ORIGIN, SEDIMENTOLOGICAL CHARACTERISTICS, AND PALEOGLACIAL SIGNIFICANCE OF LARGE LATERO-FRONTAL MORAINES IN DEGLACIATING REGIONS OF PERÚ AND ICELAND.

By

RODRIGO ALBERTO NARRO PÉREZ, B.Sc (Hons),

A Thesis

Submitted to the School of Graduate Studies

in Partial Fulfillment of the Requirements for the Degree

Doctor of Philosophy

McMaster University

Doctor of Philosophy (2021) McMaster University

(Earth, Environment and Society) Hamilton, Ontario, Canada

Title: **ORIGIN, SEDIMENTOLOGICAL CHARACTERISTICS, AND PALEOGLACIAL SIGNIFICANCE OF LARGE LATERO-FRONTAL MORAINES IN DEGLACIATING REGIONS OF PERÚ AND ICELAND.**

AUTHOR: Rodrigo Alberto Narro Pérez B.Sc (Hons)

(McMaster University, Hamilton, 2014)

SUPERVISOR: Professor Dr. Carolyn H. Eyles

NUMBER OF PAGES: xix, 322

ABSTRACT

This thesis investigates the origin, sedimentological characteristics, and paleoglacial significance of large latero-frontal moraines and moraine-dammed glacial lakes and their potential to generate glacial lake outburst flood (GLOF) events in the Cordillera Blanca, Perú and Iceland. This topic is particularly important as the potential for GLOF events in high altitude regions is increasing as ongoing global climate warming causes rapid glacier recession and the growth of lakes impounded by unstable moraines.

The first chapter of this thesis introduces the characteristics of moraine dammed lakes and GLOFs and provides details of the study areas in Perú and Iceland that were selected for this work (Chapter 1). Chapter 2 investigates the glacial history of the Cordillera Blanca, Perú through the compilation, mapping, and analysis of dated moraines in the region. The formation of moraines by different glaciers in the same region at approximately the same time is interpreted to indicate a period of regional climate conditions that were favourable for glacier expansion and/or equilibrium. Six stages of glacial activity are identified from this analysis, ranging in age from older than 35 thousand years (Stage 1) to modern (Stage 6).

The third chapter of this thesis identifies the geomorphic and sedimentologic characteristics of a moraine-dammed supraglacial lake (Llaca Lake) in the Cordillera Blanca, Perú. The combined use of imagery collected with an uncrewed-aerial vehicle (UAV), field sedimentological observations and geomorphological mapping allowed the creation of a landsystem model that summarizes the current geomorphic and

sedimentologic environment of Llaca Lake (Chapter 3). This is the first study to describe the landform-sediment assemblages in a tropical moraine-dammed supraglacial lake and provides a framework for further landsystem analysis of growing supraglacial lakes that are at risk of GLOF events.

The fourth chapter of this thesis describes the sedimentary architecture of the eastern lateral moraine of Gígjökull in southern Iceland. An uncrewed-aerial vehicle was used to acquire high resolution photographs of an exposure through the lateral moraine that allowed the identification of seven lithofacies types and three lithofacies associations. Documentation of the sedimentary architecture of the eastern lateral moraine of Gígjökull enhances understanding of moraine development and the identification of areas of hydrogeological weakness that can reduce the structural integrity of the moraine.

The research findings presented in this thesis utilize a glacial sedimentological and geomorphological approach to investigating the relationship between current and past glacial processes in the study areas, and the role that these processes play in determining the characteristics and stability of large ice marginal moraines that impound glacial lakes. This work also furthers our understanding of the dynamic surface processes at work in high altitude regions such as the Cordillera Blanca. Identifying and determining the relationships between current and past processes, sediments and landforms will enhance understanding of the role of large moraines damming glacial lakes in other high-altitude regions such as the Himalayas, British Columbia, Patagonia, and New Zealand and the associated risk of GLOF events.

TABLE OF CONTENTS

ACKNOWLEDGEMENTS

Throughout my graduate career, I learned that nothing is ever done in isolation. The culmination of my doctoral work was completed because I was fortunate to have a community that pushed me, elevated me and ensured that I was on tract throughout this journey. While I may never be able to show how truly thankful I am, I can begin by acknowledging you all.

The start of the work in this thesis can be attributed to el Ingeniero Nemesio Benjamín Morales Arnao, past Executive President of Perú's Instituto Nacional de Investigación en Glaciares y Ecosistemas de Montaña (INAIGEM), who was instrumental in establishing the research partnership between McMaster University and INAIGEM. A collaboration that continues to this day. Ing. Benjamín is one of the Cordillera Blanca's foremost geologists, who has left a lasting legacy in the region and the work in this thesis hopes to honour his work. Muchas gracias Ingeniero por todo lo que hiciste por mí y por creer en esta relación científica entre Perú y Canadá.

Thank you to all the research and field staff in INAIGEM that aided in the logistics, administration and planning of the field work of this thesis. I have learned so much from all of you and I am honoured to be one of the many Peruvians researching climate change in our country. Gracias a Oscar Vilca, Harrison Jara Infantes, Juan Carlos Torres Lázaro, Steven Wegner, José Herrera Quispe, Jesús Gómez López, y Maria Gracia Bustamante Rosell por su ayuda y amistad al largo de los años. Thank you Luzmila Dàvila Röller for all your help and friendship over the years – estoy sumamente agradecido a ti por todo.

To the Glacial Sedimentology Lab, thank you for making me the geoscientist that I am today. I started as a very naïve and perhaps clumsy undergraduate student and you all made me a better scientist. Thank you to Riley Mulligan, Jess Slomka and Stacey Puckering for putting up with my silliness as an undergrad and for being the first people to instill within me the importance of fieldwork – you all set the foundation of my field skills. Jess, thank you for teaching me the importance of beautiful figures – all my figure making skills I attribute to you! Riley, thank you for putting me in my place when I needed it but challenging me to be a critical thinker as a sedimentologist. Thank you to Chimira Andres and David Bowman for fieldwork help in Perú. Thank you to Rebecca Lee for countless hours in the field (in Perú, Iceland and Ontario) and for sticking with me while we survived that one ice storm in Sléttjökull. Thank you for all your help, discussions and insights throughout this thesis but I'm also thankful for the life long friendship we have formed.

Thank you to John Maclachlan who has been an incredible mentor throughout this journey. Thank you for putting up with all my rants and shenanigans as a student but most importantly for encouraging me and uplifting me throughout my graduate journey when I needed and more importantly those times when I didn't know I needed it. Thank you for helping in the field in Perú and for your valuable contributions and discussions regarding

the Cordillera Blanca and Llaca Lake work. And thank you to Heather and Archer for their support and smiles over the years!

Thank you to Dr. Nancy Doubleday and the Water Without Borders (WWB) program for their support and encouragement during my doctoral work. In particular, through the offering of the graduate WWB field course for the 2019 and 2020 year in Perú. This field course further strengthen the relationship between McMaster and INAIGEM.

Thank you to my whole family, those near and far, who have provided love and support throughout this journey. Para mis abuelos, Graciela, Manuel, Elsa y Alfonso, y Alinda espero haberlos hecho orgulloso. Para la abuelita Ricardina, me viste comenzar mis estudios – gracias por tanto amor y una niñez tan bonita. Esta tesis le debe mucho a mis tíos, Rosa Gamarra y Julio Mazzotti, Carlos Gamarra y Marisa Molina, Raúl Gamarra e Ivonne Dancourt, Rica Gamarra y Jorge Castillo, y Elvia Narro por todo lo que han hecho por mí y mi hermana. Gracias por todo el amor que me han dado desde pequeño y por haber inculcado en mí el valor del trabajo y la perseverancia, pero lo más importante el valor de la familia. Para mi Abu – gracias por todo el amor que siempre me has dado. Para todo el resto de mi familia, mis tíos, tías, primos y primas – gracias.

Thank you to all my friends who have shown me nothing but love and friendship throughout this journey. Thank you for putting up with all the rants about graduate school, the 'you don't get it' rants and for always ensuring that I still had fun and a social life while being a graduate student. The amount of love and encouragement you've all given me has meant so much. Thank you Alan Rheaume, Alex Young, Aneta Ratajczyk, Brandon Greiling, Daniel D'Angela, Esther Kim, Ji Kim, Jimmy Long, Justin Ganly, Kevin Monk, Nat Ferriman, Nic Patafio, Martyna Benisz, Richard Monk, Ryan LaPorte, Sam Bailey, Scott Mallon, Tristan Paul – your support has meant so much. Jessica Lieng and Magda Szlezak thank you for always being there for me, through thick and thin, for checking-in when I needed it – your love has meant a lot. Jacob Brodka, thank you for putting up with my rants, for being with me through the ups and down of graduate school, from beginning to start, and for always reminding me of the finish line – I'm incredible thankful for your friendship.

Muchas gracias a la familia Brenner Jaramillo por una amistad de más de dos décadas, gracias tía, tío y Gonzalo. Gracias Diego por la amistad más larga de mi vida y por siempre proveer un hogar donde poder ir después de todos mis trabajos de campo en Perú.

Gracias a mi nueva comunidad latinoamericana en McMaster la cual estuvo conmigo en el final de la tesis y me empujo para cruzar la meta final – gracias a Stacy Creech, Andrés Felipe Fajardo, Milly Freire-Archer, Katy Celina Sandoval, Jorge Sanchez-Perez y Sofia Palma Florido.

Thank you to my McMaster community that has provided so much love and support over the years, in particular to those who have taught me so much outside of the sciences and have provided mentorship and guidance. Thank you Daniel Coleman, Faith Ogunkoya,

Khadijeh Rakie, Sashaina Singh, Ameil Joseph, Gena Zuroski, Jordan Carrier, Kalai Saravanamuttu, Kim Dej and Vanessa Watts.

To my mom, dad, Gaby y Frosty – thank you for going through this journey with me. Mami, gracias por enseñarme a ser fuerte, por todo el amor que me has dado y por empujarme a ser una buena persona cada día de mi vida. Me enseñaste a no darme por vencido y ser un luchador. Papi, desde pequeño me enseñaste a abrir mi mente e inculcaste una curiosidad para entender el mundo en que vivimos – esta tesis es la culminación de una educación que tu comenzaste – gracias por todo. Gaby thank you for always cheering me on, answering the pone whenever I've needed you and for putting up with me throughout this journey (and if we're being honest for putting up with me since we were kids!). Para mi hermanito pequeño, gracias por trece años tan bonitos y por haber querernos tanto. Aunque no pudiste estar hasta el final de esto, yo sé que siempre estarás con nosotros. Te dedico el final de esta tesis a ti.

Thank you to my committee, Dr. Sarah Dickson-Anderson and Dr. Joe Boyce. Your encouragement and support throughout my doctoral work, it was instrumental to its completion and success. Thank you Sarah for a wonderful year in the WWB and beyond – you instilled a sense of interdisciplinarity in me that I'm deeply thankful for. Thank you Joe for instructing me throughout my undergraduate and giving me the knowledge and skills that I used throughout this work. I am deeply thankful for your mentorship over the years. I would like to thank Dr. Stephan Harrison for taking the time to review my thesis as the external examiner and for providing kind and insightful comments to strengthen this work. Thank you to Dr. Juliet Daniel for being the chair to my defense. Thank you Juliet for seeing my whole university career as a student from beginning (1st year cell bio) to end (thesis defence) and for the years of mentorship, care and kindness and thank you for pushing me to be the best I can be.

Lastly, I would like to thank my supervisor Dr. Carolyn Eyles who I owe so much and may never be able to articulate how grateful I am. In first year iSci, you opened up my eyes and mind to the endless possibilities that studying the Earth Science had. You welcomed me with open arms to the Glacial Sedimentology Lab in the summer of 2011 as an eager, and very naïve iSci student who wanted to do fieldwork. You have pushed me to be a better writer, a better researcher and a better geoscientist. You have always encouraged me to pursue my passions – whether that was to pursue being a VP for the MSU, or whether it was me joining a bunch of committees or teaching courses, you've always pushed for me to be the best that I can be. This thesis started with a question, "Hey Carolyn, do you think we could go to Perú to do my PhD work?" and I remember you saying "I've never been to Perú and I know no one there, but let's do it!" I do not have enough words to express my gratitude for allowing me to formulate the research questions and objectives that allowed me to reconnect with the country that I was born in. I am very thankful for your patience and understanding throughout my graduate journey (and during undergrad!). My mind and

my work has always gone in a thousand different directions (the number of tabs on my internet browser was a testament of that) and while you always made sure I was focused, you still let me be me. You have been an incredible teacher, mentor, supervisor, friend and the amount of memories that have been made in field experiences, Christmas parties, conferences, lunches and more will be forever treasured. As I embark on the next stage of life, I can say that without a doubt, wherever I'll end up, all of the success I'll have as a professional, are thanks to you – I'll be forever grateful for everything!

Gracias a todos,

Rodrigo Alberto Narro Pérez

LIST OF FIGURES AND TABLES

DECLARATION OF ACADEMIC ACHIEVEMENT

This thesis is comprised of four interlinked chapters containing the research led by the author. The chapters composing the body of this thesis (Chapters 2-4) have been formatted and prepared for submission to peer-reviewed scientific journals.

Chapter 2: Chronology of Late Quaternary Tropical Glaciation in the Cordillera Blanca, Perú: A Framework for Future Investigations. R. Narro Pérez & C.H. Eyles.
R. Narro Pérez conducted the compilation of the literature review, data analysis, writing of the manuscript and figure drafting. C.H. Eyles (Supervisor) provided editing of the manuscript and figures and discussion. This paper will be formatted and submitted to the *Journal of South American Earth Sciences.*

Chapter 3: Landsystem Analysis of a tropical moraine-dammed supraglacial lake, Llaca Lake, Cordillera Blanca, Perú. R. Narro Pérez, R.E. Lee, L. Davila Roller, J.C. Maclachlan & C.H. Eyles.
R. Narro Pérez performed fieldwork, conducted the literature review, drafted the figures, and prepared the manuscript. R. E. Lee assisted in fieldwork, analyzed, and prepared the photogrammetric drone data and aided in the discussing and editing of the manuscript. L. Davila Roller and J.C. Maclachlan aided in fieldwork and in the discussion of the manuscript and editing. C.H. Eyles (supervisor) visited the field site and assisted in fieldwork, and provided significant discussion and editing throughout the preparation of the manuscript. This manuscript will be formatted and submitted to the *Earth Surface Processes and Landforms.*

Chapter 4: *Sedimentary Architecture of a lateral moraine, Gígjökull, Iceland. R. Narro Pérez, R.E. Lee & C.H. Eyles.*
R. Narro Pérez led fieldwork, data collection and analysis, literature review, writing of the manuscript and drafting figures. R.E. Lee aided in fieldwork, provided insight to discussions and editing of the manuscript. C.H. Eyles (supervisor) contributed to the editing of the manuscript and figures and helpful discussions. This manuscript will be formatted for submission to Jökull – *Journal of Earth Science.*

CHAPTER 1: INTRODUCTION

1.1. INTRODUCTION

Receding glaciers are recognized as physical indicators of climate change and increasing global temperatures. The impact of glacier recession is most noticeable in high altitude and glaciated environments, where changes to the physical landscape and also to the cultural and economic well-being of the communities that live in these environments are apparent (Mark *et al.*, 2010, 2017; Huggel *et al.*, 2015; Vuille *et al.*, 2018). Much of the research regarding the social impacts of glacier recession has focused on the diminishing amounts of meltwater that will be available to communities dependent on this potable water source (Baraer *et al.*, 2009; Vuille *et al.*, 2018). However, the increased potential for catastrophic meltwater floods as glaciers continue to melt is a growing concern (Haeberli, 1983; Huggel *et al.*, 2004; Harrison *et al.*, 2018; Wilson *et al.*, 2018; Emmer *et al.*, 2020; Shugar *et al.*, 2020).

Glacial lake outburst floods (GLOFs, also known as jökulhaups or aluvíones; Quincey and Carrivick, 2015) are catastrophic floods that occur when a naturally formed dam, such as a latero-frontal moraine, fails and releases immense amounts of glacial lake water and sediment (Costa and Schuster, 1988; Hubbard *et al.*, 2005; Korup and Tweed, 2007; Harrison *et al.*, 2018). In high altitudes areas, in particular those with an increasing number of moraine-dammed glacial lakes, the risk of outburst flood generation needs to be better researched and understood (Haeberli *et al.*, 2016; Harrison *et al.*, 2018). Since the start of the 21st century, glacier outburst floods have occurred, and continue to threaten communities, in Perú, Bolivia, Nepal, India, Pakistan, Iceland, Greenland, New Zealand,

Switzerland, Russia, and North America, causing infrastructure and agricultural damage as well as loss of human life (Figure 1.1).

GLOFs released from moraine-dammed lakes dramatically increased in number between 1930 and 1970, an increase attributed to a delayed response to global warming following the Little Ice Age (LIA; Harrison *et al.*, 2018). A recent study by Shugar *et al* (2020) reports that global glacial lake volume increased by ~48% between 1990 and 2018 in response to ongoing climate warming. While there has been few GLOFs released from moraine-dammed lakes since 1970, it is assumed that GLOF frequency will increase throughout the 21st century as glacial lakes continue to increase in number and size due to ongoing climate warming (Harrison *et al.*, 2018; Shugar *et al.*, 2020).

Moraine-dammed lakes, as the name indicates, are dammed by large latero-frontal moraines that indicate the position of former glacier margins during episodes of advance, readvance, or stillstand. Moraines are not only important as natural dams but can also provide valuable information about past glacier behaviour and extent. The age of a moraine can be broadly determined through analysis of boulders found near or on the crestline of the moraine, using a variety of methodologies such as lichenometry, radiocarbon dating, and surface exposure dating (i.e. Matthews and Petch, 1982; Ivy-Ochs *et al.*, 2006; Jomelli *et al.*, 2009; Owen *et al.*, 2009; Smith and Rodbell, 2010). Determining the chronology of moraine formation can therefore help in the reconstruction of the glacial and deglacial history of an area. In addition, documentation of the composition, structure, and genetic history of moraines can greatly enhance understanding of moraine stability and factors that

Figure 1.1: High-mountain regions that are at risk of experiencing glacier floods. MDL – Moraine-dammed lakes; GTV – Glacier topped volcanoes; GDL – Glacier-dammed lakes; EO – Englacial outbursts. Adapted from Quincey and Carrivick (2015).

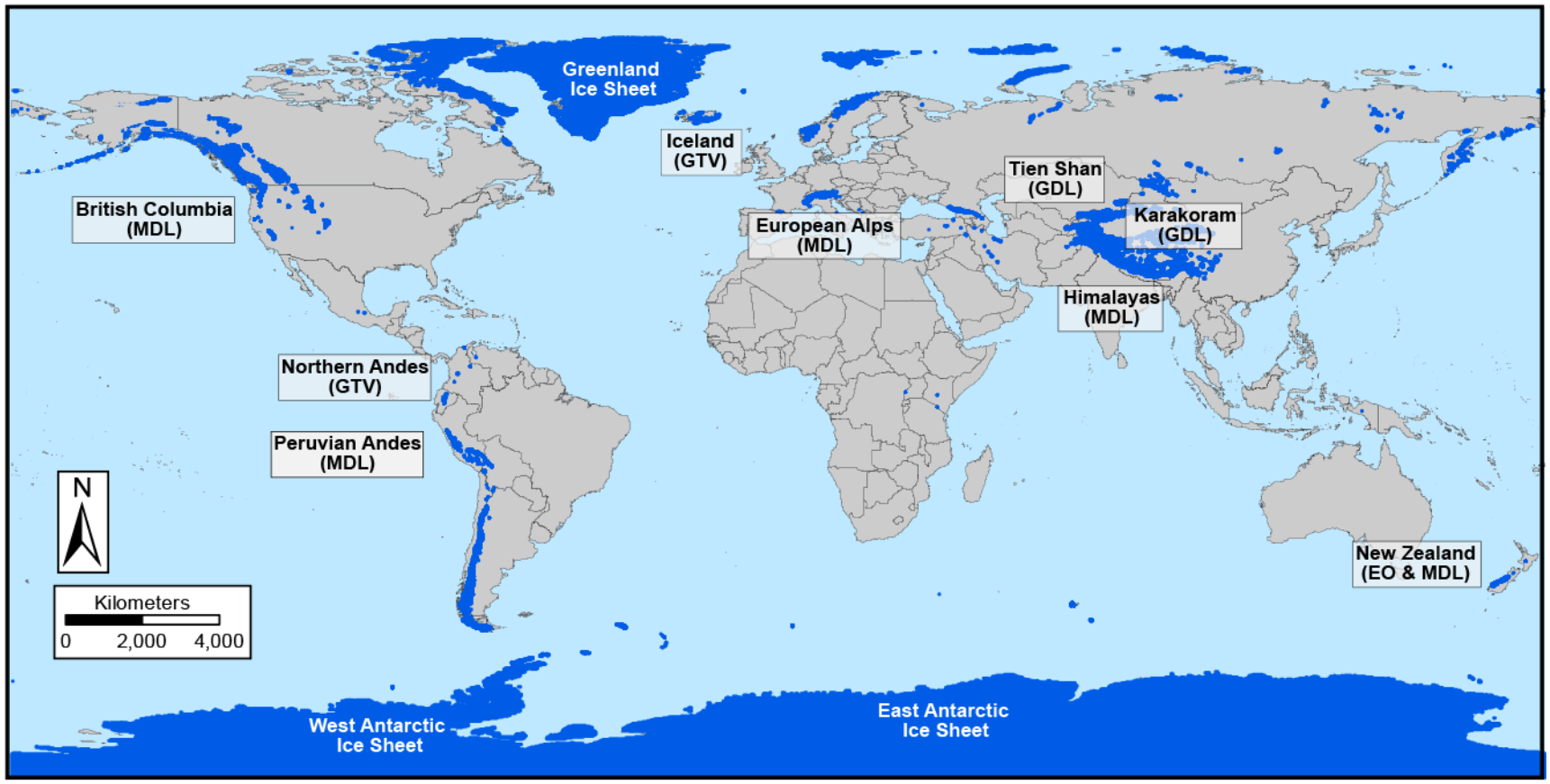
Greenland
Ice Sheet
Iceland
(GTV)
Tien Shan
(GDL)
British Columbia
(MDL)
European Alps
(MDL)
Karakoram
(GDL)
Himalayas
(MDL)
Northern Andes
(GTV)
Peruvian Andes
(MDL)
N
Kilometers
0 2,000 4,000
New Zealand
(EO & MDL)
West Antarctic
Ice Sheet
East Antarctic
Ice Sheet

can contribute to their collapse and failure (Clague and Evans, 2000; McKillop and Clague, 2007; Westoby *et al.*, 2014; Quincey and Carrivick, 2015). Thus, there is a pressing need to better understand glacial moraines, the processes involved in their formation, their sedimentological composition, and their spatial heterogeneity, in order to gain more insight into factors controlling their behaviour as natural dams and their significance for reconstructing glacial chronologies.

1.2 RATIONALE AND OBJECTIVES

This thesis aims to investigate the origin, sedimentological characteristics, and paleoglacial significance of large latero-frontal moraines in deglaciating regions of Perú and Iceland. The findings reported here may be applied to better understand the role of large moraines damming glacial lakes in other high-altitude regions such as the Himalayas, British Columbia, and New Zealand (Figure 1.1).

The thesis reports on studies that utilize a glacial sedimentological and geomorphological approach to investigate the relationship between current and past glacial processes in the Cordillera Blanca, Perú and southern Iceland, and the role that these processes play in determining the characteristics and stability of large ice marginal moraines that impound glacial lakes. The Cordillera Blanca mountain range in Perú was chosen as it contains the largest tropical glacier field in the world but also has the longest record of GLOFs that began in the 1930s (Smith, Mark and Rodbell, 2008; INAIGEM, 2018; Emmer *et al.*, 2020). Many of the glacial lakes of significant size in the Cordillera Blanca are dammed by large latero-frontal moraines (Iturrizaga, 2014; Emmer, Vilímek

and Zapata, 2018; Emmer *et al.*, 2020), but large, accessible outcrops that allow examination of the internal structure of these moraines are not easily found. Consequently, the large lateral moraines at Gígjökull, Iceland were also selected for study as they have easily accessible exposures where sedimentological data can be obtained.

Before a detailed sedimentological investigation of the moraines in the Cordillera Blanca of Perú could take place, an understanding of the past glacial history the region needed to be compiled. This was accomplished through compilation and mapping of dated moraines reported in the literature (Chapter 2). Thehe geomorphic and sedimentologic characteristics of a moraine-dammed supraglacial lake in the Cordillera Blanca, Perú (Llaca Lake) were subsequently investigated using a landsystem mapping approach (Chapter 3); and an uncrewed aerial vehicle (UAV) was used to obtain high resolution imagery of the sedimentology and architecture of the large lateral moraine at Gígjökull, southern Iceland (Chapter 4). Each of these studies contributes toward the enhanced understanding of large latero-frontal moraines, moraine-dammed glacial lakes, and their potential for the release of GLOFs.

1.3 BACKGROUND INFORMATION

1.3.1 Moraine-Dammed Glacial Lakes

Moraine-dammed glacial lakes have been reported in glaciated environments in British Columbia, Canada (Figure 1.1; Blown and Church, 1985; Clague and Evans, 2000; Kershaw, Clague and Evans, 2005; McKillop and Clague, 2007a), the Himalayas (Hewitt, 1982; Shaun D Richardson and Reynolds, 2000; Osti, Bhattarai and Miyake, 2011; Jain *et al.*, 2012; Fujita *et al.*, 2013; Aggarwal *et al.*, 2017), the European Alps (Haeberli, 1983;

Huggel *et al.*, 2002, 2004; Werder *et al.*, 2010; Magnin *et al.*, 2020), Patagonia (Loriaux and Casassa, 2013; Iribarren Anacona, Norton and Mackintosh, 2014; Wilson *et al.*, 2018), New Zealand (Blair, 1994; Allen, Schneider and Owens, 2009); Bolivia (Hoffmann and Weggenmann, 2013; Cook *et al.*, 2016), and Perú (Carey, 2005; Emmer and Vilímek, 2013; Emmer, 2017; Emmer, Vilímek and Zapata, 2018; Baťka *et al.*, 2020; Mergili *et al.*, 2020).

The majority of the moraine complexes that impound present-day proglacial lakes were constructed during the "Little Ice Age", a period of cooling associated with glacial advance that began, depending on locale, in the 13th or 14th century and ended between the end of the mid-16th and the end of the 19th century (Matthews and Briffa, 2005; Clague *et al.*, 2009; Matthews, 2014). Latero-frontal moraine formation is primarily driven by ice-marginal processes involving mass movements such as debris flows, and/or the falling, rolling and sliding of debris, and deposition from meltwater (Humlum, 1978; Small, 1983; Benn and Benn, 1989; Owen and Derbyshire, 1989; Benn and Evans, 2010; Evans, Shulmeister and Hyatt, 2010; Lukas *et al.*, 2012). The sedimentary architecture of latero-frontal moraines is characterized by an arrangement of crudely to well stratified beds of diamict, boulders, gravels and/or sands that dip away or towards the glacier margin, depending on whether the glacier snout is advancing or retreating (Boulton and Eyles, 1979; Small, 1983)(Owen and Derbyshire, 1989; Lukas *et al.*, 2012) (Humlum, 1978; Lukas, 2012). Some latero-frontal moraines also contain horizons of fine-grained glaciolacustrine material incorporated during episodes of glacier (re)advance and retreat (Evans, Shulmeister and Hyatt, 2010)

1.3.2 Components of a Glacial Lake Outburst Flood

Glacial lakes impounded by latero-frontal moraines are commonly the source of glacial lake outburst floods (GLOFs; Huggel *et al.*, 2002; Hubbard *et al.*, 2005; Korup and Tweed, 2007; Emmer and Vilímek, 2013; Westoby *et al.*, 2014; Quincey and Carrivick, 2015)). A GLOF event is often deconstructed into three key stages consisting of 1) a trigger mechanism, 2) dam break initiation and development, and 3) downstream movement of outburst flood waves (Westoby *et al.*, 2014). Figure 1.2 is a conceptual diagram describing a GLOF in the Cordillera Blanca where these three components are shown (1-3) as well as potential triggers of a GLOF (A-E), the geomorphic and geological features found in moraine-dammed glacial lakes (a-g), and factors that can influence dam failure (i-iii).

1.3.2.1 Trigger mechanism

The trigger mechanism refers to the physical event that starts ("triggers") a GLOF event (Figure 1.2 – A-E). Common triggers for GLOFs generated from moraine-dammed glacial lakes include ice and rock avalanches, landslides, heavy rainfall, and the sudden release of sub-, en- and supra glacial discharge that create large waves that overtop or puncture the moraine (Clague and Evans, 2000; Shaun D. Richardson and Reynolds, 2000; Westoby *et al.*, 2014; Harrison *et al.*, 2006; Emmer and Vilímek, 2014). Active and prolonged piping (water leakage) through the moraine can decrease moraine stability leading to moraine failure (Clague and Evans, 2000; Osti, Bhattarai and Miyake, 2011) and ground shaking caused by seismic activity (earthquakes) can also cause moraine collapse (Clague and Evans, 2000).

Figure 1.2: Conceptual model of a hazardous moraine-dammed glacial lake in the Cordillera Blanca, Perú. Geomorphic and geological features found in moraine-dammed glacial lakes: a) rockfall and avalanche fans provide supraglacial debris to glacier surface; b) ice-cored hummocks; c) buried ice underneath lake bottom; d) latero-frontal moraine damming the glacial lake; e) mountain peaks containing small slope glaciers and glaciated peaks (nevados); f) pedestal moraines and/or terminal moraines found on mountain sides of major valleys in the Cordillera Blanca; g) valley floors contain glaciofluvial rivers and deposits; h) community settlements. Potential triggers of a Glacial Lake Outburst Flood include: A) contact glacier calving; B) rapid and sudden input of water from supra-, en-, or subglacial sources; C) rockfall/snow/ice avalanches; D) high precipitation event; E) seismic event. Factors that influence dam failure: i) lake dimensions and large lake volume; ii) small dam freeboard and dam dimensions; iii) moraine sedimentary architecture that allows water seepage/piping. Key stages of a GLOF: 1) an event causes a significant water wave in the lake; 2) dam breach and formation; 3) resultant flood wave moves downvalley. Adapted from Richardson and Reynolds (2000) and Westoby et al. (2014).

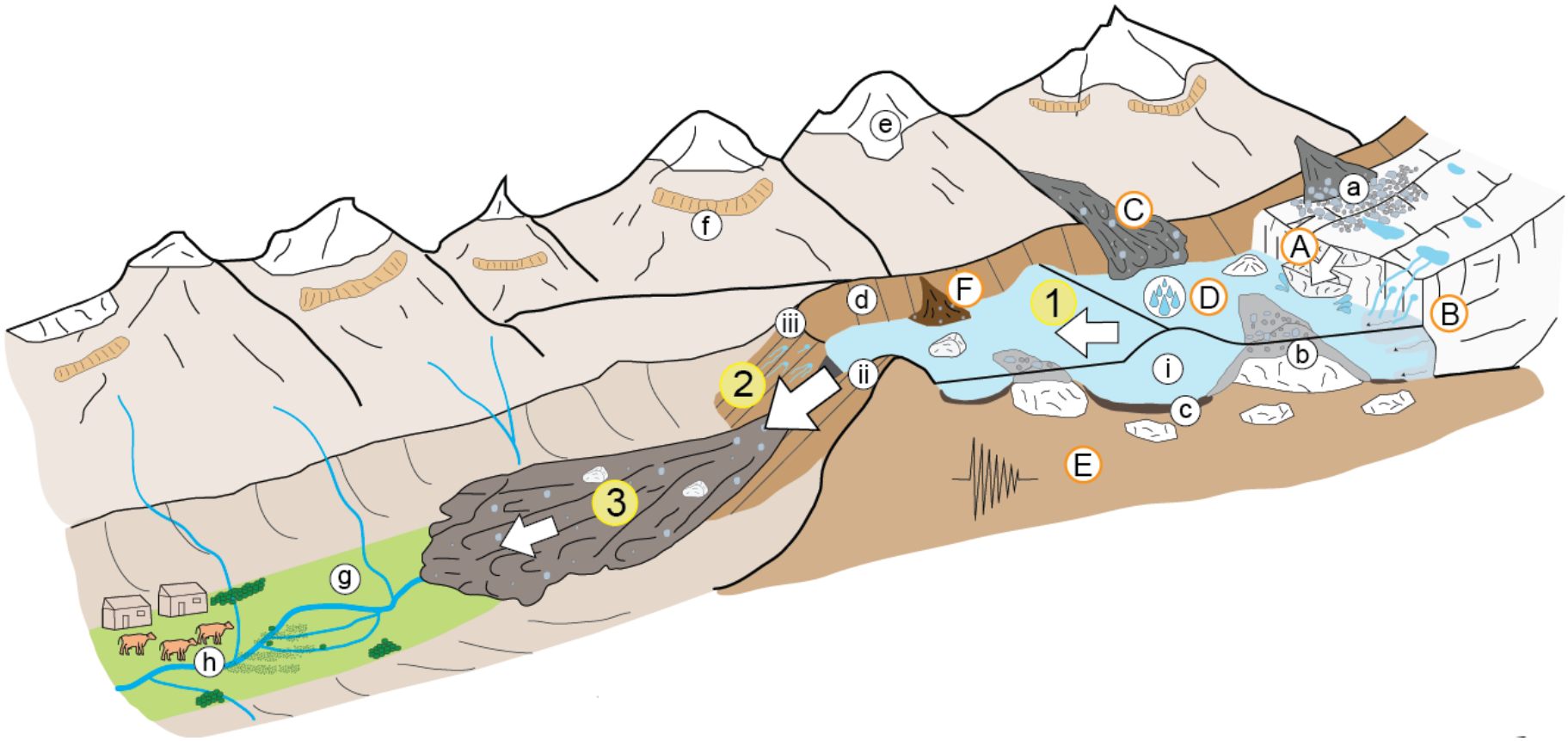
a
A
B
C
D
E
F
b
c
d
e
f
g
h
i
ii
iii
1
2
3

1.3.3.2 Breach Initiation and Development

Dam breach occurs when the natural strength of the dam is exceeded by the impounded glacial lake water mass, by high shear stresses caused by seepage or piping, and/or by the overtopping of displacement waves (Figure 1.2 – i-iii; Clague and Evans, 2000; Shaun D Richardson and Reynolds, 2000; Korup and Tweed, 2007; Westoby *et al.*, 2014). The breach commonly creates an incipient channel in the moraine dam that increases in size as the flow strength exceeds the cohesive strength of the dam material (Korup and Tweed, 2007; Westoby *et al.*, 2014). Development of the dam breach will halt when the base-level of the moraine is reached, a bedrock abutment or less erodible material is encountered, or the outflow channel becomes sufficiently armoured to halt down-cutting (Clague and Evans, 2000; Westoby *et al.*, 2014).

1.3.3.3 Downstream Movement of Outburst Flood Waves

The last stage of a GLOF is the downstream movement of the outburst flood waves through the newly formed outflow channel (breach) downstream into the valley. Depending on local factors, such as the composition and cohesiveness of the moraine material, varying mixtures of lake water, glacier ice, and moraine sediment will compose the flood waves (Clague and Evans, 2000; Kershaw, Clague and Evans, 2005; Westoby *et al.*, 2014). These debris-charged flood waves can travel long distances downstream; the GLOF generated by Lake Palcacocha in 1941 flowed down valley 23 km to the city of Huaraz causing heavy tolls on infrastructure and human life (Carey, 2005; Emmer and Vilímek, 2013; Wegner, 2014).

While the lake volume and moraine dam breach will determine the resulting flood volumes, discharges of 10-30 x 10^6 m^3 are not uncommon (Quincey and Carrivick, 2015).

In the Cordillera Blanca, most recorded GLOF events are characterized by debris-charged flows that carried large boulders (diameters of several metres) that were subsequently deposited across the valley floor (Emmer, 2017). The presence of other bodies of water encountered by a GLOF moving downvalley can dramatically change the composition and volume of the flow. For example, in the 1941 GLOF of Lake Palcacocha the flood waves incorporated the waters of Lake Jircacocha, a lake that was 8.3 km downstream from Lake Palcacocha, adding an additional 3.6 million m^3 of water to the original 10-12 million m^3 (Vilímek *et al.*, 2005; Andres *et al.*, 2018).

1.3.4 Modeling of Glacial Lake Outburst Floods

Modelling the potential of a region to generate GLOF events requires an initial comprehensive survey to identify and classify glacial lakes in the region (i.e., Emmer, Vilímek and Zapata, 2018; Guardamino *et al.*, 2019; Emmer *et al.*, 2020). Predictive models then utilize observations from past GLOF events and/or observational data to determine: 1) the likelihood of a GLOF event from occurring and/or 2) the potential flood wave scenarios and the potential damage (i.e. Clague and Evans, 2000; Huggel *et al.*, 2002; Korup and Tweed, 2007; Allen, Schneider and Owens, 2009; Benn *et al.*, 2012; Jain *et al.*, 2012; Schneider *et al.*, 2014; Westoby *et al.*, 2014; Iribarren Anacona, Norton and Mackintosh, 2014; Rivas *et al.*, 2015; Somos-Valenzuela *et al.*, 2016; Aggarwal *et al.*, 2017; Bueechi *et al.*, 2019; Mergili *et al.*, 2020; Emmer *et al.*, 2020). These models vary in their complexity and can include empirical regression models, analytical and parametric models, and physically-based numerical models (Westoby *et al.*, 2014).

Input parameters to predictive GLOF models often include factors such as current glacier behaviour and characteristics, moraine dam characteristics, lake characteristics, and

characteristics of the regional environment (Allen, Schneider and Owens, 2009; Westoby *et al.*, 2014; Quincey and Carrivick, 2015; Aggarwal *et al.*, 2017; Wilson *et al.*, 2018; Viani *et al.*, 2020). Moraine dam characteristics inputs typically include dam type (i.e. moraine, bedrock, ice), dam freeboard (vertical distance between lake level and lowest point on the moraine crest), dam width, dam height, presence of piping (yes or no), and the presence of remedial work (Clague and Evans, 2000; Huggel *et al.*, 2004; McKillop and Clague, 2007; Emmer and Vilímek, 2014). Depending on the input parameters used, the GLOF potential of any one lake may change (Emmer and Vilímek, 2013). A range of output scenarios can be created from GLOF models that can help identify the susceptibility of a specific lake to experience a GLOF event, most often in the form of qualitative scales ranging from 'high susceptibility' to 'zero susceptibility' (Emmer *et al.*, 2016), or 'high hazard probability' to 'low hazard probability' (Huggel *et al.*, 2003).

1.3.4.1 Limitations of Modeling GLOF events

It is important to note for the purposes of this thesis that in current GLOF models, moraine characteristic inputs are limited to physical dimensions such as dam width, dam height, and freeboard. The sedimentology and architecture of the moraine dams are either not included as input parameters in these models or are simplified (i.e does the moraine contains buried ice), despite the recognition that the geological characteristics of the moraine are important, particularly for assessing the stability of the dam and for predicting the type of trigger likely to initiate a dam breach (Clague and Evans, 2000; Shaun D Richardson and Reynolds, 2000; McKillop and Clague, 2007; Westoby *et al.*, 2014).

Piping or seepage will gradually weaken a dam and cause it to fail internally (Clague and Evans, 2000; Korup and Tweed, 2007). Current GLOF models are limited to

including piping in a binary format, either present or not, and do not take into account the internal structure of a moraine dam and identification of areas where piping may occur (Westoby *et al.*, 2014). Moraine dams that consist of primarily of silt and sand-rich diamicts or sand-rich gravel are considered to be particularly prone to piping and thereby potential failure (Clague and Evans, 2000). It is therefore important to determine the characteristics and sedimentological architecture of large latero-frontal moraines that serve as lake dams to better identify where areas of piping or failure may occur.

1.3.2 Moraines and Dating Techniques

The sedimentological and architectural characteristic of moraines are related to the processes associated with the formation of these landforms (Shaun D Richardson and Reynolds, 2000; Evans, Shulmeister and Hyatt, 2010; Lukas *et al.*, 2012). Determining the age of e moraines in a particular region, helps establish the glacial history of the region and provides information that can aid in the identification of past glacial processes. Thus, the research presented in this thesis also requires an understanding of how dating techniques are applied to determine the chronology of moraine emplacement. The most common methodologies used to date past glacial events in glaciated regions of the Andes include lichenometry, dendrochronology, radiocarbon dating, surface exposure dating, and sediment core analysis. In the Cordillera Blanca, lichenometric studies, which measure the size of lichens growing on boulders, have been used to estimate the age of bouldery moraines (i.e. Rodbell, 1992; Solomina *et al.*, 2007; Jomelli *et al.*, 2008). However, moraine ages calculated by this method may be inaccurate due to the influence of substrate lithology and microclimatic conditions that can affect the size and speed of colonization by

lichen (Benedict, 1967; Jochimsen, 1973; Rodbell, 1992), and/or lichen mortality (Osborn *et al.*, 2015). In addition, slope processes such as rockfalls can displace boulders on moraines which may result in inaccurate dating of the feature.

Surface exposure dating analyses cosmogenic radionuclides (CRN) and has been used extensively to date Andean moraines (i.e. Rodbell, 1992; Farber *et al.*, 2005; Benn and Lukas, 2006; Solomina *et al.*, 2007; Bromley *et al.*, 2009, 2016; Glasser *et al.*, 2009; Hall *et al.*, 2009). Cosmogenic nuclides (e.g., ^{10}Be, ^{26}Al, ^{3}He, ^{36}Cl) form and accumulate at quasi-steady rates in rocks exposed to cosmic rays. Boulders transported and eroded by glaciers are assumed to have had their surfaces "scraped clean" of any previous isotope accumulation (Gosse and Phillips, 2001; Balco *et al.*, 2008; Rodbell, Smith and Mark, 2009). Thus, measuring the concentration of cosmogenic radionuclides on a boulder found on top of a moraine can determine the amount of time since the boulder was deposited and exposed to cosmogenic rays (Briner *et al.*, 2005). However, boulders that are emplaced post-glacially by processes such as rock fall, or are covered by snow for significant periods of time, will yield ages that underestimate the age of the moraine (Rodbell, Smith and Mark, 2009). Exposure ages older than the landform can also be obtained if the boulder is not eroded sufficiently by the ice and cosmogenic radionuclides are 'inherited' from previous episodes of exposure (Briner *et al.*, 2005).

Radiocarbon dating is often done by dating organic material from lakes and/or peat lands upvalley from moraines to provide a minimum-limiting ages for the moraines, this dating provides relative dating - the minimum amount of time from ice retreat and the area which was dated (Rodbell and Seltzer, 2000; Farber *et al.*, 2005; Rodbell, Smith and Mark,

2009). In the Cordillera Blanca, radiocarbon dating on upvalley lacustrine deposits have been used in the Breque moraine to provide a minimum limiting age to describe glacial behaviour in the valley (Rodbell and Seltzer, 2000; Farber *et al.*, 2005). Radiocarbon dating and dendrochronological analysis of paleosols and tree stumps found in lateral moraines in Switzerland revealed clusters of dates, suggesting that these moraines experience several phases of stability during their formation equated with periods of negative mass balance during which glacier did not extend to the moraine crestlines (Röthlisberger and Schneebeli, 1979; Small, 1983). These findings imply an incremental formation of lateral moraines by stacking during successive advances (Lukas, 2012; Lukas *et al.*, 2012) over various amounts of time (yearly/decadal/centennial) and raise the question of which 'dates' obtained from a moraine can be ascribed to the time of its formation. While many authors have brought up the questionable reliability of dating boulders found on moraines (Benedict, 1967; Jochimsen, 1973; Osborn *et al.*, 2015), better understanding of the processes involved in the formation of these landforms will enhance understanding of the significance of any dates obtained.

1.4 STUDY SITES

The Cordillera Blanca mountain range in Perú was chosen as the primary study site as it contains the largest tropical glacier field in the world, numerous moraine-dammed lakes, and also has the longest record of GLOFs that began in the 1930s (Smith, Mark and Rodbell, 2008; INAIGEM, 2018; Emmer *et al.*, 2020). As there are few accessible exposures through large moraines in the Cordillera Blanca, a secondary study site was

identified at Gígjökull, Iceland where accessible exposures through a large lateral moraine allowed the collection of architectural and sedimentological data.

1.4.1 Cordillera Blanca, Perú

The Cordillera Blanca mountain range, located in northern Perú forms part of the larger Andes range (Figure 1.3A). It contains the largest tropical glacier field in the world (Ames Marquez and Francou, 1995; Kaser, 1999; Barnett, Adam and Lettenmaier, 2005; Bury *et al.*, 2013; Burns and Nolin, 2014; INAIGEM, 2018) and has the longest historical record of GLOF occurrence that began in the late 1930s (Carey, 2010; Emmer *et al.*, 2020).

The Cordillera Blanca forms part of the Andean mountain range which was uplifted intermittently over a period of 100 Ma (Megard, 1984; Decou *et al.*, 2013; Margirier *et al.*, 2016). Three distinct coast-parallel mountain ranges, the Cordillera Occidental, the Cordillera Central, and the Cordillera Oriental developed during uplift of the Peruvian Andes. In the region of Ancash, the Cordillera Occidental is subdivided into three physiographic regions, the Cordillera Negra to the west, the central Callejón de Huaylas valley, and the glaciated Cordillera Blanca to the east (Figure 1.4; Cobbing *et al.*, 1981). The main geological unit exposed in the Cordillera Blanca is a Neogene granodiorite, the Cordillera Blanca batholith, that intruded into shales and sandstones of the Upper Jurassic Chicama Formation approximately 14 – 5 Ma (Megard, 1984; McNulty and Farber, 2002; Giovanni *et al.*, 2010). The current physiography of the Cordillera Blanca is characterized by deep, U-shaped glacial valleys incised by glaciers during the Quaternary that trend in a northeast-southwest direction (Figure 1.5; Clapperton, 1972; Rodbell, 1992; Smith, 2005; Iturrizaga, 2014).

Figure 1.3: Study areas. A – Location of Cordillera Blanca (Chapter 2) is indicated in the red box on the inset map of Perú on bottom right corner of image. Major glacial lakes that have undergone remediation work to prevent a GLOF event have been identified. Location of Figure 1.3B is indicated on the yellow box. B – Llaca Lake and Llaca Glacier (Chapter 3) have been indicated as well as the three nevados feeding Llaca Glacier, Lake Palcacocha and the city of Huaraz. C – Location of Eyjafjallajökull is indicated on the inset map of Iceland. Gígjökull (Chapter 4) is shown in the red box.

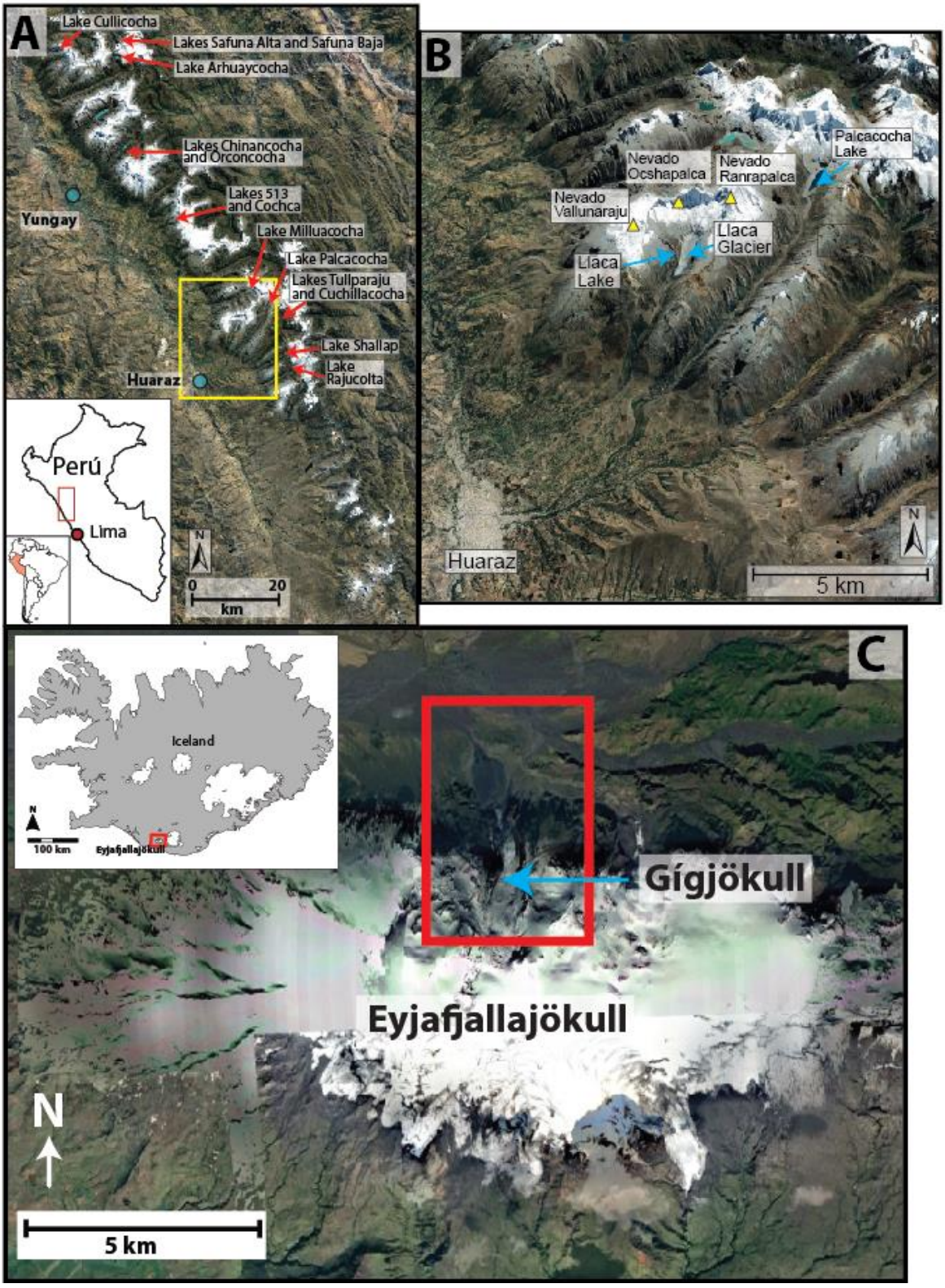
A
Lake Cullicocha
Lakes Safuna Alta and Safuna Baja
Lake Arhuaycocha
Lakes Chinancocha and Orconcocha
Lakes 513 and Cochca
Yungay
Lake Milluacocha
Lake Palcacocha
Lakes Tullparaju and Cuchillacocha
Lake Shallap
Lake Rajucolta
Huaraz
Perú
Lima
N
0 20
km
B
Palcacocha Lake
Nevado Ocshapalca
Nevado Ranrapalca
Nevado Vallunaraju
Llaca Glacier
Llaca Lake
Huaraz
N
5 km
C
Iceland
N
100 km
Eyjafjallajökull
Gígjökull
Eyjafjallajökull
N
5 km

Figure 1.4: Location of the political and physical locations discussed in text. The three main physiographic regions of the Andes in the region of Ancash are the Cordillera Negra to the west, the central Callejón de Huaylas valley and the glaciated Cordillera Blanca to the East. Huaraz is the capital of the Region of Ancash.

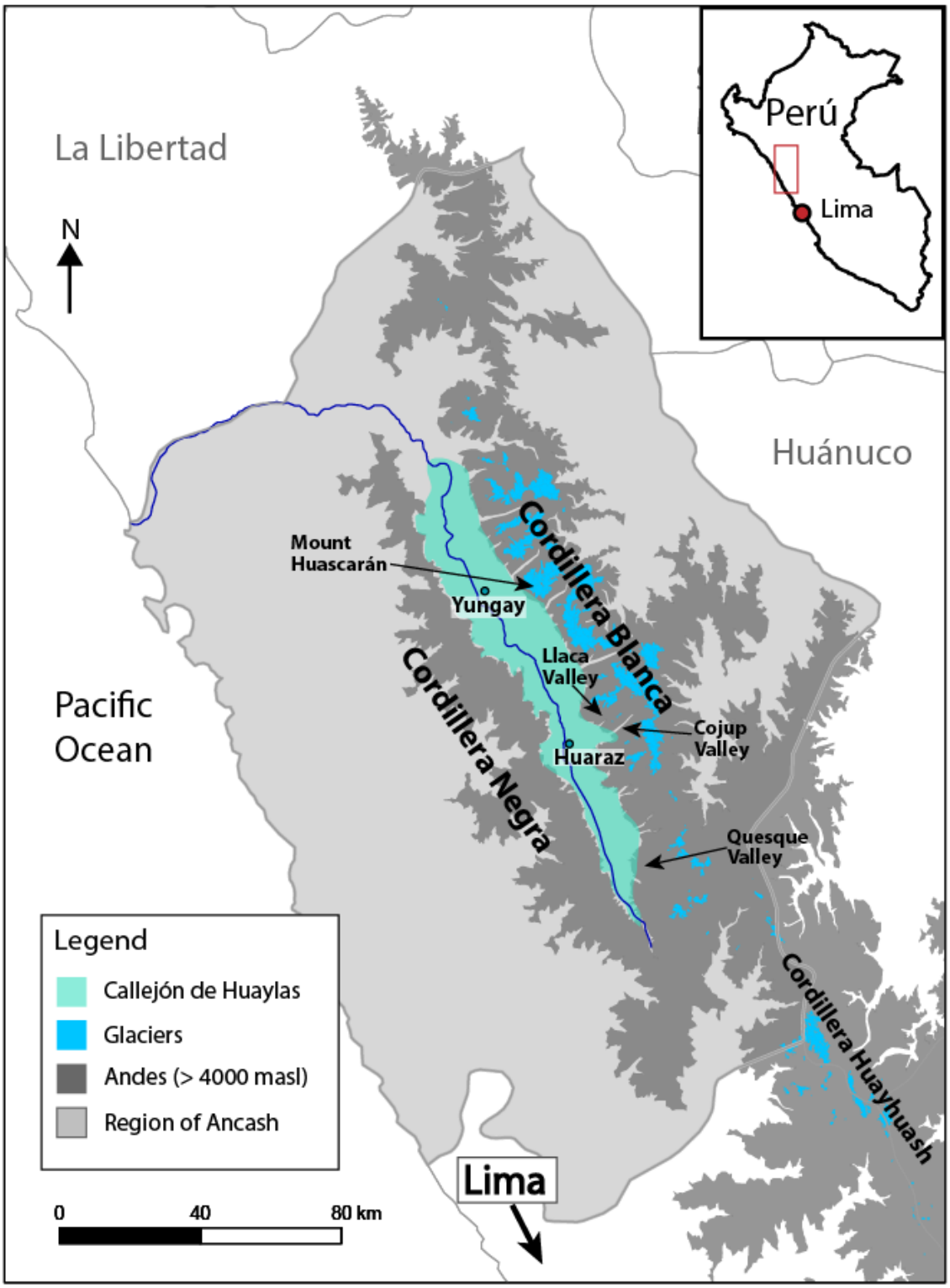
La Libertad
N
Perú
Lima
Huánuco
Mount Huascarán
Yungay
Cordillera Blanca
Llaca Valley
Cojup Valley
Huaraz
Cordillera Negra
Quesque Valley
Cordillera Huayhuash
Pacific Ocean
Legend
Callejón de Huaylas
Glaciers
Andes (> 4000 masl)
Region of Ancash
0
40
80 km
Lima

The Cordillera Blanca has experienced an annual average air temperature increase of about 0.31ºC per decade between 1969 and 1998, and of 0.13 ºC per decade from 1983 to 2012 (Mark and Seltzer, 2005; Schauwecker *et al.*, 2014). This increase in temperature is the primary cause for the reduction of the total glaciated area in the Cordillera Blanca from 800-850 km^2 in 1930 to an estimated 448.81 km^2 in 2016 (Georges, 2004; Silverio and Jaquet, 2017; INAIGEM, 2018).

While current glacier retreat in the Cordillera Blanca is primarily attributed to increased temperatures (Vuille *et al.*, 2003; Rabatel *et al.*, 2013; Schauwecker *et al.*, 2014) , precipitation changes due to the El Niño-Southern Oscillation phenomenon (ENSO) also impact the mass balance of Andean tropical glaciers(Garreaud *et al.*, 2009; Veettil, Wang, Florêncio de Souza, *et al.*, 2017). El Niño years (i.e. the warm phases of ENSO) tend to be associated with reduced precipitation, while La Niña years (i.e. the ENSO cold phases) are associated with wetter conditions. In general, Andean glaciers are expected to experience negative mass balance during El Niño years and positive or stable mass balance during La Niña conditions (Favier, Wagnon and Ribstein, 2004; Rabatel *et al.*, 2013; Veettil, Wang, Bremer, *et al.*, 2017; Veettil, Wang, Florêncio de Souza, *et al.*, 2017). Despite these generalizations, further study is needed to fully understand the relationship between tropical glaciers and ENSO as the climatic characteristics of La Niña/El Niño are not uniform across the tropical Andes and the consequences of an El Niño event can vary considerably (Garreaud *et al.*, 2009; Schauwecker *et al.*, 2014; Veettil, Wang, Florêncio de Souza, *et al.*, 2017).

Figure 1.5: Cross sectional valley morphology in the Cordillera Blanca is of the classic U-shape, characteristic of previously glaciated valleys. A – Down valley view of the Cojup Valley; the city of Huaraz can be seen in the distance (arrow indicates location). B – Down valley view of the Parón Valley taken from the Jantaraju moraine.

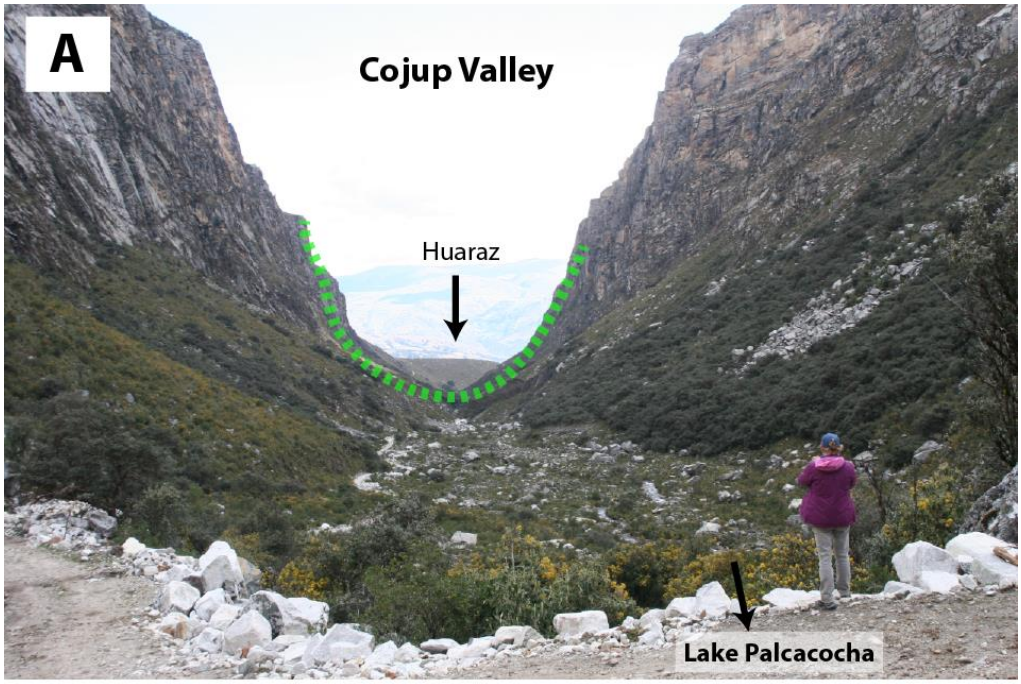
A
Cojup Valley
Huaraz
Lake Palcacocha

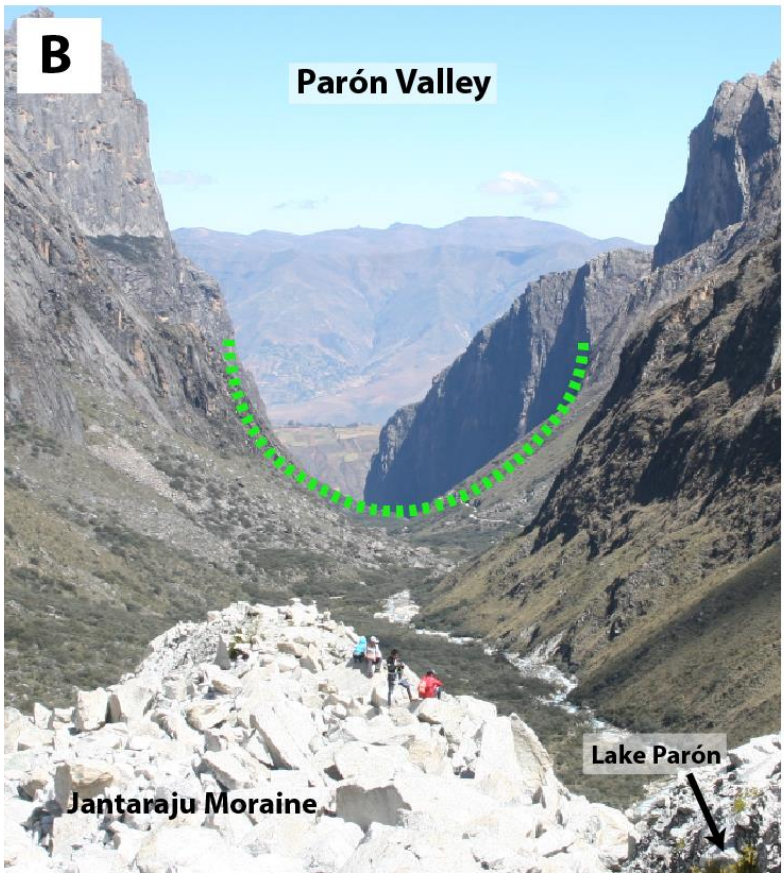
B
Parón Valley
Lake Parón
Jantaraju Moraine

1.4.1.1 GLOFS in the Cordillera Blanca

As with most glaciated regions experiencing an increase in temperature and decrease in glacial extent, the Cordillera Blanca is experiencing rapid glacial lake growth (Shugar *et al.*, 2020). Various studies have been conducted in the Cordillera Blanca to characterise and create a glacial lake inventory to assess the likelihood of a GLOF event (Morales, Zamora and Ames, 1979; Iturrizaga, 2014; Emmer *et al.*, 2016; Vilímek, Klimeš and Červená, 2016; Guardamino *et al.*, 2019). Using Google Earth data from 2012 and 2013, Vilímek et al. (2016) identified 2370 lakes of all sizes in the Cordillera Blanca; Emmer *et al.* (2016) used the same data source to identify 882 lakes of 'significant size' (lake width >20m plus lake width &length > 100 m). The most recent lake inventory (Emmer *et al.* 2020) determined that ~643 lakes existed in 1948 and ~893 lakes in 2017; total lake area also increased from approximately 29 km^2 in 1948 to 35 km^2 in 2017. In addition, of all glacial lakes analyzed, 38% were moraine-dammed(Emmer *et al.*, 2020), and the majority of large lakes identified (> 100,000 m^2) are characterized as moraine-dammed lakes (48%; Emmer *et al.*, 2016, 2020; Harrison *et al.*, 2018).

The most destructive historical GLOF to impact the Cordillera Blanca occurred on December 13, 1941, when Lake Palcacocha (Figure 1.3B) breached its moraine dam releasing a catastrophic flood that devastated the nearby city of Huaraz (Carrivick and Tweed, 2016). Two possible mechanisms have been hypothesised as triggers for the moraine dam failure: an ice calving or ice avalanche event that created impact waves that weakened the moraine dam or failure of the dam due to internal erosion of the dam structure through piping (Emmer *et al.*, 2020; Mergili *et al.*, 2020). The resulting flood waters released from the lake reached the city of Huaraz within minutes, killing approximately

2,000 people (Carey, 2005; Wegner, 2014). Since then, between 1948 and 2017, 32 smaller GLOF events have been documented in the Cordillera Blanca, with 28 occurring from moraine-dammed lakes (Emmer, 2017; Emmer *et al.*, 2020) and 4 from bedrock-dammed lakes (Carey *et al.*, 2012; Emmer *et al.*, 2016, 2020). There are three 'peaks' of GLOF incidence, the first between the late 1930s to the early 1950s with 26 events, the second occurred in 1970 (as a result of a catastrophic earthquake on May 31, 1970), and a third peak between 1997 and 2003 with four events (Emmer *et al.*, 2020). From these 28 events, 21 have known or estimated causes; the majority of these (15) are thought to have been caused by mass wasting events (i.e. ice avalanches, rock avalanches, moraine slope failures) as well as ice calving processes (Emmer, 2017; Emmer *et al.*, 2020). The most recent GLOF in Perú coccured on February 23rd, 2020 in Lake Salkataycocha, southern Perú where an avalanche landed on the lake triggering a displacement wave that overtopped and eroded the dam. The flood waves travelled 36 km downstream to the towns of Chaullay and Sahuaycaco killing five individuals and impacting hundreds of families (Vilca *et al.*, 2021)

To decrease the likelihood of a GLOF event, in particular the likelihood of a moraine dam breach, various remedial projects have been implemented (Grabs and Hanisch, 1993; Quincey and Carrivick, 2015). Between 1967 and 1999, remedial work was completed on 35 glacial lakes in the Cordillera Blanca. This work included the construction of open cuts through the moraine dam to reduce lake level (implemented in Lake Arhuaycocha, Lake Shallpa, Lake Cochca and Lake Milluacocha; Figure 1.3), and the creation of artificial dams and tunnels to increase dam freeboard and regulate water

levels (Quincey and Carrivick, 2015; Emmer, Vilímek and Zapata, 2018; INAIGEM, 2018). Artificial dams were often constructed in conjunction with open cuts at Lake Ishinca, Lake Milluacocha, Lake Palcacocha, and Lake Rajucolta (Figure 1.3; Emmer, Vilímek and Zapata, 2018; INAIGEM, 2018). Several of these lakes are also monitored continuously through live streaming of lake level data (e.g. Lake Palcacocha; INAIGEM, 2021).

1.4.1.2 Llaca Glacier and Llaca Lake, Cordillera Blanca

Llaca Lake an enlarging moraine-dammed, supraglacial lake formed at the margins of Llaca Glacier in the central west Cordillera Blanca (Figure 1.3B; Torres Amado et *al.*, 2016). In 1971, it had a surface area of approximately 63,312 m^2, a volume of about 794,000 m^3 and a maximum depth of 29 m (Santillán Portilla and Alegre Montalvo, 2003; Guardamino *et al.*, 2019). To decrease the risk of a GLOF event, remedial work was performed in 1977 that involved the construction of an open cut and artificial dam with the aim of decreasing lake level by 10 m. However, despite this remediation work, Llaca Lake continues to increase in size and volume. In 2004, it had a surface area of 43,988 m^2, a volume of 274,305 m^3 and a maximum depth of 17 m. By 2012, it had a surface area of 64,513 m^2, a volume of 495,477m^3 and a maximum depth of 19m (Torres Amado, Dávila Roller and Vilca Gómez, 2016; ANA, 2020).

Llaca Lake is located approximately 14 km northeast of the city of Huaraz (Figure 1.3B) and its enlarging volume is of concern to the local population. Using both a semi-quantitative and quantitative method to asses the potential for outburst, Emmer and Vilímek (2013) determined Llaca Lake has a medium to high potential for generation of a GLOF. Llaca Lake was also ranked 9th out of 20 lakes in terms of its susceptibility for a GLOF in

the scenario where the dam is overtopped following a slope failure or mass wasting event into the lake (Emmer and Vilímek; 2014).

One of the unique features of the Llaca Lake system is the presence of large areas of buried ice and ice-cored hummocks in the lake. Llaca Lake is one of the few supraglacial lakes in the Cordillera Blanca that is also susceptible to a GLOF event. This provides a unique opportunity to examine a growing moraine-dammed supraglacial lake.

1.4.2 Gígjökull, Southern Iceland

Gígjökull is a northern outlet glacier of the Eyjafjallajökull Ice Cap, located in south central Iceland (Figure 1.3C). Eyjafjallajökull is a central volcano rising from sea level to an elevation of approximately 1640 m.a.s.l. and has been built over the last 800,000 years through numerous eruptions characterized by varying types of volcano-ice interactions (Kristjánsson *et al.*, 1988). The volcano is currently capped by a small ice cap drained by a series of outlet glaciers (Figure 1.3C). Gígjökull is a 4 km-long outlet glacier with an average slope of 22° (Kirkbride and Dugmore, 2008) that descends from ~1550 m.a.s.l. on the northwestern flank of the volcanic crater, to 250 m.a.s.l. at its terminus. It is estimated to have an area of 7.8 km^2 and approximately 10-30% of its surface area is covered with debris, mostly on the front and lateral glacier margin (Scherler, Wulf and Gorelick, 2018). Prior to the eruption of Eyjafjallajökull in 2010, the glacial lake Gígjokulson was located in front of Gígjökull (Dunning *et al.*, 2013). Jökulhlaups (Icelandic term for GLOFs) triggered by the eruption, dramatically changed the geomorphology of the Gígjökull proglacial field, breached the latero-frontal moraine, and drained the lake (Magnússon *et al.*, 2012; Dunning *et al.*, 2013). Draining of Gígjokulson has allowed previously

inaccessible areas along the inner walls of the lateral moraines of Gígjökull's to be accessed for sedimentologic observations.

The glacial history of southern Iceland, and in particular of Eyjafjallajökull's outlet glaciers has been analyzed in various studies to understand current glacial dynamics (Thorarinsson, 1943; Dugmore, 1987; Kirkbride and Dugmore, 2008). Physical observations of the glacier margin have been recorded since the early 20th century and they indicate that the terminus of Gígjökull has been steadily retreating. Two large, steep-sided latero-frontal moraines identify the former extent of Gígjökull during the Little Ice Age. The preservation of such large latero-frontal moraines is not common in this part of Iceland; the only other south Icelandic glacier with prominent lateral moraines is Kvíárjökull which lies 150 km to the east (Spedding, 2000; Spedding and Evans, 2002; Sigurðardóttir, 2013).

1.5 STRUCTURE OF THIS THESIS

This thesis is presented as a series of chapters (Chapters 2 to 4) that form the basis of manuscripts to be submitted to scholarly journals for publication. Chapter 1 provides an introduction and Chapter 5 summarizes and concludes the thesis; these chapters are not intended for publication.

(i) Chapter 1: Introduction

This chapter introduces the problem that many high-altitude glaciated areas in the world face regarding the susceptibility and risk of glacial lake outburst floods (GLOFs) from moraine-dammed lakes, the role that moraines play in paleoglacial studies, and the limitations of the current understanding of moraine dammed glacial lakes.

(ii) Chapter 2: Chronology of Late Quaternary Tropical Glaciation in the Cordillera Blanca, Perú: A Framework for Future Investigations

Chapter 2 establishes a chronological framework of late Quaternary glacial activity in the Cordillera Blanca through the compilation, review, and analysis of published studies on the dating of frontal and lateral moraines in the region. The studies reviewed focus on the use of lichenometry, radiocarbon dating, and surface exposure dating to determine the time of emplacement of frontal and lateral moraines but fail to acknowledge the limitations and uncertainty associated with dating boulders that lay near or on the crestline of moraines (Rodbell, 1992; Solomina *et al.*, 2007; Jomelli *et al.*, 2008; Hall *et al.*, 2009; Stansell *et al.*, 2013). The genesis of these large latero-frontal moraines is complex and can take large periods of time (Humlum, 1978; Evans, Shulmeister and Hyatt, 2010; Evans *et al.*, 2013) which causes uncertainty as to the precise "age" of a dated moraine (Osborn *et al.*, 2015). Rather than focusing on a determining a very precise chronology of glacial movement for a particular region as past studies have done, this chapter aims to build a broad chronological framework for the Cordillera Blanca that can be used for future regional sedimentological and geomorphological studies. A series of six chronological stages are identified from mapping of 142 glacial moraines that span from >35 ka (Stage 1) to Stage 6 (0.85 ka – present).

(iii) Chapter 3: Landsystem Analysis of a tropical moraine-dammed supraglacial lake, Llaca Lake, Cordillera Blanca, Perú

Chapter 3 provides a detailed study of one glacial lake in the Cordillera Blanca, Perú: Llaca Lake, a tropical moraine-dammed supraglacial lake. Its proximity to the northern end of the city of Huaraz and rapid retreat of Llaca Glacier that feeds it has identified Llaca Lake to have medium-to-high risk for a GLOF (Emmer and Vilímek, 2013, 2014). Llaca Lake is one of the few glacial lakes in the Cordillera Blanca that is supraglacial in nature and it

contains extensive areas of ice-cored hummocks. These areas of exposed ice-cored sediment within the lake basin are often not included in large lake surveys that aim to document the volume of water impounded behind moraine dams (i.e., INAIGEM, 2018; Emmer *et al.*, 2020; Wood *et al.*, 2021); however, these areas are extremely important as they constitute significant volumes of water storage that could substantially increase flood volumes. A landystem approach was used here to investigate the sedimentological and geomorphological characteristics of Llaca Lake using UAV-derived photogrammetric data collected in the field. The geomorphological and sedimentological characteristics of Llaca Lake are synthesized into three landsystem zones: Zone 1: includes distal portions of Llaca Lake and the latero-frontal moraine; Zone 2: the central zone of ice-cored hummocks; and Zone 3: the active glacier margin. These zones are differentiated based on the spatial distribution of landforms, sediments, and active depositional processes. The findings presented in this chapter emphasize the importance of understanding processes operating in such supraglacial lakes including the generation of a longer-term sediment record that may be used for future paleoclimatic work. The analysis of the Llaca Lake landsystem presented in this chapter is considered a first step towards understanding the broad range of spatially and temporally variable processes operating in this type of environment.

(iv) Chapter 4: Sedimentary Architecture of a lateral moraine, Gígjökull, Iceland

Chapter 4 reports on the use of UAV-derived photographic analysis to identify and characterize the sedimentary architecture of a lateral moraine in Gígjökull, Iceland. As lateral (and latero-frontal) moraines are commonly used as chronological markers and play an important role in impounding glacial lakes susceptible to GLOFs, it is important to

understand the genesis and sedimentological architecture of these landforms. In this study seven lithofacies types were identified within the Gígjökull moraine that were grouped into three lithofacies associations: LFA 1 – 3. The geometry and spatial distribution of these lithofacies associations were mapped and allowed the identification of the sedimentary architecture of part of the moraine; this was then used to create a conceptual model describing the processes of moraine formation. This chapter of the thesis presents a novel methodology to analyze the sedimentary architecture of a moraine through the collection and analysis of UAV data. It also furthers understanding of the processes involved in moraine formation and the distribution of sediment heterogeneity that can significantly affect moraine stability and likelihood of failure.

(v) Chapter 5; Conclusion and future work

The concluding chapter of this thesis (Chapter 5) provides a summary of the major findings from each of the three investigations that comprise the bulk of the research reported here. It also presents suggestions for future work, specifically in the Cordillera Blanca, based on the approach and methodologies utilized here. The data and analysis presented in the body of this thesis provide a robust understanding and discussion of how a glacial sedimentological and morphological approach can contribute toward the better understanding of: 1) moraine formation and sedimentological architecture (Chapter 2 and Chapter 4); 2) the utility of moraines and moraine dammed lake sediments for determining the glacial history of a region (Chapter 2 and Chapter 3); and 3) the application of analytical approaches identifying landsystems (Chapter 3) and sedimentary architectures (Chapter 4) to better inform GLOF susceptibility studies.

REFERENCES

Aggarwal, S., Rai, S.C., Thakur, P.K., & Emmer, A., 2017. Inventory and recently increasing GLOF susceptibility of glacial lakes in Sikkim, Eastern Himalaya. Geomorphology 295, pp. 39–54.

Allen, S. K., Schneider, D. and Owens, I. F. 2009. First approaches towards modelling glacial hazards in the Mount Cook region of New Zealand's Southern Alps. Natural Hazards and Earth System Science, 9(2), pp. 481–499.

Ames Marquez, a. and Francou, B. 1995. Cordillera Blanca: glaciares en la historia', Bulletin de l'institut Francais d'etudes andines, 24, pp. 37–64. Available at: http://en.scientificcommons.org/51330895%5Cnhttp://en.scientificcommons.org/12740368.

ANA, 2020. Lagunas - Reservas de agua dulce en Áncash: Resultados de estudios de batimetría en 38 lagunas glaciares. Huaraz, Perú.

Andres, C. N., Eyles, C.H., Jara, H., & Narro-Pérez, R., 2018. Sedimentological Analysis of Paleolake Jircacocha, Cojup Valley, Cordillera Blanca, Peru. Revista de Glaciares y Ecosistemas de Montaña, 5, pp. 9–26.

Balco, G., Stone, J.O., Lifton, N.A., & Dunai, T.J., 2008. A complete and easily accessible means of calculating surface exposure ages or erosion rates from 10 Be and 26 Al measurements. Quaternary Geochronology, 3(3), pp. 174–195.

Baraer, M., McKenzie, J.M., Mark, B.G., Bury, J., & Knox, S., 2009. Characterizing contributions of glacier melt and groundwater during the dry season in a poorly gauged catchment of the Cordillera Blanca (Peru). Advances in Geosciences, 22,

pp. 41–49.

Baraer, M., Mark, B.G., McKenzie, J.M., Condom, T., Bury, J., Huh, K.-I., Portocarrero, C., Gómez, J., & Rathay, S., 2012. Glacier recession and water resources in Peru's Cordillera Blanca, Journal of Glaciology, 58 (207), pp. 134–150. doi: 10.3189/2012JoG11J186.

Barnett, T. P., Adam, J. C. and Lettenmaier, D. P., 2005. Potential impacts of a warming climate on water availability in snow-dominated regions', Nature, 438(7066), pp. 303–309. doi: 10.1038/nature04141.

Baťka, J., Vilímek, V., Stefanová, E., Cook, S.J., & Emmer, A., 2020. Glacial Lake Outburst Floods (GLOFs) in the Cordillera Huayhuash, Peru: Historic Events and Current Susceptibility. Water, 12(10), p. 2664. doi: 10.3390/w12102664.

Benedict, J. B., 1967. Recent Glacial History of an Alpine Area in the Colorado Front Range, U.S.A.: I. Establishing a Lichen-Growth Curve. *Journal of Glaciology*, 6, 48, pp. 817–832. doi: 10.3189/S0022143000020128.

Benn, D. I., Bolch, T., Hands, K., Gulley, J., Luckman, A., Nicholason, L.I., Quincey, D., Thompson, S., Toumi, R., & Wiseman, S., 2012. Response of debris-covered glaciers in the Mount Everest region to recent warming, and implications for outburst flood hazards. Earth-Science Reviews, 114(1–2), pp. 156–174. doi: 10.1016/j.earscirev.2012.03.008.

Benn, D. I. and Evans, D. J. A. (2010) *Glaciers & Glaciation*. 2nd edn. London: Hodder Education.

Benn, D. I. and Lukas, S., 2006. Younger Dryas glacial landsystems in North West

Scotland: an assessment of modern analogues and palaeoclimatic implications. Quaternary Science Reviews, 25 (17–18), pp. 2390–2408. doi: 10.1016/j.quascirev.2006.02.015.

Benn, Douglas I. and Benn, D. I., 1989. Debris transport by Loch Lomond Readvance glaciers in Northern Scotland: Basin form and the within-valley asymmetry of lateral moraines. Journal of Quaternary Science, 4(3), pp. 243–254. doi: 10.1002/jqs.3390040305.

Blair, R. W., 1994. Moraine and Valley Wall Collapse due to Rapid Deglaciation in Mount Cook National Park, New Zealand. Mountain Research and Development, 14(4), p. 347. doi: 10.2307/3673731.

Blown, I. and Church, M., 1985. Catastrophic lake drainage within the Homathko River basin, British Columbia. Canadian Geotechnical Journal, 22(4), pp. 551–563. doi: 10.1139/t85-075.

Boulton, G. S. and Eyles, N., 1979. Sedimentation by valley glaciers; a model and genetic classification, in Schlüchter, C. (ed.) *Proceedings of an INQUA Symposium on Genesis and Lithology of Quaternary Deposits. Zurich.* Rotterdam: A.A. Balkema, Rotterdam, pp. 11–24.

Briner, J. P., Miller, G.H., Thompson Davis, P., & Finkel, R.C., 2005. Cosmogenic exposure dating in arctic glacial landscapes: Implications for the glacial history of northeastern Baffin Island, Arctic Canada. Canadian Journal of Earth Sciences, 42(1), pp. 67–84. doi: 10.1139/E04-102.

Bromley, G.R.M., Schaefer, J.M., Winckler, G., Hall, B.L., Todd, C.E., & Rademaker, K.M., 2009. Relvative timing of last glacial maximum and late-glacial events in the central tropical Andes. Quaternary Science Reviews, 28, 2514-2526.

Bromley, G.R., Schaefer, J.M., Hall, B.L., Rademaker, K.M., Putnam, A.E., Todd, C.E., Hegland, M., Winckler, G., Jackson, M.S., & Strand, P.D., 2016. A cosmogenic 10Be chronology for the local last glacial maximum and termination in the Cordillera Oriental, southern Peruvian Andes: Implications for the tropical role in global climate. Quaternary Science Reviews, 148, 54-67.

Bueechi, E., Klimes, J., Frey, H., Huggel, C., Strozzi, T., & Cochachin, A., 2019. Regional-scale landslide susceptibility modelling in the Cordillera Blanca, Peru—a comparison of different approaches. Landslides, 16(2), pp. 395–407. doi: 10.1007/s10346-018-1090-1.

Burns, P. and Nolin, A., 2014. Using atmospherically-corrected Landsat imagery to measure glacier area change in the Cordillera Blanca, Peru from 1987 to 2010. Remote Sensing of Environment, 140, pp. 165–178. doi: 10.1016/j.rse.2013.08.026.

Bury, J., Mark, B.G., Carey, M., Young, K.R., McKenzie, J.M., Baraer, M., French, A., & Polk, M.H., 2013. New Geographies of Water and Climate Change in Peru: Coupled Natural and Social Transformations in the Santa River Watershed. Annals of the Association of American Geographers, 103(2), pp. 363–374. doi: 10.1080/00045608.2013.754665.

Carey, M., 2005. Living and dying with glaciers: people's historical vulnerability to avalanches and outburst floods in Peru. Global and Planetary Change, 47(2–4), pp.

122–134. doi: 10.1016/j.gloplacha.2004.10.007.

Carey, M., 2010. *In the Shadow of Melting Glaciers: Climate Change and Andean Society*. New York: Oxford University Press. doi: 10.1093/acprof:oso/9780195396065.001.0001.

Carey, M., Huggel, C., Bury, J., Portocarrero, C., & Haeberli, W., 2012. An integrated socio-enviornmental framework for glacier hazard management and climate change adaptation: lesssons from Lake 513, Cordillera Blanca, Peru. Climatic Change, 112, 733-767. doi: 10.1007/s10584-011-0249-8.

Carrivick, J. L. and Tweed, F. S., 2016. A global assessment of the societal impacts of glacier outburst floods. Global and Planetary Change, 144, pp. 1–16. doi: 10.1016/j.gloplacha.2016.07.001.

Chevallier, P., Pouyand, B., Suarez, W., & Condom, T., 2011. Climate change threats to environment in the tropical Andes: glaciers and water resources. Regional Environmental Change, 11(S1), pp. 179–187. doi: 10.1007/s10113-010-0177-6.

Clague, J. and Evans, S. G., 2000. A review of catastrophic drainage of moraine-dammed lakes in British Columbia. Quaternary Science Reviews, 19(17–18), pp. 1763–1783. doi: 10.1016/S0277-3791(00)00090-1.

Clague, J.J., Menounos, B., Osborn, G., Luckman, B.H., & Koch, J., 2009. Nomenclature and resolution in Holocene glacial chronogies. Quaternary Science Reviews, 28, 2231-2238. doi: 10.1016/j.quascirev.2008.11.016.

Clapperton, C.M., 1972. The Pleistocene Moraine Stages of West-Central Peru. Journal of Glaciology, 11, 62, 255-263. doi: 10.3189/S0022143000022243.

Cobbing, J., W. Pitcher, J. Baldock, W. Taylor, W. McCourt, & Snelling, N.J, 1981. Estudio geológico de la Cordillera Occidental del norte del Perú, Institute Geologico Minero y Metalurgico, Peru., 10(D), 1–252. Available at: https://hdl.handle.net/20.500.12544/330.

Condom, T., Escobar, M., Purkey, D., Pouget, J.C., Suarez, W., Ramos, C., Apaestegui, J., Zapata, M., Gomez, J., & Vergara, W., 2011. Modelling the hydrologic role of glaciers within a Water Evaluation and Planning System (WEAP): a case study in the Rio Santa watershed (Peru). Hydrology and Earth System Sciences Discussions, 8(1), pp. 869–916. doi: 10.5194/hessd-8-869-2011.

Cook, S. J., Kougkoulos, I., Edwards, L.A., Dortch, J., & Hoffmann, D., 2016. Glacier change and glacial lake outburst flood risk in the Bolivian Andes. Cryosphere, 10(5), pp. 2399–2413. doi: 10.5194/tc-10-2399-2016.

Costa, J. E. and Schuster, R. L., 1988. Formation and Failure of Natural Dams. Bulletin of the Geological Society of America, 100(7), pp. 1054–1068. doi: 10.1130/0016-7606(1988)100<1054:TFAFON>2.3.CO;2.

Decou, A., von Eynatten, H., Dunkl, I., Frei, D., Worner, G., 2013. Late Eocene to Early Miocene Andean uplift inferred from detrital zircon fission track and U-Pb dating of Cenozoic forearc sediments (15-18°S). Journal of South American Earth Sciences, 45, 6-23. doi: 10.1016/j.jsames.2013.02.003.

Dugmore, A. J., 1987. *Holocene glacier fluctuations around Eyjafjallajökull, south Iceland : a tephrochronological study*. University of Aberdeen.

Dunning, S. A., Large, A.R.G., Russell, A.J., Roberts, M.J., Duller, R., Woodward, J.,

Mériaux, A.-S., Tweed, F.S., & Lim, M., 2013. The role of multiple glacier outburst fl oods in proglacial landscape evolution: The 2010 Eyjafjallajökull eruption, Iceland. Geology, 41(10), pp. 1123–1126. doi: 10.1130/G34665.1.

Emmer, A., Klimes, Mergili, M., Vilímek, V., & Cochachin, A., 2016. 882 lakes of the Cordillera Blanca: An inventory, classification, evolution and assessment of susceptibility to outburst floods. CATENA, 147, pp. 269–279. doi: 10.1016/j.catena.2016.07.032.

Emmer, A., 2017, Geomorphologically effective floods from moraine-dammed lakes in the Cordillera Blanca, Peru. Quaternary Science Reviews, 177, pp. 220–234. doi: 10.1016/j.quascirev.2017.10.028.

Emmer, A., Harrison, S., Mergili, M., Allen, S., Frey, H., & Huggel, C., 2020. 70 years of lake evolution and glacial lake outburst floods in the Cordillera Blanca (Peru) and implications for the future. Geomorphology, 365, p. 107178. doi: 10.1016/j.geomorph.2020.107178.

Emmer, A. and Vilímek, V., 2013. Review Article: Lake and breach hazard assessment for moraine-dammed lakes: an example from the Cordillera Blanca (Peru). Natural Hazards and Earth System Sciences, 13(6), pp. 1551–1565. doi: 10.5194/nhess-13-1551-2013.

Emmer, A. and Vilímek, V., 2014. New method for assessing the susceptibility of glacial lakes to outburst floods in the Cordillera Blanca, Peru. Hydrology and Earth System Sciences, 18(9), pp. 3461–3479. doi: 10.5194/hess-18-3461-2014.

Emmer, A., Vilímek, V. and Zapata, M. L., 2018. Hazard mitigation of glacial lake outburst

floods in the Cordillera Blanca (Peru): the effectiveness of remedial works. Journal of Flood Risk Management, 11, pp. S489–S501. doi: 10.1111/jfr3.12241.

Evans, D. J. A., Rother, H., Hyatt, O.M., & Shulmeister, J., 2013. The glacial sedimentology and geomorphological evolution of an outwash head/moraine-dammed lake, South Island, New Zealand. Sedimentary Geology, 284–285, pp. 45–75. doi: 10.1016/j.sedgeo.2012.11.005.

Evans, D. J. A., Shulmeister, J. and Hyatt, O., 2010. Sedimentology of latero-frontal moraines and fans on the west coast of South Island, New Zealand. Quaternary Science Reviews, 29(27–28), pp. 3790–3811. doi: 10.1016/j.quascirev.2010.08.019.

Farber, D.L., Hancock, G.S., Finkel, R.C., & Rodbell, D.T., 2005. The age and extent of tropical alpine glaciation in the Cordillera Blanca, Peru. Journal of Quaternary Science, 20, 7-8, 759-776. doi: 10.1002/jqs.994.

Favier, V., Wagnon, P. and Ribstein, P., 2004. Glaciers of the outer and inner tropics: A different behaviour but a common response to climatic forcing. Geophysical Research Letters, 31(16), p. L16403. doi: 10.1029/2004GL020654.

Fujita, K., Sakai, A., Takenaka, S., Nuimura, T., Surazakov, A.B., Sawagaki, T., & Yamanokuchi, T., 2013. Potential flood volume of Himalayan glacial lakes. Natural Hazards and Earth System Sciences, 13(7), pp. 1827–1839. doi: 10.5194/nhess-13-1827-2013.

Garreaud, R.D., Vuille, M., Compagnucci, R., & Marengo, J., 2009. Present-day South American climate. Palaogeography, Palaeoclimtology, Palaeoecology, 281, 180-195. doi: 10.1016/j.palaeo.2007.10.032.

Georges, C., 2004. 20th-Century Glacier Flunctuations in the Tropical Cordillera Blanca, Perú. Arctic, Antarctic, and Alpine Research, 36, 1, 100-107. doi: 10.1657/1523-0430(2004)036[0100:TGFITT]2.0.CO;2.

Giovanni, M.K., Horton, B.K., Garzione, C.N., McNulty, B., & Grove, M., 2010. Extensional basin evolution in the Cordillera Blanca, Peru: Stratigraphic and isotopic records of detachment faulting and orogenic collapse in the Andean hinterland. Tectonics, 29, TC6007, 1-21. pp. 1–21. doi: 10.1029/2010TC002666.

Glasser, N.F., Clemmens, S., Schnabel, C., Fenton, C.R., & McHargue, L., 2009. Tropical glacier flunctuations in the Cordillera Blanca, Peru between 12.5 and 7.6 ka from cosmogenic 10Be dating. Quaternary Science Reviews, 28, 3448-3458. doi: 10.1016/j.quascirev.2009.10.006.

Gosse, J.C., & Phillips, F.M., 2001. Terrestrial in situ cosmogenic nuclides: theory and application. Quaternary Science Reviews, 20, 1475-1560. doi: 10.1016/S0277-3791(00)00171-2.

Grabs, W. E. and Hanisch, J., 1993. Objectives and prevention methods for glacier lake outburst floods (GLOFs). Snow and Glacier Hydrology (Proceedings of the Kathmandu Symposium, 1992), pp. 341–352.

Guardamino, L., Haeberli, W., Muñoz, R., Drenkhan, F., Tacis, A., & Cochachin, A., 2019. *Proyección de Lagunas Futuras en las Cordilleras Glaciares del Perú*. Lima, Perú.

Available at: http://repositorio.ana.gob.pe/handle/ANA/3597.

Haeberli, W., 1983. Frequency and characteristics of glacier floods in the Swiss Alps. Annals of Glaciology, 4(January 1983), pp. 85–90. doi: 10.1017/s0260305500005280.

Haeberli, W., Buetler, M., Huggel, C., Lehmann Friedli, T., Schaub, Y., & Schleiss, 2016. New lakes in deglaciating high-mountain regions – opportunities and risks. Climatic Change, 139(2), pp. 201–214. doi: 10.1007/s10584-016-1771-5.

Hall, S.R., Farber, D.L., Ramage, J.M., Rodbell, D.T., Finkel, R.C., Smith, J.A., Mark, B.G., & Kaseel, C., 2009. Geochronology of Quaternary glaciations from the tropical Cordillera Huayhuash, Peru. Quaternary Science Reviews, 28, 25-26, 2991-3009. doi: 10.1016/j.quascirev.2009.08.004.

Harrison, S., Glasser, N., Winchester, V., Haresign, E., Warren, C., & Jansson, K., 2006. A glacial lake outburst flood associated with recent mountain glacier retreat, Patagonian Andes. Holocene, 16(4), pp. 611–620. doi: 10.1191/0959683606hl957rr.

Harrison, S., Kargel, J., S., Huggel, C., Reynolds, J., Shugar, D.H., Betts, R.A., Emmer, A., Glasser, N., Haritashya, U.K., Klimes, Reinhardt, L., Shaub, Y., Wiltshire, A., Regmi, D., & Vilímek, 2018. Climate change and the global pattern of moraine-dammed glacial lake outburst floods. The Cryosphere, 12(4), pp. 1195–1209. doi: 10.5194/tc-12-1195-2018.

Hewitt, K., 1982. Natural dams and outburst floods of the Karakoram Himalaya. Hydrological Aspects of Alpine & High-Mountain Areas, Proc. Symp. Held During

First Sci. General Assembly Int. Assoc. Hyd, (138).

Hoffmann, D. and Weggenmann, D., 2013. Climate Change Induced Glacier Retreat and Risk Management: Glacial Lake Outburst Floods (GLOFs) in the Apolobamba Mountain Range, Bolivia BT . In Leal Filho, W. (ed.). *Climate Change and Disaster Risk Management.* Berlin, Heidelberg: Springer Berlin Heidelberg, pp. 71–87. doi: 10.1007/978-3-642-31110-9_5.

Hubbard, B., Heald, A., Reynold, J.M., Quincey, D., Richardson, S.D., Zapata Luyo, M., Santillan Portilla, N., & Hambrey, M.J., 2005. Impact of a rock avalanche on a moraine-dammed proglacial lake: Laguna Safuna Alta, Cordillera Blanca, Peru. Earth Surface Processes and Landforms, 30, 1251-1264. doi: 10.1002/esp.1198.

Huggel, C. *et al.* (2002) 'Remote sensing based assessment of hazards from glacier lake outbursts: A case study in the Swiss Alps', *Canadian Geotechnical Journal*, 39(2), pp. 316–330. doi: 10.1139/t01-099.

Huggel, C., Kääb, A., Haeberli, W., & Krummenacher, B., 2003. Regional-scale GIS-models for assessment of hazards from glacier lake outbursts: evaluation and application in the Swiss Alps. Natural Hazards and Earth System Sciences, 3(6), pp. 647–662. doi: 10.5194/nhess-3-647-2003.

Huggel, C., Haeberli, W., Kääb, A., Bieri, D., & Richardon, S., 2004. An assessment procedure for glacial hazards in the Swiss Alps. Canadian Geotechnical Journal, 41(6), pp. 1068–1083. doi: 10.1139/T04-053.

Huggel, C., Carey, M., Clague, J.J., Kääb, A., 2015. Introduction: human-environment dynamics in the high-mountain cryosphere. In Huggel, C. et al. (eds) *The High-*

Mountain Cryosphere - Environmental Changes and Human Risks. New York: Cambridge University Press, pp. 1–6.

Humlum, O., 1978. Genesis Of Layered Lateral Moraines. Geografisk Tidsskrift-Danish Journal of Geography, 77(1), pp. 65–72. doi: 10.1080/00167223.1978.10649094.

Instituto Nacional De Investigación en Glaciares y Ecosistemas de Montaña (INAIGEM), 2018. Inventario Nacional de Glaciares: Las Cordilleras Glaciares del Peru. Instituto Nacional de Investigación en Glaciares y Ecosistemas de Montaña Biblioteca y Publicaciones.

Iribarren Anacona, P., Norton, K. P. and Mackintosh, A., 2014. Moraine-dammed lake failures in Patagonia and assessment of outburst susceptibility in the Baker Basin. Natural Hazards and Earth System Sciences Discussions, 2(7), pp. 4765–4812. doi: 10.5194/nhessd-2-4765-2014.

Iturrizaga, L., 2014. Glacial and glacially conditioned lake types in the Cordillera Blanca, Peru: A spatiotemporal conceptual approach. Progress in Physical Geography, 38, 5, 602-636. doi: 10.1177/0309133314546344.

Ivy-Ochs, S., Kerschner, H., Reuther, A., Maisch, M, Sailer, R., Schaefer, J., Kubik, R.W., Synal, H.A., & Schlucter, C., 2006. The timing of glacier advances in the northern European Alps based on surface exposure dating with cosmogenic ^{10}Be, ^{26}Al, ^{36}Cl, and ^{21}Ne. In Situ-Produced Cosmogenic Nuclides and Quantification of Geological Processes. Geological Society of America, pp. 43–60. doi: 10.1130/2006.2415(04).

Jain, S. K., Lohani, A., K., Singh, R.D., Chaudhary, A., Thakural, L.N., 2012. Glacial lakes and glacial lake outburst flood in a Himalayan basin using remote sensing and GIS.

Natural Hazards, 62(3), pp. 887–899. doi: 10.1007/s11069-012-0120-x.

Jochimsen, M., 1973. Does the size of lichen thalli really constitute a valid measure for dating glacial deposits? Arctic and Alpine Research 5, 417–424. doi: doi.org/10.1080/00040851.1973.12003749.

Jomelli, V., Grancher, D., Brunstein, D., & Solomina, O., 2008. Recalibration of the yellow Rhizocarpon growth curve in the Cordillera Blanca (Peru) and implications for LIA chronology. Geomorphology, 93, 201-212. doi: 10.1016/j.geomorph.2007.02.021.

Jomelli, V., Favier, V., Rabate, A., Brunstein, D., Hoffman, G., & Francou, B., 2009. Fluctuations of glaciers in the tropical Andes over the last millennium and paleoclimatic implications: A review. Palaeography, Palaeoclimatology, Palaeoecology, 281, 269-282. doi: 10.1016/j.palaeo.2008.10.033.

Kaser, G., 1999. A review of the modern fluctuations of tropical glaciers. Global and Planetary Change, 22, 1-4, 93-103. doi: 10.1016/S0921-8181(99)00028-4.

Kershaw, J. A., Clague, J. J. and Evans, S. G., 2005. Geomorphic and sedimentological signature of a two-phase outburst ?ood from moraine-dammed Queen Bess Lake, British Columbia, Canada. Earth Surface Processes and Landforms, 30(1), pp. 1–25. doi: 10.1002/esp.1122.

Kirkbride, M. P. and Dugmore, A. J., 2008. Two millennia of glacier advances from southern Iceland dated by tephrochronology. Quaternary Research, 70(3), pp. 398–411. doi: 10.1016/j.yqres.2008.07.001.

Klimeš, J., Benešová, Vilímek, V., Bouška, P., & Cochachin Rapre, A., 2014. The reconstruction of a glacial lake outburst flood using HEC-RAS and its significance

for future hazard assessments: an example from Lake 513 in the Cordillera Blanca, Peru. Natural Hazards, 71(3), pp. 1617–1638. doi: 10.1007/s11069-013-0968-4.

Klimeš, J., Novotný, J., Novotná, I., Jordán de Urries, B., Vilímek, V., Emmer, A., Strozzi, T., Kusák, M., Cochachin Rapre, A., Hartvich, F., & Frey, H., 2016. Landslides in moraines as triggers of glacial lake outburst floods: example from Palcacocha Lake (Cordillera Blanca, Peru). Landslides, 13(6), pp. 1461–1477. doi: 10.1007/s10346-016-0724-4.

Korup, O. and Tweed, F., 2007. Ice, moraine, and landslide dams in mountainous terrain. Quaternary Science Reviews, 26(25–28), pp. 3406–3422. doi: 10.1016/j.quascirev.2007.10.012.

Loriaux, T. and Casassa, G., 2013. Evolution of glacial lakes from the Northern Patagonia Icefield and terrestrial water storage in a sea-level rise context. Global and Planetary Change, 102, pp. 33–40. doi: 10.1016/j.gloplacha.2012.12.012.

Lukas, S., Graf, A., Coray, S., & Schlüchter, C., 2012. Genesis, stability and preservation potential of large lateral moraines of Alpine valley glaciers - towards a unifying theory based on Findelengletscher, Switzerland. *Quaternary Science Reviews*. 38, pp. 27–48. doi: 10.1016/j.quascirev.2012.01.022.

Lukas, S., 2012. Processes of annual moraine formation at a temperate alpine valley glacier: Insights into glacier dynamics and climatic controls. Boreas, 41(3), pp. 463–480. doi: 10.1111/j.1502-3885.2011.00241.x.

Magnin, F., Haeberli, W., Linsbauer, A., Deline, P., & Ravanel, L., 2020. Estimating glacier-bed overdeepenings as possible sites of future lakes in the de-glaciating

Mont Blanc massif (Western European Alps). *Geomorphology*, 350, p. 106913. doi: 10.1016/j.geomorph.2019.106913.

Margirier, A., Audin, L., Robert, X., Herman, F., Ganne, J., & Schwartz, S., 2016. Time and mode of exhumation of the Cordillera Blanca batholith (Peruvian Andes). Journal of Geographical Research: Solid Earth, 121, 6235-6249. doi: 10.1002/2016JB013055.

Mark, B.G., Bury, J., McKenzie, J.M., French, A., & Baraer, M., 2010. Climate Change and Tropical Andean Glacier Recession: Evaluating Hydrologic Changes and Livelihood Vulnerability in the Cordillera Blanca. Annals of the Association of American Geographers, 100, 4, 794-805. doi: 10.1080/00045608.2010.497369.

Mark, B. G., French, A., Baraer, M., Carey, M., Bury, J., Young, K.R., Polk, M.H., Wigmore, O., Lagos, P., Crumley, R., McKenzie, J.M., & Lautz, L., 2017. Glacier loss and hydro-social risks in the Peruvian Andes. Global and Planetary Change, 159(483), pp. 61–76. doi: 10.1016/j.gloplacha.2017.10.003.

Mark, B. G. and Seltzer, G. O., 2003. Tropical glacier meltwater contribution to stream discharge: a case study in the Cordillera Blanca, Peru. Journal of Glaciology, 49(165), pp. 271–281. doi: 10.3189/172756503781830746.

Mark, B. G. and Seltzer, G. O., 2005. Evaluation of recent glacier recession in the Cordillera Blanca, Peru (AD 1962–1999): spatial distribution of mass loss and climatic forcing. Quaternary Science Reviews, 24(20–21), pp. 2265–2280. doi: 10.1016/j.quascirev.2005.01.003.

Matthews, J. A., 2014. Little Ice Age. *Encyclopedia of Environmental Change*, 1, pp. 504–

509. doi: 10.4135/9781446247501.n2294.

Matthews, J. A. and Briffa, K. R., 2005. The “Little Ice Age”: Re-evaluation of an evolving concept. Geografiska Annaler, Series A: Physical Geography, 87(1), pp. 17–36. doi: 10.1111/j.0435-3676.2005.00242.x.

Matthews, J. A. and Petch, J. R., 1982. Within-valley asymmetry and related problems of Neoglacial lateral moraine development at certain Jotunheimen glaciers, southern Norway. Boreas, 11(3), pp. 225–247. doi: 10.1111/j.1502-3885.1982.tb00716.x.

McKillop, R. J. and Clague, J. J., 2007. A procedure for making objective preliminary assessments of outburst flood hazard from moraine-dammed lakes in southwestern British Columbia. Natural Hazards, 41(1), pp. 131–157. doi: 10.1007/s11069-006-9028-7.

McNulty, B. and Farber, D., 2002. Active detachment faulting above the Peruvian flat slab. Geology, 30(6), p. 567. doi: 10.1130/0091-7613(2002)030<0567:ADFATP>2.0.CO;2.

Mégard, F., 1984. The Andean orogenic period and its major structures in central and northern Peru. Geological Society of America Bulletin, 95, 9, 1108-1117. doi: 10.1144/gsjgs.141.5.0893.

Mergili, M., Pudasaini, S., P., Emmer, A., Fisher, J.T., Cochachin, A., Frey, H., 2020. Reconstruction of the 1941 GLOF process chain at Lake Palcacocha (Cordillera Blanca, Peru). Hydrology and Earth System Sciences, 24(1), pp. 93–114. doi: 10.5194/hess-24-93-2020.

Morales, B., Zamora, M. and Ames, A. M., 1979. Inventario de Lagunas y Glaciares del

Perú. *Boletin de la Sociedad geologica del Peru*, 62, pp. 69–92.

Osborn, G., McCarthy, D., LaBrie, A., & Burke, R., 2015. Lichenometric dating: Science or pseudo-science? Quaternary Research, 83, 1-12. doi: 10.1016/j.yqres.2014.09.006.

Osti, R., Bhattarai, T. N. and Miyake, K., 2011. Causes of catastrophic failure of Tam Pokhari moraine dam in the Mt. Everest region. Natural Hazards, 58(3), pp. 1209–1223. doi: 10.1007/s11069-011-9723-x.

Owen, L. A., Robinson, R., Benn, D.I., Finkel, R.C., Davis, N.K., Yi, C., Putkonen, J., Li, D., & Murray, A.S., 2009. Quaternary glaciation of Mount Everest. Quaternary Science Reviews., 28(15–16), pp. 1412–1433. doi: 10.1016/j.quascirev.2009.02.010.

Owen, L. A. and Derbyshire, E., 1989. The Karakoram glacial depositional system. *Zeitschrift für Geomorphologie*, Supplement(76), pp. 33–77.

Quincey, D. and Carrivick, J., 2015. Glacier Floods. In Huggel, C. et al. (eds) *The High-Mountain Cryosphere - Environmental Changes and Human Risks*. New York: Cambridge University Press, pp. 204–226.

Rabatel., A., Francou, B., Soruco, A., Gomez, J., Cáceres, B., Ceballos, J.L., Basantes, R., Vuille, M., Sicart, J.-E., Huggel, C., Scheel, M., Lejeune, Y., Arnoud, Y., Collet, M., Condom, T., Consoli, G., Favier, V., Jomelli, V., Galarrage, R., Ginot, P., Maisincho, L., Mendoza, J., Ménégoz, M., Ramirez, E., Ribstein, P., Suarez, W., Villacis, M., & Wagnon, P., 2013. Current state of glaciers in the tropical Andes: a

multi-century perspective on glacier evolution and climate change. The Cryosphere, 7, 81-102. doi: 10.5194/tc-7-81-2013.

Richardson, S.D., and Reynolds, J. M., 2000. An overview of glacial hazards in the Himalayas. Quaternary International, 65-66, pp. 31–47.

Richardson, Shaun D. and Reynolds, J. M., 2000. Degradation of ice-cored moraine dams implications for hazard development. In Nakawo, M., Ramond, C. F., and Fountain, A. (eds) *Debris-covered Glaciers, Proceedings of a Workshop Held at Seattle, Washington, USA, September 2000.* Seattle: International Association of Hydrological Sciences Publication, 264, pp. 165–175.

Rivas, D. S., Somos-Valenzuela, M.A., Hodges, B.R., & McKinney, D.C., 2015. Predicting outflow induced by moraine failure in glacial lakes: The Lake Palcacocha case from an uncertainty perspective. *Natural Hazards and Earth System Sciences*, 15(6), pp. 1163–1179. doi: 10.5194/nhess-15-1163-2015.

Rodbell, D.T., 1992. Lichenometric and Radiocarbon dating of Holocene glaciation, Cordillera Blanca, Perú. The Holocene, 2, 1, 19-29. doi: 10.1177/095968369200200103.

Rodbell, D.T., & Seltzer, G.O., 2000. Rapid Ice Margin Flunctuations during the Younger Dryas in the Tropical Andes. Quaternary Research, 54, 328-338. doi: 10.1006/qres.2000.2177.

Rodbell, D. T., Smith, J. A. and Mark, B. G, 2009. Glaciation in the Andes during the Lateglacial and Holocene. *Quaternary Science Reviews*, 28(21–22), pp. 2165–2212. doi: 10.1016/j.quascirev.2009.03.012.

Röthlisberger, F. and Schneebeli, W., 1979. Genesis of lateral moraine complexes, demonstrated by fossil soils and trunks: indicators of prglacial climatic flunctuations. In Schlüchter, C. (ed.) *INQUA Symposium on Genesis and Lithology of Quaternary Deposits. Zürich, 10-20 September 1978. Moraines and varves: origin, genesis and classification.* Rotterdam, pp. 387–419.

Santillán Portilla, N. and Alegre Montalvo, C., 2003. *Monitoreo de Lagunas - Laguna Llaca*. Unidad de Glaciología y Recursos Hídricos UGRH - Huaraz, Perú.

Schauwecker, S., Roher, M., Acuña, D., Cochachin, A., Dávila, L., Frey, H., Giráldez, C., Gómez, J., Huggel, C., Jacques-Coper, M., Loarte, E., Salzmann, N., & Vuille, M., 2014. Climate trends and glacier retreat in the Cordillera Blanca, Peru, revisited. Global and Planetary Change, 119, 85-97. doi: 10.1016/j.gloplacha.2014.05.005.

Schneider, D., Huggel, C., Cochachin, A., Guillén, S., & García, J., 2014. Mapping hazards from glacier lake outburst floods based on modelling of process cascades at Lake 513, Carhuaz, Peru. Advances in Geosciences, 35, 145-155. doi: 10.5194/adgeo-35-145-2014.

Shugar, D. H., Burr, A., Haritashya, U.K., Kargel, J.S., Watson, C.S., Kennedy, M.C., Bevington, A.R., Betts, R.A., Harrison, S., & Strattaman, K., 2020. Rapid worldwide growth of glacial lakes since 1990. Nature Climate Change, 10(10), pp. 939–945. doi: 10.1038/s41558-020-0855-4.

Sigurðardóttir, M., 2013. *The sedimentology and formation of the Gígjökull and Kvíárjökull latero-frontal moraines, Iceland*. University of Iceland.

Silverio, W. and Jaquet, J. M., 2017. Evaluating glacier fluctuations in Cordillera Blanca

(Peru) by remote sensing between 1987 & 2016 in the context of ENSO. *Archives des Sciences*, 69(2), pp. 145–161. Available at: https://archive-ouverte.unige.ch/unige:98197.

Small, R. J., 1983. Lateral Moraines of Glacier De Tsidjiore Nouve: Form, Development, and Implications. *Journal of Glaciology*, 29(102), pp. 250–259. doi: 10.3189/S0022143000008303.

Smith, J. A., Seltzer, G.O., Farber, D.L., Rodbell, D.T., Finkel, R.C., 2005. Early Local Last Glacial Maximum in the Tropical Andes. Science, 308(5722), pp. 678–681. doi: 10.1126/science.1107075.

Smith, J. A., Mark, B. G. and Rodbell, D. T., 2008. The timing and magnitude of mountain glaciation in the tropical Andes. Journal of Quaternary Science, 23(6–7), pp. 609–634. doi: 10.1002/jqs.1224.

Smith, J. A. and Rodbell, D. T., 2010. Cross-cutting moraines reveal evidence for north atlantic influence on glaciers in the tropical Andes. Journal of Quaternary Science, 25(3), pp. 243–248. doi: 10.1002/jqs.1393.

Solomina, O., Jomelli, V., Kaser, G., Ames, A., Berger, B., Pouyaud, B., 2007. Lichenometry in the Cordillera Blanca, Peru: "Little Ice Age" moraine chronology. Global and Planetary Change, 59, 225-235. doi: 10.1016/j.gloplacha.2006.11.016.

Somos-Valenzuela, M. A., Chisolm, R.E., Rivas, D.S., Portocarrero, C., & McKinney, D.C., 2016. Modeling a glacial lake outburst flood process chain: the case of Lake Palcacocha and Huaraz, Peru. *Hydrology and Earth System Sciences*, 20(6), pp. 2519–2543. doi: 10.5194/hess-20-2519-2016.

Spedding, N., 2000. Hydrological controls on sediment transport pathways : implications for debris-covered glaciers. Debris Covered Glaciers (Proceedings of a workshop held at Seattle, Washington, USA, September 2000), IAHS Publication no. 264.

Spedding, N. and Evans, D. J., 2002. Sediments and landforms at Kvíárjökull, southeast Iceland: a reappraisal of the glaciated valley landsystem. Sedimentary Geology, 149(1–3), pp. 21–42. doi: 10.1016/S0037-0738(01)00242-1.

Stansell, N. D., Rodbell, D.T., Abbott, M.B., & Mark, B.G., 2013. Proglacial lake sediment records of Holocene climate change in the western Cordillera of Peru. Quaternary Science Reviews, 70, pp. 1–14. doi: 10.1016/j.quascirev.2013.03.003.

Thorarinsson, S., 1943. Oscillations of the Iceland glaciers during the last 250 years. Geografiska Annaler, 25(2), p. 1. doi: 10.2307/519895.

Torres Amado, L. N., Dávila Roller, L. R. and Vilca Gómez, O., 2016. *Informe Técnico N°03 - Monitoreo Glaciológico en el Glaciar Llaca*. Huaraz, Perú.

Veetil, B.K., Wang, S., Souza, S.F., Bremer, U.S., & Simões, J.C., 2017. Glacier monitoring and glacier-climate interactions in the tropical Andes: A review. Journal of South American Earth Sciences, 77, 281-246. doi: 10.1016/j.jsames.2017.04.009.

Veettil, B. K., Wang, S., Bremer, U. F., de Souza, S.F., & Simões, J.C., 2017. Recent trends in annual snowline variations in the northern wet outer tropics: case studies from southern Cordillera Blanca, Peru. Theoretical and Applied Climatology, 129(1–2), pp. 213–227. doi: 10.1007/s00704-016-1775-0.

Viani, C., Machguth, H., Huggel, C., Godio, A., Franco, D., Perotti, L., & Giardino, M.,

2020. Potential future lakes from continued glacier shrinkage in the Aosta Valley Region (Western Alps, Italy). *Geomorphology*, 355, p. 107068. doi: 10.1016/j.geomorph.2020.107068.

Vilca, O., Mergili, M., Emmer, A., Frey, H., Huggel, C., 2021. The 2020 glacial lake outburst flood process chain at Lake Salkantaycocha (Cordillera Vilcabamba, Peru). *Landslides*. Landslides, 18(6), pp. 2211–2223. doi: 10.1007/s10346-021-01670-0.

Vilímek, V., Zapata, M.L., Klimes, J., Patzel, Z., & Santillán, N., 2005. Influence of glacial retreat on natural hazards of the Palcacocha Lake area, Peru. *Landslides*, 2(2), pp. 107–115. doi: 10.1007/s10346-005-0052-6.

Vilímek, V., Klimeš, J. and Červená, L., 2016. Glacier-related landforms and glacial lakes in Huascarán National Park, Peru. Journal of Maps, 12(1), pp. 193–202. doi: 10.1080/17445647.2014.1000985.

Viviroli, D., Archer, D.R., Buytaer, W., Fowler, H.J., Greenwood, G.B., Hamlet, A.F., Huang, Y., Koboltsching, G., Litaror, M.I., López-Moreno, J.I., Lorentz, S., Schadler, B., Schreier, H., Schwaiger, K., Vuille, M, & Woods, R., 2011. Climate change and mountain water resources: overview and recommendations for research, management and policy. Hydrology and Earth System Sciences, 15(2), pp. 471–504. doi: 10.5194/hess-15-471-2011.

Vuille, M., Bradley, R.S., Werner, M., & Keimig, F., 2003. 20th century climate change in the tropical Andes: Observations and model results. Climatic Change, 59(1–2), pp. 75–99. doi: 10.1023/A:1024406427519.

Vuille, M., Carey, M., Huggel, C., Buytaert, W., Rabatel, A., Jacobsen, D., Soruco, A., Villacis, M., Yarleque, C., Elison Timm, O., Condom, T., Salzmann, N., & Sicart, J.-E., 2018. Rapid decline of snow and ice in the tropical Andes – Impacts, uncertainties and challenges ahead. Earth-Science Reviews, 176, 195-213. doi: 10.1016/j.earscirev.2017.09.019.

Watanabe, T., Lamsal, D. and Ives, J. D., 2009. Evaluating the growth characteristics of a glacial lake and its degree of danger of outburst flooding: Imja Glacier, Khumbu Himal, Nepal. Norsk Geografisk Tidsskrift - Norwegian Journal of Geography, 63(4), pp. 255–267. doi: 10.1080/00291950903368367.

Wegner, S. A., 2014. Nota Técnica 7 - Lo que el Agua se Llevó: Consecuencias y Lecciones del Aluvión de Huaraz de 1941. *Notas Técnicas sobre Cambio Climáatico - MInisterio del Ambiente, Perú*. Lima, p. 85.

Werder, M. A., Bauder, A., Funk, M., Keusen, H.-R., 2010. Hazard assessment investigations in connection with the formation of a lake on the tongue of Unterer Grindelwaldgletscher, Bernese Alps, Switzerland. Natural Hazards and Earth System Sciences, 10(2), pp. 227–237. doi: 10.5194/nhess-10-227-2010.

Westoby, M. J., Glasser, N.F., Brasington, J., Hambrey, M.J., Quincey, D.J., Reynolds, J.M., 2014. .Modelling outburst floods from moraine-dammed glacial lakes. *Earth-Science Reviews*, 134, pp. 137–159. doi: 10.1016/j.earscirev.2014.03.009.

Wilson, R., Glasser, N.F., Reynolds, J.M., Harrison, S., Iribarren Anacona, P., Schaefer, M., Shannon, S., 2018. Glacial lakes of the Central and Patagonian Andes. Global and Planetary Change, 162, pp. 275–291. doi: 10.1016/j.gloplacha.2018.01.004.

Wood, J. L., Harrison, S., Wilson, R., Emmer, A., Yarlenque, C., Glasser, N.F., Torres, J.C., Caballero, A., Araujo, J., Bennett, G.L., Diaz-Moreno, A., Garay, D., Jara, H., Poma, C., Reynolds, J.M., Riveros, C.A., Romero, E., Shannon, S., Tinoco, T., Turpo, E., & Villafane, H., 2021. Contemporary glacial lakes in the Peruvian Andes. Global and Planetary Change, 204, p. 103574. doi: 10.1016/j.gloplacha.2021.103574.

CHAPTER 2: CHRONOLOGY OF LATE QUATERNARY TROPICAL GLACIATION IN THE CORDILLERA BLANCA, PERÚ: A FRAMEWORK FOR FUTURE INVESTIGATIONS

ABSTRACT

The Cordillera Blanca, Perú, forms part of the Andean Mountain range and hosts the largest concentration of tropical glaciers in the world. Rapid retreat of these glaciers is threatening local communities as enlarging, but unstable moraine-dammed glacial lakes increase the risk of glacial outburst floods and long-term water supplies are diminished. In order to better understand the characteristics of these moraine-dammed glacial lakes and the potential risks posed by continued glacier retreat in the Cordillera Blanca, this paper aims to establish a chronological framework of past glacial activity and moraine formation in the region. Review of published data on the dating of glacial landforms, such as frontal and lateral moraines that record the position of glacier termini under maximum advance or still-stand conditions, allows the identification and mapping of six stages of Late Quaternary glacial activity in the region. 142 glacial moraines are identified and mapped in the Cordillera Blanca and fall within the following chronological stages: Stage 1 (>35 ka); Stage 2 (35-19 ka – including glacial events broadly synchronous with the Global Last Glacial Maximum); Stage 3 (19-11.7ka - including glacial events broadly synchronous with global climatic events such as the Late Glacial, the Antarctic Cold Reversal, and Younger Dryas); Stage 4 (11.7 – 1 ka - including early, mid and late Holocene glacial events); Stage 5 (1 – 0.85 ka – including glacial events of the last 1ka as well as the Little Ice Age [LIA]); Stage 6 (0.85 ka – present - including current glacial retreat since the LIA). These chronological stages provide a qualitative framework of late Quaternary glacial activity that reflects glacier response to regional climatic conditions. A major limitation of this work lies in the reliability of obtaining accurate dates for the development of glacial moraines in

high relief Andean environments prone to frequent mass movements. Despite these limitations, the chronological framework of regional glacial activity presented here, serves as a framework for future studies that aim to better understand glaciation of the Cordillera Blanca, and in turn other Andean glaciated regions.

2.1 INTRODUCTION

The Cordillera Blanca mountain range in northwestern Perú, part of the larger Andes range (Figure 2.1), contains the largest tropical glacier field in the world. Recent climate warming has greatly impacted these glaciers (Barnett et al., 2005), decreasing the total glaciated area in the Cordillera Blanca from 800-850 km2 in 1930 to 448.81 km2 in 2016 (Georges, 2004; INAIGEM, 2018). Glacial meltwater from the Cordillera Blanca drains into the Santa River which sustains agricultural, industrial and hydroelectric operations as well as numerous communities within the Santa River Basin (Bury et al., 2011; Drekhan et al., 2015; INAIGEM, 2018; Figure 2.2).

Glacial retreat in the Cordillera Blanca poses several threats to the cultural and economic well-being of the region. Reduced amounts of meltwater, particularly during the dry season, threaten communities dependent upon this water source (Mark et al., 2010; Vuille et al., 2018). In addition, recent glacial retreat has allowed the development of numerous glacial lakes, impounded by unstable moraine dams, which have the potential to fail and release large volumes of meltwater as catastrophic floods (Carey, 2005; Carey et al., 2012; Schneider, et al., 2014; Emmer et al., 2016). It is therefore important to understand the history of glaciation in the region, and the chronology of landform development, to evaluate the impact of current climate warming on glacial lake expansion, moraine stability, and future water supply. This paper aims to augment current understanding of past glacial advances and retreats in the Cordillera Blanca, past processes that have occurred in valleys draining the mountains, and the effect of changing glacial regimes on geologic processes, natural hazards, and water resources.

Figure 2.1: Map of South America with Perú in black outline. The Andes mountain range is shown in dark grey (elevations of 1000-4000 masl). and light grey (elevations over 4000 masl.). Dashed red boxes indicate approximate ranges of Andean glacier types: A) Inner Tropical Glaciers; B) Outer Tropical Glaciers; C) Temperate Glaciers. Yellow Box indicates location of Cordillera Blanca within Peru (Figure 2.2).

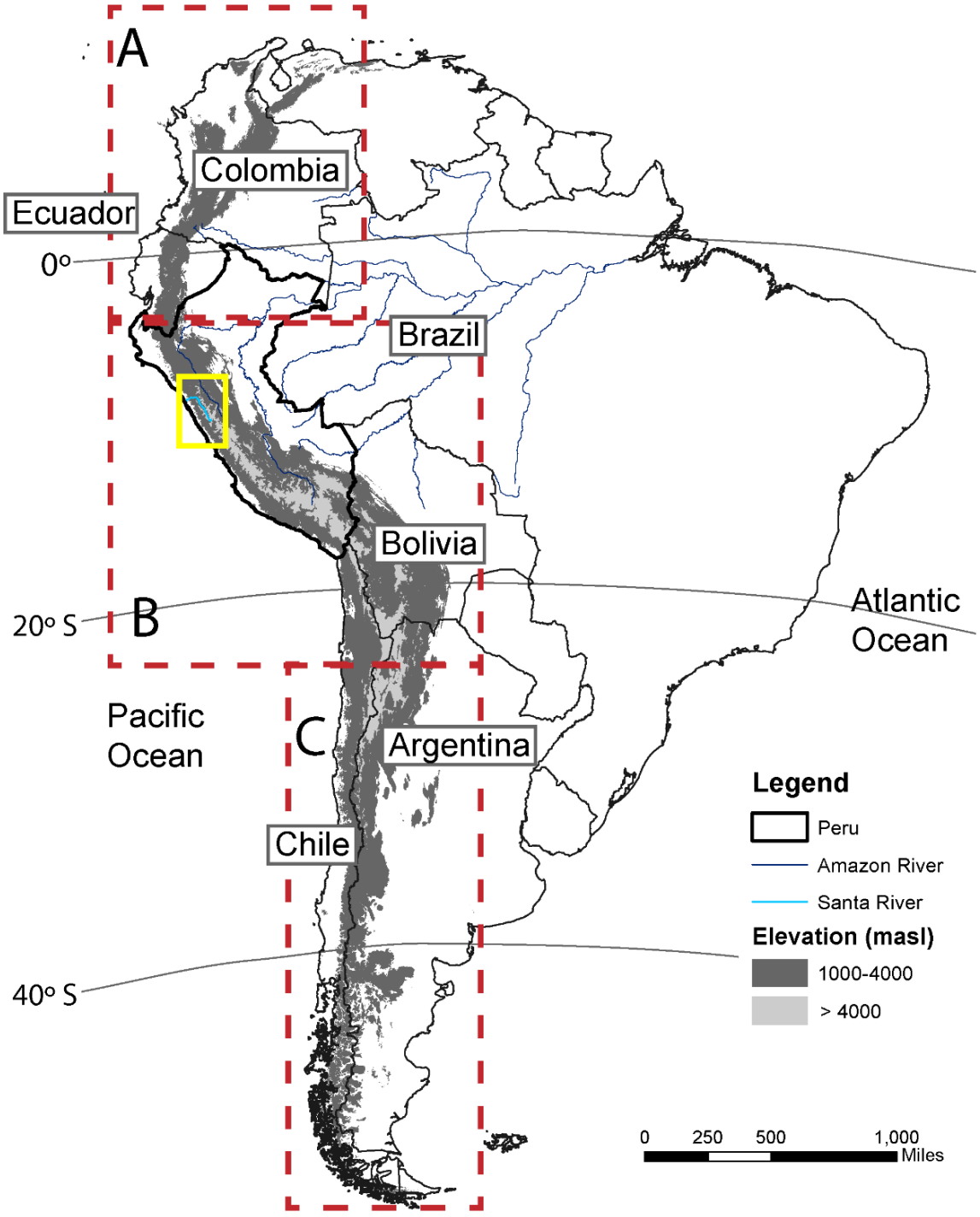
A
Colombia
Ecuador
0°
Brazil
Bolivia
20° S
B
Atlantic
Ocean
Pacific
Ocean
C
Argentina
Chile
40° S
Legend
Peru
Amazon River
Santa River
Elevation (masl)
1000-4000
> 4000
0
250
500
1,000
Miles

Figure 2.2: Location of the political and physical locations discussed in text. The Santa River Basin lies predominantly in the Region of Ancash and drains north and westward into the Pacific Ocean. Huaraz is the capital of the Region of Ancash.

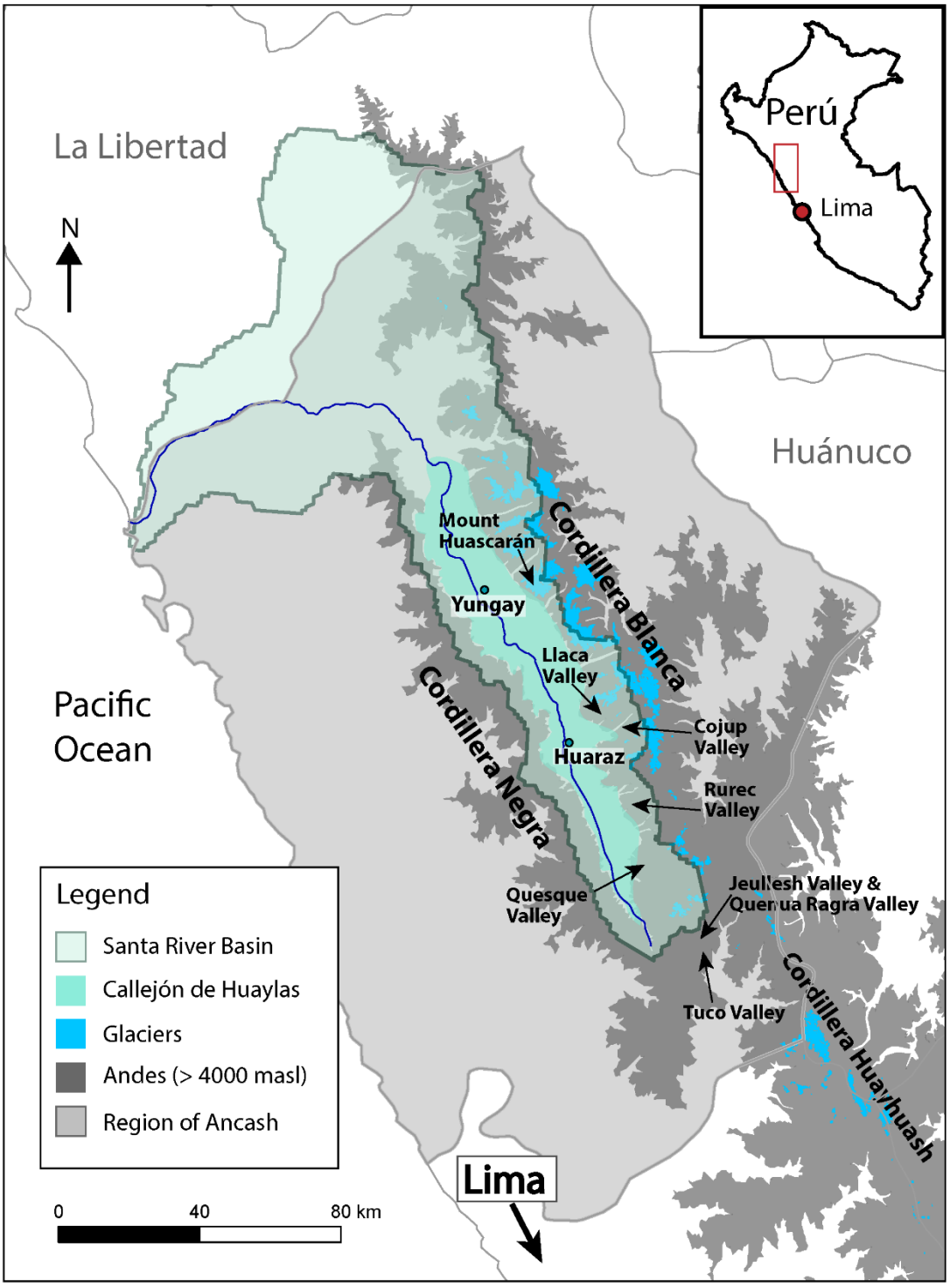
La Libertad
N
Perú
Lima
Huánuco
Mount Huascarán
Yungay
Cordillera Blanca
Llaca Valley
Cojup Valley
Huaraz
Rurec Valley
Cordillera Negra
Pacific Ocean
Quesque Valley
Jeullesh Valley & Quenua Ragra Valley
Tuco Valley
Cordillera Huayhuash
Lima
Legend
Santa River Basin
Callejón de Huaylas
Glaciers
Andes (> 4000 masl)
Region of Ancash
0
40
80 km

A considerable amount of previous research has attempted to establish the chronology of glacial events in the Cordillera Blanca and broader Perú. Many of these past studies rely on chronometric analysis (including radiometric, lichenometry and surface exposure dating) of surface landforms associated with glacial advances, stillstands or readvances (Rodbell, 1993; Solomina et al., 2007; Glasser et al, 2009; Smith and Rodbell, 2010). While many of these studies aim to create precise chronologies of site-specific glaciation in the tropical Andes, the objective of this study is to synthesize a relative chronology of glaciation that can be used as a framework to investigate surface processes and landsystems throughout the Cordillera Blanca. In order to understand the factors that have controlled the development of glaciation in the tropical Andes it is necessary to first consider the geological setting of both the Andes and the Cordillera Blanca.

2.1.1 Geology of the Andes

The Cordillera Blanca falls within the larger Andes mountain ranges. The Andes mountain ranges extend approximately 7,000 km along the western edge of South America from northern Venezuela and Colombia to southern Chile and Argentina (Figure 2.1) and consist of a complex assemblage of parallel, near-parallel and sometimes diverging ranges of different ages, lithology and history. The Andes can be divided into three distinct tectonic segments, the Northern Andes (12°N-5°S), Central Andes (5°S -33°S) and Southern Andes (33°S-56°S), differentiated by surface and structural features, volcanic activity, geophysical evidence and tectonic boundaries (James, 1971; Sillitoe, 1975; Hall and Wood, 1985; Stern, 2004).

The Andean orogeny, generated by subduction of the oceanic Nazca Plate beneath the continental South American plate, has caused intermittent uplift of the Andean mountain ranges for more than 100 Ma (Mégard, 1984; Decou et al., 2013; Mangirier et al., 2016). Regional orogenic processes, resulting in uplift of the Cordillera Blanca and the rest of northern Perú, began in the Early Cretaceous (Dalmayrac & Molnar, 1981; Schwartz, 1988; Petford & Atherton, 1996; Giovanni et al., 2010). Currently, the Nazca Ridge, a divergent ocean ridge lying on the Nazca plate, is being subducted along the Perú-Chile Trench beneath the South American plate (Wipf, et al., 2005; Figure 2.3). The thickened basaltic ocean crust of the Nazca Ridge is buoyant and causes low angle, flat-slab subduction along the Andean margin. Seismic data identify three flat slab segments along the Andean Margin, one of them being the Peruvian flat-slab segment, characterized by a subduction angle of less than 30 degrees, which lies between the Gulf of Guayaquil at 5°S and Arequipa at 14°S (Figure 2.3; Ramos, 1999; Ramos and Folguera, 2009). This region is also associated with the inland migration and eventual cessation of arc magmatism (which ended in the northern part of the region around 12 Ma), coincident with the complete subduction of the Inca Plateau (a former oceanic plateau) and the intersection of the Nazca Ridge with the Perú-Chile trench (Gutscher et al., 1999; Ramos, 2009; Ramos and Folguera, 2009).

The central Andes of Perú and Bolivia, which developed close to sea level during the mid-Cenozoic, underwent a prolonged spell of tectonic quiescence before a pulse of late Miocene tectonism elevated it to its present average altitude of 4,200-4,400 m.a.s.l (Wilson, 1983). Uplift rates in the Andean range have varied over time (Decou et al., 2013),

Figure 2.3: Nazca-South American Plate convergence system. The Nazca Plate is being subducted beneath the South American Plate along the Peru-Chile Trench, resulting in uplift of the Cordillera Blanca and Andes. This uplift was a likely a trigger for glaciation as a result of the creation of high-altitude land masses starting in the late Miocene.


South American Plate
N
C. Oriental
C. Central
C. Occidental
Cordillera Huayhuash
Junin Plain
Lima
Peru-Chile Trench
Nazca Plate
6-8 cm/yr
Cordillera Vilcanota
Quelccaya Ice Cap
Nevado Coropuna
Altiplano
Nazca Ridge
Pacific Ocean
0
400
km

and many parts of the Andes have experienced periods of both uplift and subsidence during the late Cenozoic. However, the majority of mountain uplift appears to have been achieved during the late Miocene. Uplift rates in the Central Andes are estimated to be approximately 0.25 mm/year between 25 Ma and 10 Ma, and 0.2-0.3 mm/year from 10 Ma to present (Gregory-Wodzicki, 2000; Fox et al., 2015; Margirier et al., 2018). The dramatic increase in elevation experienced along the Andes ranges during the Miocene is thought to have been sufficient to trigger localized glaciation. A number of glacial deposits, dated to between 6 and 5 Ma, have been identified in Patagonia, and indicate the existence of localized glaciation in South America prior to the development of large ice sheets over temperate lands in the Northern Hemisphere, around 3.5 Ma (Meyers & Hinnov, 2010; Bartoli et al., 2011).

2.1.2 Geology of the Cordillera Blanca

In northern Perú, the central Andes form three distinct coast-parallel mountain ranges, the Cordillera Occidental, the Cordillera Central, and the Cordillera Oriental (Figure 2.3). In the region of Ancash, the Cordillera Occidental can be further subdivided into physiographic regions that comprise the Cordillera Negra to the west, the central Callejón de Huaylas valley, and the glaciated Cordillera Blanca to the east (Figure 2.2; Wilson, 1963). The main body of the Cordillera Blanca is composed of Neogene granodiorite, intruded into shales and sandstones of the Upper Jurassic Chicama Formation, and forms a steep-sided flat-roofed batholith (Giovanni et al., 2010; coloured red on Figure 2.4). The Cordillera Blanca batholith is a young granitic pluton (14 – 5 Ma), ~200 km long by ~20 km wide, that plunges to the south, and forms the footwall of the 200 km long

Figure 2.4: Geological map of the Cordillera Blanca. Adapted from Giovinalli et al., 2011.

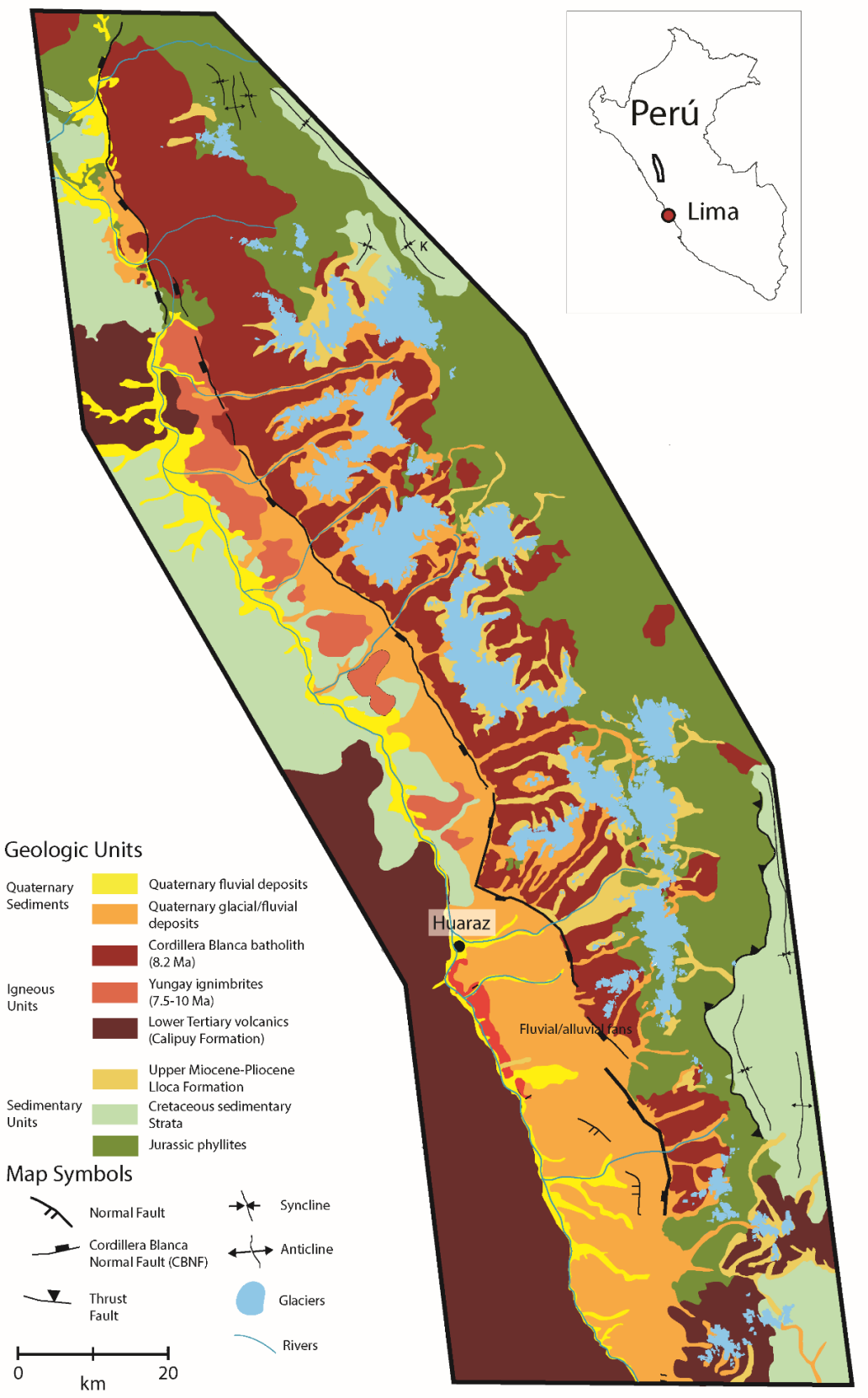
Perú
Lima
Huaraz
Fluvial/alluvial fans
Geologic Units
Quaternary Sediments
Quaternary fluvial deposits
Quaternary glacial/fluvial deposits
Igneous Units
Cordillera Blanca batholith (8.2 Ma)
Yungay ignimbrites (7.5-10 Ma)
Lower Tertiary volcanics (Calipuy Formation)
Sedimentary Units
Upper Miocene-Pliocene Lloca Formation
Cretaceous sedimentary Strata
Jurassic phyllites
Map Symbols
Normal Fault
Cordillera Blanca Normal Fault (CBNF)
Thrust Fault
Syncline
Anticline
Glaciers
Rivers
0
20
km

Cordillera Blanca Normal Fault (CBNF, Figure 2.4; McNulty and Farber, 2002; Giovanni et al.,2010; Horton, 2012). The batholith is estimated to have experienced an exhumation rate of ~1mm/year between 4 Ma and the present time. The high summits (>6000 m) of the Cordillera Blanca and the internal fabric of the batholith suggest its emplacement along a pre-existing lithospheric fault (Cobbing et al., 1981; McNulty et al., 1998). However, there is considerable debate regarding the processes driving exhumation of the Cordillera Blanca and how magmatism and normal fault activity have influenced Andean relief (Dalmayrac and Molnar, 1981; Margirier et al., 2016).

The Cordillera Blanca batholith and the associated magmas of the Fortalzeza (7.4Ma) and Yungay ignibrites (8-3 Ma) were emplaced during the last period of magmatic activity in northern Perú around 12Ma (Cobbing et al., 1981). The batholith is dissected by a series of subparallel valleys that trend approximately northeast-southwest and intersect the northwest-southeast trending CBNF along the Callejon de Huaylas basin (Figure 2.2). While there is little discussion of the factors that created the valleys that lie semi-perpendicular to the CBNF along the western flank of the Cordillera Blanca, weaknesses caused by brittle deformation during NE-SW extension of the crust during the past 5 Ma may have contributed to their development (Sebrier et al., 1988; Marginier et al., 2017). These weaknesses have been exploited by glacial, fluvial and mass wasting processes to produce the narrow, linear valleys that can be seen today (Figure 2.5).

The Callejón de Huaylas (see Figure 2.2 for location) lies in a supradetachment basin and is situated on the hanging wall of the active 20-45º westward-dipping Cordillera

Figure 2.5: Cross sectional valley morphology in the Cordillera Blanca is of the classic U-shape, characteristic of previously glaciated valleys. A – Down valley view of the Cojup Valley; the city of Huaraz can be seen in the distance (arrow indicates location). B – Down valley view of the Parón Valley taken from the Jantaraju moraine.

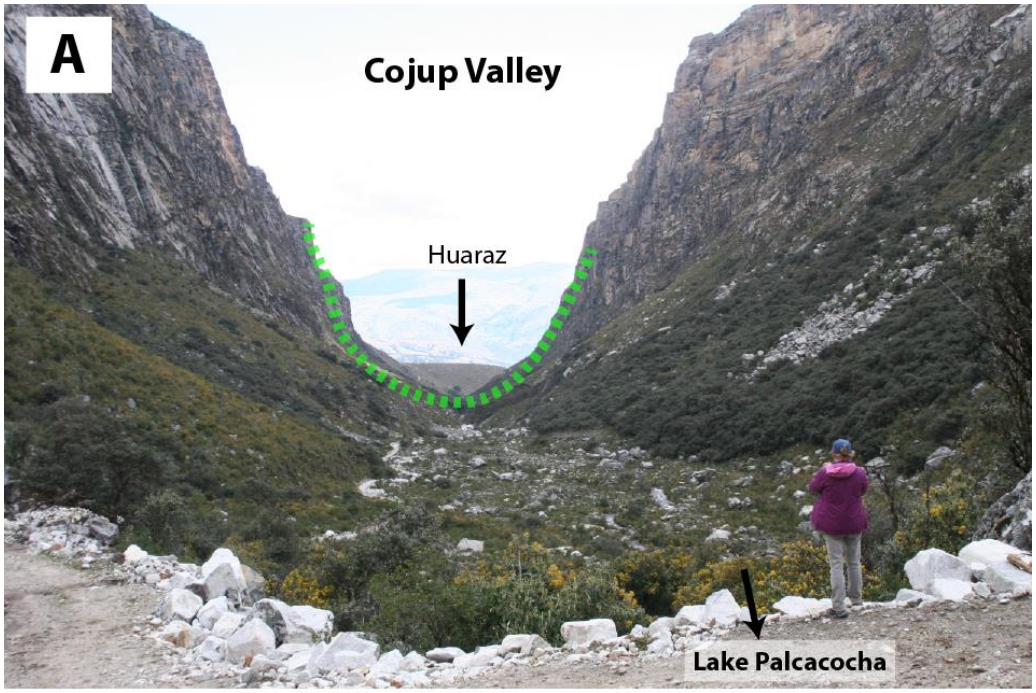
A
Cojup Valley
Huaraz
Lake Palcacocha

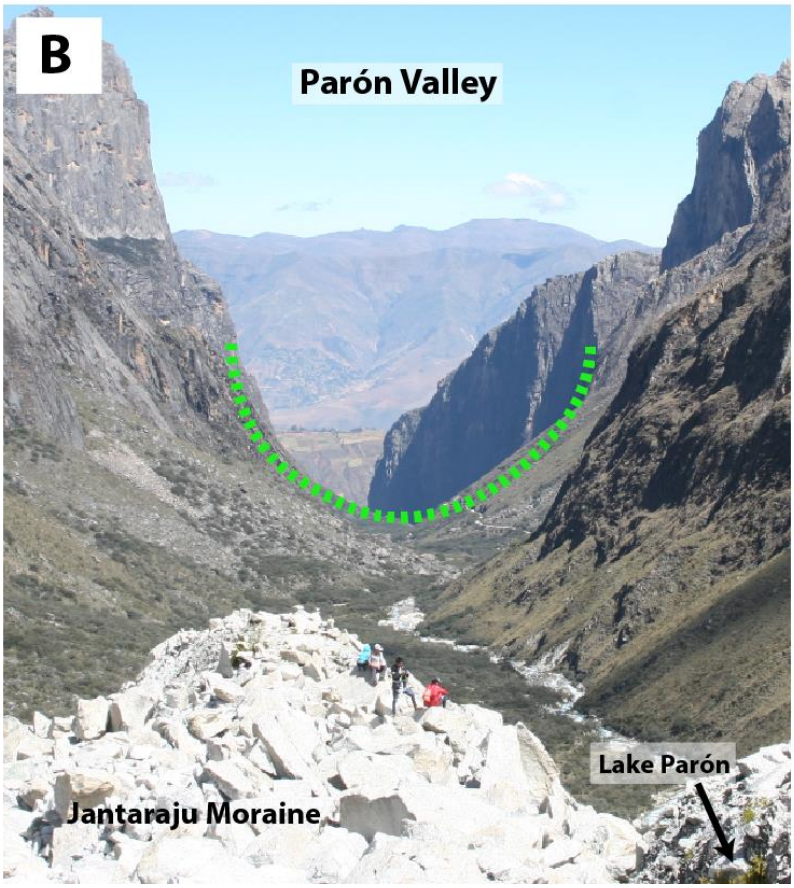
B
Parón Valley
Lake Parón
Jantaraju Moraine

Blanca Normal Fault (CBNF) which runs parallel to the regional strike of active fold-thrust structures farther east (Giovanni et al., 2010). Vertical slip rates estimated for the past 30ka on the CBNF range from 5.1 ± 0.8 mm/yr to 0.6 ± 0.2 mm/yr and decrease from north to south (Schwartz, 1988; Siame et al., 2006). The Callejón de Huaylas basin is infilled with ~1300 m of conglomerate, sandstone, siltstone and limited carbonates of the upper Miocene-Pliocene Lloclla Formation and overlying glacial and fluvial deposits (Figure 2.4; Giovanni et al., 2010). The Lloclla formation is an upward-coarsening sedimentary succession interpreted to have formed by the progradation of stream-dominated alluvial fans into lacustrine fan-delta systems (Giovanni et al., 2010; Figure 2.4) and is overlain unconformably by subhorizontal Quaternary glacial deposits (10's-100's m thick) deposited during the last glacial maximum at ~13,200 ka (Rodbell, 1992; Rodbell & Seltzer, 2000). In the northern part of the Callejón de Huaylas basin, glacial and fluvial deposits cap ignimbrites of the upper Miocene Yungay Formation, Eocene to middle Miocene Calipuy volcanic rocks, and Jurassic to Cretaceous clastic units (Figure 2.4).

The relatively young volcanic and sedimentary rocks of the Cordillera Blanca have influenced the activity and effectiveness of erosional and depositional processes caused by mass movements, and fluvial and glacial agents. Modern tropical glaciers can be found at high elevations at the head of many of the northeast-southwest trending valleys that dissect the Cordillera Blanca (Figure 2.4); these glaciers were much more extensive during the Quaternary and reached as far west as the Callejón de Huaylas basin (Clapperton, 1972; Farber et al., 2005; Bromley et al., 2009). Glacial erosion of valley walls and the subglacial sculpting of undulating valley floors have been strongly influenced by the geology and

lithology of the underlying substrate (Eyles, 1983; Fisher et al., 2006; Cook and Swift, 2012); however, cross-sectional valley morphology throughout the Cordillera Blanca is of the classic U-shape, characteristic of most glaciated valleys (Eyles, 1983; Benn & Evans, 2010; Figure 2.5). The highest mountain summits (such as Mount Huascarán, >6000m.a.s.l.; Figure 2.2) are located in the northern and central parts of the Cordillera Blanca. In contrast, the southern part of the Cordillera Blanca has a lower relief but a higher mean elevation. This difference may be in part due to regional differences in bedrock lithology resulting in a greater amount of valley carving in the northern and central part of the Cordillera Blanca and less erosion in the southern part (Margirier et al., 2016; Figure 2.4).

Quaternary age sediments that overlie bedrock and infill valleys in the Cordillera Blanca have complex stratigraphies and variable spatial thickness and facies characteristics. The dominant facies types identified in the previously glaciated valleys are coarse-grained boulder-gravels deposited by mass-wasting, fluvial and glacial processes (Eyles, 1979; Hambrey & Glasser, 2012). The abundance of supraglacial debris supplied to and transported by the tropical glaciers confined within the steep and narrow valleys of the Cordillera Blanca, allows large end-moraine complexes to form (Figures 2.6 & 2.7). These large moraine complexes often disrupt drainage through the valleys and form dams impounding large glacial lakes which are prone to failure and can cause catastrophic floods (Glacial Lake Outburst Floods – GLOFs; Reynolds, 1992; Hubbard et al., 2005; Schneider, et al., 2014; Emmer et al., 2016). Sedimentation along deglaciated valley floors is dominated by fluvial processes as glaciers recede and by sediment input from valley walls

Figure 2.6: Llaca Lake (location shown in Figure 2.10C) is impounded by a large frontal moraine and overlies buried ice of the Llaca Glacier. A – Aerial view of the Llaca Lake and glacier. B – Ice melting beneath a cover of coarse-grained, angular supraglacial debris within Llaca Lake. C – Down valley view of the moraine dam impounding Llaca Lake.

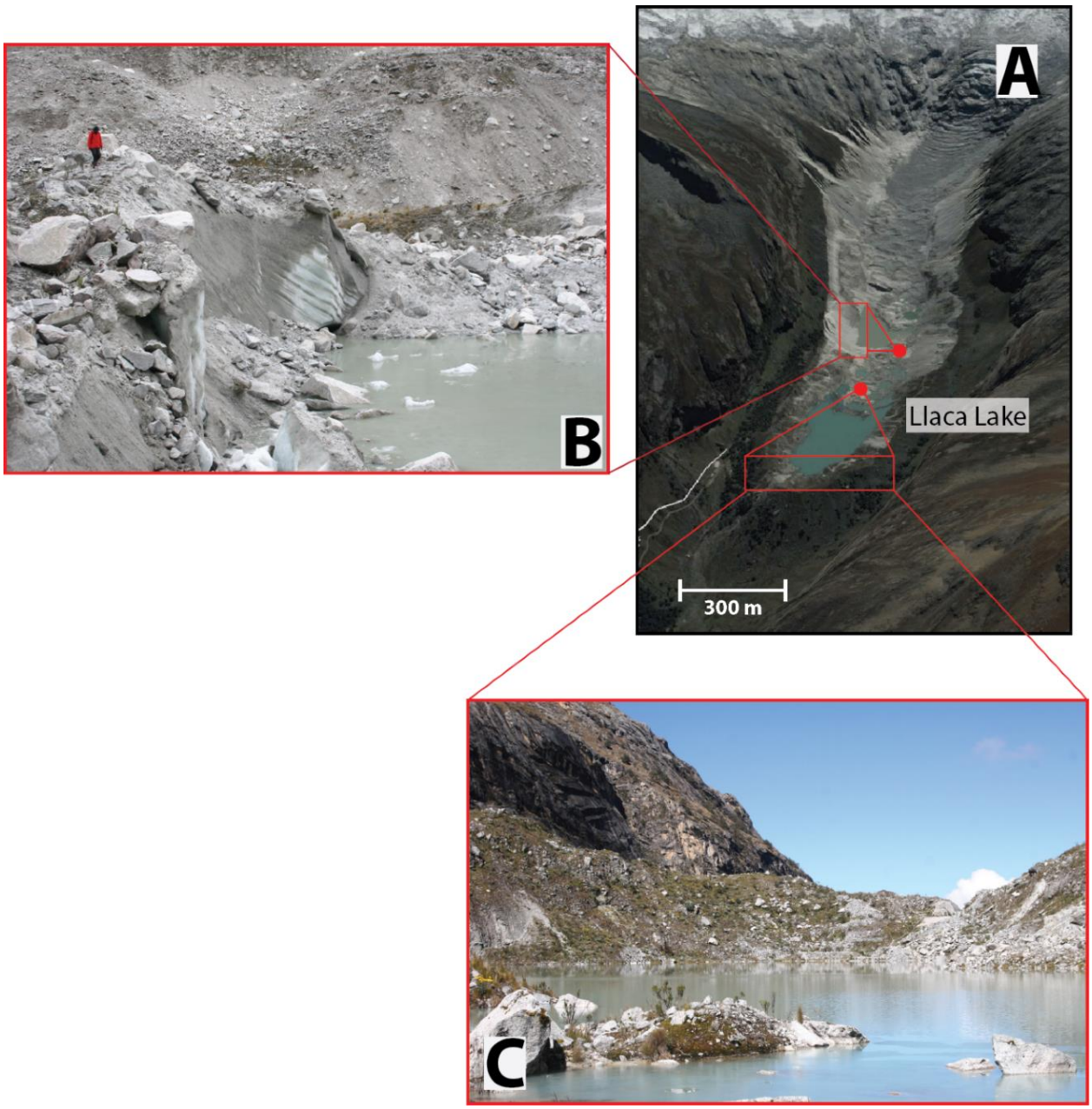
A
B
C
Llaca Lake
300 m

Figure 2.7: A – Palcacocha Lake (see Figure 2.10D for location) is dammed by steep-sided frontal and lateral moraines (B,C). The height of the Palcacocha Moraine (C) reaches approximately 146 m above the valley floor (Klimes et al., 2016).

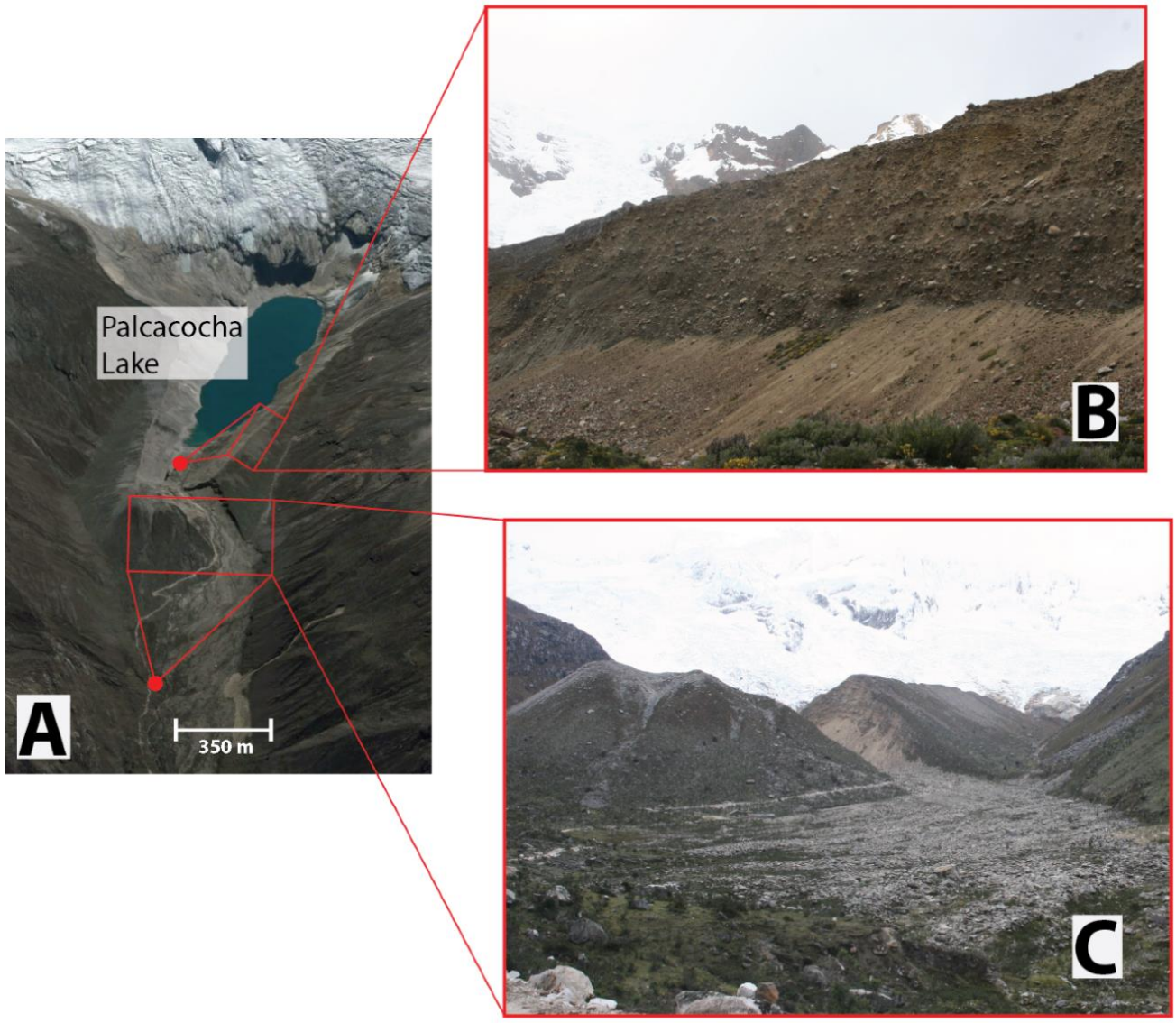
Palcacocha
Lake
A
350 m
B
C

in the form of angular rockfall material on screes and debris cones (Hambrey and Ehrmann, 2004; Hambrey & Glasser, 2012).

2.2 CHARACTERISTICS OF ANDEAN TROPICAL GLACIERS

The Andes mountain ranges contain some of the wettest and driest mountainous regions in the world, as well as a diverse range of glaciated environments. Modern glaciers within the Andean Cordillera Blanca are located at latitudes of between 8°30' and 10°10'S and can therefore be considered as tropical glaciers (Kaser and Osmaston, 2002; Rodbell et al., 2009; Veetil et al., 2017). Precipitation in these tropical regions of the Andes results from an easterly flow of moisture from the Atlantic Ocean and Amazon Basin via tropical easterlies (e.g. Garreaud et al., 2003) and is transported to the high Andes via convective circulation. In contrast, temperate Andean glaciers are found south of 29°S latitude in Chile and Argentina, where precipitation is derived from the Pacific Ocean and where strong orographic effects result in greater amounts of precipitation on the western (windward) side of the Andes than on the eastward (leeward) side (Rodbell et al., 2009).

Tropical glaciers of the Andes can be further subdivided into outer and inner tropical glaciers according to the seasonality of the precipitation they receive (Figure 1; Rabatel et al., 2013; Rodbell et al., 2009; Veetil et al., 2017). Regions within the inner tropics (Ecuador, Venezuela and Colombia) experience year-round precipitation whereas the glaciated regions of Perú and Bolivia are considered to belong to the outer tropics where precipitation is affected by one dry season (April-September) and one wet season (October-March: Kaser, 2001; Rabatel et al., 2013). The movement of the Intertropical Convergence Zone (ITCZ), the area in which the northeast and southeast trade winds converge, is

responsible for the occurrence of two rainy seasons in the inner tropics and one in the outer tropics (Kaser and Ostamon, 2002; Veetil et al., 2017). For both the inner and outer tropics, incident solar radiation is more or less constant throughout the year, resulting in a small annual temperature range that is exceeded by more extreme diurnal temperature variability (Benn et al., 2005).

Precipitation in the Andean region is also affected by the El Niño-Southern Oscillation phenomenon (ENSO: Francou and Pizarro, 1985; Aceituno, 1988; Vuille et al., 2000; Garreaud et al., 2009). El Niño years (i.e. the warm phases of ENSO) tend to be warm and dry, while La Niña years (i.e. the ENSO cold phases) are associated with cold and wet conditions. In general, Andean glaciers are expected to experience negative mass balance during El Niño conditions and positive or stable mass balance during La Niña conditions (Veemil et al., 2017). However, the climatic characteristics of La Niña/El Niño are not uniform across the tropical Andes and the consequences of an El Niño event can vary considerably (Garreaud et al., 2009).

Tropical glaciers show distinctive sensitives to past, and current, variations in temperature and precipitation. The annual cycle of mass balance for tropical glaciers differs substantially to that of temperate glaciers in the Andes (Figure 2.8). Ablation is generally restricted to the summer season at temperate glaciers (Figure 2.8 C), whereas tropical glaciers experience ablation throughout the year owing to the relatively constant annual temperatures (Figure 2.8A, 8B). Glaciers of the Cordillera Blanca, which lie in the outer tropics, gain mass predominantly during the wet season in the peak austral summer months when slightly higher ablation rates also occur (Figure 2.8B; Kaser and Osmaston, 2002;

Figure 2.8: Idealized mass balance characteristics for three types of Andean Glaciers. A) – inner tropical glaciers experience two marked wet/accumulation seasons; constant warm temperatures maintain consistent ablation rates throughout the year; B) – outer tropical glaciers gain mass during the austral summer months when precipitation rates are high; ablation occurs throughout the year but at higher rates during the summer; C) – temperate glaciers gain mass during the austral winter month and are prone to high ablation rates during the summer.

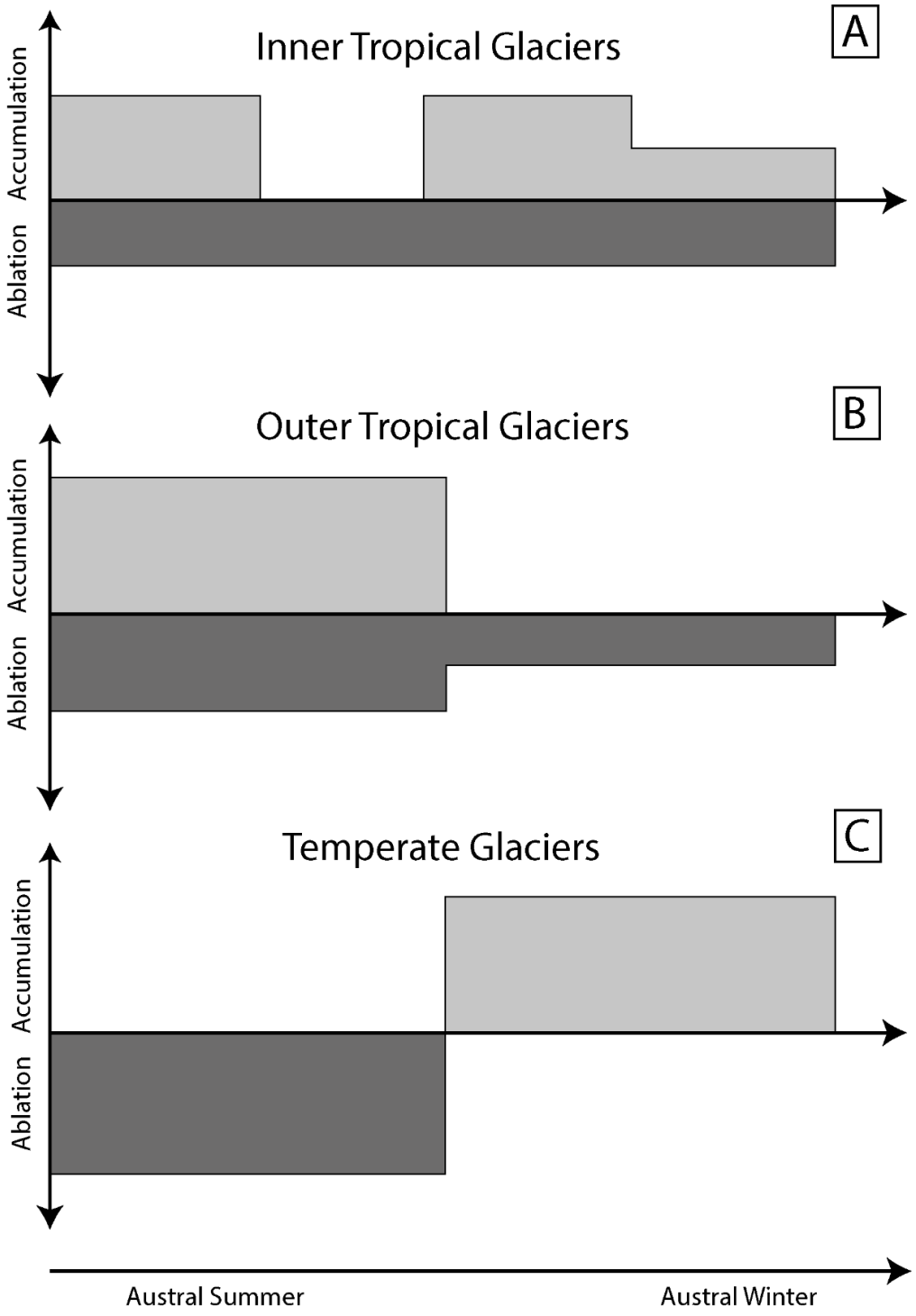
Inner Tropical Glaciers
A
Accumulation
Ablation
Outer Tropical Glaciers
B
Accumulation
Ablation
Temperate Glaciers
C
Accumulation
Ablation
Austral Summer
Austral Winter

Kaser et al., 2003; Rodbell et al., 2009). Accumulation gradients on tropical glaciers are small and the thermal homogeneity of the tropics promotes ablation by melting in the lower parts of most glaciers year round. This makes tropical glacier termini highly responsive to climate variability, particularly changes in precipitation (Licciardi et al., 2009).

2.2.1 Glacier of the Cordillera Blanca

Most modern glaciers in the Cordillera Blanca are small (average size of about 0.7km2), steeply inclined, and occasionally have pronounced glacier tongues (e.g. Jantajaru Glacier in the Parón Valley; Portocarrero et al., 2014; Iturrizaga, 2013). Despite the highest precipitation values occurring on the eastern side of the Andes, the predominant glacier orientation is toward the south-west and west with 32% of all glaciers facing these directions (Tacsi Palacios et al., 2014). Approximately 77% of all glaciers are found on slopes of over 25° and 26.5% of all glaciers are on slopes greater than 65° (Tacsi Palacios et al., 2014). Glaciers in the Cordillera Blanca are found at elevations of between 4249 and 6701 masl (Tacsi Palacios et al., 2014); the snow line altitude in this region ranges 5000-5200 masl. (Smith et al., 2005; Iturrizaga, 2014). Smaller glaciers (< 1km2) are concentrated at elevations between 4500-5500 masl while glaciers greater than 1 km2 are found at elevations of between 4500-5000 masl. Most glaciers in the Cordillera Blanca are diminishing in size, and transitioning from short valley glaciers to slope glaciers, or glacier patches (Iturrizaga, 2014); in 1970, ~37% of all glaciers had a size ranging from 1-5 km2, whereas today only 20% of glaciers are greater than 1 km2 in area (Portocarrero et al., 2010).

Recently acquired remote sensing and photogrammetry data have allowed actual measurement of retreat rates experienced by glaciers in the Cordillera Blanca. A comprehensive overview of the region based on SPOT satellite images and digitized maps, suggests an overall decline in glacier coverage from ~850–900 km2 during the Little Ice Age (LIA) to 800–850 km2 in 1930, 660–680 km2 in 1970, and 620 km2 in 1990. Ice coverage at the end of the 20th century was estimated to be slightly less than 600 km2 (Georges, 2004). A similar study on the basis of Landsat TM data detected 643 km2 of glacial cover in 1987, and 600 km2 in 1991; estimates based on 2016 Landsat 8 data suggest a further reduction to 449 ±56 km2 (Silverio and Jaquet, 2005). The most recent national glacier survey in 2016 states that the Cordillera Blanca has total of 755 glaciers with a total estimated ice covered area of 448.81 km2 (INAIGEM, 2018). Given that the 1930 estimate of ice cover was 830 km2, the Cordillera Blanca appears to have experienced a loss of 46% of ice cover over a period of 86 years (Silverio & Jacquet, 2016). This rapid rate of ice loss is well illustrated by the Yanamarey Glacier, whose terminus receded over 800 m between 1948 and 2008, and experienced an accelerated rate of retreat (greater than 30 m/year) between 2002 and 2008 (Bury, et al., 2011; Figure 2.9).

The Santa River Basin and the Cordillera Blanca have been significantly impacted by recent climate warming which has undoubtedly contributed toward glacier recession in the region (Bury et al., 2012; Mark et al., 2010). Analysis of data from over 100 weather stations in the Cordillera Blanca identified an air temperature rise of about 0.31ºC per decade between 1969 and 1998, and of 0.13 ºC per decade from 1983 to 2012 (Mark and

Figure 2.9: Terminus positions identified for the Yanamarey Glacier (see Figure 2.10D for location) which has experienced rapid retreat during the past 5 decades (1969 – 2016). Image source: Google Earth, (1969, 2011, 2016a).

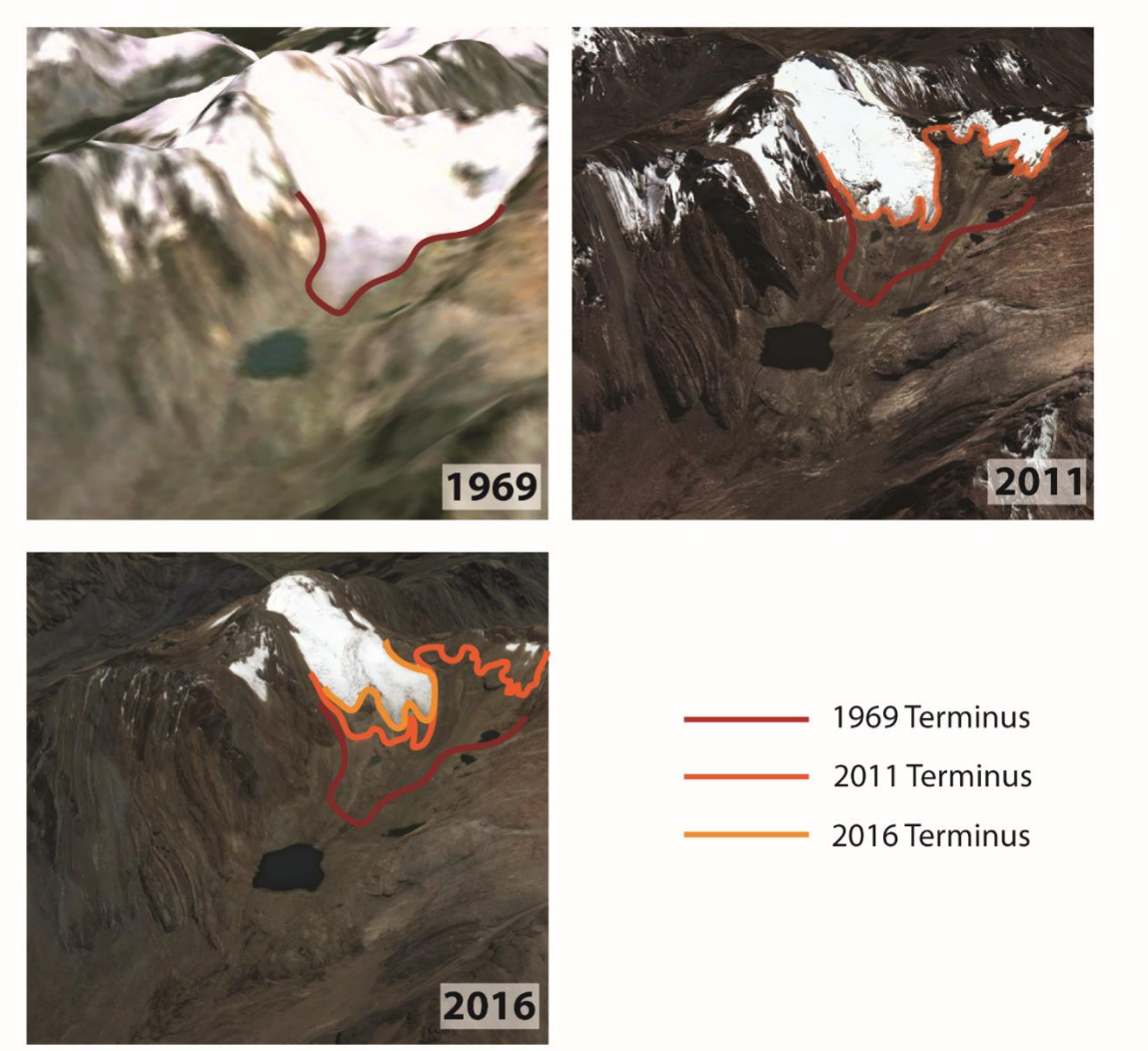
1969
2011
2016
1969 Terminus
2011 Terminus
2016 Terminus

Seltzer, 2005; Schauwecker et al., 2014). This mirrors the overall temperature increase of 0.13°C/ decade from 1950-2010 in the tropical Andes (Vuille et al., 2015). An associated increase in precipitation of about 60 mm/decade since the early 1980s has also been documented. However, Schauwecker et al. (2014) caution that the rapid glacier recession noted to have occurred between 1980 and 2012 may have been caused by other factors than just recent changes in temperature and precipitation; glaciers may be still reacting to air temperature increases that occurred prior to 1980.

2.3 GLACIAL HISTORY OF THE CORDILLERA BLANCA

In the Northern Hemisphere, glacial deposits, in particular till sheets, are used to establish the history of glacial advance and retreat in a region (e.g. Boulton, 1996; Karrow, et al., 2000; Svendesen et al., 2004; Evans et al., 2008; Cummings et al., 2011). The approximate age of ice advances is determined through radiocarbon dating of organic materials and thermoluminesence dating of intervening interglacial or interstadial deposits (e.g. Southern Ontario, Canada; Barnet, 1992; Berger & Eyles, 1994). In the Cordillera Blanca, and other parts of the tropical Andes, thick successions of preserved glacial sediment are not reported (Cobbing, 1981; Giovanni et al., 2009) as preservation of glacial material is relatively rare in these Andean environments due to reworking by mass wasting, fluvial processes, and erosive events such as glacial lake outburst floods (Reynolds, 2000; Hubbard et al., 2005; Benn and Evans, 2010). Thus, establishing a chronology of glacial events relies on the relative and absolute dating of landforms and surface features, in particular moraines, created by the most recent glacial advances and subsequent retreats.

Documenting the dynamics of tropical glaciers and their response to climatic change in the past century is integral to understanding past glacier behavior and the nature of associated processes. There is evidence to suggest that glaciers in the tropical Andes were subject to moderate retreat between the early 1940s and the early 1960s (Rabatel et al., 2013). From the mid-1960s to the second half of the 1970s glacier termini remained almost stationary, and in the late 1970s glacier retreat accelerated in a stepwise manner: the first acceleration occurred in the late 1970s, the second in the mid-1990s and the third in the early 2000s. Glacier shrinkage in the last three decades appears to be unprecedented since the glacial maximum of the Little Ice Age (LIA; Rabatel et al., 2013).

The timing and geographic extent of past glaciation in the Cordillera Blanca has been determined largely through the analysis of trimlines on exposed bedrock, and the dating of end and lateral moraines (e.g. Rodbell, 1992, Glasser et al., 2009; Solomina et al., 2007; Rodbell et al., 2009). It is assumed that these landscape features provide evidence for the former location of a glacier during advance, at stillstand, or retreat (Rodbell et al., 2009).

2.3.1 Techniques used for dating glacial landforms

The most common techniques used to date past glacial events in the Andes include lichenometry, dendrochronology, radiocarbon dating, surface exposure dating, and sediment core analysis. Forested moraines are limited to the southern Andes, and the use of dendrochronology to date trees growing on moraines and to infer a minimum age for the moraines has also been limited to a few studies in the southern Andes (Villalba, 1990; Koch and Killian, 2005). In the Cordillera Blanca, lichenometric studies, which measure the size

of lichens growing on boulders, have been used to estimate the age of bouldery moraines (e.g. Rodbell, 1992; Solomina et al., 2007; Jomelli et al., 2008). Lichen of the subgenus Rhizocarpon are most commonly used for this form of dating in the Andes (e.g. Rodbell, 1992; Solomina et al., 2007; Jomelli et al., 2009); this methodology assumes that the size of the largest lichen living on a substrate indicates the length of time that the surface has been exposed to colonization and growth (Beschel, 1958; Rodbell, 1992). However, moraine ages calculated by this method may also be influenced by substrate lithology and microclimatic conditions that can affect the size and speed of colonization by lichen (Rodbell, 1992; Benedict, 1967; Jochimsen, 1973), and/or lichen mortality (Osborn et al., 2015). In addition, slope processes such as rockfalls can displace boulders on moraines which may result in inaccurate dating of the feature.

Radiocarbon dating can be used to determine limiting ages for moraines if organic material is present (Rodbell et al., 2009). Maximum-limiting ages give the oldest possible calculated date of the sample, while minimum-limiting ages give the youngest possible calculated date. Organic matter found in lakes and peatlands immediately up-valley from a moraine, can provide a minimum age for the moraine. However, care must be taken to ensure that the organic material being sampled is found within sediment that has accumulated post-glacially and is not material that has survived being overridden by glacial ice (Thompson et al., 2006). Dates that provide a maximum age for glaciation can be determined when organic material is incorporated in till that underlies a moraine or in soil A-horizons buried by till (Rodbell et al., 2009). The majority of maximum-limiting radiocarbon ages are reported in the southern Andes where glaciers advanced into forests

or peatlands (Lowell et al., 1995). Organic matter found within outwash sand and gravels down-valley from moraines has also been dated to provide a maximum age for the glacial advance (Mercer and Palacios, 1978). However, since the stratigraphic relationship between the outwash deposits and the moraines is rarely known, it is difficult to correlate the two deposits with any certainty.

Surface exposure dating that analyses cosmogenic radionuclides (CRN) has been used extensively to date Andean moraines (e.g. Rodbell, 1992; Farber et al 2005; Douglass et al 2006; Solomina et al., 2007; Rodbell et al., 2009; Bromley et al., 2009; Glasser et al., 2009; Bromley et al., 2016). Cosmogenic nuclides (e.g., 10Be, 26Al, 3He, 36Cl) form and accumulate at quasi-steady rates, in rocks exposed to cosmic rays. Boulders transported and eroded by glaciers are assumed to have had their surfaces "scraped clean" of any previous isotope accumulation (Gosse & Phillips, 2001; Balco et al., 2008; Rodbell et al., 2009). Thus, measuring the concentration of cosmogenic radionuclides in the upper surface of a boulder found on the upper surface of a moraine can determine the amount of time since the boulder was deposited and exposed to cosmogenic rays (Briner et al., 2005). However, boulders that are emplaced post-glacially by processes such as rock fall, or are covered by snow for significant periods of time, will yield ages that underestimate the age of the moraine (Rodbell et al., 2009). Exposure ages older than the landform can also be obtained if the boulder is not eroded sufficiently by the ice and cosmogenic radionuclides are 'inherited' from previous episodes of exposure (Briner et al., 2005). The ages obtained can also be affected by elevation as at any given latitude and longitude the rates for in situ cosmogenic radionuclide production increase with increasing altitude above sea level. This

factor must be taken into consideration when calculating surface exposure dates in the tectonically active Santa River Basin (Rodbell, 1991, 1992; Rodbell et al., 2009).

Other methodologies, including sediment flux analysis of lake deposits and rock weathering features have been used to estimate the age of glacial advance/retreat cycles in the Andes (Rodbell, 1993; Ariztegui, D., et al., 1997; Polissar et al., 2006; Rodbell et al., 2008). However, given the wide range of factors that can affect both sediment influx and weathering rates in such a region as the Cordillera Blanca, these techniques are not widely used for dating purposes.

2.4. LATE QUATERNARY GLACIAL HISTORY OF THE CORDILLERA BLANCA

Early studies that aimed to establish glacial chronologies in the Cordillera Blanca, identified a series of 'moraine groups', each formed within distinct episodes of glacial activity (i.e. the four moraine groups identified separately by Clapperton, 1992 and by Rodbell, 1992). Subsequent studies attempted to relate these four groupings of moraines to glacial stages identified elsewhere (e.g. Farber et al., 2005; Glasser et al., 2009). However, this task proved difficult due to the wide range of dates obtained for the moraine groups, and the inconsistent nomenclature and locational data provided for individual features.

This paper presents a new interpretation of the late Quaternary glacial chronology of the Cordillera Blanca based on the spatial grouping of moraines dated by others, into 6 stages of glacial activity (Figure 2.10A – 10F; see below); these stages may be used to identify regional patterns of ice growth and decay. The methodology used is similar to that used by La Frenierre et al. (2011) in which dated moraines and sampling locations reported in the literature are geoferenced using the coordinates provided, or by identifying the

Figure 2.10A: Five distinct regions on the western side of the Cordillera Blanca have ben delineated on the basis of the dated glacial landforms (moraines) they contain (red boxes, see Figure 2.10B – 10F). The glacial landforms have been grouped according to their estimated ages into one of 6 stages ranging from Stage 1 (greater than 35 ka) to Stage 6 (0.15ka – present). Coloured lines within the boxes represent the position of landforms dated to have formed during these Stages.

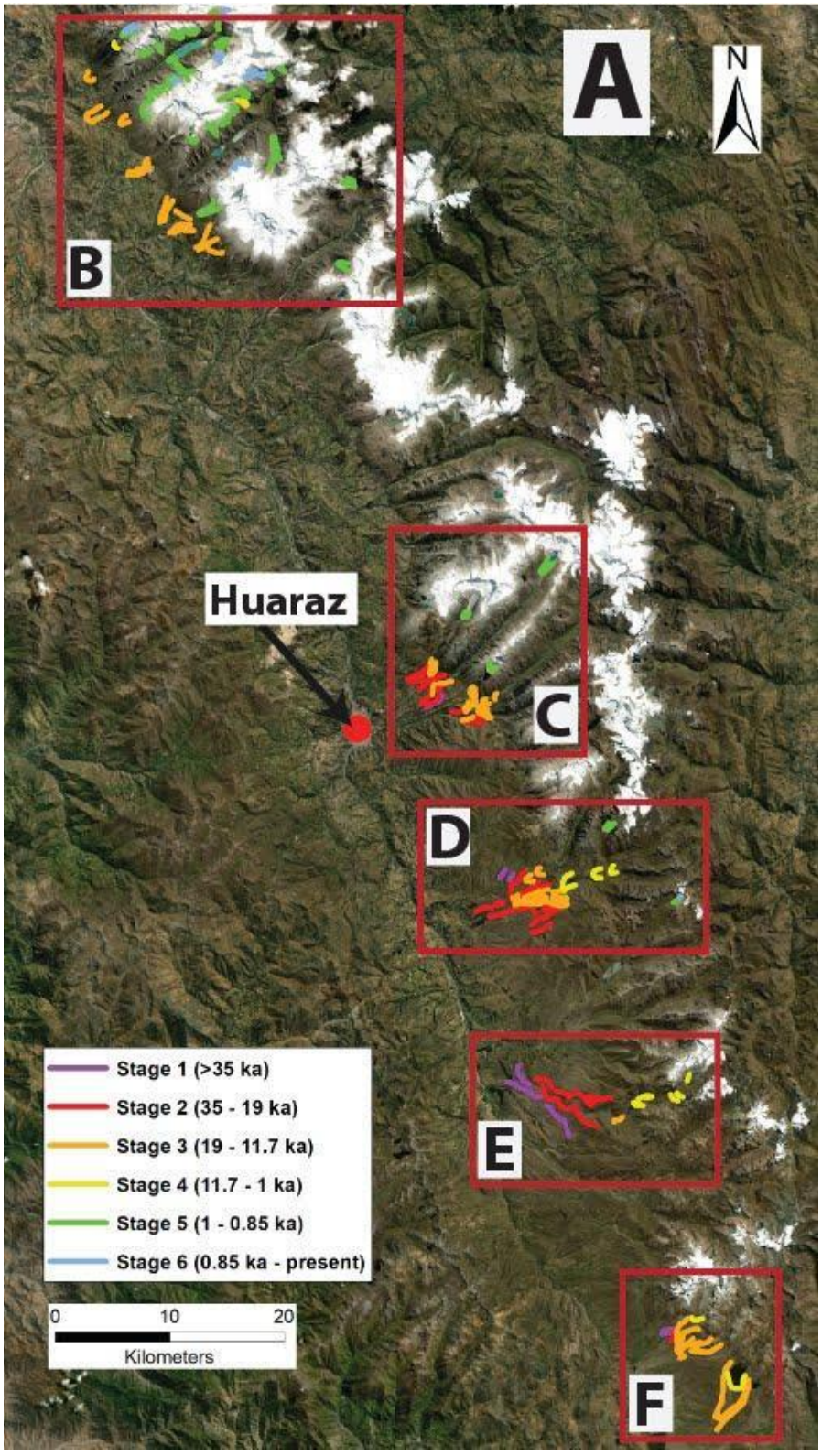
A
N
B
Huaraz
C
D
E
F
Stage 1 (>35 ka)
Stage 2 (35 - 19 ka)
Stage 3 (19 - 11.7 ka)
Stage 4 (11.7 - 1 ka)
Stage 5 (1 - 0.85 ka)
Stage 6 (0.85 ka - present)
0
10
20
Kilometers

Figure 2.10B: The northern most region of the Cordillera Blanca includes prominent landforms such as Mount Huascarán and the Parón and Llanganuco Valleys. Moraines found at the western end of these valleys are attributed to Stage 3 (19-11ka, formed the local glacial maximum). Numerous younger moraines fall within Stage 5 or Stage 6 (0.5 to present). Data from Clapperton (1992); Solomina et al., (2007) and La Frenierre et al. (2011).

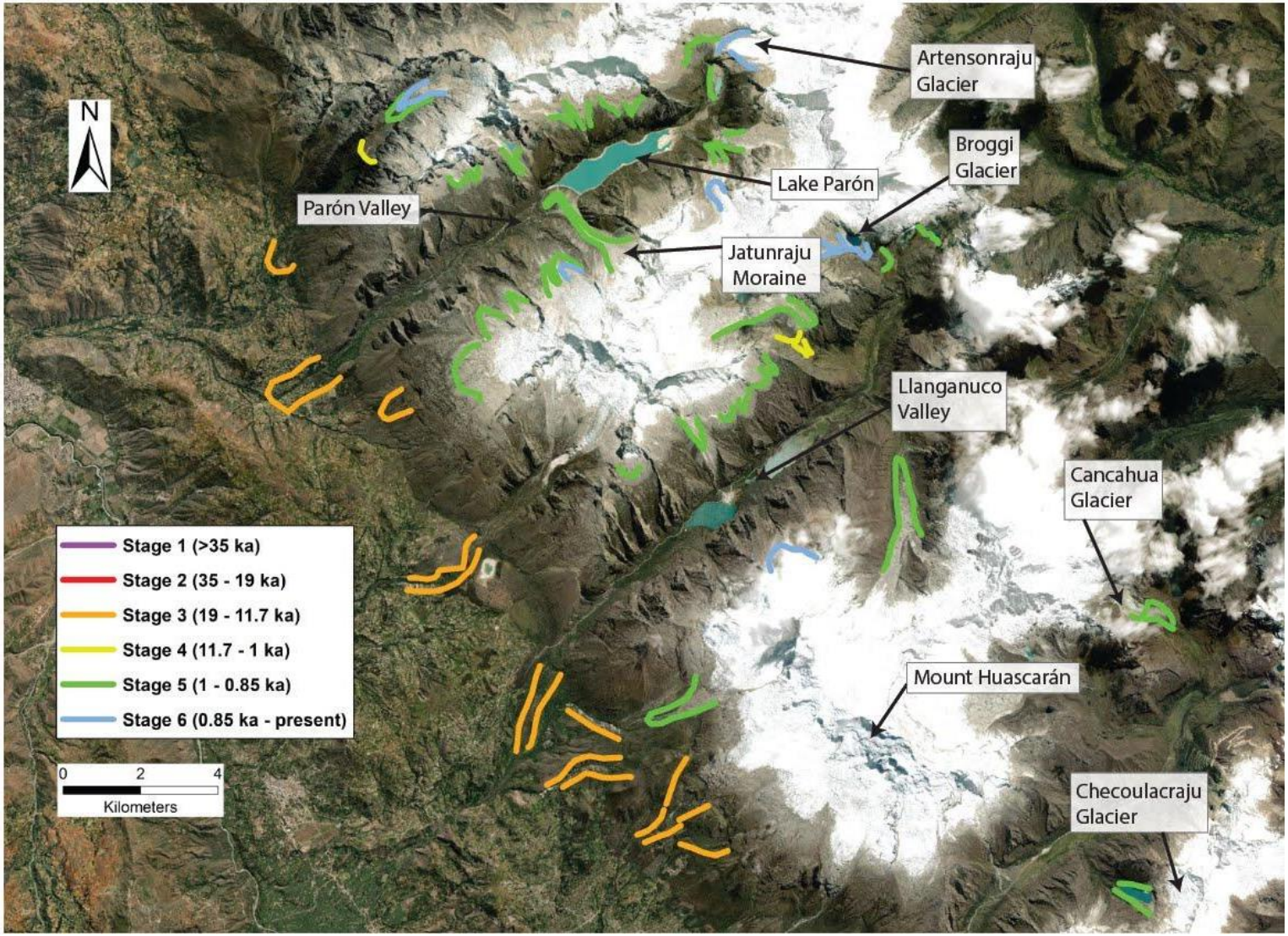
N
Artensonraju Glacier
Broggi Glacier
Lake Parón
Parón Valley
Jatunraju Moraine
Llanganuco Valley
Cancahua Glacier
Mount Huascarán
Checoulacraju Glacier
Stage 1 (>35 ka)
Stage 2 (35 - 19 ka)
Stage 3 (19 - 11.7 ka)
Stage 4 (11.7 - 1 ka)
Stage 5 (1 - 0.85 ka)
Stage 6 (0.85 ka - present)
0 2 4
Kilometers

Figure 2.10C: The valleys of Llaca, Cojup, Quilcayhuanca and Pariac drain toward the City of Huaraz (location is at the bottom left corner of the image). Moraines at the mouths of all four valleys are some of the oldest moraines dated in the Cordillera Blanca. Two moraine crests dated to Stage 1 (>35ka) are located close to the mouth of the Cojup valley. Several Stage 2 moraines (35-19ka) are found downvalley of Stage 3 moraines that are dated to between 19-11ka. The frontal and lateral moraines that impound both Llaca and Palcacocha lakes are considered to be Stage 5 moraines formed during the LIA. It is worth noting that no moraines or other landforms are considered to belong to Stage 4 in these valleys. Data from Clapperton, 1972; Solomina et al., 2007; Farber et al., 2005; Bromley et al., 2009; La Frenierre et al. 2011; Emmer et al., 2019.

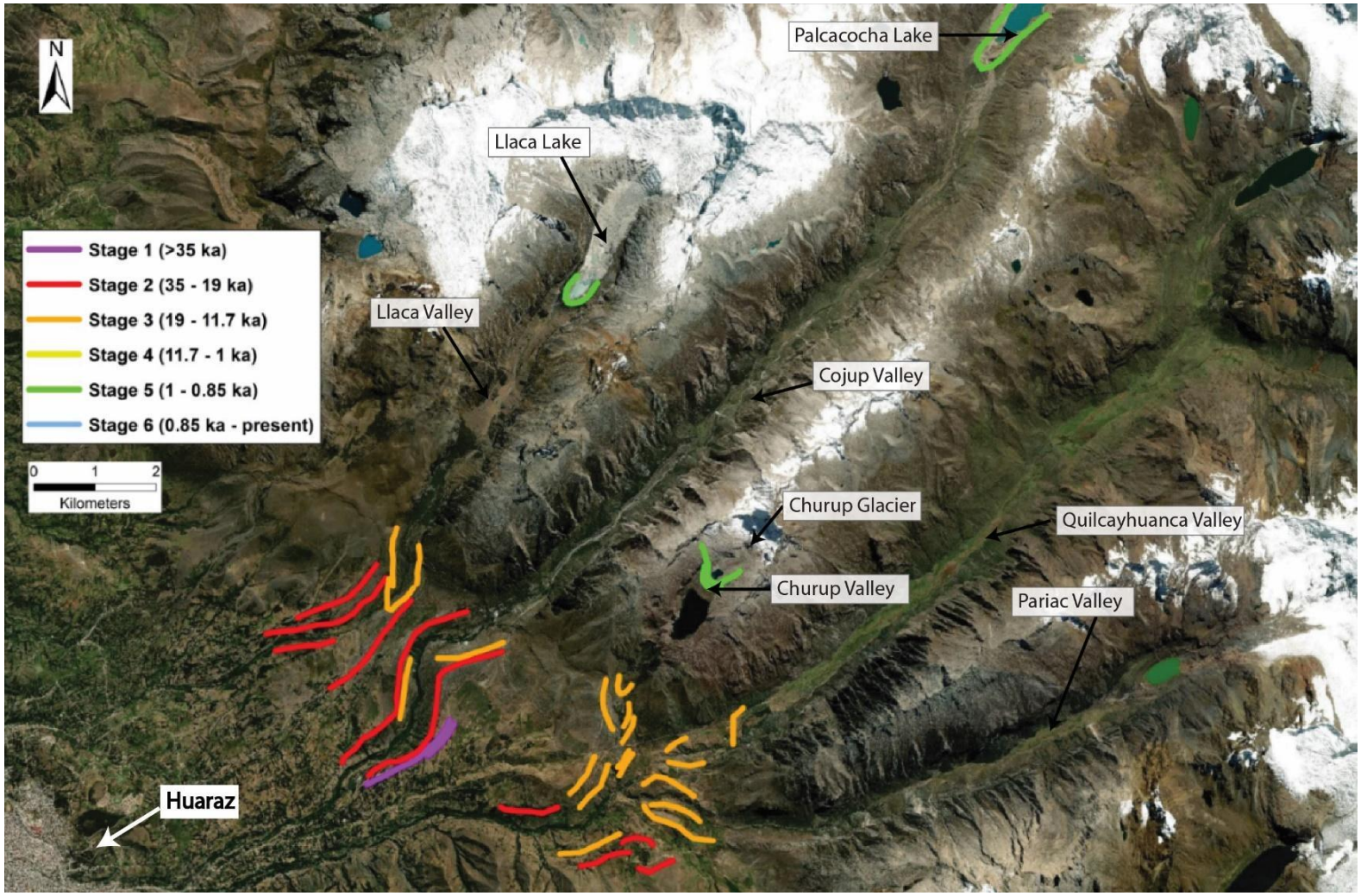
N
Palcacocha Lake
Llaca Lake
Llaca Valley
Cojup Valley
Churup Glacier
Quilcayhuanca Valley
Churup Valley
Pariac Valley
Huaraz
Stage 1 (>35 ka)
Stage 2 (35 - 19 ka)
Stage 3 (19 - 11.7 ka)
Stage 4 (11.7 - 1 ka)
Stage 5 (1 - 0.85 ka)
Stage 6 (0.85 ka - present)
0 1 2
Kilometers

Figure 2.10D: This region is dominated by moraines dated to have formed during Stage 2 (35 – 19 ka) and Stage 3 (19-11.7 ka). Glacial Lake Breque is thought to have existed between 12.8 ka and 11.3 ka and was dammed by Stage 3 moraines (19-11 ka). The Uquian Valley contains a series of Stage 4 moraines dated to ~10.9ka and ~7.3ka. Data from Rodbell (1993); Rodbell and Seltzer (2000); Solomina et al. (2007); La Frenierre et al. (2011).

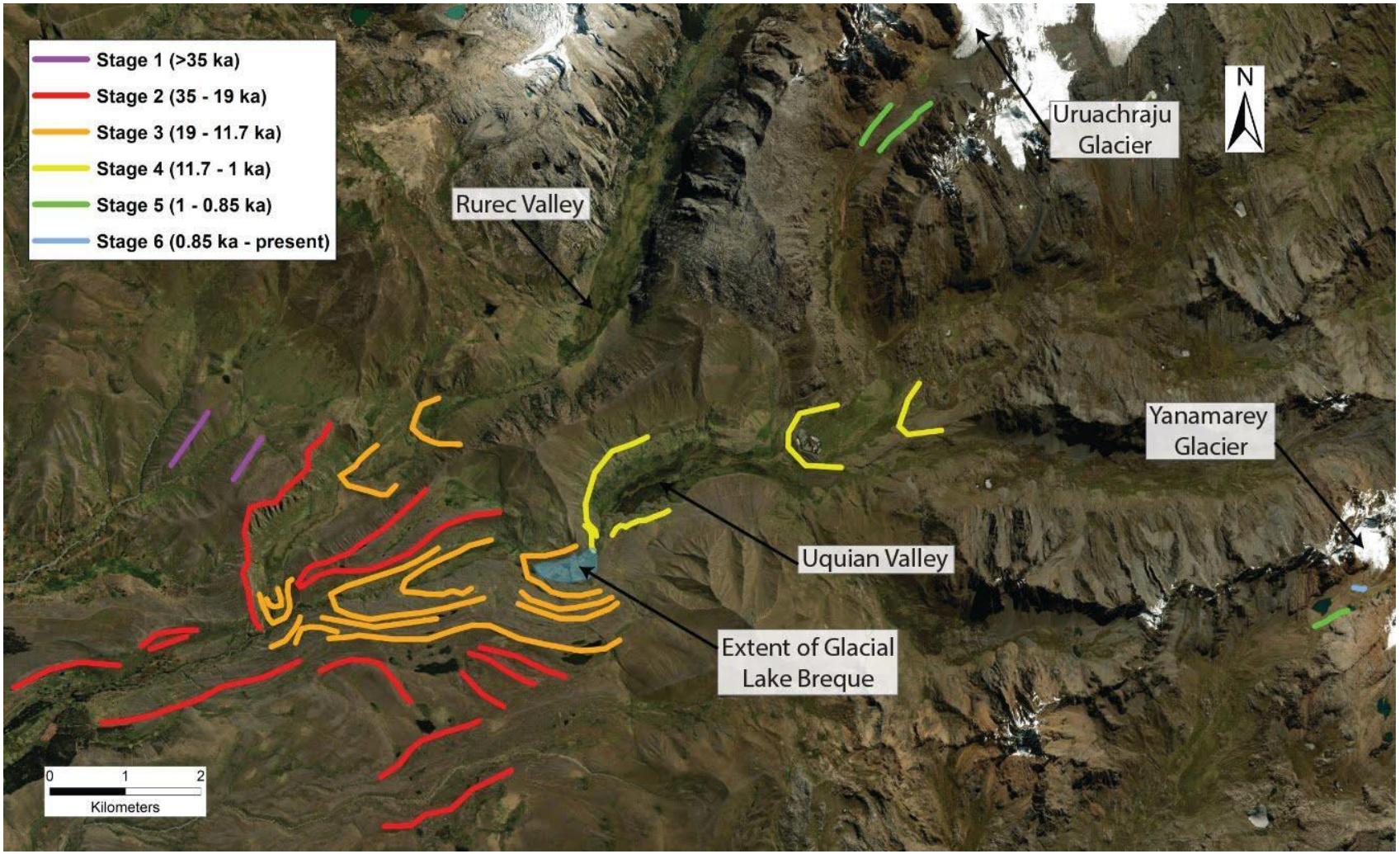
Stage 1 (>35 ka)
Stage 2 (35 - 19 ka)
Stage 3 (19 - 11.7 ka)
Stage 4 (11.7 - 1 ka)
Stage 5 (1 - 0.85 ka)
Stage 6 (0.85 ka - present)
Rurec Valley
Uruachraju Glacier
N
Yanamarey Glacier
Uquian Valley
Extent of Glacial Lake Breque
0 1 2
Kilometers

Figure 2.10E: The Gueshque valley is one of the few valleys in the Cordillera Blanca that contains a succession of moraines dating from Stage 1 (>35 ka) to Stage 4 (11.7-0.5 ka) that formed during progressive glacial retreat upvalley. Data from: La Frenierre et al. (2011); Stansell et al. (2017).

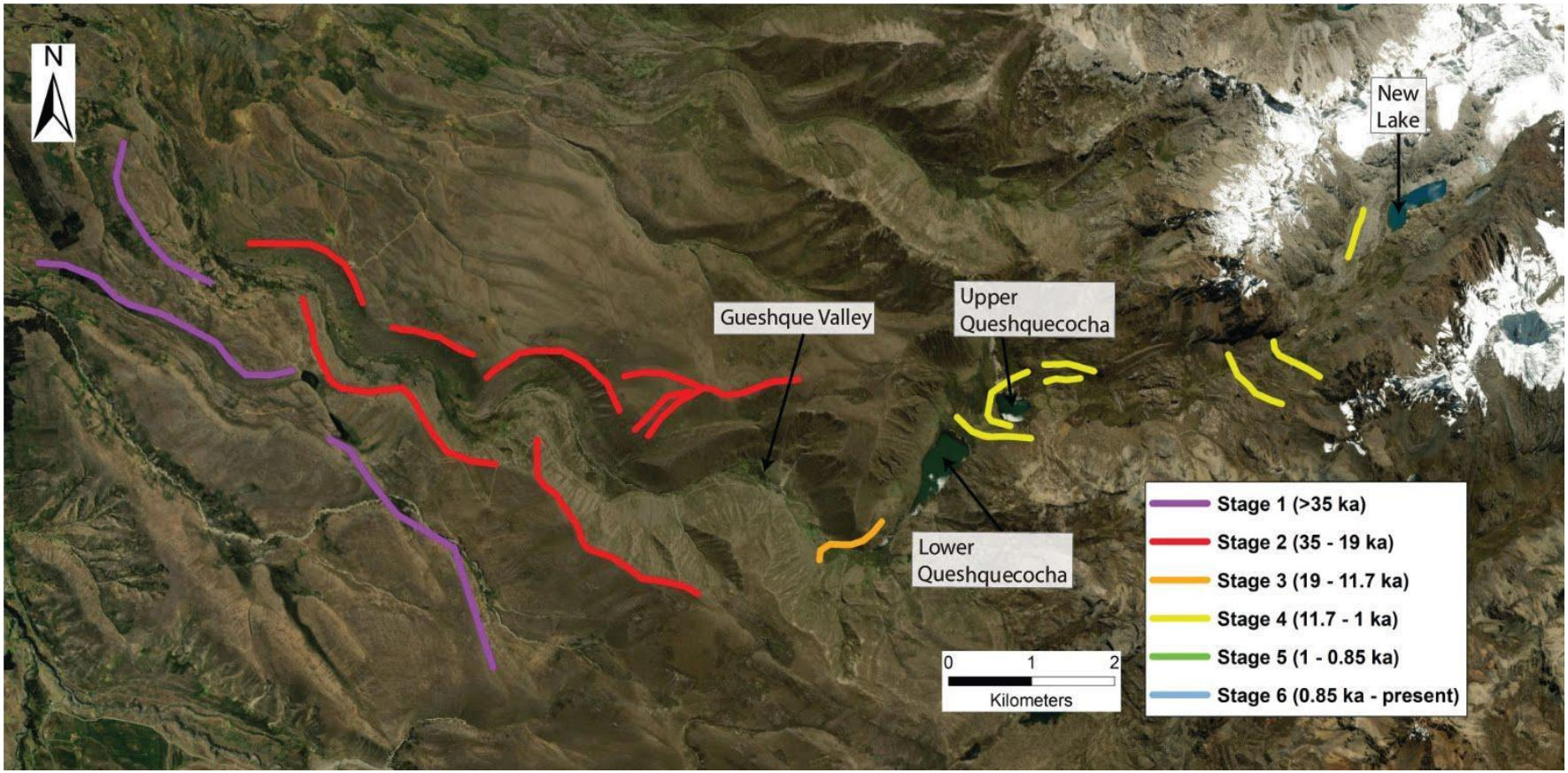
N
New Lake
Upper Queshquecocha
Gueshque Valley
Lower Queshquecocha
0 1 2
Kilometers
Stage 1 (>35 ka)
Stage 2 (35 - 19 ka)
Stage 3 (19 - 11.7 ka)
Stage 4 (11.7 - 1 ka)
Stage 5 (1 - 0.85 ka)
Stage 6 (0.85 ka - present)

Figure 2.10F: The southernmost region of the Cordillera Blanca contains moraines dated to fall within Stage 1 (> 35ka) – Stage 4 (11- 0.5ka). Stage 3 (19-11ka) moraines are the most numerous and prominent in all three valleys in this region. Data from Glasser et al. (2009); Smith and Rodbell (2010).

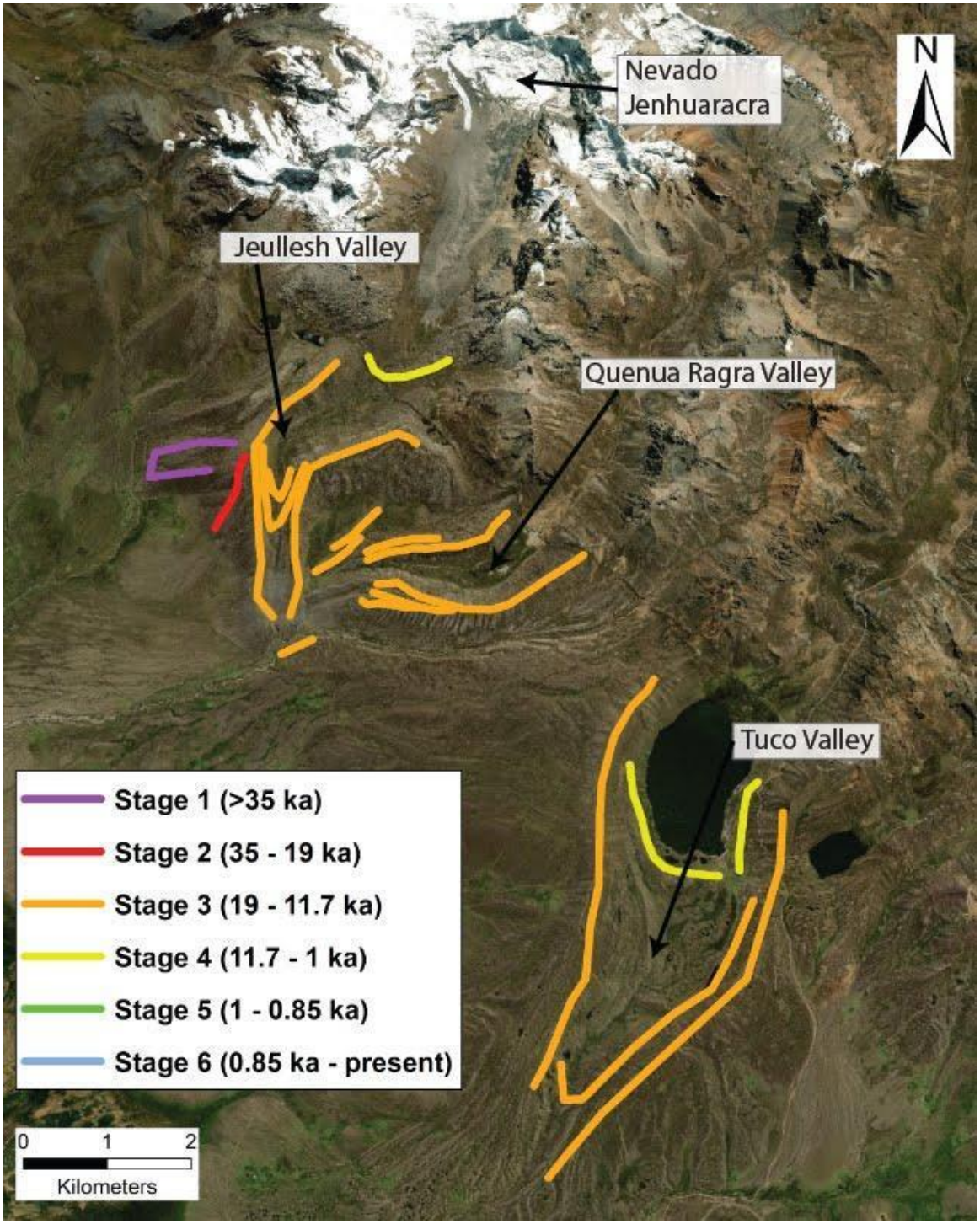
Nevado
Jenhuaracra
N
Jeullesh Valley
Quenua Ragra Valley
Tuco Valley
Stage 1 (>35 ka)
Stage 2 (35 - 19 ka)
Stage 3 (19 - 11.7 ka)
Stage 4 (11.7 - 1 ka)
Stage 5 (1 - 0.85 ka)
Stage 6 (0.85 ka - present)
0
1
2
Kilometers

features on Google Earth imagery. Each individual feature is hand-digitized and attributed a date based on the information provided by each contributing study. Features (moraines) have been drawn on top of an ArcGIS basemap. In this study, 142 individual features in the Cordillera Blanca were mapped and grouped according to their ages; six broad groupings (or Stages) were identified starting with the oldest stage (Stage 1), which includes glacial features older than approximately 35 ka, and extending to the youngest stage (Stage 6), which includes features created after the end of the Little Ice Age ~1850 AD (Table 1; Figures 2.10A – 10F; for studies used in this paper see Appendix 2.1).

Note: In this review we report ages of glacial features as reported in the original literature without recalculation. Many of the radiocarbon dates obtained for glacial events in the Cordillera Blanca were recalibrated by Rodbell et al. (2009), La Frenierre et al., (2011), and Mark et al., (2017) and are presented in terms of 'ka' in reference to thousands of calibrated 14C years BP (where present is 1950 AD). For cosmogenic ages we use values reported by specific studies as 'ka' (thousand years before 2000).

Stage 1 (Before 35 ka)

Although the Peruvian Andes attained most of their present elevation by 5-6 Ma (Smith et al., 2008) and probably had sufficiently high elevations at that time to support glaciation, there are few preserved glacial features dated to be older than 35 ka in the Cordillera Blanca (Farber, et al., 2005; Smith and Rodbell, 2010). The earliest evidence of glaciation in the broader Andes is based on dated tills found in southern Argentina estimated to be between 7.0 and 4.6 Ma (Mercer and Sutter, 1981); the oldest glacial features in Bolivia are dated at between 3.27 ± 0.14 Ma and 3.28 ± 0.13 Ma (Clapperton,

Table 2.1: Number of features identified and mapped for each glacial episode (Stage) recognized in this study. See Figures 2.10A to 10F for mapped distribution of features.

Stage	Number of features mapped
1 (Before 35 ka)	7
2 (34 – 19 ka)	28
3 (18 – 11.7 ka)	50
4 (11.7 - 1 ka)	13
5 (1 ka– 0.15 ka)	37
6 (0.15 ka – present)	7
Total	142

1979). Glacial moraines thought to have formed prior to 35 ka are found in Perú to the east of the Junin Plain, and are dated to be at least 67 ka (Figure 2.3; Mercer and Palacios, 1977); moraines found in the Cordillera Vilcanota are dated at 41.5 ka (Figure 2.3; Goodman et al., 2001). The distribution of these dated features suggests that at least one phase of regional glaciation did occur in Perú prior to 35ka.

In the Cordillera Blanca, moraines located at the western end of the Cojup valley (termed the 'Cojup moraines'; Rodbell, 1993; Figures 2.10A, C), were initially dated using rock weathering stages and were calculated to range between > 4.3 Ma and 46 – 29 ka (Rodbell, 1993). These dates were later refined using 10Be CRN to suggest two potential glacial advances around 440 and 120 ka (Farber et al., 2005). Towards the north-western section of the Rurec Valley (Figures 2.10A, D), two moraines, also identified as belonging to the 'Cojup' moraine group by Rodbell (1993), are considered here to belong to Stage 1 due to the estimated age range of 120 ka to 140 ka as recalculated by Bromley et al. (2009). Three moraines in the Quesque valley (Figures 2.10A, E) are considered to be 'Cojup' moraines and are included here in Stage 1 together with a moraine dated at between 65 ka and 39 ka (Figures 2.10A, F) in the Jeullesh Valley at the southern end of the Cordillera Blanca. This latter moraine is the oldest moraine dated in the southern part of the study area (Smith and Rodbell, 2010).

Stage 2 (35 – 19 ka)

Synchronicity between the global Last Glacial Maximum (LGM; 22 – 19 ka) and the maximum extent of glaciation in the southern hemisphere, in particular the broader Andes in South America, is a controversial topic. There is considerable uncertainty

regarding the timing of the local LGM in the Peruvian and Bolivian Andes (La Frenierre et al., 2011; Mark et al., 2017) and the most recent approximation for the timing of this is 25.1 ka (based on averaging terrestrial cosmogenic nuclide data from 12 mountain ranges in Perú and Bolivia; Smith et al., 2008). However, there are large uncertainties with this date (up to ± 7.2 ka) and statements regarding the timing of the local LGM should be interpreted with caution. An early local LGM at between 32 – 28 ka is postulated to have occurred in the tropical Andes on the basis of moraine dates obtained from Ecuador, Perú, and Bolivia (Smith et al., 2008). In other parts of the Peruvian Andes near Lake Titicaca, the local LGM is estimated to have occurred between 22 – 19 ka (Seltzer et al., 2002) and to have been relatively modest in comparison to previous glaciations.

In the Cordillera Blanca, the moraine group 'Rurec' is classified here as belonging to Stage 2 (Rodbell, 1993) and includes moraines found at the mouths of the glaciated valleys Llaca, Cojup and Quilcayhuanca (Figures 2.10A, C); in the Rurec and Uquian valleys (Figures 2.10A, D); and the Quesque Valley (Figures 2.10A, E). This grouping of 'Rurec' moraines was initially assigned a large age range (32-20.5 ka, 45.6-27 ka, 132 -75 ka; Rodbell, 1993), but subsequent revision of these dates has reduced the range to 29-20.5 ka with a mean age of 23.4 ka (Farber et al., 2005) or 20.5 ka (Bromley et al., 2009). In the Jeullesh Valley, one moraine considered to fall within Stage 2 has an estimated age of between 32-27ka (Smith and Rodbell, 2010; Figures 2.10A, F).

Outside the Cordillera Blanca, a moraine group in the Cordillera Huayhuash (Figure 2.3) has been dated to a minimum age of 26 ka, and is interpreted to have formed during ice recession following a glacial maximum during Marine Isotope Stage (MIS) 2 (29-14

ka; Lisiecki & Raymo, 2005). A second moraine group in the same region has been dated at ~22-20 ka and is interpreted to represent a local ice advance prior to the onset of an extended period of retreat (Hall et al., 2009). In the Junin Plain (Figure 2.3), a moraine group is thought to have formed around 31 ka (Smith et al., 2008) during the local LGM and prior to the global LGM (22-19 ka). In the Cordillera Vilcanota (Figure 2.3), a cluster of well-nested moraines in the Upismayo and Jalacocha valley, classified as the U3 sequence by Mark et al. (2004), was determined to be of MIS 2 age based on a maximum-limiting radiocarbon date of ~34.4-31.7 ka and a minimum-limiting radiocarbon date of 16.8 ka (Goodman et al., 2001). Mark et al. (2002) determined a minimum-limiting age from nearby Laguna Casercocha of about ~20 ka, and concluded that the U3 moraine sequence represents two different MIS 2 advances, one at 16.65 ka and the other at ~20 ka. At the southern end of the Cordillera Occidental (Figure 2.3), a group of moraines on Nevado Coropuna, thought to be concurrent with the Group C (Junin Plain) and Rurec (Cordillera Blanca) moraines (Bromley et al., 2009), were estimated to have an age of 21.4-20.7 ka (Bromley et al., 2009). Another series of moraines identified ~14 km SW of the Quelccaya Ice cap (Figure 2.3) are constrained by a minimum-limiting radiocarbon date of 25.5 ka (Goodman et al., 2001).

Stage 3 (19 – 11.7 ka)

The moraines classified here as having formed during Stage 3 in the Cordillera Blanca formed post local LGM (after ~ 19ka). The abundance of moraines belonging to this stage suggests that post-LGM cooling in the tropical Andes was substantial and may have been coincident with the Younger Dryas chronozone (12.8-11.5 ka; La Frenierre, In

Huh, & Mark, 2011; Jomelli et al., 2014). However, this could also reflect a period in which higher rates of sediment supply provided the material to build these landforms. Post-LGM climatic cooling was preceded by the Antarctic Cold Reversal (ACR; 14.5-12.9 ka) in the southern hemisphere; both cooling events may be recorded by advances of the Andean tropical glaciers (Jomelli et al., 2017). Ice core records from Nevado Huascarán indicate periods of cooling at the onset of the Antarctic Cold Reversal just prior to the start of the Younger Dryas (Thompson et al., 1995).

In this study, the largest number of dated morainic features (n = 50) identified within the Cordillera Blanca fall within Stage 3. These moraines, often found at the mouths of linear valleys, are some of the largest and most pronounced in the region and indicate that this stage was a significant ice expansion/moraine building period. In addition, the size and morphology of these moraines has allowed them to be preserved despite the many tectonic and surface processes (e.g. landslides, flooding) active within the Cordillera Blanca.

In the northern part of the Cordillera Blanca., Stage 3 moraines can be found at the mouths of the Parón and Llanganuco valleys as well as in areas bordering adjacent mountains, such as Mount Huascarán (Figures 2.10A, B). Stage 3 moraines can also be found farther south at the mouths of the LLaca, Cojup and Quilcayhuanca valleys (Figure 2.10A, C) and can be found up-valley from Stage 2 moraines in the Rurec and Uquian valleys (Figures 2.10A, D). In the Quesque Valley (Figures 2.10A, E) the sole moraine that falls within this stage is dated to have a mean age of 13.8 ± 0.4 ka and is interpreted to have formed during the last glacial advance before a period of ice retreat (Stansell et al., 2017).

Rodbell and Setlzer (2000) examined a lacustrine sedimentary sequence from a former glacial lake (Glacial Lake Breque; Breque Site in Figure 2.10D) and were able to determine through radiocarbon dating, a glacial readvance in the Uquian valley that culminated at 12.9 ka; the age of this readvance was later supported by cosmogenic dating of the moraine in this area at between 13.2 ±0.5 and 10.4 ±0.4. ka (Farber et al., 2005). This event followed the formation of moraines down-valley prior to 18 ka (Rodbell, 1993).

In the southern part of the Cordillera Blanca, the oldest moraines dated post-local LGM can be found in the Jeullesh, Quenua Ragra and Tuco valleys (Figures 2.10A, F). A significant moraine-building period occurred in the Jeuleush Valley at 12.4 ka and in the Tuco Valley at 12.5 ka (Glasser et al., 2009). Moraines in the Jeullesh and Quenua Ragra valleys have been dated at between 18 and 15 ka (Smith and Rodbell, 2010), consistent with evidence indicating a late-glacial readvance or still stand at this time (Garreaud et al., 2003). It has been noted that there are no moraines in these valleys that date to within the Younger Dryas between 12.8 and 11.6 ka (Mark et al., 2017).

A series of moraines in the Junin Plain region of Perú (Figure 2.3) have been dated to around 16.1 ± 1.7 ka (Bromley et al., 2009). In the Cordillera Oriental (Figure 2.3), radiocarbon data suggest that by ~14ka there was a 50% reduction in glacier extent relative to MIS 2 maxima at between 29 and 14 ka (Rodbell, 1993). There is further evidence of a re-expansion of ice between ~14.2 and 12 ka, followed by rapid deglaciation, and the area became ice free between 12.0 and 11.0 ka (Rodbell, 1993; La Frenierre et al., 2011). Additional data to indicate Stage 3 glacial expansion in Perú comes from moraine groups in the Cordillera Huayhuash, (dated to 14-13 ka; Hall et al., 2009), the Quelccay Ice Cap

(with a minimum-limiting radiocarbon date of 13.1 and 12.7 ka; Mercer and Palacios, 1977; Goodman et al., 2001) and in the Nevado Coropuna (moraines dated to 14.2-10.6 ka; Bromley et al., 2009). Evidence for glacial expansion in both the Cordillera Blanca and other parts of Perú during Stage 3 is also congruent with the results of sedimentation flux analysis of 13 lakes in Perú and Bolivia conducted by Rodbell et al. (2008) who identified a period of increase clastic sediment flux from 18 to ~14 ka.

Stage 4 (11.7 – ~1 ka)

Moraines and features mapped here as recording Stage 4 glacial events are considered to have formed between the start of the Holocene (after 11.7 ka, Pillans and Gibbard, 2012) and approximately one thousand years before present (i.e., prior to the Little Ice Age).

It is interesting to note that there is no record of Stage 4 (mid-to-late Holocene (7-5 ka) glacial readvances or stillstands recorded by moraines or other features in the northern valleys of the Cordillera Blanca such as Cojup, Llaca, or Parón (Figures 2.10A, B, C); all glacial features considered to have formed during this stage are located in the southern valleys. At the Glacial Lake Breque site (Figures 2.10A, D), Rodbell (1993) dated a series of moraines up-valley of the former lake and determined that the ice front retreated ≥ 1 km from the location of the former lake by ~10.9 ka and had retreated ≥ 5km prior to ~7.3 ka. The moraines up-valley from the Glacial Lake Breque site are therefore considered to belong to Stage 4 (Figure 2.10A, D).

In the Queshque Valley (Figures 2.10A, E) a series of moraines immediately up-valley from the Lower Queshcocha lake are dated to 10.8 ±0.1 ka; further up-valley, a

nested pair of end moraines enclosing Upper Queshquecocha lake date to 10.5 ± 0.4 ka (n = 4), and a belt of closely spaced right-lateral moraines further up-valley and adjacent to Upper Queshquecocha date to 10.4 ± 0.5 ka (Figure 2.10E; Stansell et al., 2017). Approximately 3 km up-valley from Upper Queshquecocha, three boulders on an end moraine yield a mean age of 9.4 ± 0.3 ka, and an end moraine located ~0.75 km inside the ~9.4 ka ice limit yields boulder ages ranging from 6.2 ± 0.1 to 0.21 ± 0.02 ka (Figure 2.10E; Stansell et al., 2017). Lastly, a right-lateral moraine crest perched 150 m above New Lake dates from 3.5 ± 0.1 to 0.25 ± 0.01 ka (Stansell et al., 2017). These latter dates have large ranges that may result from inherited cosmogenic radionuclides or post-depositional boulder instability (Stansell et al., 2017).

In the Jeullesh Valley in the southern part of the Cordillera Blanca (Figures 2.10A, F), three moraines date to 10.8 ka, 9.7 ka, and 7.6 ka (Glasser et al., 2009) and in the Tuco Valley, two moraines date to 11.3 and 10.7 ka (Glasser et al., 2009). These moraines are interpreted to have formed as a result of three (or four) stillstands or minor advances during glacier recession between the period of 12.5 – 7.6 ka.

Outside of the Cordillera Blanca, in the Cordillera Huayhuash (Figure 2.3), Hall et al. (2009) interpret their Stage 4 moraines to have originated from a minor middle Holocene advance between ~5.6 and 3.5 ka. Elsewhere in the Andes, such as in the Patagonian Ice fields and Tierra del Fuego, there is ample evidence of late Holocene glacial readvances and stillstands during the Late Holocene (i.e. Glasser *et al.*, 2004; Haberzettl *et al.*, 2007; Rodbell, Smith and Mark, 2009; Davies *et al.*, 2020).

Stage 5 (1 ka – 0.15 ka)

Glacial Stage 5 includes features produced by glacial fluctuations between ~1 ka and 0.15 ka (~1000 CE – 1850 CE). The most prominent climatic chronozone in this Stage is the Little Ice Age (LIA), a period of cooling experienced in Europe between 1200 CE and 1900 CE (Matthews and Brifa, 2005; Clague et al., 2009). Ongoing research in Perú and the Cordillera Blanca, is attempting to determine if the cooling experienced during the LIA in Europe was synchronous with cooling in the tropical Andes (Jomelli et al., 2007; Solomina et al., 2007; Jomelli et al., 2009; Solomina et al., 2016; Mark et al., 2017; Emmer et al., 2021).

In the Cordillera Blanca, two different moraine groups (Group 3 and Group 4 of Rodbell, 1972) are considered to have formed by glacial readvances that terminated before 1750-1800 CE and during the late 1800s respectively (Rodbell, 1972). These moraines are included here in Stage 5 (Figures 2.10A, B, C, D, E). In the northern part of the Cordillera Blanca (Figures 2.10A, B), moraines reclassified here as Stage 5 moraines (formerly Group 3 of Rodbell, 1992) occur on the valley sides of both the Parón and Llanganuco valleys. Lichenometric studies of the frontal and lateral moraines of the Artensonraju, Broggi, Cancahua, and Checoulacraju glaciers (Figure 2.10B) identify them to be of LIA age (Solomina et al., 2007). The large J-shaped moraine of the Jatunraju glacier is estimated to have formed in the past few hundred years (Clapperton, 1972; Seltzer and Rodbell, 2005) and is considered here to be a Stage 5 moraine. Towards the south (Figures 2.10A, C), the frontal moraines of Llaca Lake and Lake Palcacocha are determined to be of LIA age and fall into glacial Stage 5 (Solomina et al., 2007) as do the lateral moraines of the Uruachraju and Yanamarey glaciers (Figures 2.10A, D; Solomina et al., 2007). In the Churup Valley,

two frontal-lateral moraines are identified to be around LIA age and also fall into Stage 5 (Emmer et al., 2019; Figure 2.10C). There are no dated moraines that fall within Stage 5 in the southern part of the Cordillera Blanca (Figure 2.10A, D, E).

Lichenometric studies have identified the time between 1590-1720 CE as the period in which numerous prominent terminal and lateral moraines formed in the Cordillera Blanca (Solomina et al., 2007); this period of ice advance is coincident with cold and wet phases interpreted from ice-core data from the Quelccaya Ice Cap that signal increased net accumulation in the region (Thompson et al., 2000). Two less prominent ice advances were also identified between 1780 and 1880 (Solomina et al., 2007). Compilation of data from 123 moraines associated with 24 glaciers in the Cordillera Blanca determined that an early LIA advance occurred around 1330 ± 29 CE, the LIA maximum glacial advance was reached around 1630 ± 27 CE, and was followed by three minor glacial advances at 1670 ± 24 CE, 1730 ± 21 CE, and 1760 ± 19 CE (Jomelli et al. 2007).

Beyond the Cordillera Blanca, five successive moraines at Qori Kalis Glacier on the Quelccaya Ice Cap (Figure 2.3) in southern Perú, are dated to have formed at CE 1500 ± 20, 1635 ± 20, 1685 ± 20, 1705 ± 10, and 1795 ± 10 (Jomelli et al., 2009). Comparing the timing of the Qori Kalis Glacier advances and the Quelccaya Summit Dome ice core records (Thompson et al., 2013) Stroup et al. (2014) deduced that temperature rather than accumulation rate was the main driver of the glacial fluctuations. A synthesis of LIA data for tropical glaciers in Perú, Bolivia, Ecuador, Colombia and Venezuela made by Jomelli et al. (2009) determined synchronicity of several glacial advances within the tropical Andes. It appears that the maximum glacier extent during the LIA in Perú and Bolivia

occurred between 1680-1730 CE and around 1730 CE in Ecuador, Colombia and Venezuela (Jomelli et al., 2009).

Stage 6 (0.15 ka / 1850 CE – present)

Stage 6 glacial events are those that occurred between the end of the LIA (~1850 CE) and the present. This time period is marked by rapid glacier recession in the Cordillera Blanca. In the northern region (Figures 10A, B), five moraines identified as belonging to Stage 6 at Broggi Glacier range in age from 1850 to 1970 CE (Figures 2.9A, B; Solomina et al., 2007). At Yanamarey Glacier (Figure 2.10D), subglacially-formed roche moutonées were dated to 1980 CE (Solomina et al., 2007). Moraines or other glacial features formed in this time period have not been identified or dated in the southern region of the Cordillera Blanca.

Tropical glaciers are noted to have retreated at faster rates than in other mountainous regions of the world during the 20th century (Rabatel et al., 2013). Between the LIA maximum extent and the beginning of the 20th century, individual glaciers in the Cordillera Blanca retreated an average distance of ~1000m (~30% of their length; Vuille et al., 2008a). The majority of glacier shrinkage and tongue retreat recorded in the Cordillera Blanca during the 20th century, occurred between 1940 and 1950 CE, when a significant rise of the ELA was also documented (Vuille et al., 2008a). However, at least three phases of advance may also have occurred during the 20th century; one in the mid-1930s (Kaser, 1999), one in the late 1970s (Kaser and Georges, 1997), and one in the early 1990s (Ames and Francou, 1995; Georges, 2004).

Glacier margin retreat during the 20th century has been accompanied by significant loss of ice volume. From 1948 to 1982 CE volume loss on Yanamarey glacier (Figure 2.10D) was estimated at 22×106 m3, with an additional loss of 7×106 m3 between 1982 and 1988 CE (Hastenrath and Ames, 1995). Mark and Seltzer (2005) estimated a loss of 57×106 m3 in glacier volume between 1962 and 1999 CE in the Queshque Massif of the southern Cordillera Blanca (Figure 2.10E). This translates into an area-averaged glacier ice thinning of 5–22 m and an estimated ELA rise of 25–125m, depending on the aspect of the glacier.

2.5 DISCUSSION

2.5.1 Late Quaternary Glaciation in the Cordillera Blanca

This study synthesizes and maps previously published data pertaining to the dating of late Quaternary glacial features in the Cordillera Blanca and has identified six major stages of glacial advance and/or moraine building. The proposed stages provide a relative chronology of late Quaternary glacial events, span geographic areas within the Cordillera, and provide a framework for future researchers aiming to reconstruct past glacier behavior in tropical Andean regions (Figure 2.11).

The majority of the age estimates for each of the six stages are based on lichenometric or CRN dates obtained from boulders located on end and lateral moraines within or at the mouths of narrow linear valleys draining the Cordillera Blanca. It is assumed that the moraines formed at times when the glacier occupying the valley advanced to a stillstand position that allowed glacially transported debris to accumulate along its margin. The identification of numerous moraines formed by different glaciers in the same region at

Figure 2.11: Reconstructed retreat of ice in the Gueshque Valley (35 - 9.4ka; see Figure 2.10E for location) based on the location of dated moraines in the valley (dates from Stansell et al. 2017). Image source: Google Earth (2016b).

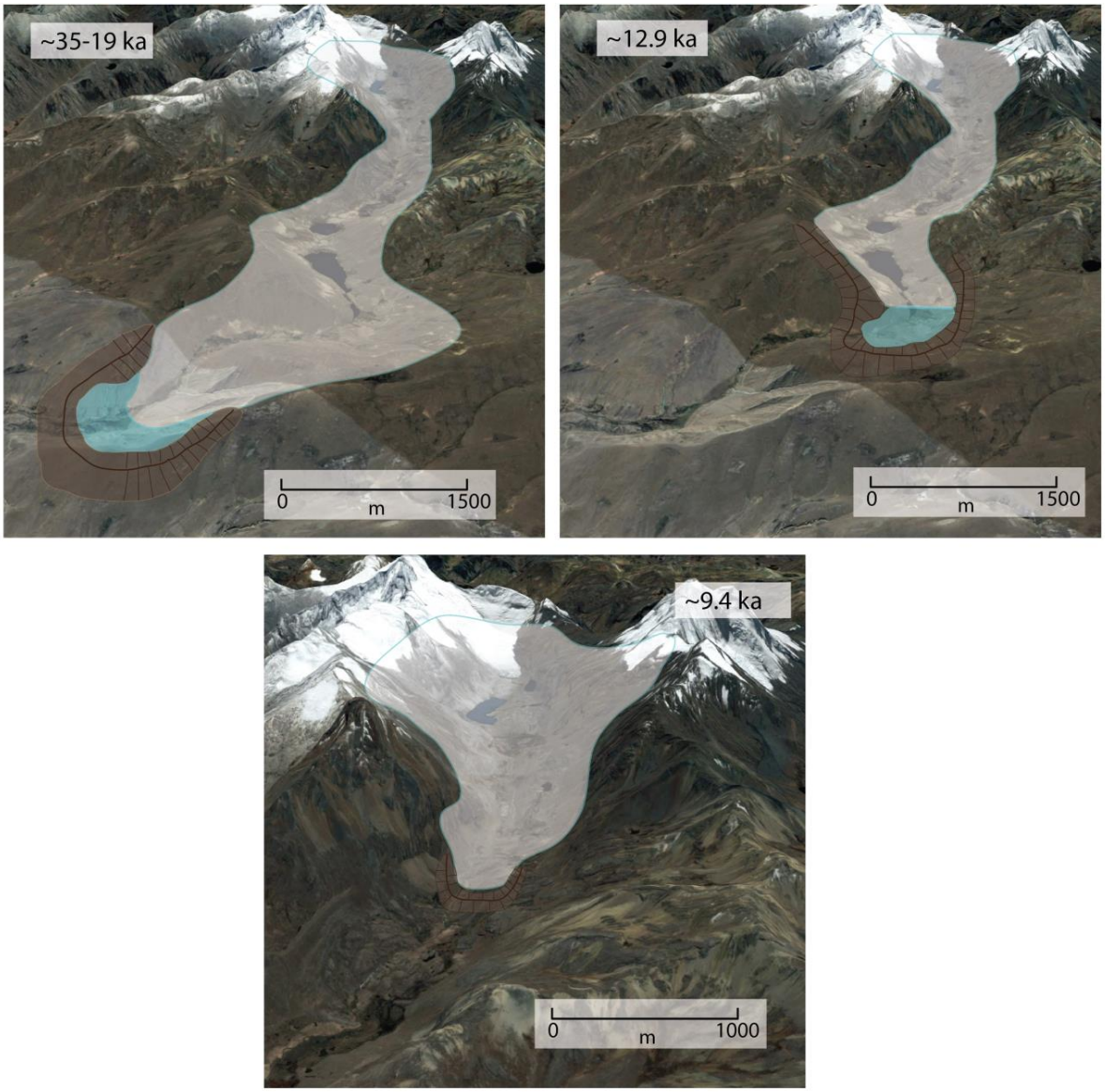
~35-19 ka
0
m
1500
~12.9 ka
0
m
1500
~9.4 ka
0
m
1000

approximately the same time can be interpreted to indicate that regional climatic conditions were favourable for glacier expansion and/or equilibrium. The six stages of glacial expansion identified here are therefore interpreted to reflect regional climatic conditions conducive to glacier growth. The broader question of whether these regional stages are more broadly synchronous with those documented in South America, the Northern Hemisphere, and globally will be examined below. Figure 2.12 illustrates the approximate age ranges of the glacial features dated in the Cordillera Blanca in the five regions shown in Figure 2.10 B-F together with the estimated age of significant climate events of importance in the southern hemisphere. The synchronicity or asynchroniticty of glacial behaviour in the Cordillera Blanca relative to these larger climate events needs further research (Mark, Stansell and Zeballos, 2017) as factors such as local climatic forcing (i.e. ENSO) are major influences on glacial behaviour (Shakun *et al.*, 2015; Veettil and Kamp, 2017). The dated features in the Cordillera Blanca suggest a broadly synchronous pattern of glacial behavior within the region that spans several global cooling events.

Moraines classified in this study as having formed during Stage 1 include those dated to be older than 35 ka; only seven such features were mapped for the Cordillera Blanca. The earliest dated evidence of late Quaternary glaciation in the Cordillera Blanca comes from a frontal moraine in the Cojup Valley dated to 441 ka (Farber et al., 2005); elsewhere in Perú ages of 67 ka (Junin Plain; Mercer and Palacios, 1977) and 41.5 ka (Cordillera Vilcanota; Goodman et al., 2001) have been obtained. In contrast, in other parts of the Andes, much earlier evidence of Late Quaternary glaciation is recorded. In Argentina and Chile substantial ice caps were established by 14 Ma (Heusser, 2003; Rabassa, 2008);

Figure 2.12: Chart summarizing the age ranges of the dated glacial features in each of the five regions identified within the Cordillera Blanca (Figures 2.10A-F) and the timing of significant global cooling events. Each vertical bar represents the minimum and maximum age of landforms within the region. A dashed line represents data given as age ranges. The timing of the Younger Dryas (12.8-11.5 ka) and the Antarctic Cold Reversal (14.5-12.9 ka) are based on ages presented by Jomelli et al. (2017), and the age of the Oldest Dryas is based on Pausata and Löfverström (2015). The age range for the Global Last Glacial Maximum (GLGM; 23 – 19 ka) is from Hughes et al. 2013.

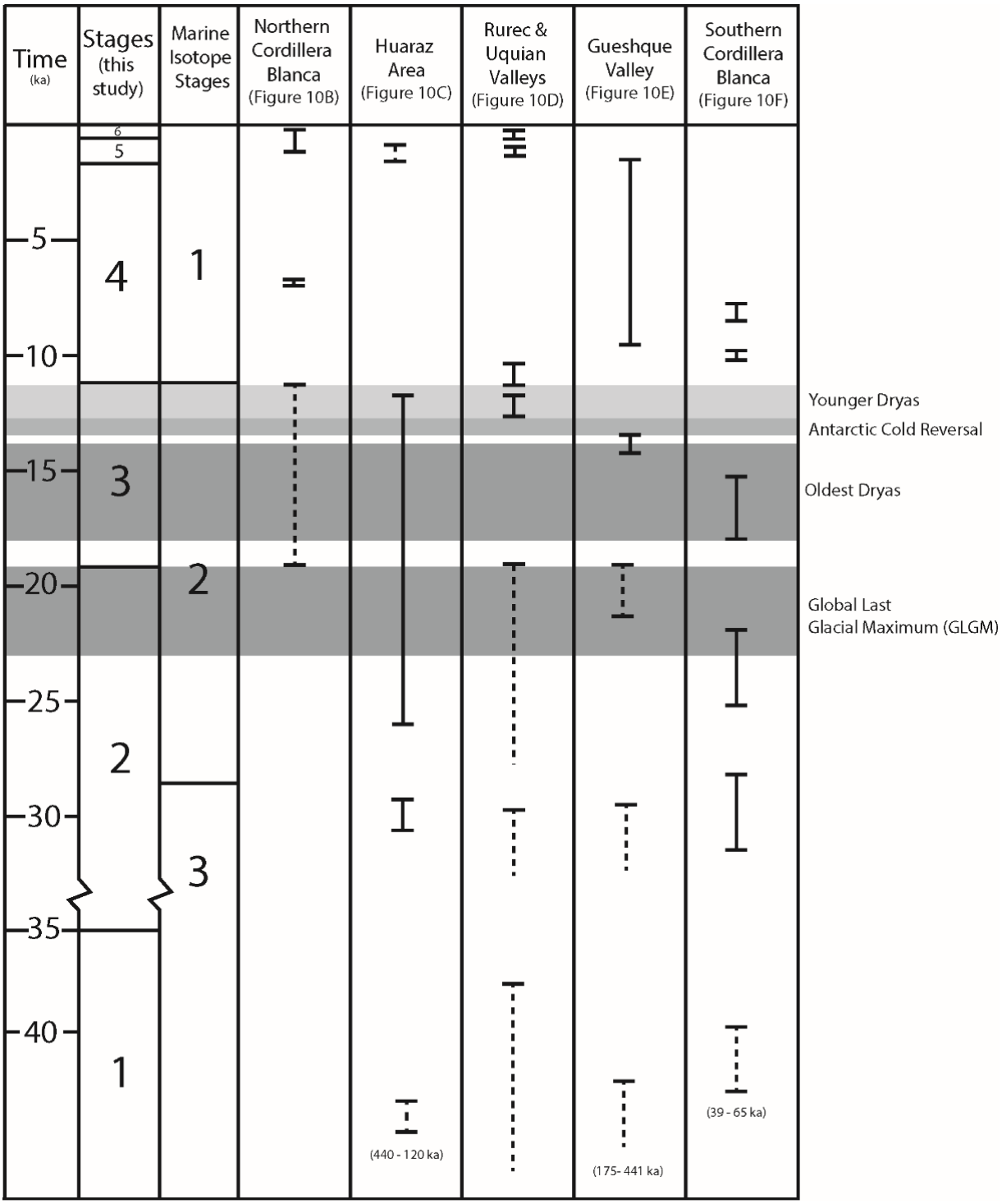
Time
(ka)
Stages
(this
study)
Marine
Isotope
Stages
Northern
Cordillera
Blanca
(Figure 10B)
Huaraz
Area
(Figure 10C)
Rurec &
Uquian
Valleys
(Figure 10D)
Gueshque
Valley
(Figure 10E)
Southern
Cordillera
Blanca
(Figure 10F)
6
5
4
3
2
1
2
3
1
5
10
15
20
25
30
35
40
Younger Dryas
Antarctic Cold Reversal
Oldest Dryas
Global Last
Glacial Maximum (GLGM)
(440 - 120 ka)
(175- 441 ka)
(39 - 65 ka)

in Bolivia the earliest late Quaternary glaciation is dated to at least 3.25 Ma (Clapperton, 1983), and in Colombia to 2.6 Ma (Helmens, 2011). In Europe and North America substantial late Quaternary ice sheets had developed by 1.2 – 1 Ma (Ehlers and Gibbard, 2011). These regional differences in the timing of the glacial activity. It is very likely that glaciation may have affected the Cordillera Blanca much earlier and more extensively than current evidence suggests; the highly dynamic environments of the Cordillera Blanca that promote the reworking of sediments and landforms have prevented preservation of any record of these earlier events.

Twenty percent of all the glacial features mapped in the Cordillera Blanca (Figures 2.10A – 10F) are considered to belong to Stage 2 and are dated between 35ka and 19 ka. This Stage is coincident with the period of greatest global ice volumes during the last glacial cycle (the Global Late Glacial Maximum: GLGM; Martinson et al., 1987) and is associated with the global eustatic sea level low dated to 18 14C ka Bp (Yokoyoma et al., 2000). The GLGM has been given an assigned chronozone between 23-19 ka (Hughes et al., 2013).

The majority of Stage 2 moraines in the Cordillera Blanca have been dated to around 20.5 ka (Figures 2.10C, 2.10D, 2.10E; Rodbell, 1993; Farber et al., 2005; Bromley et al., 2009). Other moraine clusters elsewhere in Perú and Bolivia have similar ages: in the Cordillera Huayhuash these are dated at 22-20ka (Perú; Hall et al., 2009); in the Junin Plain and Cordillera Real at 25-22 ka (Bolivia; Wright, 1983; Smith et al., 2005a, b); and in the Nevado Coropuna at ~23.5-24.5ka and ~21.1-20.7 ka (Bromley et al., 2009). These dates indicate there was an MIS 2 advance in the Cordillera Blanca that reached its maximum sometime between 25-20 ka and agree reasonably well with the timing of the GLGM.

However, there is still some debate about the placement of the local Late Glacial Maximum within the tropical Andes. Studies that involve surface exposure dating with CRNs suggest that the local LGM may have been either much earlier (32-28 ka; Smith et al., 2005a, b) or close to (24 ka; Zech et al., 2007) the timing of the GLGM depending on the scaling method used (Smith et al., 2008). Most recently, Mark et al. (2017) calculated the mean cosmogenic ages for all moraines considered to have formed during the LLGM (i.e. Stage 2) to be about 25.1 ka ± 4 ka. While consensus on the precise timing of LLGM in the tropical Andes has yet to be reached, there is evidence to suggest a significant late glacial stillstand or readvance sometime between 18-15 ka (Smith et al., 2008; Zech et al., 2008, Zech et al., 2010; Mark et al., 2017 In contrast, the temperate glaciers of Chile and Argentina (lying between 30 to 40 S°) are stated to have reached their maximum extent much earlier at 35-40 ka, while glaciers south of 40 S° experienced maxima synchronous with the Global LGM around 23 – 19 ka (Zech et al., 2008; Medelova et al., 2017; Mark et al., 2017; Davies et al., 2020). The variability in local glacial maxima in different regions of the Andes suggests that strong local forcing factors controlled glacier behaviour and may have overwhelmed global climatic signals (Hughes et al., 2013).

The moraines included in Stage 3 formed in the time interval between 18 and 11.7 ka and record glacial activity that occurred after the local LGM and into the beginning of the Holocene. Stage 3 includes the greatest number of moraines mapped in the Cordillera Blanca (35.7%) which are interpreted to record stillstands or readvances as glaciers retreated upvalley from their LLGM position. Stage 3 encompasses three widely recognized cooling periods: the Oldest Dryas (also known as Heinrich event 1), a major

cooling event recorded in the Northern Hemisphere that spanned from ~18 ka – 14.7 ka (Pausata and Löfverström, 2015), the Antarctic Cold Reversal (14.5-12.9 ka), and the Younger Dryas (12.8-11.6 ka).

The Oldest Dryas events in the Cordillera Blanca, are considered to have a mean date of ~15.4 ka (Rodbell, 1993a, Farber et al., 2005; La Frenierre et al., 2011). This date is consistent with Oldest Dryas features reported from other regions of the tropical Andes, including the Junin Plain and Cordillera Real in Perú at 16.1 ka (Smith et al., 2005a,b; Zech et al., 2007; Bromley et al., 2009), the Rucu Pichichan and Poetrerillos Platea in Ecuador at ~15.4 ka (Heine and Heine, 1996), and the Cordillera Vilcanota in Bolivia at 16.9ka (Mark et al., 2002). The abundance of moraines dated within the Oldest Dryas period suggests that cooling climatic conditions caused numerous glaciers in the tropical Andes to experience either stillstand or readvance.

Following the Oldest Dryas, southern polar latitudes experienced a period of cooling, the Antarctic Cold Reversal (ACR: 14.5-12.9 ka), that also influenced glaciation in the tropical Andes (Jomelli et al., 2017). Although only seven moraines date from this stage in the Cordillera Blanca (Figure 2.10C, 10D, 10F; Bromley et al., 2009; Smith and Rodbell, 2010; Stansell et al., 2017), a recalculation of 226 ages from 53 moraines within the Tropical Andes of Venezuela, Colombia, Perú, Bolivia and northern Argentina by Jomelli et al. (2017) determined that most Andean glaciers reached their maximum extent during the ACR. Several other regions in Perú record synchronous glacial advance or stillstand events coincident with the timing of the ACR: in the Cordillera Huayshuash (14-13ka; Hall et al., 2009); Quellccaya Ice Cap (13.3-12.9ka; Goodman et al., 2001; Mark et

al., 2002), and Nevado Coropuna (13 ka; Bromley et al., 2009). In addition, Mark et al., 2017, calculated a mean age for ACR boulders on moraines in Perú and Bolivia to be 13.7 ka.

Following the ARC a period of cooling (the Younger Dryas: 12.8-11.6 ka) is recorded over most of the Northern Hemisphere (Jomelli et al., 2017; Mark et al., 2017). In the Cordillera Blanca three moraines are dated to near the beginning of the YD: in the Queshque Valley (Figure 2.10E; Stansell et al., 2017); at the Breque Site (Figure 2.10D; (Rodbell and Seltzer, 2000), and in the Jeullesh and Tuco valleys (Figure 2.10D; Glasser et al., 2009). This suggests that some regions of the tropical Andes experienced cooling conditions synchronous with those in the Northern Hemisphere, although some studies suggest that the Younger Dryas had minimal impact on tropical glaciers (Smith et al., 2008).

Stage 4 features developed in the time interval between the start of the Holocene (11.7ka) and 1 ka. Only 9.3% of features mapped in the Cordillera Blanca formed during this time, suggesting that there may have been little variability in ameliorating climatic conditions as the glaciers receded up-valley. Features that formed during Stage 4 are found mostly in the southern region of the Cordillera Blanca, in the Uquian (Figure 2.10D); Quesque (Figure 2.10E); Jeullesh and Tuco Valleys (Figure 2.10F). In the Jeulleush Valley a terminal moraine dated to 7.6 ka located 1.5 km below the present-day glacier terminus was suggested to be coincident with an 8,200 year cooling event recorded in Greenland and elsewhere (Glasser et al., 2009). The apparent absence of features formed during the early to mid-Holocene is also noted in other regions of the Tropical Andes; the few features that

have been dated are located at Cordillera Vilcamba (~8.6 ka; Perú; Licciardi et al., 2009), Cordillera Vilcanota (2.9 ka; Perú; Goodman et al., 2001), Cordillera Cochamamba (7.0 ka; Bolivia; Zech et al., 2007) and Nevado Sajama (7.1-4.05 ka; Bolivia; Smith et al., 2009).

During the Holocene, glaciation in the Northern Hemisphere followed a general trend of recession during the period from early-mid Holocene to the late Holocene, followed by several advances during the Neoglacial (after 5 ka into the LIA) corresponding to general cooling periods in the North Atlantic (Solomina et al., 2015). Glaciers in the tropical Andes follow a similar pattern in having the largest advances/stillstands during a period of overall retreat at the beginning of the Holocene, followed by less frequent advances of moderate amplitude in the middle of the Holocene (Solomina et al., 2015). Unfortunately, few glacial features dated to the mid Holocene are preserved within the Cordillera Blanca to allow more detailed correlation with events that occurred during this period in the Northern Hemisphere.

Stage 5 includes features that have been dated from 1 ka to 0.85 ka. Twenty-five percent of the features mapped in the Cordillera Blanca belong to this stage. Most of these features are located in the northern Cordillera Blanca where most of the lichenometric studies have been undertaken (Jomelli et al., 2007). It is important to note that glaciers across Europe were advancing during this time period due to cooler climatic conditions ascribed to the Little Ice Age (LIA: Matthews and Brifa, 2005; Clague et al., 2009).

Jomelli et al. (2007) examined lichenometric data from 123 moraines associated with 24 glaciers in the Cordillera Blanca and identified an early LIA glacial advance ~1330 CE, a second advance (classified as the LIA maximum) at 1630 CE, and three other

advances at 1670 CE, 1730 CE and 1760 CE. While the maximum glacial extent during the Little Ice Age for the Cordillera Blanca is considered to have occurred around 1630 CE, in Bolivia it occurred between 1657-1686 CE (Rabatel et al., 2006, 2008), in Ecuador between 1720 CE (Hastenrath, 1981) and 1830 CE (Jomelli et al., 2007b), and in Venezuela two advances were recorded between 1640 and 1730 CE (Polissar et al., 2006; Jomelli et al., 2007). Overall, it appears that in Bolivia and Perú (the outer tropics) the maximum LIA extent was around 1630-1680 CE and in Ecuador, Colombia and Venezuela (the inner tropics) it occurred earlier around 1730 CE (Jomelli et al., 2009). This may reflect a shift from wetter conditions between 1650 CE and 1750 CE to drier and colder conditions during the 19th century (Jomelli et al., 2009).

Stage 6 covers the time between 1850 CE and present time, encompassing the end of the 19th century and recent glacier fluctuations. Only 7 features of this age are mapped in the Cordillera Blanca (Figure 2.10B). The absence of Stage 6 features in the region may be due to the absence of chronological data for features that lie close to current ice margins and the current mode of progressive glacial retreat that does not allow significant morainic features to develop. However, the direct monitoring of glacier activity during Stage 6 is facilitated by the plethora of aerial imagery and remote sensing data available (Silverio and Jaquet, 2016). These data indicate that tropical glaciers have retreated at faster rates than in other mountainous regions of the world during the 20th century (Rabatel et al., 2013).

Much of the glacier shrinkage and tongue retreat recorded in the Cordillera Blanca during the 20th century, occurred between 1940-1950, when a significant rise of the ELA

was documented (Vuille et al., 2008a). In Bolivia, glacier retreat started in the late 19th century, experienced a relative slowdown between the 1910s and the 1930s, increased again after the 1940s, and very rapid retreat rates resumed during the 1980s and 1990s (Rabatel et al., 2006).

2.5.3 Distribution of dateable glacial features in the Cordillera Blanca

Figures 2.10 A-F demonstrate regional differences in the spatial distribution of dated glacial features between the northern and southern regions of the Cordillera Blanca. The majority of the Stage 4 moraines (11.7 – 1 ka) are found in the southern region, in particular in the Rurec (Figure 2.10D), Quesque (Figure 2.10E), and the Jeullesh and Tuco Valleys (Figure 2.10F). Few features have been identified and dated in the northern region that fall within the time period of Stage 4.

The lack of dateable glacial features in the northern region of the Cordillera Blanca is likely due to differences in bedrock type, valley morphology, and the dominance of certain surface processes, such as rock avalanches and slope failures. Marginier et al. (2016) showed that maximum relief (~3km) in the Cordillera Blanca is located in the central and northern regions, where most of the 6000 m high summits are found. In contrast, relief is ~1km in the southern part of the Cordillera Blanca (Marginier et al., 2016). The greater topographic relief in the northern and central parts of the Cordillera Blanca may encourage higher rates of valley erosion by glacial and fluvial processes than in southern regions, and enhance the effectiveness of mass wasting processes in the redistribution of material from steep valley walls.

In addition, the valleys in northern and central regions of the Cordillera Blanca are carved into the Cordillera Blanca granodiorite batholith (Figure 2.4), while the valleys of the southern region are carved into Jurassic phyllites (Uquian and Quesque valleys; Figures 2.10 D, E) or Tertiary volcanic tuffs (Jeullesh and Tuco valleys; Figure 2.10F). The less resistant sedimentary bedrock of the southern region has allowed much broader and less deeply incised valleys to develop. All of the valleys along the western margin of the Cordillera Blanca lie perpendicular or orthogonal to the NW-SE trending Callejón de Huaylas Valley and the CBNF (Figure 2.4). It is therefore likely that the orientation of these valleys is fault-controlled.

While it is likely that numerous moraines and other glacial features were formed during the early to mid-Holocene (Stage 4) in the northern parts of the Cordillera Blanca, the absence of these features today may be attributed to reworking by the dynamic surface processes that operate on the steep valley slopes in this region; avalanches, rock falls, slumps or GLOFs are all mass wasting processes that could have removed or remoulded glacial landforms and sedimentary features such as moraines leaving an imperfect record of past glacial activity (Fischer et al. ,2006; Fischer et al, 2012). In addition, there may be a sampling bias from previous studies which may require a more comprehensive sampling method for all valleys throughout the Cordillera Blanca.

2.5.3 Limitations of glacial landform dating

It is important to recognize the limitations of dating landforms in order to construct the history and timing of glacial events in a region such as the Cordillera Blanca. The assumption that glacial moraines dated by lichenometry or surface exposure (CRN) dating

provide an accurate estimate of the timing of a period of glacial standstill or advance, does not account for the many dynamic moraine building or post-depositional processes that can occur. When a sample is taken from a boulder on a moraine for surface exposure dating, the calculated date reports the date the boulder (and the moraine) were stabilized rather than the extent of the glacier at that time. It is possible that a substantial amount of time elapsed between the period of glacier contact with the moraine and when it became stable (Roe and O'Neal, 2009).

Post-depositional processes related to intermittent snow cover, variable uplift, erosion of the moraine, erosion of the boulders, and/or mass wasting, create a significant amount of uncertainty in the surface exposure dating of moraines as they affect the initiation and duration of exposure. The dynamic nature of the Cordillera Blanca, in particular due to the prevalence of mass wasting and slope processes in the region, must be taken into account when considering the reliability of the dates compiled for this study (Hambrey and Ehrmann, 2004; Hambrey & Glasser, 2012). It is very likely that many of the moraines from which boulders were sampled for dating purposes were impacted by post-depositional mass wasting processes.

While this paper has relied on previously published chronological data to map and classify moraines in the Cordillera Blanca, the authors acknowledge that there is both dating and geomorphic ambiguity inherent in the data that have been used. The new interpretation of chronological data presented in this paper is meant to serve as a guide and framework for future studies that aim to better understand the glacial history of the Cordillera Blanca and broader Andean region.

2.6 CONCLUSIONS

The Cordillera Blanca is the largest tropical glaciated region in the world, yet a well-constrained and detailed glacial history of this region is still not available. This study aims to synthesize a chronology of glaciation for the Cordillera Blanca that may be used as a framework for subsequent investigations of the glacial history of the region. Six stages of Late Quaternary glacial activity in the Cordillera Blanca are proposed here, spanning from >35 ka (Stage 1) to the present (Stage 6). These stages are defined on the basis of the identification and dating of glacial features (predominantly moraines) created during the advance or stillstand of glacier margins and have been mapped throughout the Cordillera (Figure 2.10A-F). While the dates provided in this review are derived from current literature on the dating of landforms, there is a considerable amount of uncertainty regarding the accuracy of dating techniques that focus on establishing the timing of emplacement of individual boulders on glacial landforms. Despite this constraint, it is hoped that the stages of past glacial activity identified in this study provide an enhanced understanding of the regional development and history of glaciation in the region.

In parallel with glacier retreat, climate in the tropical Andes has changed significantly over the past 50–60 years. Temperature in the Andes has increased by approximately 0.1 °C/decade, with only two of the last 20 years experiencing average temperatures below those of the 1961–90 CE average (Vuille et al., 2015). Precipitation has increased slightly in the second half of the 20th century in the inner tropics and decreased in the outer tropics. The general pattern of moistening in the inner tropics and drying in the subtropical Andes is consistent with observed changes in large-scale

circulation patterns, and suggests a strengthening of tropical atmospheric circulation (Vuille et al., 2008a, 2008b). In contrast, in the central Andes of Argentina and Chile, and the Patagonian Andes, several post-LIA re-advances have been recorded over the past 100-110 years, despite the overall regional pattern of glacier recession and significant ice loss (Masiokas, et al., 2009).

The chronology of late Quaternary glacial events in the Cordillera Blanca proposed here:

1) Stage 1 (> 35 ka) includes glacial events that occurred after 800 ka with three possible discrete advances dated at 440 ka, 225 ka and 125 ka (Farber et al., 2005). A later glaciation is postulated to have terminated around 65 ka (Smith and Rodbell, 2010).

2) Stage 2 (35 – 19 ka) includes glacial events that may have occurred within the Local Last Glacial Maximum (LLGM) and the Global Last Glacial Maximum (GLGM). The earliest glaciation event within this stage is postulated to have culminated at 32 ka (Smith and Rodbell, 2010); several other glacial events followed at 23. 4 ka (Farber et al., 2005) and 20.5 ka (Bromley et al, 2009).

3) Stage 3 (19-11.7ka) is a period of overall glacial retreat that was interrupted by various episodes of stillstand and readvance that may have been synchronous with global climatic changes (e.g. the Older Dryas, Antarctic Cold Reversal, Younger Dryas).

4) Stage 4 (11.7-1ka) records a period of overall glacial retreat with occasional episodes of standstill and readvance. Most of the moraines included in this stage are found in the southern region of the Cordillera Blanca.

5) Stage 5 (1 – 0.85ka) includes evidence of glacial activity associated with the Little Ice Age, most of which has been dated with lichenometry. The earliest evidence for a LIA advance in the Cordillera Blanca occurred around 1330 ± 29 CE, followed by subsequent advances at 1630 ± 27 CE, 1670 ± 24, 1730 ± 21, and 1760 ± 19 CE (Jomelli et al. 2007).

6) Stage 6 (1850 AD – present) is the final stage that records glacial activity from 1850 CE to the present time. Glaciers in the Cordillera Blanca have experience rapid retreat in recent times and overall ice coverage has decreased from 830 km 2 in 1930 to 449 ± 56 km2 in 2016 CE.

This relative chronology of glacial activity in the Cordillera Blanca provides a foundation for future investigations of past and present geological, surface and hydrological processes operating in the region. Issues regarding the accuracy of methodologies used to establish the age of glacially-emplaced landforms and features (see Osborn et al., 2015; La Frenierre et al., 2011) continue to impede the establishment of a more complete timeline of glacial events within the Cordillera Blanca and the broader tropical Andes. It is important to establish a detailed timeline of past glacial activity in this region to better understand the duration and impact of the current rapid retreat rates experienced by tropical glaciers. Diminishing glacial coverage in the Cordillera Blanca is already impacting water supply to local communities for human consumption, agriculture and ecosystems (e.g. Buytaert et al., 2006; Vuille et al., 2008b; Mark et al., 2010; Mark et al., 2017). It has been suggested that once glaciers of the Cordillera Blanca completely melt, annual discharge to streams and rivers will be reduced by 2-30% depending on the

watershed (Baraer et al., 2012). In addition, the unstable termini of retreating glaciers often sit within glacial lakes impounded by moraine dams that are prone to failure and have the potential to release catastrophic outburst floods. Enhanced understanding of the current and past behavior of these glaciers in relation to projected climate changes will aid in developing predications of how future change will affect glacier dynamics, landscape stability, and water supply. The Cordillera Blanca is a unique area with the highest concentration of tropical glaciers on Earth; understanding its glacial history has the potential to provide insight into the nature and mechanism of past and present tropical glacier fluctuations and their relationship with atmospheric processes at local, regional and global scales.

APPENDIX 2.1

Articles used as sources of chronological data

Stages		Type of dating used	Paper
Stage 1	Before 35 ka	Rock-weathering features Radiocarbon dates	Rodbell, 1993
		Radiocarbon dating	Mercer and Palacios, 1997
		Soil weathering data Radiocarbon dating	Goodman et al., 2001
		Cosmogenic radionuclide dating (^{10}Be)	Smith and Rodbell, 2010.
		Cosmogenic radionuclide dating (^{10}Be)	Farber et al., 2005
Stage 2	34 – 19 ka	Soil weathering data Radiocarbon dating	Goodman et al., 2001
		Cosmogenic radionuclide dating (^{10}Be)	Farber et al., 2005
		Cosmogenic radionuclide dating (^{10}Be)	Smith et al., 2008
		Cosmogenic radionuclide dating (^{10}Be)	Hall et al., 2009
		Cosmogenic radionuclide dating (^{3}He)	Bromley et al., 2009
		Review	La Frenierre et al., 2011
		Review	Mark et al., 2017
Stage 3	18 – 11.7 ka	Rock-weathering features Radiocarbon dates	Rodbell, 1993
		Soil weathering data Radiocarbon dating	Goodman et al., 2001
		Radiocarbon dating	Rodbell and Seltzer, 2000
		Cosmogenic radionuclide dating (^{10}Be)	Farber et al., 2005
		Cosmogenic radionuclide dating (^{10}Be)	Glasser et al., 2009
		Cosmogenic radionuclide dating (^{10}Be)	Hall et al., 2009
		Cosmogenic radionuclide dating (^{3}He)	Bromley et al., 2009
		Cosmogenic radionuclide dating (^{10}Be)	Smith and Rodbell, 2010
		Review	Mark et al., 2017
		Cosmogenic radionuclide dating (^{10}Be) Radiocarbon dating	Stansell et al., 2017
Stage 4	11.7 – 1 ka	Rock-weathering features Radiocarbon dates	Rodbell, 1993
		Cosmogenic radionuclide dating (^{10}Be)	Glasser et al., 2009
		Cosmogenic radionuclide dating (^{10}Be)	Hall et al., 2009
		Review	Rodbell et al. 2009
		Cosmogenic radionuclide dating (^{10}Be) Radiocarbon dating	Stansell et al., 2017
Stage 5	1 – 0.85 ka	Geological mappin	Clapperton 1972
			Georges, 2004
		Radiocarbon dating	Seltzer and Rodbell, 2005
		Satellite imagery	Silverio and Jacquet, 2005
		Lichenometry	Jomelli et al., 2007
		Lichenometry	Solomina et al., 2007

		Lichenometry	Emmer et al., 2019
		Review	Jomelli et al., 2009
		Review	Solomina et al., 2016
			Silverio & Jacquet, 2016
			INAIGEM, 2018
Stage 6	0.85 ka - present	Aerial Imagery	Hastenrath and Ames, 1995
		Aerial imagery	Georges, 2004
		Satellite imagery	Silverio and Jaquet, 2005
		Satellite imagery	Silverio & Jacquet, 2016
		Satellite imagery	INAIGEM, 2018

APPENDIX 2.2

Chronological data used in Chapter 2

Sample ID	Latitude (deg S)	Longitude (deg W)	Age (BP)	Uncertainty	Method	Source
Gueshque1-A-QG1			50		Lichenometry	Rodbell (1992)
Guesque1-B-QG4			100		Lichenometry	Rodbell (1992)
Guesque1-I-QQ2			100		Lichenometry	Rodbell (1992)
Gueshque1-G-RN21			625		Lichenometry	Rodbell (1992)
Gueshque1-A-QG2			975		Lichenometry	Rodbell (1992)
Gueshque1-B-QG6			400		Lichenometry	Rodbell (1992)
Gueshque1-I-QQ3			1100		Lichenometry	Rodbell (1992)
Gueshque1-I-QQ4			1225		Lichenometry	Rodbell (1992)
Gueshque2-K-QQ6			750		Lichenometry	Rodbell (1992)
Gueshque2-J-QQ6			625		Lichenometry	Rodbell (1992)
Guesque2-L-QC1			750		Lichenometry	Rodbell (1992)
Guesque2-O-Ql			1800		Lichenometry	Rodbell (1992)
Guesque2-E-RN3			550		Lichenometry	Rodbell (1992)
Guesque2-F-RN8			1225		Lichenometry	Rodbell (1992)
Guesque2-D-RN12			475		Lichenometry	Rodbell (1992)

Guesque2-C-RN15			250		Lichenometry	Rodbell (1992)
Guesque2-G-RN20			975		Lichenometry	Rodbell (1992)
Guesque2-H-RN29			2550		Lichenometry	Rodbell (1992)
Guesque2-A-QG4			2500		Lichenometry	Rodbell (1992)
Guesque2-B-QG7			2800		Lichenometry	Rodbell (1992)
Quesque2-L-QC2			2550		Lichenometry	Rodbell (1992)
Quilloc-O-QL2			2225		Lichenometry	Rodbell (1992)
Quilloc-E-RN4			3500		Lichenometry	Rodbell (1992)
Quilloc-E-RN5			3225		Lichenometry	Rodbell (1992)
Quilloc-D-RN13			3225		Lichenometry	Rodbell (1992)
Quilloc-C-RN16			1425		Lichenometry	Rodbell (1992)
Quilloc-F-RN9			2225		Lichenometry	Rodbell (1992)
Quilloc-O-QLL1			3500		Lichenometry	Rodbell (1992)
Quilloc-H-RN28			6200		Lichenometry	Rodbell (1992)
Quilloc-A-QG3			6525		Lichenometry	Rodbell (1992)
Quilloc-B-QG8			5650		Lichenometry	Rodbell (1992)
Quilloc-K-QQ7			6200		Lichenometry	Rodbell (1992)
RioNegro-E-RN7			7300		Lichenometry	Rodbell (1992)
RioNegro-E-RN6			7300		Lichenometry	Rodbell (1992)
RioNegro-D-RN14			7330		Lichenometry	Rodbell (1992)
RioNegro-F-RN11			5800		Lichenometry	Rodbell (1992)
RioNegro-I-QQ5			6525		Lichenometry	Rodbell (1992)
HU-41	9.651	77.361	11800	290	^{10}Be	Farber et al. (2005)
HU-43	9.651	77.361	11340	350	^{10}Be	Farber et al. (2005)
PE98RU-43a	9.651	77.361	13160	460	^{10}Be	Farber et al. (2005)
PE98RU-43b	9.651	77.361	10430	450	^{10}Be	Farber et al. (2005)

PE98RU-C41	9.651	77.361	10430	420	^{10}Be	Farber et al. (2005)
PE98RUC42	9.651	77.361	10650	370	^{10}Be	Farber et al. (2005)
PE98RU-C44	9.653	77.365	12670	420	^{10}Be	Farber et al. (2005)
PE98RU-C45	9.652	77.65	10660	390	^{10}Be	Farber et al. (2005)
GV-22	9.31	77.306	19460	460	^{10}Be	Farber et al. (2005)
GV-23	9.31	77.306	15530	1140	^{10}Be	Farber et al. (2005)
GV-24	9.831	77.7307	14690	350	^{10}Be	Farber et al. (2005)
K-13	9.488	77.474	14230	670	^{10}Be	Farber et al. (2005)
K-6a	9.478	77.468	15240	580	^{10}Be	Farber et al. (2005)
K-6b	9.478	77.468	15280	730	^{10}Be	Farber et al. (2005)
K-8a	9.477	77.468	16070	790	^{10}Be	Farber et al. (2005)
K-8b	9.477	77.468	15970	730	^{10}Be	Farber et al. (2005)
K-9	9.491	77.41	14940	830	^{10}Be	Farber et al. (2005)
P98GV-C19	9.83	77.304	11940	750	^{10}Be	Farber et al. (2005)
P98GV-C20	9.83	77.304	13080	340	^{10}Be	Farber et al. (2005)
P98GV-C21	9.83	77.304	12830	580	^{10}Be	Farber et al. (2005)
HU-1	9.486	77.453	19240	580	^{10}Be	Farber et al. (2005)
HU-2	9.486	77.453	18280	430	^{10}Be	Farber et al. (2005)
HU-4	9.486	77.452	19050	470	^{10}Be	Farber et al. (2005)
K-1	9.485	77.464	28410	1900	^{10}Be	Farber et al. (2005)
K-10	9.493	77.461	29330	1200	^{10}Be	Farber et al. (2005)
K-2	9.484	77.471	16730	1700	^{10}Be	Farber et al. (2005)
K-3	9.486	77.48	20330	890	^{10}Be	Farber et al. (2005)
K-4	9.484	77.476	18620	890	^{10}Be	Farber et al. (2005)
K-5a	9.479	77.473	23610	720	^{10}Be	Farber et al. (2005)
K-5b	9.479	77.473	23920	1100	^{10}Be	Farber et al. (2005)

K-7	9.477	77.468	16980	780	^{10}Be	Farber et al. (2005)
Peru-18	9.492	77.46	17040	550	^{10}Be	Farber et al. (2005)
Peru-21	9.488	77.454	19600	740	^{10}Be	Farber et al. (2005)
K-12a	9.494	77.463	133600	5000	^{10}Be	Farber et al. (2005)
K-12b	9.494	77.463	145600	4300	^{10}Be	Farber et al. (2005)
PE-98-981	9.821	77.367	782400	24000	^{10}Be	Farber et al. (2005)
PE-98-982	9.821	77.367	207000	5000	^{10}Be	Farber et al. (2005)
Peru-1	9.502	77.463	869800	25000	^{10}Be	Farber et al. (2005)
Peru-10	9.505	77.46	237300	9400	^{10}Be	Farber et al. (2005)
Peru-12	9.495	77.464	210400	4800	^{10}Be	Farber et al. (2005)
Peru-13	9.496	77.464	205400	5900	^{10}Be	Farber et al. (2005)
Peru-16	9.494	77.463	58900	2300	^{10}Be	Farber et al. (2005)
Peru-3	9.504	77.464	285300	3300	^{10}Be	Farber et al. (2005)
Peru-4	9.504	77.464	1886200	5200	^{10}Be	Farber et al. (2005)
Peru-5	9.505	77.466	197300	2400	^{10}Be	Farber et al. (2005)
Peru-6	9.505	77.466	90780	3100	^{10}Be	Farber et al. (2005)
Peru-7	9.505	77.466	243200	5000	^{10}Be	Farber et al. (2005)
Peru-8	9.505	77.466	234400	8600	^{10}Be	Farber et al. (2005)
Peru-9	9.505	77.466	226600	5200	^{10}Be	Farber et al. (2005)
Glacial Lake Breque Moraine	9.6	7.4	12700	800	^{14}Radiocarbon	Farber et al. (2005)
Broggi - Moraine and Sandur	8.999167	77.584333	30		Lichenometry	Solomina et al. (2007)
Broggi- Moraine and Sandur	8.999167	77.584333	60		Lichenometry	Solomina et al. (2007)
Broggi - End Moraine	8.999167	77.584333	140-150		Lichenometry	Solomina et al. (2007)
Broggi - End Moraine of	8.999167	77.584333	300-340		Lichenometry	Solomina et al. (2007)

hanging glaciers						
Cancahua - End Moraine	9.086	77.548833	300-340		Lichenometry	Solomina et al. (2007)
Cancahua - End Moraine	9.086	77.548833	140-150		Lichenometry	Solomina et al. (2007)
Cancahua - Left lateral moraine	9.086	77.548833	200-220		Lichenometry	Solomina et al. (2007)
Cancahua - End Moraine overalyed by 3	9.086	77.548833	200-220		Lichenometry	Solomina et al. (2007)
Cancahua - Uppermost lateral moraine	9.086	77.548833	490-570		Lichenometry	Solomina et al. (2007)
Cancahua - External lateral moraine	9.086	77.548833	1000-1200		Lichenometry	Solomina et al. (2007)
Yanamarey 2002 - right lateral moraine	9.654333	77.27	320-360		Lichenometry	Solomina et al. (2007)
Yanamarey 2002 - right lateral moraine	9.654333	77.27	200-220		Lichenometry	Solomina et al. (2007)
Yanamarey 2002 - left lateral moraine	9.654333	77.27	340-390		Lichenometry	Solomina et al. (2007)
Yanamarey 2002 - left lateral moraine	9.654333	77.27	190-200		Lichenometry	Solomina et al. (2007)
Llaca - right lateral moraine	9.415	77.431667	300-340		Lichenometry	Solomina et al. (2007)
Llaca - right lateral moraine	9.415	77.431667	120-130		Lichenometry	Solomina et al. (2007)
Llaca - Left lateral moraine	9.415	77.431667	280-320		Lichenometry	Solomina et al. (2007)
Llaca - end moraine	9.415	77.431667	320-360		Lichenometry	Solomina et al. (2007)
Uruachraju - Left lateral moraine	9.586667	77.315167	300-340		Lichenometry	Solomina et al. (2007)

Uruachraju - right lateral moraine	9.586667	77.315167	320-360		Lichenometry	Solomina et al. (2007)
Uruachraju - left lateral moraine	9.586667	77.315167	150-160		Lichenometry	Solomina et al. (2007)
Artesonraju - left lateral moraine	8.958	77.626333	280-320		Lichenometry	Solomina et al. (2007)
Artensonraju -left lateral moraine	8.958	77.626333	170-190		Lichenometry	Solomina et al. (2007)
Checouiacraju - left lateral moraine	9.166667	77.5345	320-360		Lichenometry	Solomina et al. (2007)
Checouiacraju - right lateral moraine	9.166667	77.5345	300-340		Lichenometry	Solomina et al. (2007)
Pisco - right lateral moraine	9.015167	77.631833	340-390		Lichenometry	Solomina et al. (2007)
Huandoy (paron) - right lateral moraine	8.97133	77.698833	300-340		Lichenometry	Solomina et al. (2007)
JEU01	10.012194	77.271056	11600	400	^{10}Be	Glasser et al. (2009)
JEU02	10.006417	77.271472	12200	400	^{10}Be	Glasser et al. (2009)
JEU03	10.004333	77.271611	12800	400	^{10}Be	Glasser et al. (2009)
JEU04	10.006056	77.270111	10400	300	^{10}Be	Glasser et al. (2009)
JEU05	10.006056	77.270083	10900	300	^{10}Be	Glasser et al. (2009)
JEU06	10.00622	77.268056	11000	300	^{10}Be	Glasser et al. (2009)
JEU07	10.005722	77.266889	12800	400	^{10}Be	Glasser et al. (2009)
JEU08	10.007528	77.267194	10300	300	^{10}Be	Glasser et al. (2009)
JEU09	9.990722	77.253806	7800	200	^{10}Be	Glasser et al. (2009)
JEU10	9.990806	77.253917	7300	200	^{10}Be	Glasser et al. (2009)
JEU11	9.990889	77.254222	7900	300	^{10}Be	Glasser et al. (2009)
JEU12	9.991056	77.254639	7400	200	^{10}Be	Glasser et al. (2009)
JEU13	9.991056	77.254639	7500	800	^{10}Be	Glasser et al. (2009)

JEU14	10.004417	77.268583	9600	300	^{10}Be	Glasser et al. (2009)
JEU15	10.004667	77.268639	9700	300	^{10}Be	Glasser et al. (2009)
TUC02	10.040917	77.213944	11700	400	^{10}Be	Glasser et al. (2009)
TUC03	10.040972	77.213944	13300	400	^{10}Be	Glasser et al. (2009)
TUC04	10.053972	77.220222	11000	400	^{10}Be	Glasser et al. (2009)
TUC05	10.052778	77.218944	11500	400	^{10}Be	Glasser et al. (2009)
TUC09	10.043889	77.22125	10700	300	^{10}Be	Glasser et al. (2009)
TUC09	10.043611	77.221028	10600	300	^{10}Be	Glasser et al. (2009)
PE05-JEU-17	10.0017	77.276433	65025	3444	^{10}Be	Smith and Rodbell (2010)
PE05-JEU-21	10.001767	77.277183	58073	1755	^{10}Be	Smith and Rodbell (2010)
PE05-JEU-18	10.001717	77.276483	38927	1650	^{10}Be	Smith and Rodbell (2010)
PE05-JEU-19	10.001617	77.27645	39127	1716	^{10}Be	Smith and Rodbell (2010)
PE05-JEU-24	9.998967	77.27605	58615	3839	^{10}Be	Smith and Rodbell (2010)
PE05-JEU-23	9.998967	77.27605	55624	1906	^{10}Be	Smith and Rodbell (2010)
PE05-JEU-26	9.999117	77.276217	37315	1140	^{10}Be	Smith and Rodbell (2010)
PE05-JEU-10	10.00125	77.273183	46594	1499	^{10}Be	Smith and Rodbell (2010)
PE05-JEU-06	10.0042	77.27355	41959	2002	^{10}Be	Smith and Rodbell (2010)
PE05-JEU-08	10.002033	77.273367	29223	798	^{10}Be	Smith and Rodbell (2010)
PE05-JEU-05	10.00445	77.273817	31886	1170	^{10}Be	Smith and Rodbell (2010)
PE05-JEU-07	10.003733	77.273417	27351	1318	^{10}Be	Smith and Rodbell (2010)
PE05-JEU-09	10.001717	77.273317	28327	779	^{10}Be	Smith and Rodbell (2010)
PE05-JEU-04	9.999083	77.271517	14307	1108	^{10}Be	Smith and Rodbell (2010)
PE05-JEU-12	9.999283	77.271583	13619	466	^{10}Be	Smith and Rodbell (2010)
PE05-JEU-02	10.00885	77.27095	14852	744	^{10}Be	Smith and Rodbell (2010)
PE05-JEU-03	10.001783	77.271667	13091	602	^{10}Be	Smith and Rodbell (2010)
PE05-JEU-13	10.0014	77.265533	14798	488	^{10}Be	Smith and Rodbell (2010)

PE05-JEU-11	9.99775	77.256583	11783	560	^{10}Be	Smith and Rodbell (2010)
PE05-JEU-10	9.997533	77.25605	11348	474	^{10}Be	Smith and Rodbell (2010)
PE05-JEU-12	9.998117	77.25745	10947	454	^{10}Be	Smith and Rodbell (2010)
PE05-JEU-15	10.003533	77.2666283	7993	378	^{10}Be	Smith and Rodbell (2010)
PE05-JEU-16	10.005697	77.27005	102488	276	^{10}Be	Smith and Rodbell (2010)
PE05-JEU-14	10.0069	77.27	30224	825	^{10}Be	Smith and Rodbell (2010)
PE05-JEU-15	10.005967	77.27005	11900	510	^{10}Be	Smith and Rodbell (2010)
PE05-JEU-27	10.007767	77.268883	17714	1167	^{10}Be	Smith and Rodbell (2010)
PE05-JEU-04	10.006317	77.268	15546	594	^{10}Be	Smith and Rodbell (2010)
PE05-JEU-02	10.0073	77.2687	15052	875	^{10}Be	Smith and Rodbell (2010)
PE05-JEU-03	10.006467	77.2682	14607	520	^{10}Be	Smith and Rodbell (2010)
PE07-JEU-08	10.004317	77.269333	14315	600	^{10}Be	Smith and Rodbell (2010)
PE07-JEU-07	10.00445	77.26905	14177	767	^{10}Be	Smith and Rodbell (2010)
PE07-JEU-05	10.004667	77.268667	12353	715	^{10}Be	Smith and Rodbell (2010)
PE07-JEU-09	10.004267	77.269367	11402	382	^{10}Be	Smith and Rodbell (2010)
PE07-JEU-06	10.004683	77.268533	11078	528	^{10}Be	Smith and Rodbell (2010)
PE07-QUE-23	10.0101	77.2611	13192	627	^{10}Be	Smith and Rodbell (2010)
PE07-QUE-22	10.009683	77.260867	11487	721	^{10}Be	Smith and Rodbell (2010)
PE07-QUE-14	10.006997	77.259217	52786	231	^{10}Be	Smith and Rodbell (2010)
PE07-QUE-11	10.0095	77.26255	18521	958	^{10}Be	Smith and Rodbell (2010)
PE07-QUE-12	10.009333	77.2623	16125	913	^{10}Be	Smith and Rodbell (2010)
PE07-QUE-10	10.00985	77.262783	14206	636	^{10}Be	Smith and Rodbell (2010)
PE07-QUE-13	10.008717	77.26095	9508	469	^{10}Be	Smith and Rodbell (2010)
PE07-QUE-18	10.009733	77.257	15802	860	^{10}Be	Smith and Rodbell (2010)
PE07-QUE-17	10.009617	77.255983	13750	693	^{10}Be	Smith and Rodbell (2010)
PE05-JEU-37	10.010067	77.255017	15867	794	^{10}Be	Smith and Rodbell (2010)

PE07-QUE-25	10.010133	77.255397	14439	775	^{10}Be	Smith and Rodbell (2010)
PE05-JEU-33	10.015583	77.259683	18127	593	^{10}Be	Smith and Rodbell (2010)
PE05-JEU-34	10.015983	77.259067	17645	690	^{10}Be	Smith and Rodbell (2010)
PE05-JEU-36	10.01555	77.2553	17532	699	^{10}Be	Smith and Rodbell (2010)
PE05-JEU-35	10.01575	77.257483	15565	804	^{10}Be	Smith and Rodbell (2010)
PE07-QUE-03	10.013583	77.255833	14496	712	^{10}Be	Smith and Rodbell (2010)
PE07-QUE-05	10.015033	77.253433	14218	569	^{10}Be	Smith and Rodbell (2010)
PE07-QUE-09	10.014133	77.255017	13160	544	^{10}Be	Smith and Rodbell (2010)
PE07-QUE-10	10.01355	77.25695	14206	639	^{10}Be	Smith and Rodbell (2010)
PE07-QUE-13	10.013833	77.2558	9508	469	^{10}Be	Smith and Rodbell (2010)
PE07-CON-07	10.021417	77.26755	17898	791	^{10}Be	Smith and Rodbell (2010)
PE07-CON-04	10.02068	77.266983	13778	753	^{10}Be	Smith and Rodbell (2010)
PE07-CON-05	10.020517	77.267767	12773	505	^{10}Be	Smith and Rodbell (2010)
PE07-CON-01	10.0291	77.2849	49778	1552	^{10}Be	Smith and Rodbell (2010)
PE07-CON-02	10.029467	77.285033	42529	2332	^{10}Be	Smith and Rodbell (2010)
PE07-CON-03	10.030017	77.2846	40778	1771	^{10}Be	Smith and Rodbell (2010)
DRPE14-09	9.83394	77.32154	136360	190	^{10}Be	Stansell et al. (2017)
DRPE14-11	9.83394	77.32154	13490	160	^{10}Be	Stansell et al. (2017)
DRPE14-11	9.83406	77.3182	13140	130	^{10}Be	Stansell et al. (2017)
DRPE14-22	9.83399	77.31853	13020	210	^{10}Be	Stansell et al. (2017)
DRPE14-12	9.83399	77.31919	12740	180	^{10}Be	Stansell et al. (2017)
DRPE14-10	9.83399	77.31919	12660	180	^{10}Be	Stansell et al. (2017)
DRPE14-02	9.82233	77.30528	10400	250	^{10}Be	Stansell et al. (2017)
DRPE14-03	9.82256	77.30401	10280	140	^{10}Be	Stansell et al. (2017)
DRPE14-01	9.82175	77.30611	10160	310	^{10}Be	Stansell et al. (2017)
DRPE14-07	9.82013	77.30389	17180	590	^{10}Be	Stansell et al. (2017)

DRPE14-05	9.82049	77.30384	10430	410	^{10}Be	Stansell et al. (2017)
DRPE14-05	9.82104	77.30378	10170	180	^{10}Be	Stansell et al. (2017)
DRPE14-04	9.82104	77.3035	9710	220	^{10}Be	Stansell et al. (2017)
DRPE14-08	9.81999	77.30383	9670	260	^{10}Be	Stansell et al. (2017)
DRPE14-16	9.81644	77.2956	10310	140	^{10}Be	Stansell et al. (2017)
DRPE14-17	9.81498	77.29372	10250	230	^{10}Be	Stansell et al. (2017)
DRPE14-13	9.81614	77.2947	9990	150	^{10}Be	Stansell et al. (2017)
DRPE14-14	9.81634	77.29549	9400	140	^{10}Be	Stansell et al. (2017)
DRPE14-18	9.81546	77.2942	9200	170	^{10}Be	Stansell et al. (2017)
DRPE14-31	9.81533	77.27495	9240	150	^{10}Be	Stansell et al. (2017)
DRPE14-33	9.81472	77.27519	8760	110	^{10}Be	Stansell et al. (2017)
DRPE14-32	9.81472	77.27519	8700	130	^{10}Be	Stansell et al. (2017)
DRPE14-30	9.81362	77.27246	5910	110	^{10}Be	Stansell et al. (2017)
DRPE14-29	9.81374	77.27231	2780	70	^{10}Be	Stansell et al. (2017)
DRPE14-28	9.81379	77.27232	1800	30	^{10}Be	Stansell et al. (2017)
DRPE14-19	9.81379	77.27235	200	20	^{10}Be	Stansell et al. (2017)
DRPE14-25	9.79775	77.26404	3350	50	^{10}Be	Stansell et al. (2017)
DRPE14-24	9.79775	77.26404	1230	20	^{10}Be	Stansell et al. (2017)
DRPE14-26	9.7978	77.26408	520	10	^{10}Be	Stansell et al. (2017)
DRPE14-27	9.79834	77.26443	240	10	^{10}Be	Stansell et al. (2017)
CH_09	9.47655	77.4214	60-70		Lichenometry	Emmer et al. (2019)
CH_10	9.476589	77.421233	55-65		Lichenometry	Emmer et al. (2019)
CH_11	9.47535	77.420567	10-20		Lichenometry	Emmer et al. (2019)
CH_13	9.474583	77.420167	15-25		Lichenometry	Emmer et al. (2019)
CH_16	9.472467	77.4208	20-30		Lichenometry	Emmer et al. (2019)
CH_19	9.473533	77.422217	15-25		Lichenometry	Emmer et al. (2019)

CH_20	9.47435	77.422583	70-80		Lichenometry	Emmer et al. (2019)
CH_21	9.475322	77.425467	190-21		Lichenometry	Emmer et al. (2019)
CH_22	9.4779	77.42305	350-390		Lichenometry	Emmer et al. (2019)
CH_23	9.79233	77.4249	510-560		Lichenometry	Emmer et al. (2019)
CH_24	9.479	77.425617	580-640		Lichenometry	Emmer et al. (2019)
CH_25	9.485	77.42985	>1000		Lichenometry	Emmer et al. (2019)
CH_26	9.487183	77.431033	>1500		Lichenometry	Emmer et al. (2019)

REFERENCES

Aceituno, P., 1988. On the functioning of the Southern Oscillation in the South American sector. Part I: surface climate. Monthly Weather Review, 116, 505-524.

Ames Marquez, A., & Francou, 1995. Cordillera Blanca Glaciares en la Historia. El Bulletin de l'Institut Français d'Études Andines, 24, 1, 37-64.

Ariztegui, D., Bianchi, M.M, Masaferro, J., LaFague, E., & Niessen, F., 1997. Inter-hemispheric synchrony of Late-glacial climatic instability as recorded in proglacial Lake Mascardi, Argentina. Journal of Quaternary Science, 12, 333-338.

Balco, G., Stone, J.O., Lifton, N.A., & Dunai, T.J., 2008. A complete and easily accessible mans of calculating surface exposure ages or erosion rates from 10Be and 26 Al measurements. Quaternary Geochrnology, 3, 174-195.

Barnett, T.P., Adam, J.C., & Lettenmaier, D.P., 2005. Potential impacts of a warming climate on water availability in snow-dominated regions. Nature, 438, 303-309.

Bartoli, G., Hönisch, B., & Zeebe, R.E., 2011. Atmospheric CO2 decline during the Pleicone intensification of Northern Hemisphere glaciation. Paleoceonagraphy, 26, PA4213, 1-14.

Benedict, J.B., 1967. Recent Glacial History of an Alpine Area in the Colorado Front Range, U.S.A. I. Establishing a Lichen-Growth Curve. Journal of Glaciology, 6, 48, 817-832.

Benn, D.I., Owen, L.A., Osmaston, H.A., Seltzer, G.O., Porters, S.C., Mark., B., 2005. Reconstruction of equilibrium-line altitudes for tropical and sub-tropical glaciers. Quaternary International, 138-139.

Benn, D., & Evans, D.J.A., 2010. Glaciers and Glaciation. 2nd Ed. Routeledge.

Berger, G.W., & Eyles, N., 1994. Thermoluminescence chronology of Toronto-area Quaternary sediments and implication for the extent of the midcontinent ice sheet(s). Geology, 22, 31-34.

Beschel, R.E., 1958. Lichenometric studies in west Greenland. Arctic, 11, 254.

Boulton, G.S. 1996. The origin of till sequences by subglacial sediment deformation beneath mid-latitude ice sheet. Annals of Glaciology, 22, 75-84.

Briner, J.O., Kaugaman, D.S., Manley, W.F., Finkel, R.C., Caffee, M.W., 2005. Cosmogenic exposure dating of late Pleistocene moraine stabilization in Alaska. Geological Society of America Bulletin, 117, 1108-1120.

Bromley, G.R.M., Schaefer, J.M., Winckler, G., Hall, B.L., Todd, C.E., & Rademaker, K.M., 2009. Relvative timing of last glacial maximum and late-glacial events in the central tropical Andes. Quaternary Science Reviews, 28, 2514-2526.

Bromley, G.R., Schaefer, J.M., Hall, B.L., Rademaker, K.M., Putnam, A.E., Todd, C.E., Hegland, M., Winckler, G., Jackson, M.S., & Strand, P.D., 2016. A cosmogenic 10Be chronology for the local last glacial maximum and termination in the Cordillera Oriental, southern Peruvian Andes: Implications for the tropical role in global climate. Quaternary Science Reviews, 148, 54-67.

Bury, J.T., Mark, B.G., McKenzie, J.M., French, A., Baraer, M., In huh, K., Zapata Luyo, M.A., Gómez López, R.J., 2011. Glacier recession and human vulnerability in the Yanamarey watershed of the Cordillera Blanca, Peru. Climatic Change, 105, 176-906.

Carey, M., 2005. Living and dying with glaciers: people's historical vulnerability to avalanches and outburst floods in Peru. Global and Planetary Change, 47, 122-134.

Carey, M., Huggel, C., Bury, J., Portocarrero, C., & Haeberli, W., 2012. An integrated socio-enviornmental framework for glacier hazard management and climate change adaptation: lesssons from Lake 513, Cordillera Blanca, Peru. Climatic Change, 112, 733-767.

Clague, J.J., Menounos, B., Osborn, G., Luckman, B.H., & Koch, J., 2009. Nomenclature and resolution in Holocene glacial chronogies. Quaternary Science Reviews, 28, 2231-2238. doi: 10.1016/j.quascirev.2008.11.016.

Clapperton, C.M., 1972. The Pleistocene Moraine Stages of West-Central Peru. Journal of Glaciology, 11, 62, 255-263. doi: 10.3189/S0022143000022243.

Clapperton, C.M., 1983. The Glaciation of the Andes. Quaternary Science Reviews, 2, 83-155.

Clapperton, C.M., 1979. Glaciation in Bolivia before 3.27 Myr. Nature, 277, 375-377.

Cobbing, J., W. Pitcher, J. Baldock, W. Taylor, W. McCourt, & Snelling, N.J, 1981. Estudio geológico de la Cordillera Occidental del norte del Perú, Institute Geologico Minero y Metalurgico, Peru., 10(D), 1–252.

Cummings, D.I., Gorrell, G., Guilbault, J.-P., Hunter, J.A., Logan, C., Ponomarenko, D., Pugin, A.J.-M., Pullan, Russell, H.A.J., Sharpe, D.R., 2011. Sequence Stratigraphy of a glaciated basin fill with focus on esker sedimentation. GSA Bulletin, 123, 7-8, 1478-1496.

Dalmayrac, B., & Molnar, P., 1981. Parallel thurst and normal faulting in Peru and constraints on the state of stress. Earth and Planetary Science Letters, 55, 473-481.

Davies, B.J., Darvill, C.M., Lovell, H., Bendle, J.M., Dowdeswell, J.A., Fabel, D., García, J.-L., Geiger, A., Glasser, N.F., Gheorghiu, D.M., Harrison, S., Hein, A.S., Kaplan, M.R., Martin, J.R.V., Mendelova, M., Palmer, A., Pelto, M., Rodés, Á., Sagredo, E.A., Smedley, R.K., Smellie, J.L., & Thorndycraft, V.R., 2020. The evolution of the Patagonian Ice Sheet from 35 ka to the present day (PATICE). Earth-Science Reviews, 204, 103152.

Decou, A., von Eynatten, H., Dunkl, I., Frei, D., Worner, G., 2013. Late Eocene to Early Miocene Andean uplift inferred from detrital zircon fission track and U-Pb dating of Cenozoic forearc sediments (15-18°S). Journal of South American Earth Sciences, 45, 6-23. doi: 10.1016/j.jsames.2013.02.003.

Douglass, D.C., Singer, B.S., Kaplan, M.R., Mickelson, D.M., Caffee, M.W., 2006. Cosmogenic nuclide surface exposure dating of boulders on last-glacial and late-glacial moraines, Lago Buenos Aires, Argentina: interpretive strategies and paleoclimate implications. Quaternary Geochronology 1, 43–58.

Drenkhan, F., Carey, M., Huggel, C., Seidel, J., & Oré, M.T., 2015. The changing water cycle: climatic and socioeconomic drivers of water-related changes in the Andes of Peru. WIREs Water, 2, 715-733.

Ehlers, J., & Gibbard, P., 2011. Quaternary Glaciation. In Singh, V.P., Singh, P., Haritashya, U.K (Eds.) Encyclopedia of Snow, Ice and Glaciers. Pp 873-882. Springer. doi.org/10.1007/978-90-481-2642-2_423

Emmer, A., Vílímek, V., Zapata, M.L., 2016. Hazard mitigation of glacial lake outburst floods in the Cordillera Blanca (Peru): the effectiveness of remedial Works. Journal of Flood Risk Management, 11, S1, 1-13.

Emmer, A., Juricová, A. & Veetil, B.K., 2019. Glacier retreat, rock weathering and the growth of lichens in the Churup Valley, Peruvian Tropical Andes. Journal of Mountain Science, 16, 7, 1485-1499.

Evans, D.J.A., Clark, C.D., & Rea, B.R., 2008. Landform and sediment imprints of fast glacier flow in the southwest Laurentide Ice sheet. Journal of Quaternary Science, 23, 3, 249-272.

Eyles, N., 1979. Facies of supraglacial sedimentation on Icelandic and Alpine temperate glaciers. Canadian Journal of Earth Science, 16, 1341-1361.

Eyles, N., 1983. The glaciated valley landsystem. In: Eyles, N. (Ed). Glacial geology. Pergamon: Oxford, pp.91-110.

Francou, B., & Pizarro, L., 1985. El Niño y la sequía en los altos Andes Centrales (Perú y Bolivia). Bulletin de l'Institut français d'etudes andines, 14, 2, 1-18.

Farber, D.L., Hancock, G.S., Finkel, R.C., & Rodbell, D.T., 2005. The age and extent of tropical alpine glaciation in the Cordillera Blanca, Peru. Journal of Quaternary Science, 20, 7-8, 759-776. doi: 10.1002/jqs.994.

Fischer, L., Kääb, A., Huggle C., & Noetzli, J., 2006. Geology, glacier retreat and permafrost degradation as controlling factors of slope instabilities in a high-mountain rock wall: the Monte Rosa east face. Natural Hazards and Earth Systems Sciences, 6, 761-772.

Fisher, L., Purves, R.S., Huggle, C., Noetzli, J., & Haeberli, W., 2012. On the influence of topographic, geological and cryospheric factors on rock avalanches and rockfalls in high-mountain areas. Natural Hazards and Earth Sciences, 12, 1, 241-254.

Fox, M., Bodin, T., Schuster, D.L., 2015. Abrupt changes in the rate of Andean Plateau uplift from reversible jump Markov Chain Monte Carolo inversion of river profiles. Geomorphology, 283, 1-14.

Garreaud, R., Vuille, M., Clement, A., 2003. The climate of the Altiplano: observed current conditions and mechanisms of past changes. Palaeogeography, Palaeoclimatology, Palaeoecology 194, 5–22.

Garreaud, R.D., Vuille, M., Compagnucci, R., & Marengo, J., 2009. Present-day South American climate. Palaogeography, Palaeoclimtology, Palaeoecology, 281, 180-195. doi: 10.1016/j.palaeo.2007.10.032.

Georges, C., 2004. 20th-Century Glacier Flunctuations in the Tropical Cordillera Blanca, Perú. Arctic, Antarctic, and Alpine Research, 36, 1, 100-107. doi: 10.1657/1523-0430(2004)036[0100:TGFITT]2.0.CO;2.

Giovanni, M.K., Horton, B.K., Garzione, C.N., McNulty, B., & Grove, M., 2010. Extensional basin evolution in the Cordillera Blanca, Peru: Stratigraphic and isotopic records of detachment faulting and orogenic collapse in the Andean hinterland. Tectonics, 29, TC6007, 1-21. doi: 10.1029/2010TC002666.

Glasser, N.F., Clemmens, S., Schnabel, C., Fenton, C.R., & McHargue, L., 2009. Tropical glacier flunctuations in the Cordillera Blanca, Peru between 12.5 and 7.6 ka from

cosmogenic 10Be dating. Quaternary Science Reviews, 28, 3448-3458. doi: 10.1016/j.quascirev.2009.10.006.

Goodman, A.Y., Rodbell, D.T., Seltzer, G.O., & Mark, B.G., 2001. Subdivision of Glacial Deposits in Southeastern Peru Based on Pedogenic Development and Radiometric Ages. Quaternary Research, 56, 31-50.

Google Earth V 7.3.2.5776 (December 31, 1969). Yanamaray Glacier, Cordillera Blanca, Peru. 9°39'19.39"S, 77°16'14.81"W. Eye alt. 7100 m. U.S. Geological Survey. http://www.earth.google.com [May 25, 2019].

Google Earth V 7.3.2.5776 (July 26, 2011). Yanamaray Glacier, Cordillera Blanca, Peru. 9°39'19.39"S, 77°16'14.81"W. Eye alt. 7100 m. Landsat/Copernicuz, Maxar Technologies 2019. http://www.earth.google.com [May 25, 2019].

Google Earth V 7.3.2.5776 (December 30, 2016a). Yanamaray Glacier, Cordillera Blanca, Peru. 9°39'19.39"S, 77°16'14.81"W. Eye alt. 7100 m. CNES 2019, Airbus, Landsat/ Copernicus http://www.earth.google.com [May 25, 2019].

Google Earth V 7.3.2.5776 (August 5, 2016b). Gueshque Valley, Cordillera Blanca, Peru. 9°48'59.99"S, 77°16'45.75"W. Eye Alt, 7000m. Google 2018, CNES 2019 / Airbus. http://www.earth.google.com [May 29, 2019].

Gosse, J.C., & Phillips, F.M., 2001. Terrestrial in situ cosmogenic nuclides: theory and application. Quaternary Science Reviews, 20, 1475-1560. doi: 10.1016/S0277-3791(00)00171-2.

Gregory-Wodzicki, K.M., 2000. Uplift history of the Central and Northern Andes: A review. GSA Bulletin, 112, 7, 1091-1005.

Gutscher, M.A., Oliver, J.L., Aslanian, D., Eissen, J.P., & Maury, R., 1999. The "lost Inca Plateau": Cause of glat subduction beneath Peru?, Earth and Planetary Science Letter, 171, 335-341.

Hambrey, M.J., & Glasser, N.F., 2012. Discriminating glacier thermal and dynamic regimes in the sedimentary record. Sedimentary Geology, 251-252, 1-33.

Hambrey, M.J., & Ehrmann, W., 2004. Modification of sediment characteristics during glacial transport in high-alpine catchments: Mount Cook area, New Zealand. Boreas, 33, 300-318.

Hall, M.L., & Wood, C.A., 1985. Volcano-tectonic segmentation of the northern Andes. Geology, 13, 203-207.

Hall, S.R., Farber, D.L., Ramage, J.M., Rodbell, D.T., Finkel, R.C., Smith, J.A., Mark, B.G., & Kaseel, C., 2009. Geochronology of Quaternary glaciations from the tropical Cordillera Huayhuash, Peru. Quaternary Science Reviews, 28, 25-26, 2991-3009. doi: 10.1016/j.quascirev.2009.08.004.

Hansen, B.C.S., & Rodbell, D.T., 1995. A Late-glacial/Holocene Pollen Record from the Eastern Andes of Northern Peru. Quaternary Research, 44, 216-227.

Hastenrath, S., 1981. The glaciation of the Ecuadorian Andes. Rotterdam, Balkema.

Hastenrath, S., & Ames, A., 1995. Recession of Yanamarey Glacier in the Cordillera Blanca, Peru, during the 20th Century. Journal of Glaciology, 41, 137, 191-196.

Heine, K., & Heine, J.T., 1996. Late glacial climatic fluctuations in Ecuador: glacier retreat during younger dryas times. Arctic Alpine Research, 28, 496-501.

Heine, K., 1995. Late Quaternary glacier advances in the Ecuadorian Andes: a preliminary report. Quaternary of South American and Antarctica Peninsula, 9, 1-22

Helmens, K.F., 2011. Chapter 58 - Quaternary Glaciations of Colombia. In: Developments in Quaternary Science: Quaternary Glaciations – Extent and Chronology A Closer Look, ed. Ehlers, J., Gibbard, P.L., & Hughes, P.D., 2011. Elsevier

Heusser, C.J., 2003. Ice Age Southern Andes – A Chronicle of Paleoecological Events. Developments in Quaternary Sciences, 3. Elsevier.

Horton, B.K., 2012. Chapter 21 – Cenozoic evolution of hinterland basins in the Andes and Tibet. In Busby, C., & Azor, A. (Eds.). Tectonics of Sedimentary Basis: Recent Advances. John Wiley and Sons.

Hughes, P.D., Gibbard, P.L., & Ehlers, J., 2013. Timing of glaciation during the last glacial cycle: Evaluating the concept of a global 'Last Glacial Maximum' (LGM). Earth-Science Reviews, 125, 171-198.

Hubbard, B., Heald, A., Reynold, J.M., Quincey, D., Richardson, S.D., Zapata Luyo, M., Santillan Portilla, N., & Hambrey, M.J., 2005. Impact of a rock avalanche on a moraine-dammed proglacial lake: Laguna Safuna Alta, Cordillera Blanca, Peru. Earth Surface Processes and Landforms, 30, 1251-1264. doi: 10.1002/esp.1198.

Instituto Nacional De Investigación en Glaciares y Ecosistemas de Montaña (INAIGEM), 2018. Inventario Nacional de Glaciares: Las Cordilleras Glaciares del Peru. Instituto Nacional de Investigación en Glaciares y Ecosistemas de Montaña Biblioteca y Publicaciones.

Iturrizaga, L., 2013. Bent glacier tongues: A new look at Lliboutry's model of evolution of the crooked Jantunraju Glacier (Parón Valley, Cordillera Blanca, Perú). Geomorphology, 198, 147-162.

Iturrizaga, L., 2014. Glacial and glacially conditioned lake types in the Cordillera Blanca, Peru: A spatiotemporal conceptual approach. Progress in Physical Geography, 38, 5, 602-636. doi: 10.1177/0309133314546344.

James, D.E., 1971. Plate tectonic model for the evolution of the central Andes. Bulletin of the Geological Society of America, 32, 189-206.

Jochimsen, M., 1973. Does the size of lichen thalli really constitute a valid measure for dating glacial deposits? Arctic and Alpine Research 5, 417–424. doi: doi.org/10.1080/00040851.1973.12003749.

Jomelli, V., Grancher, D., Brunstein, D., & Solomina, O., 2008. Recalibration of the yellow Rhizocarpon growth curve in the Cordillera Blanca (Peru) and implications for LIA chronology. Geomorphology, 93, 201-212. doi: 10.1016/j.geomorph.2007.02.021.

Jomelli, V., Favier, V., Rabate, A., Brunstein, D., Hoffman, G., & Francou, B., 2009. Fluctuations of glaciers in the tropical Andes over the last millennium and paleoclimatic implications: A review. Palaeography, Palaeoclimatology, Palaeoecology, 281, 269-282. doi: 10.1016/j.palaeo.2008.10.033.

Jomelli, V., Khodri, M., Favier, V., Brunstein, D., Ledru, M.P, Wagnon, P., Blard, P.H., Sicart, J.E., Brauhcer, R., Grancher, D., Bourles, D.L., Braconnot, P., & Vuille M., 2011. Irregular tropical glacier retreat over the Holocene epoch driven by progressive warming. Nature, 474, 196-199.

Jomelli, V., Favier, V., Vuille, M., Braucher, R., Martin, L., Blard, P.H., Colose, C., Brunstein, D., He, F., Khodri, M., Bourlès, Leanni, L., Rinterknecht, V., Grancher, D., Francou, B., Ceballos, J.L., Fonseca, H., Liu, Z., & Otto-Bliesner, B.L., 2014. Nature, 513, 224-228.

Jomelli, V., Martin, L., Blard, P.H., Favier, V., Vuille, M., & Ceballos, J.L., 2017. Revisiting the Andean tropical glacier behavior during the Antarctic cold reversal. Geographical Research Letters, 43, 2, 629-648.

Karrow, P.F., Dreimanis, A., & Barnett, P.J., 2000. A Proposed Diachrnonice Revision of Late Quaternary Time-Stratigraphic Classification in the Eastern and Northern Great Lakes Area. Quaternary Research, 54, 1-12.

Kaser, G., & Georges, C., 1997. Changes of the equilibrium-line altitude in the tropical Cordillera Blanca, Peru, 1930-50, and their spatial variations. Annals of Glaciology, 24, 344-349.

Kaser, G., 1999. A review of the modern fluctuations of tropical glaciers. Global and Planetary Change, 22, 1-4, 93-103. doi: 10.1016/S0921-8181(99)00028-4.

Kaser, G., 2001. Glacier-climate interaction at low latitudes. Journal of Glaciaology, 47, 157, 195-204.

Kaser, G., & Osmaston, H., 2002. Tropical Glaciers. Cambridge University Press.

Kaser, G., Juen, I., Georges, C., Gómez, K., Tamayo, W., 2003. The impact of glacier on the runoff and the reconstruction of mass balance history from hydrological data in the tropical Cordillera Blanca, Peru. Journal of Hydrology, 282, 130-144.

Koch, J., & Kilian, R., 2005. 'Little Ice Age' glacier flunctuations, Gran Campo Nevado, southernmost Chile. The Holocene, 15, 1, 20-28.

La Frenierre, J., In Huh, K., & Mark, B.G., 2011. Chapter 56: Ecuador, Peru and Bolivia. In: Developments in Quaternary Science: Quaternary Glaciations – Extent and Chronology A Closer Look, ed. Ehlers, J., Gibbard, P.L., & Hughes, P.D., 2011. Elsevier

Licciardi, J.M., Schaefer, J.M., Taggart, J.R., Lund, D.C., 2009. Holocene glacier fluctuations in the Peruvian Andes indicate northern climate linkages. Science, 325, 1677-1679.

Lisiecki, L., & Raymon, M.E., 2005. A Pliocene-Pleistocene stack of 57 globally distributed benthic δ18O records. Paleoceanography, 20, 1, PA1003.

Lowell, T.V., Heusser, C.J., Anderson, B.G., Moreno, P.I., Hauser, A., Heusser, L.E., Schlüchter, C., Marchant, D.R., Denton, G.H., 1995. Interhemispheric correlation of late Pleistocene glacial events. Science, 269, 1541-1549.

Margirier, A., Audin, L., Robert, X., Herman, F., Ganne, J., & Schwartz, S., 2016. Time and mode of exhumation of the Cordillera Blanca batholith (Peruvian Andes). Journal of Geographical Research: Solid Earth, 121, 6235-6249. doi: 10.1002/2016JB013055.

Marginier, A., Audin, L., Robert, X., Pêcher, A., & Schwartz, S., 2017. Stress field evolution above the Peruvian flat-slab (Cordillera Blanca, northern Peru). Journal of South American Earth Sciences, 77, 58-69.

Margirier, A., Braun, J., Robert, X., & Audin, L., 2018. Role of erosion and isostasy in the Cordillera Blanca uplift: Insights from landscape evolution modeling (northern Peru, Andes). Tectnophysics, 728-729, 119-129.

Mark B.G., Seltzer, G.O., Rodbell, D.T., & Goodman, A.Y., 2002. Rates of Deglaciation during the Last Glaciation and Holocene in the Cordillera Vilcanota-Quelccaya Ice Cap Region, Southeastern Perú. Quaternary Research, 57, 287-298.

Mark, B.G., Seltzer, G.O., & Rodbell, D.T., 2004. Later Quaternary glaciations of Ecuador, Peru and Bolivia. In: Ehlers, J., Gibbard, P.L., (Eds.), Quaternary Glaciations – Extent and chronology Part III. Elsevier, Amsterdam.

Mark and Seltzer, 2005. Evaluation of recent glacier recession in the Cordillera Blanca, Peru (AD 1962-1999): spatial distribution of mass loss and climatic forcing. Quaternary Science Reviews, 24, 2265-2280.

Mark, B.G., Bury, J., McKenzie, J.M., French, A., & Baraer, M., 2010. Climate Change and Tropical Andean Glacier Recession: Evaluating Hydrologic Changes and Livelihood Vulnerability in the Cordillera Blanca. Annals of the Association of American Geographers, 100, 4, 794-805. doi: 10.1080/00045608.2010.497369.

Mark, B., Stansell, N., & Zeballos, G., 2017. The Last Deglaciation of Peru and Bolivia. Geographical Research Letters, 43, 2, 591-628.

Masiokas, M.H., Rivera, A., Espizua, L.E., Villalba, R., Delgado, S., Aravena, J.C., 2009. Glacier fluctuations in extratropical South America during the past 1000 years. Palaeogeography, Palaeoclimatology, Palaecology, 281, 242-268.

Matthews, J.A., & Briffa, K.R., 2005. The 'Little Ice Age': reevaluation of an evolving concept. Geografiska Annaler: Series A, Physical Geography, 87A, 1, 17-36.

Mendelova, M., Hein, A.S., McCulloch, R., & Davies, B., 2017. The Last Glacial Maximum and Deglaciation in Central Patagonia, 44°S-49°S. Cuadernos de Investigación Geográfica, 43, 2, 719-750.

McNulty, B., & Farber, D., 2002. Active detachment faulting above the Peruvian flat slab. Geology, 30, 6, 567-570. doi: 10.1130/0091-7613(2002)030<0567:ADFATP>2.0.CO;2.

Mégard, F., 1984. The Andean orogenic period and its major structures in central and northern Peru. Geological Society of America Bulletin, 95, 9, 1108-1117.

Mercer, J.H., & Sutter, J.F., 1982. Late Miocene-Earliest Pliocene Glaciation in Southern Argentina: Implications for Global Ice-Sheet History. Palaeogeography, Palaeoclimatology, Palaeoecology, 38, 185-206.

Mercer, J.H., & Palacios, M.O., 1977. Radiocarbon dating of the last glaciation in Peru. Geology, 5, 600-604.

Meyers, S.R., & Hinnov, L.A., 2010. Northern Hemisphere glaciation and evolution of Plio-Pleistocene climate noise. Paleoceanography, 25, PA3207

Osborn, G., McCarthy, D., LaBrie, A., & Burke, R., 2015. Lichenometric dating: Science or pseudo-science? Quaternary Research, 83, 1-12. doi: 10.1016/j.yqres.2014.09.006.

Pausata, F. S.R., & Löfverström, M., 2015. On the enigmatic similarity in Greenland δ18O between the Oldest and Younger Dryas. Geophysical Research Letters, 42, 23, 10470-10477.

Petford, N., & Atherton, M., 1996. Na-rich partial melts from newly underplated basaltic crust: The Cordillera Blanca Batholith, Peru. Journal of Petrology, 37, 6, 1491-1521

Pillans, B., & Gibbard, P., 2012. The Quaternary Period. In Gradstein, F.M., Ogg, J.G.., Schmitz, M.D., & Ogg, G.M (eds). The Geological Time Scale 2012. Volume 2. Elsevier. 979-1010.

Polissar, P.J., Abbott, M.B., Wolfe, A.P., Bezada, M., Rull, V., Bradley, R.S., 2006. Solar modulation of Little Ice Age climate in the tropical Andes. Proceedings of the National Academy of Sciences USA 103, 8937–8942.

Portocarrero, C., Zapata, M., López, J.G., Cochachín, A., Egas, G., Santillán, N., 2010. Inventario de Glaciares Cordillera Blanca. Unidad de Glaciología y Recursos Hídricos (UGRH), Autoridad Nacional del Agua (ANA), Huaráz.

Rabassa, J., 2008. Late Cenozoic Glaciations in Patagonia and Tierra del Fuego. Developments in Quaternary Sciences, 11, 151-204.

Rabatel, A., Machaca, A., Francou, B., & Jomelli, V., 2006. Glacier recession on the Cerro Charquini (Bolivia 16°S) since the máximum of the Little Ice Age (17th century). Journal of Glaciology, 52, 110-118.

Rabatel., A., Francou, B., Soruco, A., Gomez, J., Cáceres, B., Ceballos, J.L., Basantes, R., Vuille, M., Sicart, J.-E., Huggel, C., Scheel, M., Lejeune, Y., Arnoud, Y., Collet, M., Condom, T., Consoli, G., Favier, V., Jomelli, V., Galarrage, R., Ginot, P.,

Maisincho, L., Mendoza, J., Ménégoz, M., Ramirez, E., Ribstein, P., Suarez, W., Villacis, M., & Wagnon, P., 2013. Current state of glaciers in the tropical Andes: a multi-century perspective on glacier evolution and climate change. The Cryosphere, 7, 81-102. doi: 10.5194/tc-7-81-2013.

Ramos, V.A., & Folguera, A., 2009. Andean flat-slab subduction through time. Geological Society of London, Special Publications, 327, 31-54.

Ramos, V.A., 1999. Plate tectonic setting of the Andean Cordillera. Episodes, 22, 3, 183-190.

Ramos, V.A., 2009. Anatomy and global context of the Andes: Main geologic features and the Andean orogenic cycle. Memoir of the Geological Society of America, Memoir 204.

Reynolds, J.M., 2000. On the formation of supraglacial lakes on debris-covered glaciers. In Nakawo, N., Fountain, A., Raymond, C. (Eds.)., Debris Covered Glaciers: IAHS Publications, 264, pp. 153-161.

Rodbell, D.T., 1992. Lichenometric and Radiocarbon dating of Holocene glaciation, Cordillera Blanca, Perú. The Holocene, 2, 1, 19-29. doi: 10.1177/095968369200200103.

Rodbell, D.T., 1993. Subdivision of Late Pleistocene Moraines in the Cordillera Blanca, Peru, Based on Rock-Weathering Features, Soils and Radiocarbon Dates. Quaternary Research, 39, 133-143.

Rodbell, D.T., & Seltzer, G.O., 2000. Rapid Ice Margin Flunctuations during the Younger Dryas in the Tropical Andes. Quaternary Research, 54, 328-338. doi: 10.1006/qres.2000.2177.

Rodbell, D.T., Seltzer, G.O., Mark, B.G., Smith, J.A., & Abbot, M.B., 2008. Clastic sediment flux to tropical Andean lakes: records of glaciation and soil erosion. Quaternary Science Reviews, 27, 1612-1626.

Rodbell, D.T., Smith, J.A., & Mark, B.G., 2009. Glaciation in the Andes during the Lateglacial and Holocene. Quaternary Science Reviews, 28, 2165-2212.

Roe, G.H., & O'Neal, M.A., 2009. The response of glaciers to intrinsic climate variability: observations and models of late-Holocene variations in the Pacific Northwest. Journal of Glaciology, 55, 193, 839-854.

Schauwecker, S., Roher, M., Acuña, D., Cochachin, A., Dávila, L., Frey, H., Giráldez, C., Gómez, J., Huggel, C., Jacques-Coper, M., Loarte, E., Salzmann, N., & Vuille, M., 2014. Climate trends and glacier retreat in the Cordillera Blanca, Peru, revisited. Global and Planetary Change, 119, 85-97. doi: 10.1016/j.gloplacha.2014.05.005.

Schwartz, D.P., 1988. Paleoseismicity and neontectonics of the Cordillera Blanca fault zone, northern Peruvian Andes. Journal of Geophysical Research, 93, 85, 4712-4730.

Schneider, D., Huggel, C., Cochachin, A., Guillén, S., & García, J., 2014. Mapping hazards from glacier lake outburst floods based on modelling of process cascades at Lake 513, Carhuaz, Peru. Advances in Geosciences, 35, 145-155. doi: 10.5194/adgeo-35-145-2014.

Sébrier, M., Mercier, J.L., Macharé, J., Bonnot, D., Cabera, J., Blanc, J.L., 1988. The state of stress in an overring plate situated above a flat slab: the Andes of Central Peru. Tectonics, 7, 4, 895-928.

Seltzer, G.O., Rodbell, D.T., Baker, P.A., Fritz, S.C., Tapia, P.M., Rowe, H.D., & Dunbar, R.B., 2002. Early warming of tropical South America at the last glacial-interglacial transition. Science, 296, 1685–1686.

Seltzer, G.O., & Rodbell, D.T., 2005. Delta progradation and Neoglaciation, Laguna Parón, Cordillera Blanca, Peru. Journal of Quaternary Science, 20, 7-8, 715-722

Siame, L.L., Sébrier, M., Bellier, O., & Bourles, D., 2006. Can cosmic ray exposure dating reveal the normal fault activity of the Cordillera Blanca Fault, Peru? Revista de la Asociasión Geologica de Argetina, 61, 4, 536-544.

Silverio, W., & Jacquet, J.M., 2005. Glacial cover mapping (1987-1996) of the Cordillera Blanca (Peru) using satellite imagery. Remote Sensing of the Environment, 95, 342-350.

Silverio, W., & Jacquet, J.M., 2016. Evaluating glacier fluctuations in the Cordillera Blanca (Peru) by remote sensing between 1987 and 2016 in the context of ENSO. Archives de Sciences, 69, 145-162.

Sillitoe, R.H., 1974. Tectonic segmentation of the Andes: implications for magmatism and metallogeny. Nature, 250, 542-545

Smith, C.A., & Caffee, M.W., 2009. Lateglacial and Holocene cosmogenic surface exposure age glacial chronology and geomorphological evidence for the presence

of cold-based glaciers at Nevado Sajama, Bolivia. Journal of Quaternary Science, 24, 4, 360-372.

Smith, J.A., & Rodbell, D.T., 2010. Cross-cutting moraines reveal evidence for North Atlantic influence on glaciers in the tropical Andes. Journal of Quaternary Science, 25, 3, 243-248.

Smith, J.A., Finkel, R.C., Farber, D.L., Rodbell, D.T., & Seltzer, G.I., 2005a. Moraine preservation and boulder erosion in the tropical Andes: interpreting old surface exposure ages in glaciated valleys. Journal of Quaternary Science, 20, 7-8, 735-758.

Smith, J.A., Seltzer, G.O., Farber, D.L., Rodbell, D., & Finkel, R.C., 2005b. Early Local Last Glacial Maximum in the Tropical Andes. Science, 308, 678-671.

Smith, J.A., Mark, B.G., Rodbell, D.T., 2008. The timing and magnitude of mountain glaciation in the tropical Andes. Journal of Quaternary Sciencie, 23, 609-634.

Schneider, D., Huggel, C., Cochachin, A., Guillén, S., & García, J., 2014. Mapping hazards from glacier lake outburst floods based on modelling of process cascades at Lake 513, Carhuaz, Peru. Advances in Geosciences, 35, 145-155.

Solomina, O., Jomelli, V., Kaser, G., Ames, A., Berger, B., Pouyaud, B., 2007. Lichenometry in the Cordillera Blanca, Peru: "Little Ice Age" moraine chronology. Global and Planetary Change, 59, 225-235. doi: 10.1016/j.gloplacha.2006.11.016.

Solomina, O.N., Bradley, R.S., Hodgson, D.A., Ivy-Ochs, S., Jomelli, V., Mackintosh, A.N., Nesje, A., Owen, L.A., Wanner, H., Wiles, G.C., & Young, N.E., 2015. Holocene glacier fluctuations. Quaternary Science Reviews, 111, 9-34.

Solomina, O.N., Bradley, R.S., Jomelli, V., Geirsdottir, A., Kaufman, D.S., Koch, J., McKay, N.P., Masiokas, M., Miller, G., Nesje, A., Nicolussi, K., Owen, L.A., Putnam, A.E., Wanner, H., Wiles, G., & Yang, B., 2016. Glacier fluctuations during the past 200- years. Quaternary Science Reviews., 149, 61-90.

Stansell, N.D., Licciardi, J.M., Rodbell, D.T., & Mark, B.G., 2017. Tropical ocean-atmospheric forcing of Late Glacial and Holocene glacier flunctuations in the Cordillera Blanca, Peru. Geophysical Research Letters, 44, 4176-4185.

Stern, 2004. Active Andean volcanism: its geologic and tectonic setting. Revista geologica de Chile, 31, 2, 161-206.

Svendsen, J.I., Alexanderson, H., Astakhov, V., Demidov, I., Downdeswell, J.A., Funder, S., Gataullin, V., Henriksen, M., Hjort, C., Houmark-Nielsen, M., , Hubberten, H.W., Ingolfsson, O., Jakobsson, M., Kjaer, K.H., Larsen, E., Lokrantz, H., Lunkka, J..P., Lysa, A., Mangeru, J., Matiouchkov, A., Murray, A., Moller, P., Niessen F., Nikolskaya, O., Polyak, L., Saarnisto, M., Siegert, C., Sieger, M. J., Spielhagen, R., & Stein R., 2004. Late Quaternary ice sheet history of northern Eurasia. Quaternary Science Reviews, 23, 11-13, 1229-1271.

Tacsi Palacios, A., Colonia Ortiz, D., Torres Castillo, J., Santiago Martel, A., 2014. Inventario de Glaciares Del Peru. Unidad de Glaciologia y Recursis Hidricos (UGRH), Autoridad Nacional del Agua (ANA), Huaráz.

Thompson, L.G., Mosley-Thompson, E., Davis, M.E., Lin, P.-N., Henderson, K.A., Cole-Dai, J., Bolzan, J.F., & Liu, K.-b. 1995. Late Glacial Stage and Holocene tropical Ice Core Records from Huascarán, Peru. Science, 269, 46-50.

Thompson, L.G., Mosley-Thompson, E., & Henderson, K.A., 2000. Ice-core paleoclimate records in tropical South America since the Last Glacial Maximum. Journal of Quaternary Science, 15, 4, 377-394.

Thompson, L.G., Mosely-Thompson, E., Brecher, H., Davis, M.E., Leon, B., Les, D., Lin, P-N., Mashiotta, T., & Mountain, K., 2006. Abrupt tropical climate change: past and present. Proceedings of the National Academy of Sciences 14, 1-8.

Veetil, B.K., Wang, S., Souza, S.F., Bremer, U.S., & Simões, J.C., 2017. Glacier monitoring and glacier-climate interactions in the tropical Andes: A review. Journal of South American Earth Sciences, 77, 281-246. doi: 10.1016/j.jsames.2017.04.009.

Villalba, R., 1990. Climatic fluctuations in northern Patagonia during the last 1000 years as inferred from tree-ring records. Quaternary Research 34, 346–360.

Vuille, M., Bradley, R.S., Wener, M., & Keimig, F., 2008a. 20th Century Climate Change in the Tropical Andes: Observations and Model Results. Climate Change, 59, 75-99.

Vuille, M., Francou, B., Wagnon, P., Juen, I., Kaser, G., Mark, B.G., Bradley, R.S., 2008b. Climate and tropical Andean glaciers; Past, present and future. Earth Science Review, 89, 79-96.

Vuille, M., Bradley, R.S., & Keimig, F., 2000. Interannual climate variability in the Central Andes and its relation to tropical Pacific and Atlantic forcing. Journal of Geophysical Research, 105, 12, 12,447 – 12,460.

Vuille, M., Franquist, E., Garreaud, R., Lavado Casimiro, W.S., & Cáceres, B., 2015. Impact of the global warming hiatus on Andean temperatura. Journal of Geophysical Research: Atmospheres, 120, 3745-3757.

Vuille, M., Carey, M., Huggel, C., Buytaert, W., Rabatel, A., Jacobsen, D., Soruco, A., Villacis, M., Yarleque, C., Elison Timm, O., Condom, T., Salzmann, N., & Sicart, J.-E., 2018. Rapid decline of snow and ice in the tropical Andes – Impacts, uncertainties and challenges ahead. Earth-Science Reviews, 176, 195-213. doi: 10.1016/j.earscirev.2017.09.019.

Wilson, J.J., 1963. Cretaceous Stratigraphy of Central Andes of Peru. Bulletin of the American Association of Petroleum Geologists, 47, 1, 1-34.

Wipf, M., Zeilinger, G., Seward, D., Schlunegger, F., 2005. Geomorphic Effects in Western Peru due to Subduction of the Nazca Ridge. Geophysical Research Abstracts, 7, 04873.

Wright, H.E., 1983. Late-Pleistocene Glaciation and Climate around the Junín Plain, Central Peruvian Highlands. Geografiska Annalre Series A, Physical Geography, 65, 1-2, 35-43.

Yokoyama, Y., Lambeck, K., De Deckker, P., Johnston, P., Fifield, L.K., 2000. Timing of the last glacial maximum from observed sea-level minima. Nature, 406, 713-716.

Zech, R., Kull, C., Kubik, P.W., Veit, H., 2007. LGM and late-glacial glacier advances in the Cordillera Real and Cochambaba (Bolivia) deduced from 10Be surface expoiusre dating. Climate of the Past 3, 623-635.

Zech, R., May, J.H., Kull, C., Ilgner, J., Kubik, P.W., & Veit, H., 2008. Timing of the late Quaternary glaciation in the Andes from ~15 to 40° S. Journal of Quaternary Science, 23, 6-7, 635-647.

Zech, J., Zech, R., May, J.H., Kubik, P.W., & Weit, H., 2010. Lateglacial and early Holocene glaciation in the tropical Andes caused by la Niña-like conditions. Paleogeography, Palaeoclimatology, Palaeoecology, 29, 248-254.

CHAPTER 3: LANDSYSTEM ANALYSIS OF A TROPICAL MORAINE-DAMMED SUPRAGLACIAL LAKE, LLACA LAKE, CORDILLERA BLANCA, PERÚ

3.1 INTRODUCTION

Glaciers in high-altitude mountain environments, such as the Cordillera Blanca in Perú, are considered some of the most sensitive in their response to climate change and increasing temperatures (Evans and Clague, 1994; Huggel et al., 2015; Rangwala et al., 2015). Recent climate warming has caused rapid melt of these glaciers (Barnett, Adam and Lettenmaier, 2005; Hock et al., 2019), and an associated increase in the number and size of high-altitude mountain glacial lakes has been documented (Harrison et al., 2018). These high-altitude glacial lakes are often impounded by unstable moraine dams that can fail, causing the release of large volumes of water and sediment as glacial lake outburst floods (GLOFs) that severely impact communities downstream (Clague and Evans, 2000; Vilímek et al., 2005; Korup and Tweed, 2007; Emmer and Vilímek, 2013; Westoby et al., 2014). Unfortunately, little is known about the modern geomorphological processes operating in and around these deglaciating lakes or the characteristics of the sediments they contain.

This study focuses on identifying and classifying the geomorphology and sedimentology of an enlarging moraine-dammed, supraglacial lake (Llaca Lake) formed at the margins of the Llaca Glacier in the Cordillera Blanca, Perú (Figures 3.1 & 3.2). Llaca Lake was chosen for this study as previous studies have identified it to have medium-to-high risk for a GLOF (Emmer and Vilímek, 2013). Its proximity to the northern end of the city of Huaraz and the potential danger of a GLOF prompted remediation work on the moraine barrier and the construction of a strengthening dam in 1977 (Torres Amado, Dávila Roller and Vilca Gómez, 2016). This lake is also of particular interest as it lies on top of buried glacier ice which is melting below a cover of supraglacial and lacustrine sediment

Figure 3.1: Location of Llaca Valley within the Cordillera Blanca, close to the city of Huaraz, shown in the red box (Figure 3.2).

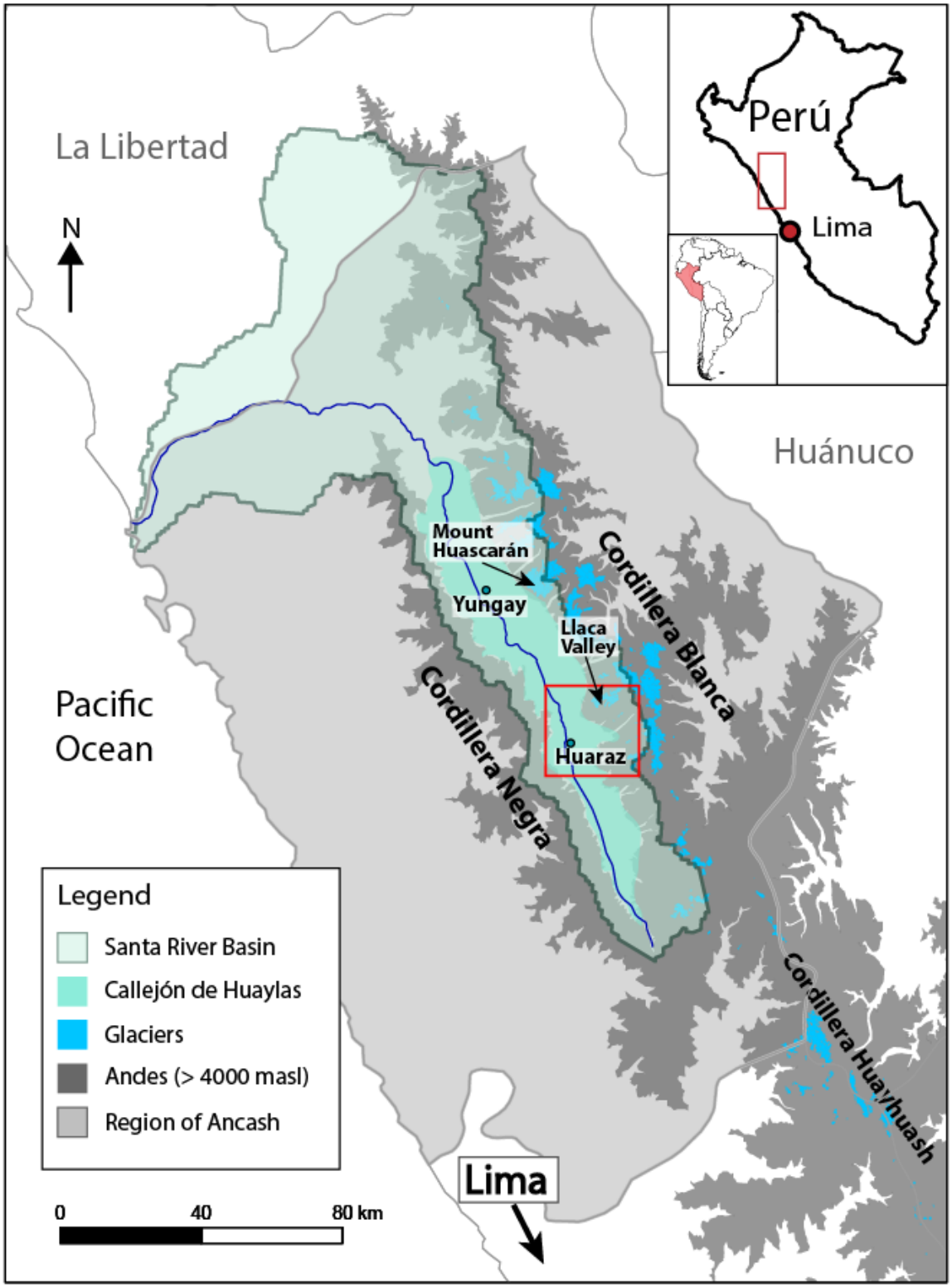
La Libertad
N
Perú
Lima
Huánuco
Mount Huascarán
Yungay
Llaca Valley
Huaraz
Cordillera Blanca
Cordillera Negra
Cordillera Huayhuash
Pacific Ocean
Lima
Legend
Santa River Basin
Callejón de Huaylas
Glaciers
Andes (> 4000 masl)
Region of Ancash
0
40
80 km

Figure 3.2: Location of Llaca Lake, Llaca Glacier, and surrounding mountains. The Cojup Valley, Lake Palcacocha Lake, Quilcayhuanca Valley and the city of Huaraz are also shown on this map. Location of this map within the Cordillera Blanca is shown by the red box on Figure 3.1.

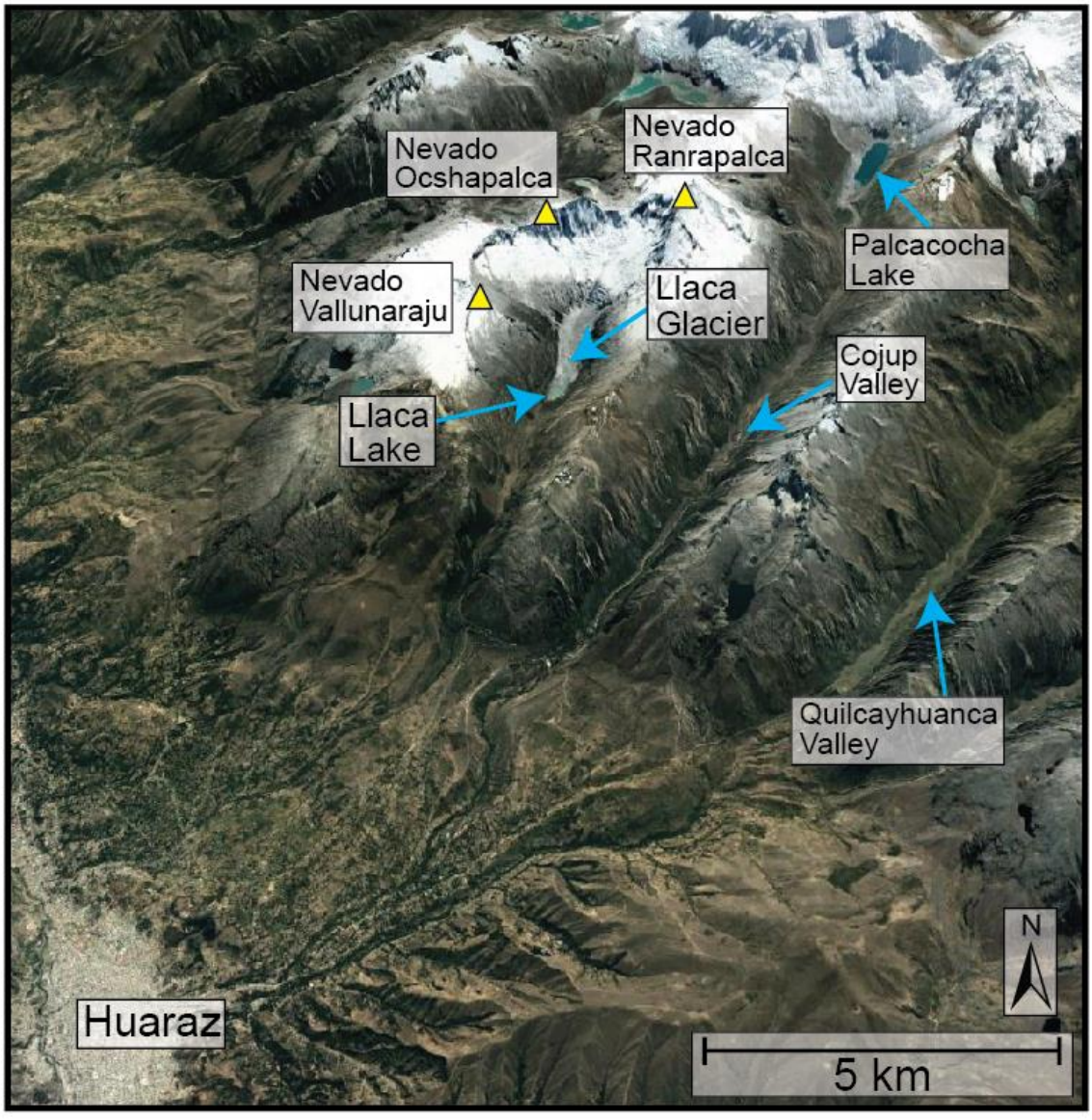
Nevado
Ocshapalca
Nevado
Ranrapalca
Palcacocha
Lake
Nevado
Vallunaraju
Llaca
Glacier
Cojup
Valley
Llaca
Lake
Quilcayhuanca
Valley
N
Huaraz
5 km

and provides an excellent example of a growing moraine-dammed supraglacial lake. Many recent glacier and glacial lake surveys (i.e (Iturrizaga, 2014; Harrison *et al.*, 2018; INAIGEM, 2018; Emmer *et al.*, 2020; Wood *et al.*, 2021) identify Llaca Lake as a large lake, yet calculations of water volume in the lake do not account for the volume of water stored in ice buried beneath lacustrine sediments. The exlusion of this water underestimates water volume calculations that aid in understanding the GLOF risk of Llaca Lake. Glacial lakes in the Cordillera Blanca take the form of moraine-dammed lakes, debris-dammed lakes, bedrock-dammed lakes, piedmont lakes, moraine-dammed ponds, supraglacial lakes, and a combination of these types (Emmer and Vilímek, 2013; Iturrizaga, 2014; Emmer *et al.*, 2020). Iturrizaga (2014) states that glacial lakes in the Cordillera Blanca undergo various transition phases between lake types as glaciers retreat. While Llaca Lake may be one of the few supraglacial lakes currently in the region, it is possible that many of the lake systems present today may have had supraglacial phases in the past.

A landsystems approach is used in this study to combine analysis of the sedimentology and geomorphology of Llaca Lake, and to identify the environmental changes experienced by lakes developing on the margins of modern glaciers in high altitude areas such as the Cordillera Blanca. This study will greatly enhance our understanding of environmental responses to climate change in high altitude glacial environments of the southern hemisphere, and will aid in the development of effective strategies for hazard analysis, management and remediation of GLOFs (Carey, 2005; Watanabe, Lamsal and Ives, 2009; Carey *et al.*, 2012; Emmer and Vilímek, 2013; Emmer *et al.*, 2016; Somos-Valenzuela *et al.*, 2016). Detailed analysis of geomorphological and sedimentological

conditions within Llaca Lake will also provide valuable data with which to evaluate lake volumes and water resource management in a region where most communities rely on a supply of glacial meltwater for drinking, agricultural and industrial uses (Mark and Seltzer, 2003, 2005; Chevallier *et al.*, 2011; Condom *et al.*, 2011; Viviroli *et al.*, 2011; Baraer *et al.*, 2012; Bury *et al.*, 2013).

3.2 ANDEAN TROPICAL GLACIERS AND CLIMATE CHANGE

Tropical glaciers in the Andes are shrinking at a considerable rate (Silverio and Jaquet, 2017; INAIGEM, 2018; Veettil, 2018; Vuille et al., 2018). In Perú, which lies in the outer tropics, precipitation is generally considered to have the strongest influence on glacier mass balance (Vuille et al., 2008) and occurs mostly in the wet season between November and March (Kaser, 2001; Rabatel et al., 2013; Veettil et al., 2017). A delayed wet season will lead to high ablation rates as the low albedo of the mostly debris-covered glacier surface at the end of the dry season causes high rates of absorption of solar radiation and enhanced melting. However, since there is no evidence to suggest that precipitation amounts have decreased during the 20th century, it is likely that increased average annual temperatures are the main cause for the documented shrinking of the Andean cryosphere (Vuille et al., 2003, 2008; Rabatel et al., 2013). Analysis of data from over 100 weather stations in the Cordillera Blanca has identified an annual average air temperature increase of about 0.31ºC per decade between 1969 and 1998, and of 0.13 ºC per decade from 1983 to 2012 (Mark and Seltzer, 2005; Schauwecker et al., 2014). This average temperature increase has greatly enhanced melting of glaciers in the Cordillera Blanca (Barnett, Adam

and Lettenmaier, 2005), decreasing the total glaciated area from 800-850 km2 in 1930 to 448.81 km2 in 2016 (Georges, 2004; INAIGEM, 2018).

3.3. STUDY AREA: CORDILLERA BLANCA

The Cordillera Blanca is a 250km long mountain range that lies within the Peruvian Cordillera Occidental, and contains the largest tropical glacier field in the world (Figure 3.1; Mark et al., 2010; Lynch, 2012; Bury et al., 2013; INAIGEM, 2018; Vuille et al., 2018). The majority of mountain summits within the Cordillera Blanca lie between 5000 and 6000 masl, with several reaching over 6000 masl in the northern and central part of the mountain range (Deverchère, Dorbath and Dorbath, 1989; Margirier et al., 2016). Nevado Huascarán, in the central part of the Cordillera Blanca, is the highest summit reaching an altitude of 6,757 masl (Margirier et al., 2016; INAIGEM, 2018). Granodiorites of the Cordillera Blanca Batholith (emplaced approximately 14-5 Ma; McNulty and Farber, 2002; Margirier et al., 2016) form the dominant geological units in this region and intrude into shales and sandstones of the Upper Jurassic Chicama Formation (Schwartz, 1988; Margirier et al., 2016, 2018). The Cordillera Blanca Batholith has been deeply incised by glaciers during the Quaternary creating the deep, U-shaped glacial valleys prominent throughout the mountain range (Clapperton, 1972; Rodbell, 1992; Smith, 2005).

As the glaciers of the Cordilla Blanca rapidly retreat, the previously glaciated valleys and deeply scoured basins they contain, are quickly infilled by glacial meltwater creating a variety of ice contact and non-ice contact glacial lakes (Figures 3.2, 3.3). The first inventory of glacial lakes in the Cordillera Blanca, compiled in 1951, identified 230 lakes of ‘significant size’ (Concha, 1951); the most recent national inventory (2014) reports

over 2370 glacial lakes in the Cordillera Blanca, 830 of which have a surface area greater than 5,000 m2 (Tacsi Palacios et al., 2014). Vilímek et al. (2016) identified 2370 lakes of all sizes in the Cordillera Blanca; Emmer et al. (2016) used the same data source to identify 882 lakes of 'significant size' (lake width >20m plus lake width &length > 100 m). The most recent lake inventory (Emmer et al. 2020) determined that ~643 lakes existed in 1948 and ~893 lakes in 2017; total lake area also increased from approximately 29 km2 in 1948 to 35 km2 in 2017. In addition, of all glacial lakes analyzed, 38% were moraine-dammed (Emmer et al, 2020), and the majority of large lakes (> 100,000 m2) identified are characterized as moraine-dammed lakes (48%; Emmer et al., 2016, 2020; Harrison et al., 2018).

A major concern is that many of these glacial lakes are impounded by large, often unstable, latero-frontal moraines that act as naturally occurring dams (Kershaw, Clague and Evans, 2005; Emmer and Vilímek, 2013; Miles et al., 2018); in the Cordillera Blanca, ~31% of lakes can be classified as moraine-dammed (Emmer et al., 2016). Displacement of proglacial lake water caused by various mechanisms such as landslides, rockfalls or icefalls, can lead to moraine dam breach and the sudden release of water as glacial lake outburst floods (GLOFs). These floods can be catastrophic to communities living down-valley of the moraine impounded lakes (Figure 3.3; Carey, 2005; Hubbard et al., 2005; Kershaw, Clague and Evans, 2005; Emmer et al., 2016). In 1941, a catastrophic flood released by failure of the moraine dam of Lake Palcacocha took the lives of 1800 people in and around the city of Huaraz (Carey, 2005; Wegner, 2014). Since this event, the water levels in many lakes within the Cordillera Blanca are monitored and remediation efforts

Figure 3.3: Location of major cities in the Callejón de Huaylas (green dots) and glacial lakes (red arrows) in the Cordillera Blanca that have undergone remediation works and/or have been identified with potential for GLOFs (Vilímek *et al.*, 2005; Emmer and Vilímek, 2013; Klimeš *et al.*, 2014, 2016; Schneider *et al.*, 2014; Emmer *et al.*, 2016; Emmer, Vilímek and Zapata, 2018; INAIGEM, 2018; Mergili *et al.*, 2020). Image source from Google Earth (2020).

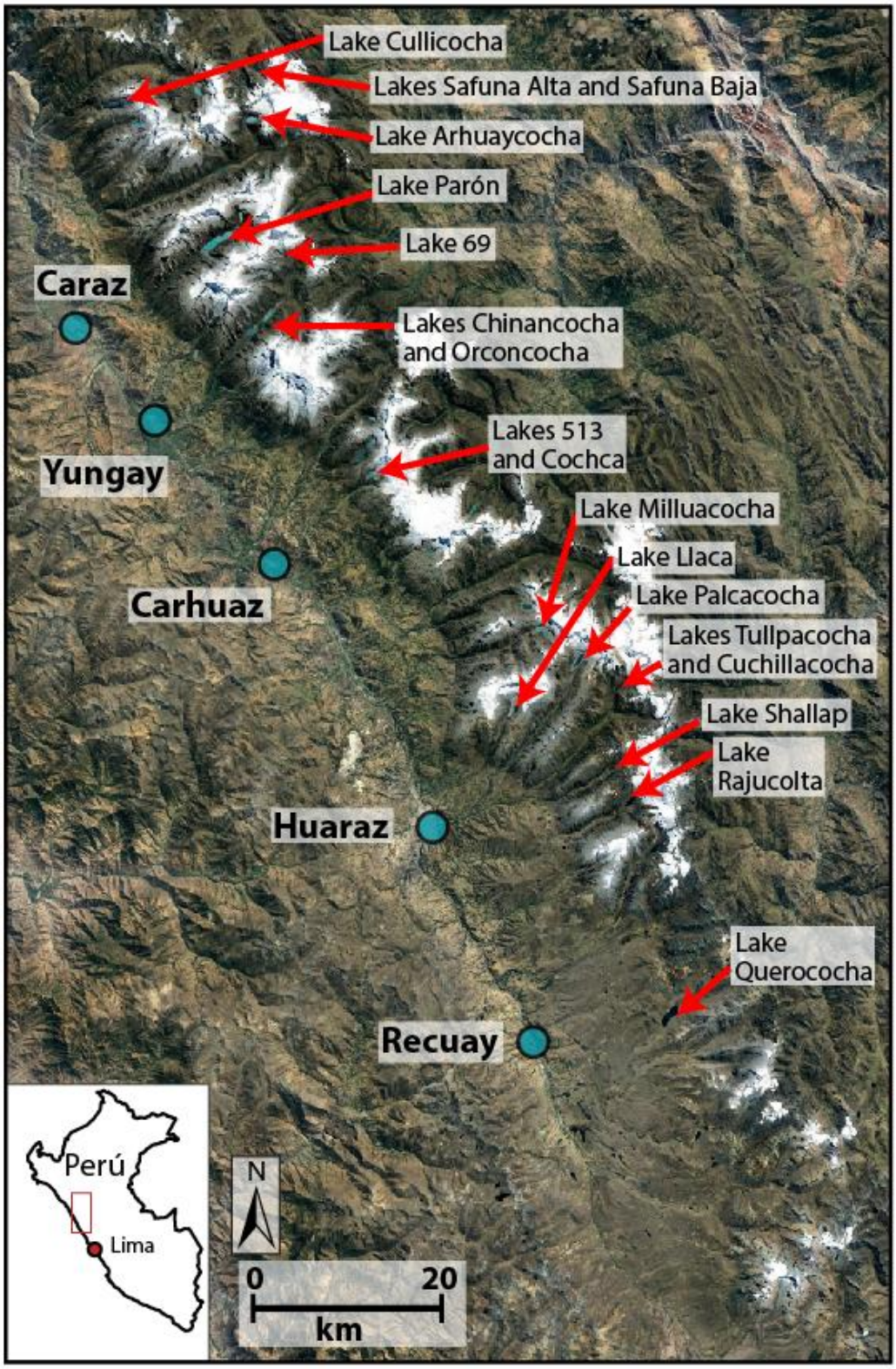
Lake Cullicocha
Lakes Safuna Alta and Safuna Baja
Lake Arhuaycocha
Lake Parón
Lake 69
Caraz
Lakes Chinancocha and Orconcocha
Yungay
Lakes 513 and Cochca
Lake Milluacocha
Lake Llaca
Carhuaz
Lake Palcacocha
Lakes Tullpacocha and Cuchillacocha
Lake Shallap
Lake Rajucolta
Huaraz
Lake Querococha
Recuay
Perú
Lima
N
0
20
km

have strengthened the moraine dams of approximately 40 lakes (Emmer, Vilímek and Zapata, 2018); efforts have also been made to predict and model the occurrence of these hazardous GLOF events (Klimeš, Vilímek and Omelka, 2009; Carey, 2010; Carey et al., 2012; Klimeš et al., 2014; Portocarrero, 2014; Schneider et al., 2014; Emmer et al., 2016; Somos-Valenzuela et al., 2016).

3.3.1 Llaca Glacier and Llaca Lake

Llaca Glacier is situated at the head of the Llaca Valley, a linear and relatively narrow valley (~500 m) that extends from a large cirque bordered by Nevado Vallunaraju (5686 masl) in the west, Nevado Ocshapalca (5888 masl) in the north, and Nevado Ranrapalca (6162 masl) in the east (Figure 3.2; Torres Amado, Dávila Roller and Vilca Gómez, 2016). The tributary glaciers Ocshapalca and Ranrapalca extend into the valley to join as Llaca Glacier, which terminates in Lake Llaca at an elevation of ~4500 masl. Supraglacial debris, sourced from the steep valley walls and lateral moraines that surround the glacier, covers much of the glacier surface and is > 1m thick at its terminus in Llaca Lake (Wigmore and Mark, 2017). Llaca Lake fronts the active ice margin, overlies stagnant glacier ice in the basin, and is impounded by a large latero-frontal moraine (Figure 3.4, 3.5). This supraglacial moraine-dammed lake is approximately 1km long (Figure 3.5, 3.6) and lies approximately 14 km northeast of the city of Huaraz (Figure 3.2; Torres Amado, Dávila Roller and Vilca Gómez, 2016). The water that flows from Llaca Lake is part of the sub-basin Casca that drains into the larger Santa River, the most important freshwater river in the region (Figure 3.1, 3.3; Torres Amado, Dávila Roller and Vilca Gómez, 2016).

In 1973, Llaca Lake was reported to have a volume of 794,000 m3 and an area of 63,312m2 (Torres Amado, Dávila Roller and Vilca Gómez, 2016; ANA, 2020). In an effort to mitigate the potential of a GLOF, a 10 m high earth dam was constructed in 1977 to control and elevate the lake outflow on the latero-frontal moraine (Figure 3.4; Portocarrero, 2014). In 2004, a new survey indicated the lake to have a reduced volume of 274,305 m3, an area of 43,988 m2, and a maximum depth of 16.8m (Torres Amado, Dávila Roller and Vilca Gómez, 2016). Estimates of the lake size made in 2017 show the lake has since expanded and now has a volume of 495,477m3, an area of 65,513 m2, and an approximate dam freeboard of 14 m (Figure 3.4; INAIGEM, 2018).

As with most glaciers in the Cordillera Blanca (Silverio and Jaquet, 2017; INAIGEM, 2018), Llaca Glacier has undergone significant marginal retreat and loss of mass over the past several decades. Between 2005 and 2019 the active glacier margin retreated between 250 and 330 m (Figure 3.5). It is not known exactly when ice stagnated in the basin now covered by Llaca Lake but the presence of Llaca Lake as a body of water was first reported in 1973 (Torres Amado, Dávila Roller and Vilca Gómez, 2016). The lake began to form and grow as the underlying stagnant ice progressively melted; this dynamic process can be clearly seen on satellite imagery of the region taken between 2005 and 2019 (Figure 3.5). Differential melting of stagnant ice buried beneath the water and sediment cover has created a constantly changing topography of exposed ice-cored hummocks and water filled basins (Figure 3.5; Iturrizaga, 2014). The exposed hummocks provide important information regarding the nature of sediments accumulating in such supraglacial lake basins.

Figure 3.4: A – Downvalley view of Llaca Valley from the top of the Llaca Dam. Coarse-grained debris comprising the latero-frontal moraine is visible on the left side of the image. Note the constructed dam and outflow channel which were emplaced to reduce the risk of dam breaching. B – View up-valley of the Llaca Lake dam (the dam is approximately 14 m high). Llaca Lake lies between the dam and Llaca Glacier in the background.

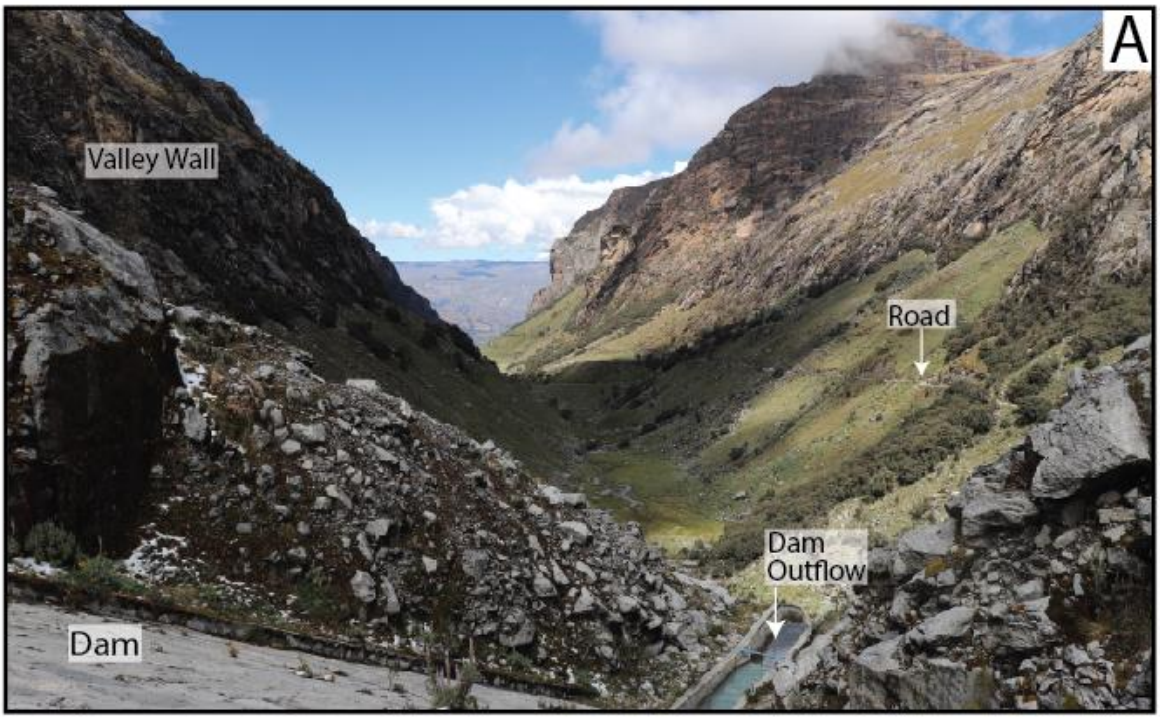
A
Valley Wall
Road
Dam
Outflow
Dam

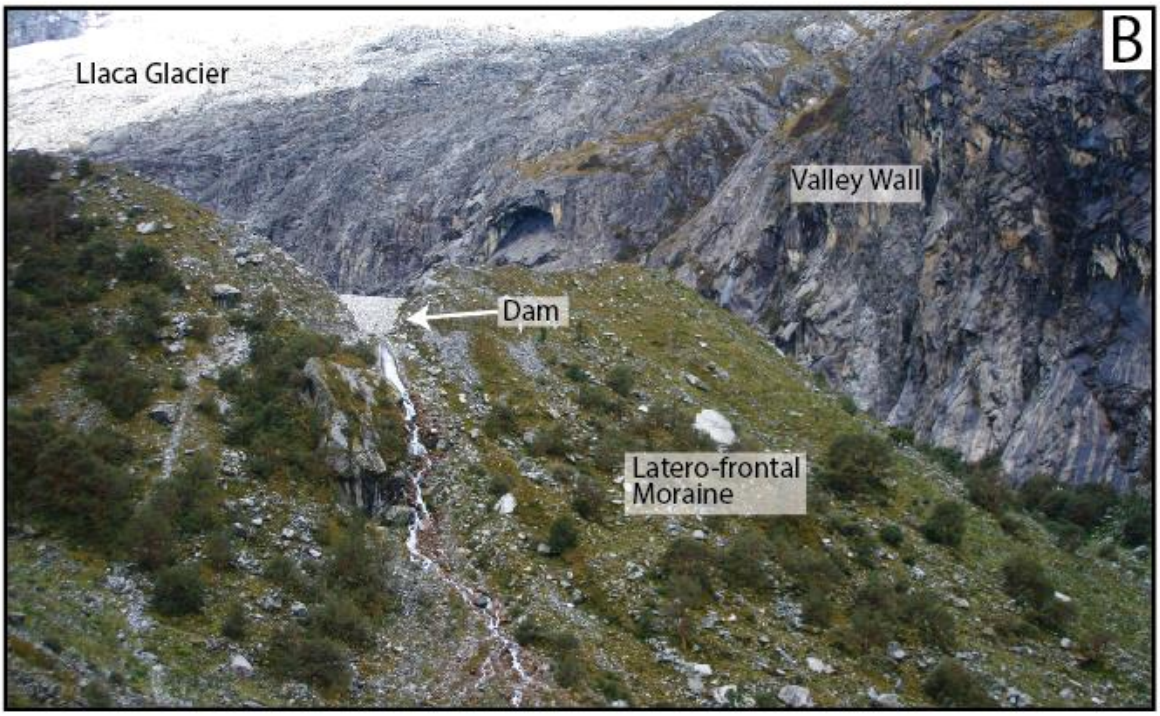
B
Llaca Glacier
Valley Wall
Dam
Latero-frontal
Moraine

Figure 3.5: Mapped satellite imagery showing changes in the distribution of lake water and exposed sediment/ice cored hummocks in Lake Llaca as Llaca Glacier receded between 2005 and 2019. Satellite imagery from Google Earth.

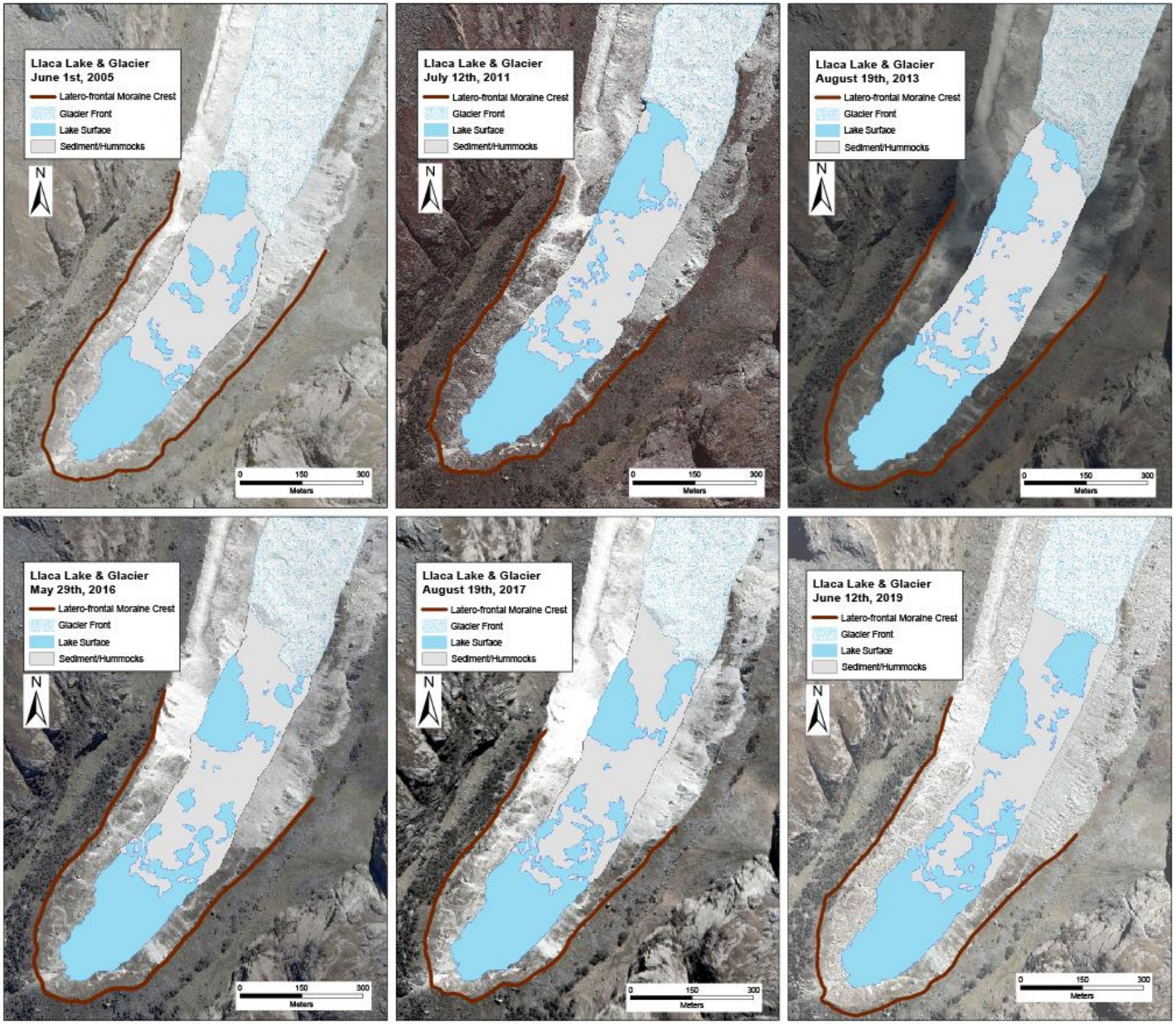
Llaca Lake & Glacier
June 1st, 2005
Latero-frontal Moraine Crest
Glacier Front
Lake Surface
Sediment/Hummocks
N
0 150 300
Meters
Llaca Lake & Glacier
July 12th, 2011
Latero-frontal Moraine Crest
Glacier Front
Lake Surface
Sediment/Hummocks
N
0 150 300
Meters
Llaca Lake & Glacier
August 19th, 2013
Latero-frontal Moraine Crest
Glacier Front
Lake Surface
Sediment/Hummocks
N
0 150 300
Meters
Llaca Lake & Glacier
May 29th, 2016
Latero-frontal Moraine Crest
Glacier Front
Lake Surface
Sediment/Hummocks
N
0 150 300
Meters
Llaca Lake & Glacier
August 19th, 2017
Latero-frontal Moraine Crest
Glacier Front
Lake Surface
Sediment/Hummocks
N
0 150 300
Meters
Llaca Lake & Glacier
June 12th, 2019
Latero-frontal Moraine Crest
Glacier Front
Lake Surface
Sediment/Hummocks
N
0 150 300
Meters

3.4 METHODOLOGY

This study involves the integration of remotely sensed data with field-based sedimentological observations and geomorphological mapping. Google Earth satellite imagery (taken in 2005, 2011, 2013, 2016, 2017, 2019) was utilized in this study to provide high resolution images (< 0.5 m) that allowed identification of geomorphological features within Llaca Lake and documentation of their changes over time (Figure 3.5). Vector shapefiles (points, lines, and polygons) of these surface features were created for each of the Google Earth datasets available for selected years between 2005 and 2019 and were imported into ArcMap for analysis of their dimensions (Figure 3.5).

Field work at Llaca Lake was conducted during May 2017 and May 2019 and included the observation and measurement of sedimentological and geomorphological features and the completion of aerial surveys by an uncrewed aerial vehicle (UAV). The locations of logs recorded from sedimentary lithofacies exposed in hummocks on the ice surface and in two excavated pits on the lake margin are shown in Figure 3.6. Sedimentary lithofacies were photographed and logged using standard sedimentological techniques recording texture, field-estimated particle size, clast shape, clast lithology, sedimentary structures and/or deformation structures.

To allow a more detailed analysis of the geomorphology of Llaca Lake and its associated landforms and sediments, a DJI Phantom 4 Advanced uncrewed aerial vehicle (UAV) was used to complete 7 photogrammetric aerial surveys of the Llaca Lake region, covering a total area of 2 km^2. The aerial surveys were flown 50 – 60 m above the ground surface, depending on proximity to the surrounding valley walls and obstacles to the

Figure 3.6: Orthomosaic model of Llaca Lake created from UAV photogrammetry (2019) showing the frontal section of the latero-frontal moraine and the margin of Llaca Glacier (upper right). Location of sedimentary logs recorded from excavations in ice-cored hummocks is indicated by the orange dots; the location of sedimentary logs recorded from pits excavated on alluvial fans is indicated by yellow dots. Resolution of orthomosaic model is 5 cm. B. Orthomosaic model overlaid on a 5cm DEM.

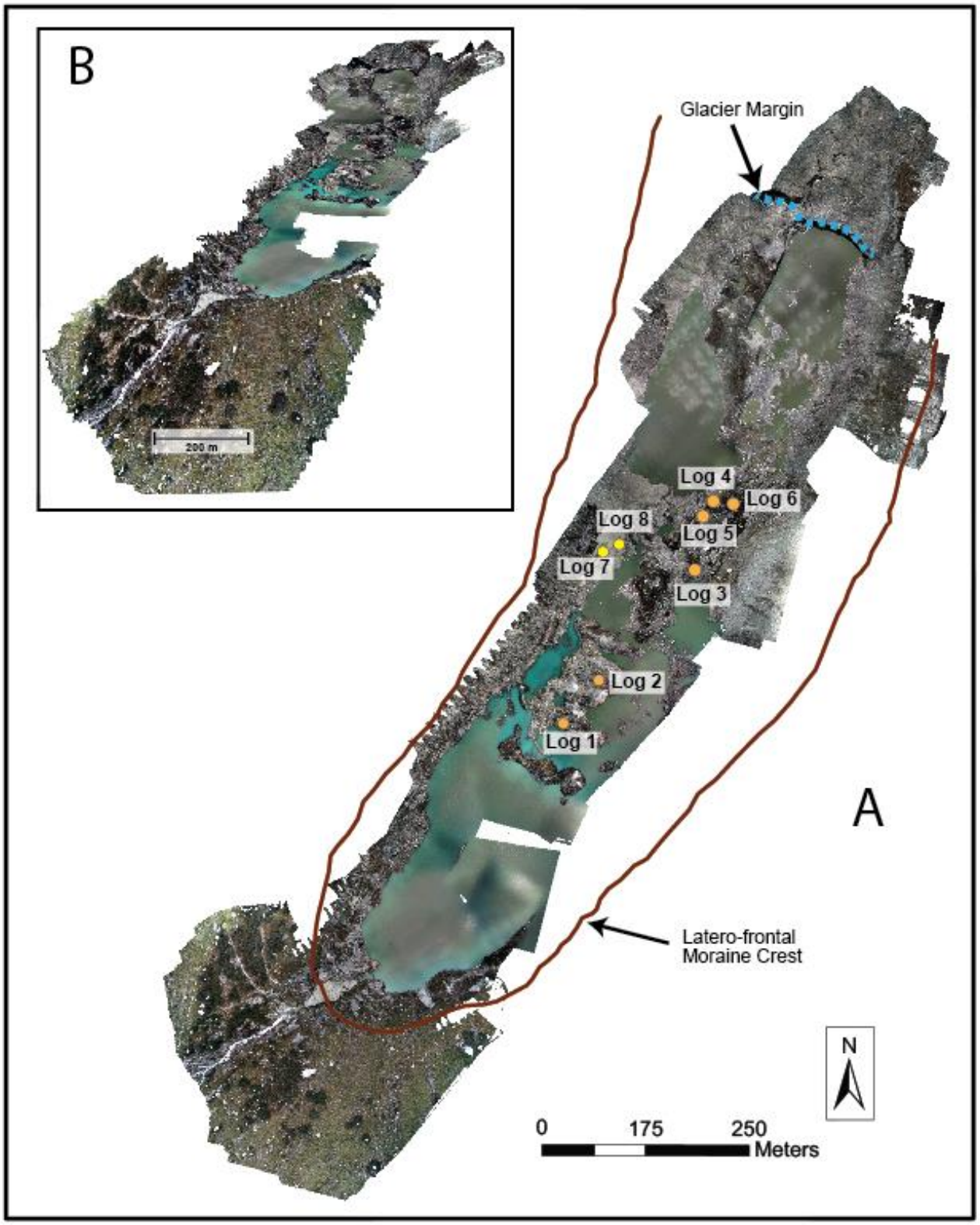
B
200 m
Glacier Margin
Log 4
Log 6
Log 8
Log 5
Log 7
Log 3
Log 2
Log 1
A
Latero-frontal
Moraine Crest
N
0
175
250
Meters

flight path, resulting in a pixel resolution of 5 cm. Ground control points (GCPs) were established in accessible locations using a portable GPS (SXBlue GNSS); these GCPs allowed georectification of the photogrammetric point cloud generated from UAV surveys and the creation of "check points" for accuracy assessment of derived Digital Elevation Models (DEMs). A model of the study area was created from the photogrammetric imagery using Agisoft Metashape Professional software (Figure 3.6). Data processing of the imagery followed a standard Structure from Motion (SfM) workflow (Gauthier, Wood and Hutchinson, 2015; Evans, Ewertowski and Orton, 2016; Ely et al., 2017), including alignment of photos, point cloud generation, input of GCPs, model generation, and the final output of a high-resolution DEM (5 cm) and orthophotos (5 cm).

The sedimentological and geomorphological data were combined to determine process-form relationships within the Llaca Lake landsystem and to identify landsystem elements. A geomorphological map of the landsystem elements was created using data from the model developed from the UAV survey, field observations, and recent aerial imagery (Google Earth, 2020, ESRI 2019; Figure 3.7). Landform elements were then grouped into landsystem zones which are the product of spatially differentiated processes operating within the landsystem (Nick Eyles, 1983; Evans, 2003). Landsystem analysis is a powerful tool that has been used in a range of glacial environments to understand both modern glaciers and ice sheets and for paleoglacial reconstruction (Evans, Lemmen and Rea, 1999; Evans, 2003; Fitzsimons, 2003; Glasser and Hambrey, 2003; Schomacker, Benediktsson and Ingólfsson, 2014; Stokes et al., 2015; Evans, Ewertowski and Orton, 2016, 2017; Chandler et al., 2020). By linking the geomorphology of the terrain with its subsurface

Figure 3.7: Landsystem element map based on data compiled from the 2019 UAV survey and othomosaic model, field observations, and recent aerial imagery (Google Earth, 2020; ESRI, 2019).

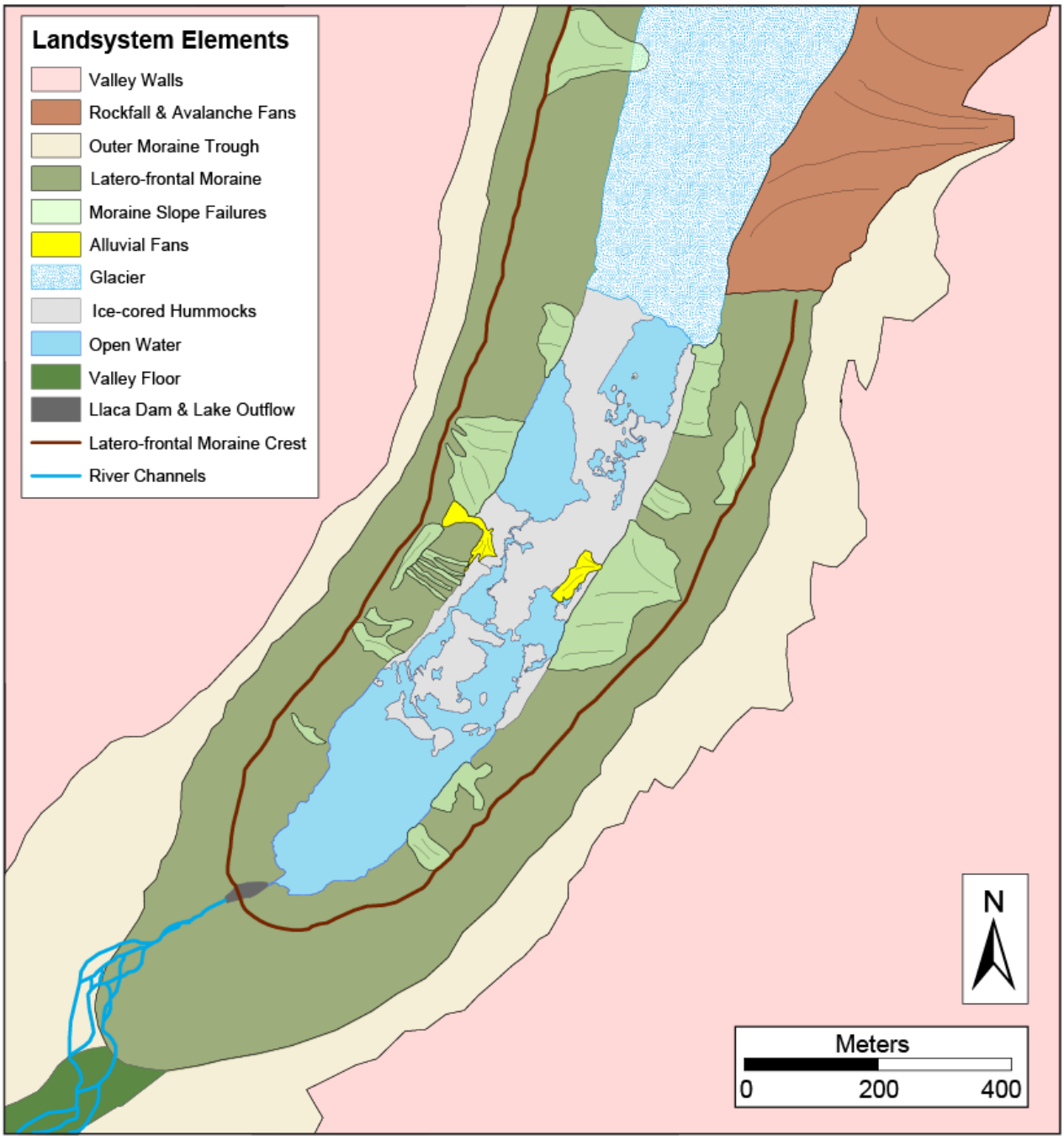
Landsystem Elements
Valley Walls
Rockfall & Avalanche Fans
Outer Moraine Trough
Latero-frontal Moraine
Moraine Slope Failures
Alluvial Fans
Glacier
Ice-cored Hummocks
Open Water
Valley Floor
Llaca Dam & Lake Outflow
Latero-frontal Moraine Crest
River Channels
N
Meters
0
200
400

material and depositional processes, the delineation of glacial landsystems also allows for subsurface conditions to be predicted from surface morphological features.

3.5 GEOMORPHOLOGICAL CHARATERISTICS OF LLACA LAKE

Geomorphological mapping of surface landforms identified from Google Earth imagery and from the DEMs and orthomosaic model created from the UAV survey allowed delineation of eight landsystem elements (Figure 3.7). These elements include the valley walls, outer moraine valley trough, rockfall and avalanche fans, the latero-frontal moraine damming the lake, the debris-covered glacier tongue, moraine slope failures, ice-cored hummocks, and alluvial fans.

Valley Walls

Valley walls that enclose the Lake Llaca landsystem are composed of granodiorite (Cobbing et al., 1981; Giovanni et al., 2010) and are subject to a variety of mass wasting processes including rockfalls and rock slides. The Llaca Valley is relatively narrow, ranging from 500 – 800m wide (Figure 3.2 & 3.7) and has a northeast - southwest orientation (Wigmore and Mark, 2017). At the narrowest part of the valley, around the position of the front of the latero-frontal moraine, valley walls are extremely steep (ranging from 68°-83°); as the valley widens towards the active glacier face, the valley walls are less steep (approximately 57°-77°). These steep valley rockwalls are the primary sediment source for rockfalls and debris flows and contribute a significant amount of debris into the Llaca Lake system.

Outer Moraine Trough

The outer moraine trough is located between the valley walls and the distal slope of the latero-frontal moraine and is vegetated by grasses, small shrubs, and trees (Figure 3.5). The width of the trough varies from 20m to 150m, and it generally widens in the down-valley direction; the western valley trough is narrower than the eastern valley trough (Figure 3.7). The outer moraine trough acts as a gutter, trapping debris and sediment from rockfall debris. Rockfall and avalanche fans that supply coarse material to the trough floors are also present, particularly along the eastern moraine valley trough (Figure 3.5).

Latero-frontal Moraine

Approximately 60-80 m in height and with varying widths of between 150-300 m, the large latero-frontal moraine (Figures 3.4, 3.5, 3.7) that currently impounds Llaca Lake is an imposing geomorphic feature. This large moraine is composed of poorly-sorted sediments of glacial or glacially transported origin which were likely deposited by a combination of processes including debris falls, slumps, and slides from supraglacial and englacial sources (Owen and Derbyshire, 1989; Benn et al., 2003). The latero-frontal moraine passes up-valley into lateral moraines fringing the current glacier margins (Figures 3.4, 3.5). Internally, these lateral moraines display crude stratification and variable sorting (Figure 3.8C, 3.8D) suggesting they may have resulted from the alternating accumulation of sediment supplied by supraglacial debris flows and glaciofluvial streams on the lateral ice margins (Kirkbride and Spedding, 1996; Benn and Owen, 2002; Sigurðardóttir, 2013). The northwestern side of the latero-frontal moraine is well vegetated with shrubs, trees, and grasses; vegetation is sparse on the southeaster side of the moraine, although small clusters of trees grow on the ridge between the latero-frontal moraine and valley wall (Figure 3.5).

Rockfall and Avalanche Fans

Large rockfall and avalanche fans (> 100 m in length) are generated by the downslope transport of large amounts of coarse-grained debris from the valley walls onto the glacier surface and into the valley (Figure 3.8A, 3.8B). Close to the active glacier margin, rock failures originate from the adjacent valley walls and contribute debris to both lateral moraines and the lake basin. Rockfall and avalanche fans are also present on the margins of the outer moraine valley troughs (Figure 3.5).

Debris-covered glacier tongue

The active tongue of Llaca Glacier terminates as a steep, debris-covered ice cliff in the northeastern portion of Llaca Lake (Wigmore and Mark, 2017; Figure 3.8A). The combination of high relief and frequent rockfalls and avalanches, triggered by events that include earth movements associated with ongoing tectonic uplift of the region, ensures that the tongue of Llaca Glacier is debris-covered (Figure 3.8A, 3.8B). This debris is typically dominated by angular clasts, with large boulders reaching up to several meters in diameter. As the ice cliff undergoes backwasting, this coarse-grained supraglacial debris is deposited into the lake basin (Figure 3.8A). The receding glacier tongue can be either in direct contact with the open water of the lake (e.g. Figure 3.9A, 3.9D), or covered by variable thicknesses of supraglacial debris (e.g. Figure 3.9B). The presence of this debris, combined with the many dynamic sedimentary processes operating in the region of the glacier tongue (e.g. sediment gravity flows, surface water flows) often make it difficult to determine the exact location of the active ice margin.

Figure 3.8: A – Annotated photograph of the margin of Llaca Glacier showing cover of supraglacial debris, exposed glacier ice and rockfall and avalanche fans. B – Upvalley view of Llaca Lake and Llaca Glacier. Alluvial fans entering the lake are outlined in orange; fine-grained sediment exposed on ice-cored hummocks is outlined in blue. C – Ice cored hummocks overlain by coarse, angular supraglacial debris. D – Supraglacial sediment on top of buried ice.

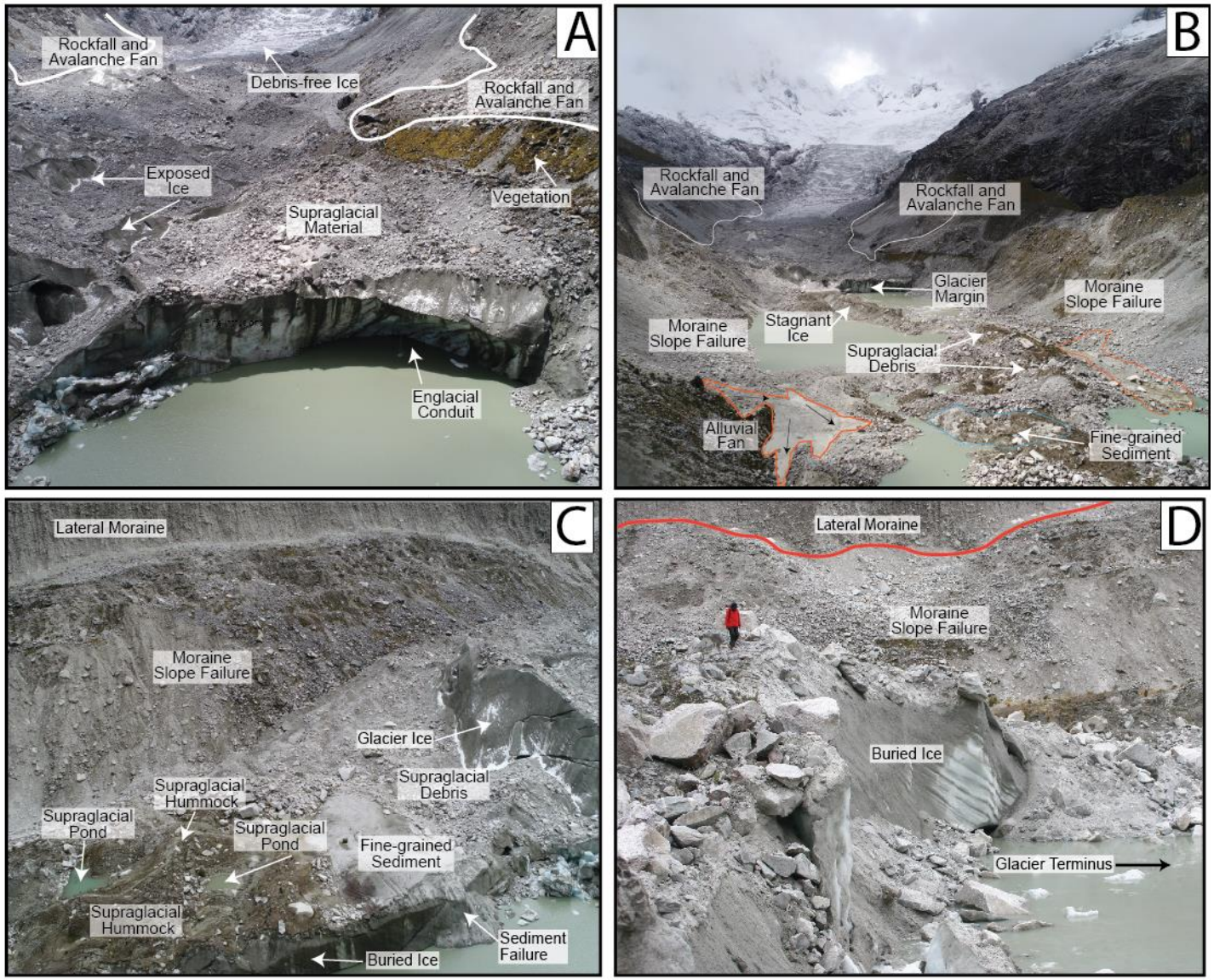
A
Rockfall and Avalanche Fan
Debris-free Ice
Rockfall and Avalanche Fan
Exposed Ice
Vegetation
Supraglacial Material
Englacial Conduit
B
Rockfall and Avalanche Fan
Rockfall and Avalanche Fan
Glacier Margin
Moraine Slope Failure
Moraine Slope Failure
Stagnant Ice
Supraglacial Debris
Alluvial Fan
Fine-grained Sediment
C
Lateral Moraine
Moraine Slope Failure
Glacier Ice
Supraglacial Debris
Supraglacial Hummock
Supraglacial Pond
Supraglacial Pond
Fine-grained Sediment
Supraglacial Hummock
Sediment Failure
Buried Ice
D
Lateral Moraine
Moraine Slope Failure
Buried Ice
Glacier Terminus

Moraine Slope Failures

There is abundant evidence to indicate intermittent failure of the steep moraine slopes bordering Llaca Lake (Figures 3.5, 3.7). These slope failures form coarse-grained sediment aprons, smaller (50-90 m in length) than the large rockfall and avalanche fans found up-valley and are common along the base of the latero-frontal moraine surrounding Llaca Lake (Figure 3.8B, 3.8C, 3.8D). Moraine slopes in the ice-distal (southwestern) section of the lake are often vegetated (with mosses and shrubs); removal of this vegetation when a failure event occurs allows the slope failure to be easily identified (Figure 3.10).

Ice-cored Hummocks

Large ice-cored sediment hummocks are found throughout the area of Llaca Lake (Figure 3.8B). These are created through differential melting of buried ice beneath the thick cover of lacustrine and supraglacial material that covers and insulates the decaying ice (Lukas, 2008; Bennett et al., 2010). Sediments exposed in the hummocks are mostly composed of either large angular or subangular boulders of supraglacial origin (Figures 3.6, 3.8B, 3.8C), or laminated fine-grained silts and fine sands deposited under lacustrine conditions (Figures 3.6, 3.8B, 3.8C). Some of the surficial debris present on the hummocks may also have been supplied by inflowing streams or the failure and transport of sediment from the steep and unstable moraine walls surrounding the lake. Variable thicknesses of supraglacial debris covering the buried stagnant ice permits differential rates of ablation and melting, creating a chaotic and constantly changing hummocky topography within the lake basin (Figures 5,3. 5.8B; Nicholson et al., 2018). The most ice-distal region of ice-cored hummocks was significantly reduced in aerial extent between 2005 and 2009

Figure 3.9: Changes in the Llaca Glacier debris-covered glacier tongue between 2013 and 2019. Red outline in all images marks the position of the visible glacier terminus in 2013. The blue outline in B (2016) shows the location of the water body that was present in front of the glacier margin in 2013 (A). The blue outlines in C (2017) show the location of small ponds that were present in 2016. The blue outline in D (2019) shows the location of the water body in 2017 (C).

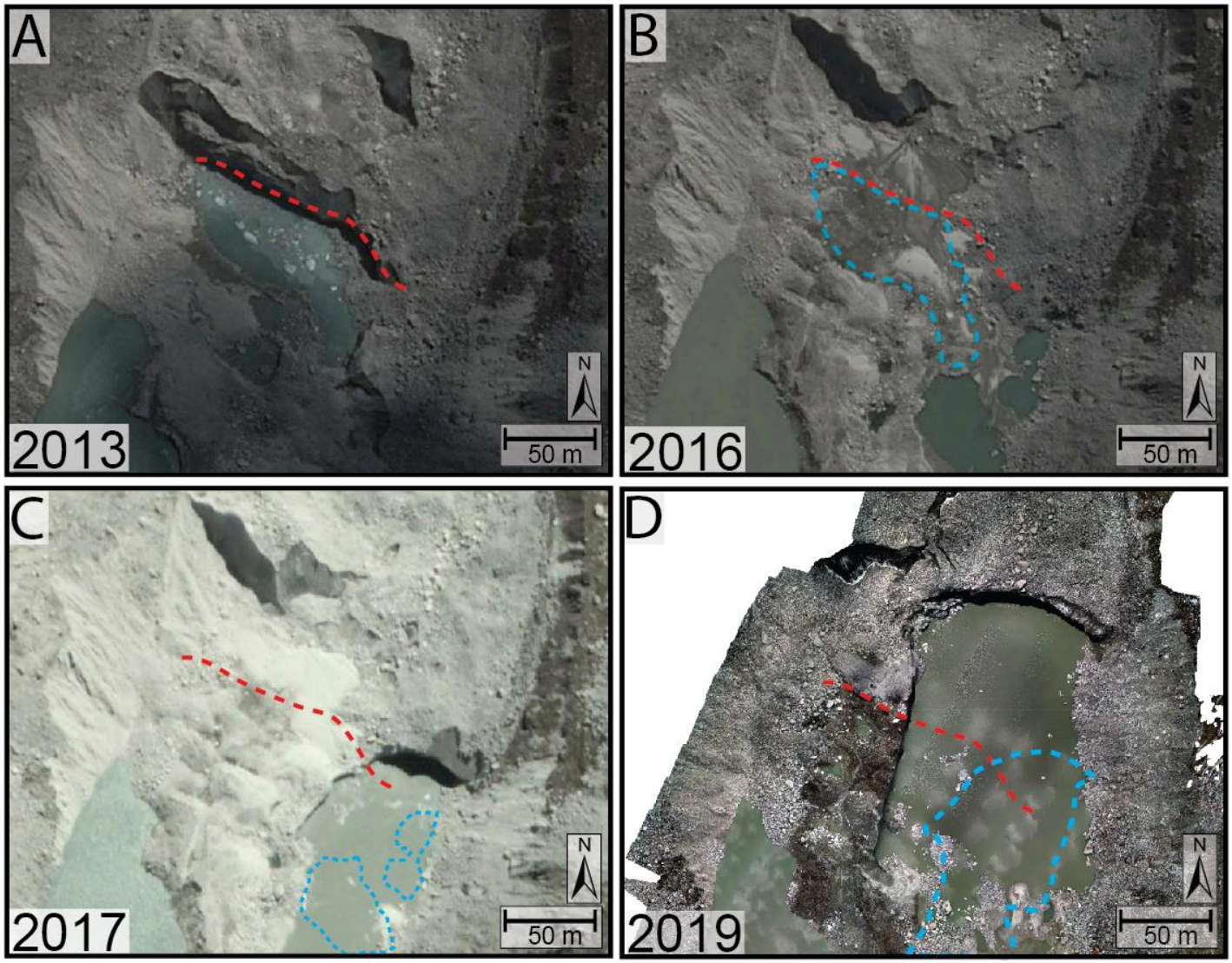
A
2013
N
50 m
B
2016
N
50 m
C
2017
N
50 m
D
2019
N
50 m

Figure 3.10: Moraine slope failures occur along the inner side of the latero-frontal moraine and transport sediment into the lake. A moraine slope failure that occurred at some time between 2013 (A) and 2016 (B) is recorded by satellite images taken in 2016 (red arrow; Google Earth, 2013, 2016).

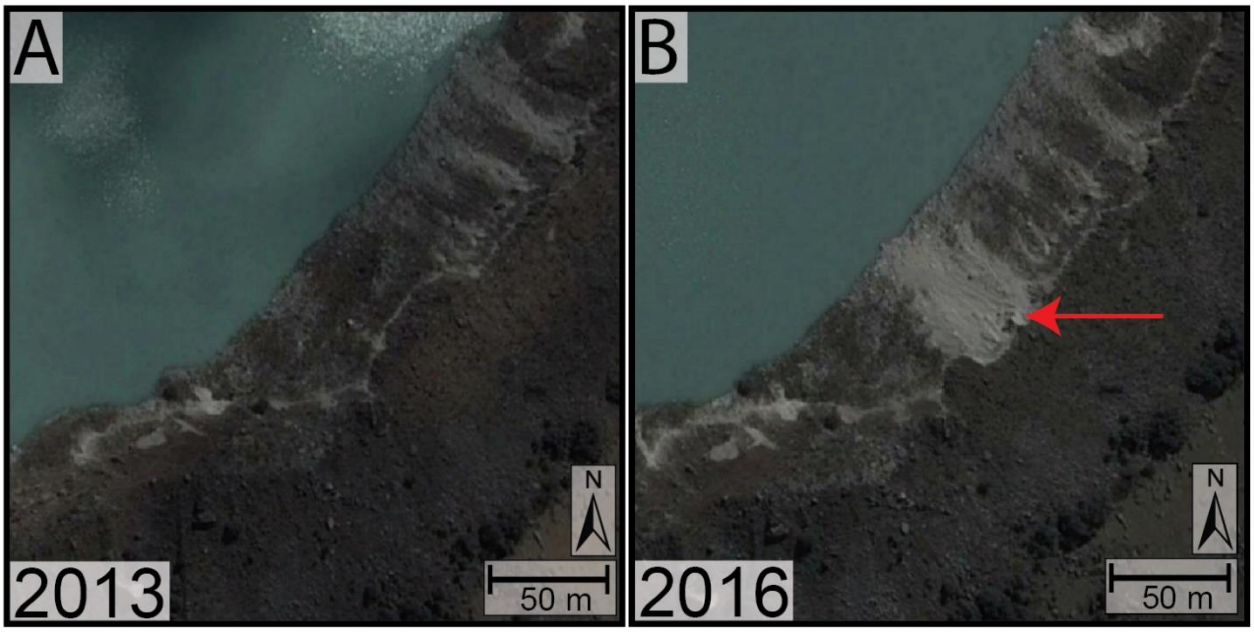
A
2013
N
50 m
B
2016
N
50 m

(Figure 3.11), but the overall form and location of the ice-cored region remained relatively uniform. In comparison, the ice-cored hummocks in the central section of the lake show a high degree of variability in the extent and form of the hummocks and associated open water bodies (Figure 3.12). The progressive changes in the topography of this region strongly suggest the continual melt of buried ice and progressive subsidence of the debris covered ice surface. Buried ice can also be observed in exposures through the hummocks close to the glacier margin (Figure 3.8C, 3.8D) and the hummocky surface topography elsewhere suggests that stagnant ice likely underlies most of the lake basin. The sedimentary facies present in these ice-cored hummocks (Figure 3.13, 3.14) are described in detail in the following section.

Alluvial fans

Alluvial fans generated by surface water flows transporting and reworking unstable sediment along the inner side of the lateral moraines, form fan-shaped bodies lying between Llaca Lake and the lateral moraines (Figure 3.7, 8B, 15). Sediments exposed in these fans are characterized by massive sand with pebbles (Sm, Gm; Figure 3.15B) deposited from the episodic rapid influx of sediment and are interbedded with occasional silt horizons.

3.6 SEDIMENTOLOGICAL CHARACTERISTICS

The sedimentary characteristics of two elements of the Llaca Lake landsytem are described here and include sediment exposed on the margins of ice-cored hummocks (logs 1-6; Figure 3.14) and in pits dug into an alluvial fan (logs 7 & 8; Figure 3.15). Eight lithofacies types

Figure 3.11: Change in size and shape of exposed ice-cored hummocks in the most ice-distal region of Llaca Lake between 2005 and 2019. Outline in red in B, C and D illustrate the size and shape of the area of ice-cored hummocks in 2005. Satellite Imagery for the years 2005, 2013, 2017 is from Google Earth (Google Earth, 2005, 2013, 2017). The 2019 image is from the model created in this study.

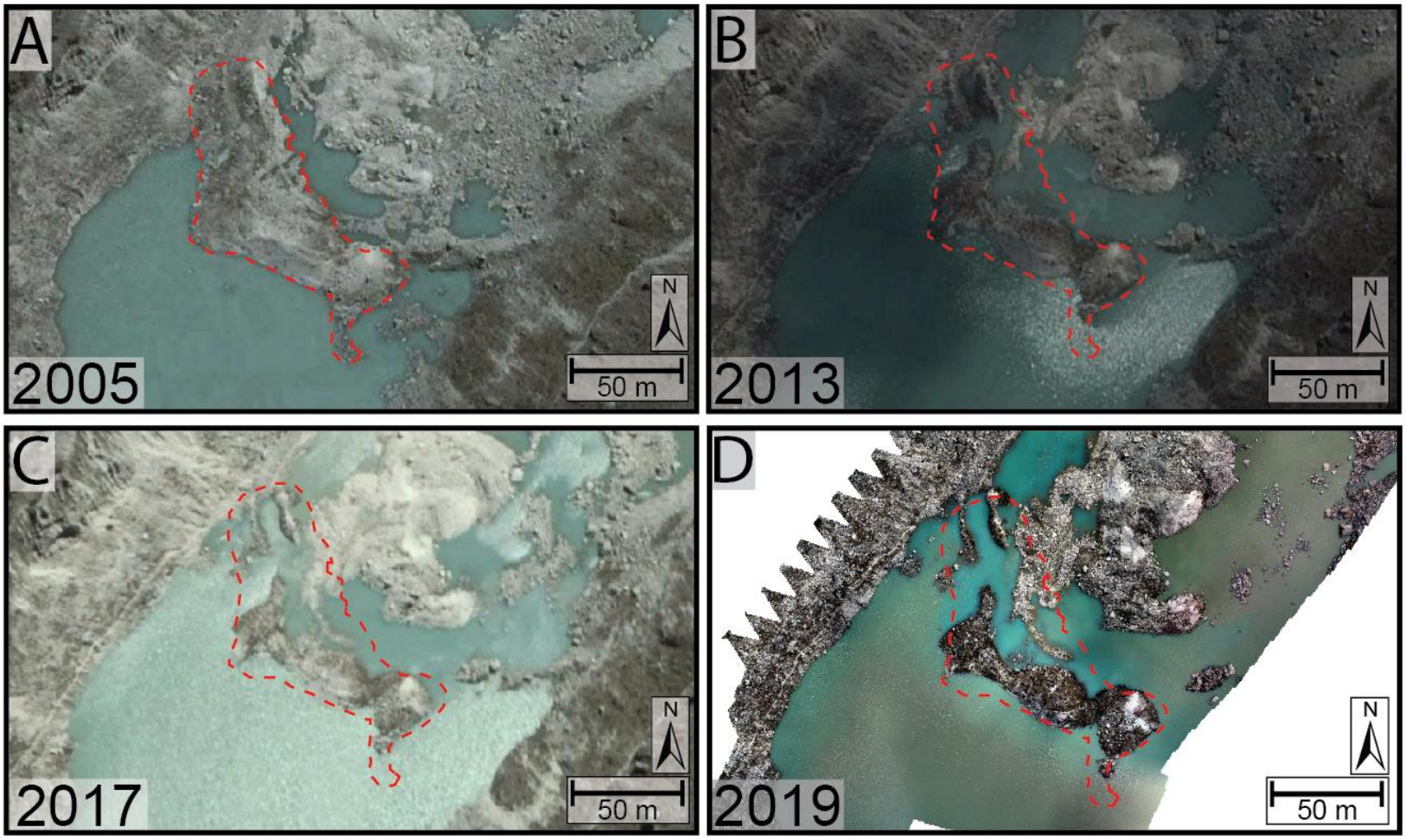
A
2005
N
50 m
B
2013
N
50 m
C
2017
N
50 m
D
2019
N
50 m

Figure 3.12: Ice-cored hummocks and water filled depressions in the central section of Llaca Lake between 2005 and 2019. Blue outlines in B show the location of open water in 2005 (A). The yellow outline on the 2016 image (C) shows the location of debris-covered, ice-cored hummocks in 2011 (B). Large areas of open water characterize this region in 2016. The 2019 image (D), derived from UAV photogrammetry, shows further development of these open water areas. Satellite imagery for 2005, 2011, and 2016 is from Google Earth (Google Earth, 2005, 2013, 2017).

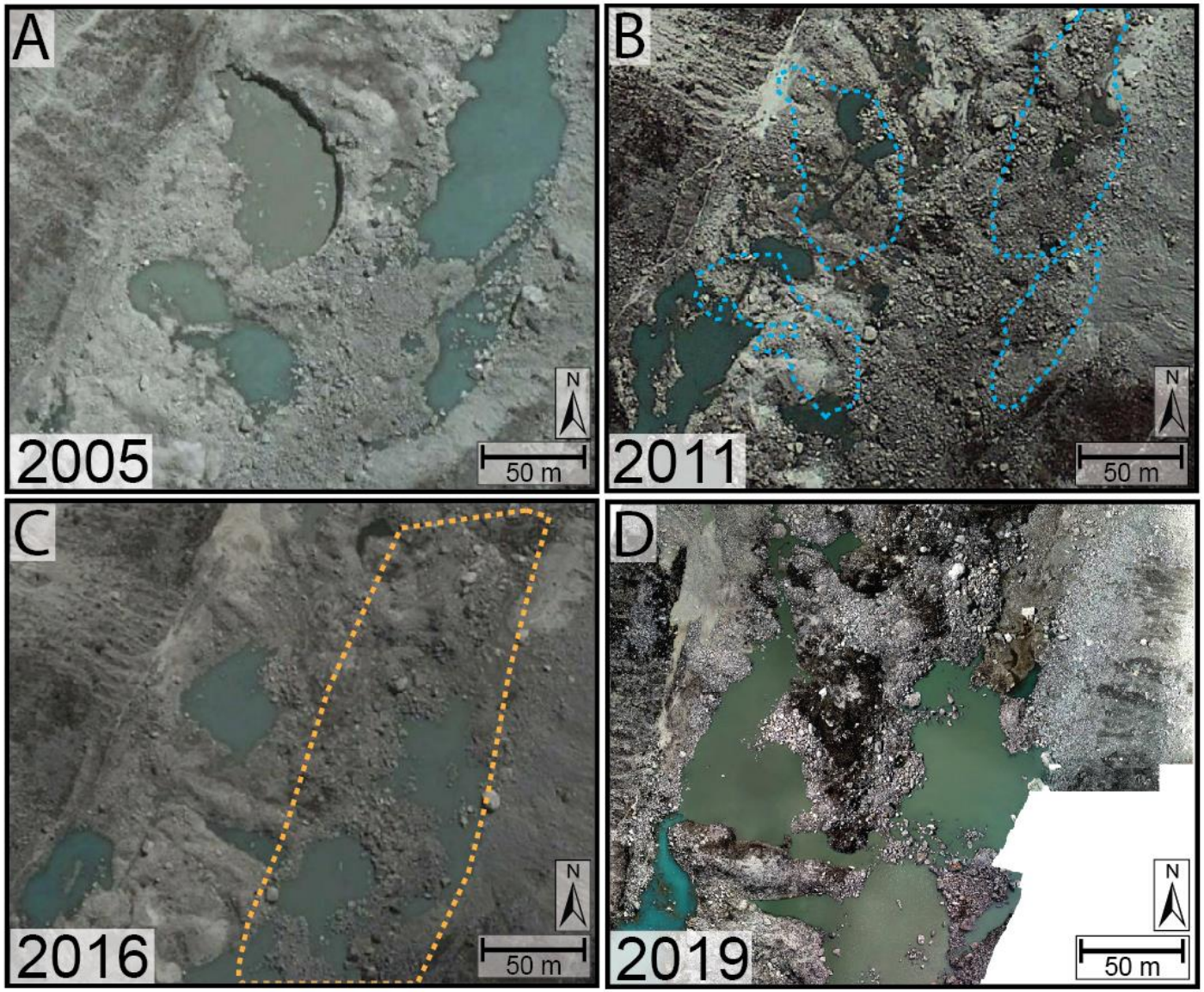
A
2005
N
50 m
B
2011
N
50 m
C
2016
N
50 m
D
2019
N
50 m

Figure 3.13: Sediments within ice-cored hummocks. A – massive gravel (Gm), subrounded to subangular clasts range from 5mm to 2-3cm; B – interbedded medium sand (Sh, Sm) and laminated silts and muds (Fl). Trowel is 25 cm long; C – two distinct beds of massive sand (Sm) overlain by interbedded sand and laminated fines (Sh, Fl); D – normally graded sand beds (Sg) overlain by massive sand with thin silt interbeds; E – medium-grained rippled sand unit (arrowed) within horizontally laminated sand; F – micro-faults within medium-grained laminated sand; G – Deformed fine to coarse sand (Sd) and silty sand; H – small dewatering structures within deformed sand; I – finely laminated silt and clay (Fl); J – deformed sand and deformed fines (Sd, Fd) showing a transition from severe to slight deformation from left to right of the image. Undeformed facies are shown beneath (Sh, Fl); K – clasts on the surface of an ice-cored hummock. Clasts are angular to subangular; surrounding matrix is composed of silt to fine sand; L – clast-rich surficial sediment comprising clasts from small granules 0.5cm to clasts ~1m in diameter.

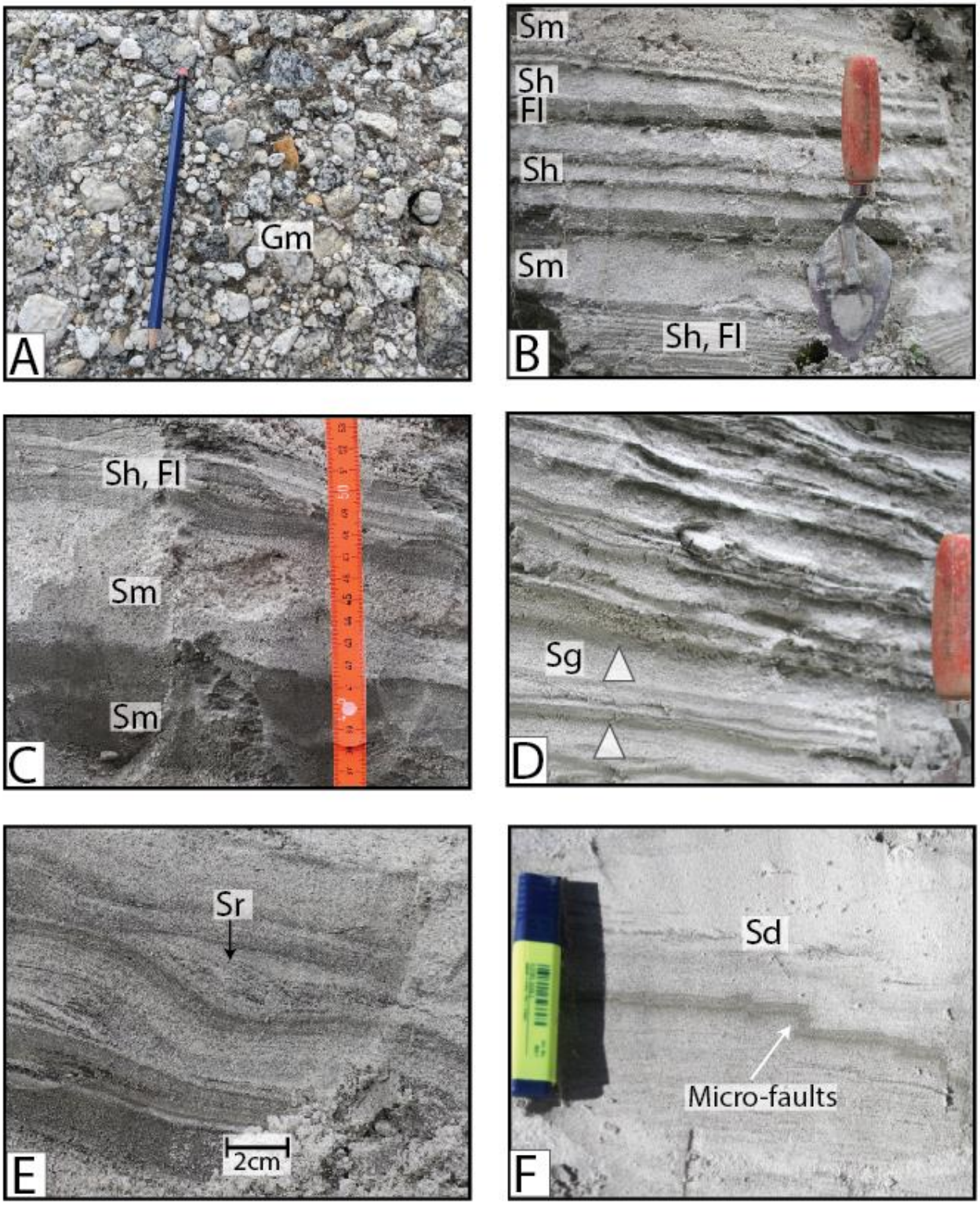
Gm
A
Sm
Sh
Fl
Sh
Sm
Sh, Fl
B
Sh, Fl
Sm
Sm
C
Sg
D
Sr
2cm
E
Sd
Micro-faults
F

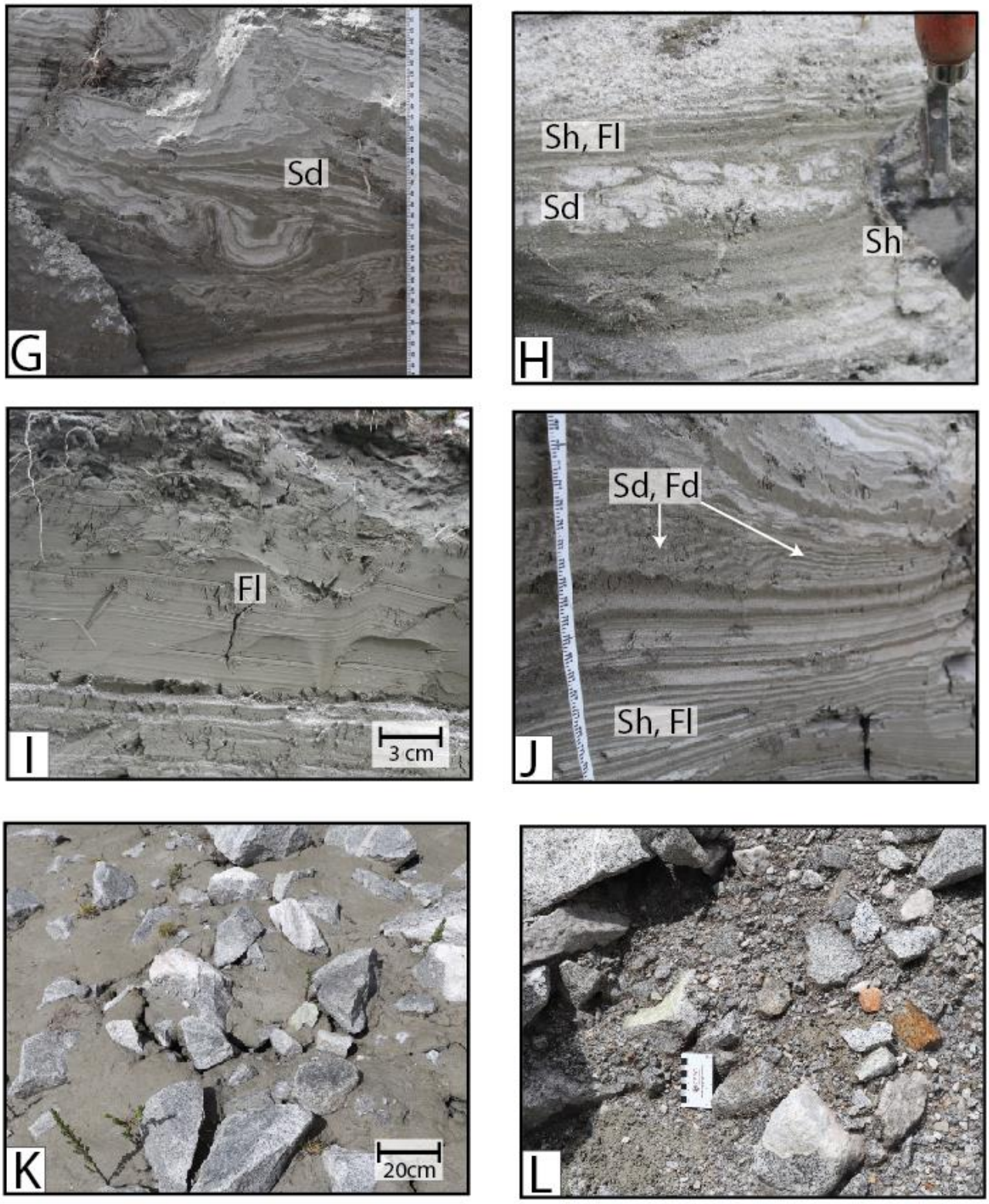
Sd
G
Sh, Fl
Sd
Sh
H
Fl
3 cm
I
Sd, Fd
Sh, Fl
J
20cm
K
L

Figure 3.14: Sedimentary logs recorded from exposures through ice-cored hummocks on Llaca Lake (see Figure 6 for log locations) with areas of interest outlined by red boxes. Box A – coarsening-upwards succession of interbedded sand and fine silt; B – unit of deformed sand (Sd) and silt (Fd). C –interbedded laminated silt and sand (Fl, Sh). D - interbedded laminated silt and sand (Fl, Sh) with thick packages of fine silt (Fl) recording fluctuating energy regimes and/or sediment supply to the lake. Log 5 is dominated by interbedded laminated silt and sand (Fl, Sh) as well as deformation structures (Fd, Sd). Log 6 is dominated by sand facies (Sd, Sm, Sg, Sh, Sr) with some interbedded fines (Fl).

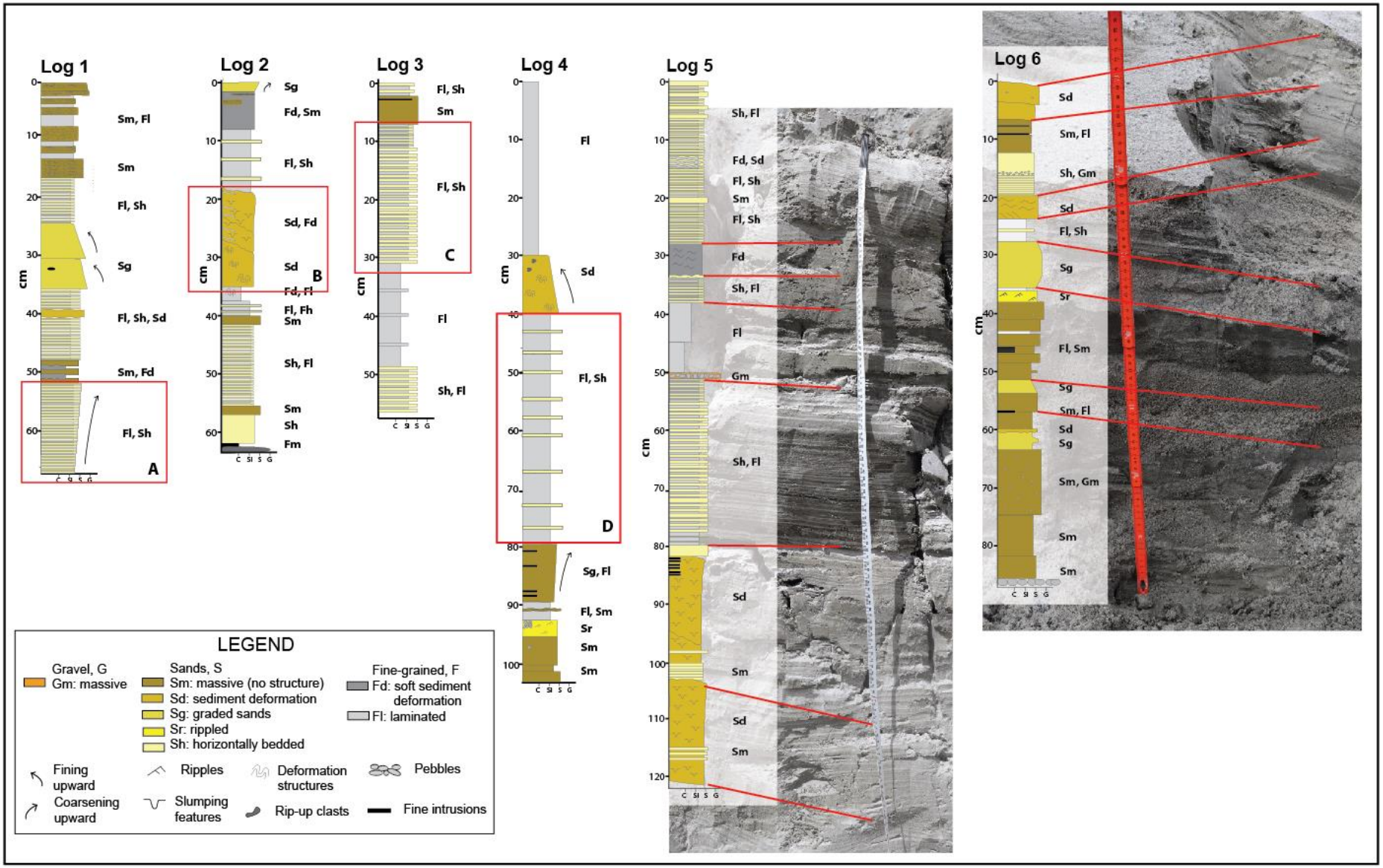
Log 1
Sm, Fl
Sm
Fl, Sh
Sg
Fl, Sh, Sd
Sm, Fd
Fl, Sh
A
Log 2
Sg
Fd, Sm
Fl, Sh
Sd, Fd
Sd
Fd, Fl
Fl, Fh
Sm
Sh, Fl
Sm
Sh
Fm
B
Log 3
Fl, Sh
Sm
Fl, Sh
Fl
Sh, Fl
C
Log 4
Fl
Sd
Fl, Sh
D
Sg, Fl
Fl, Sm
Sr
Sm
Sm
Log 5
Sh, Fl
Fd, Sd
Fl, Sh
Sm
Fl, Sh
Fd
Sh, Fl
Fl
Gm
Sh, Fl
Sd
Sm
Sd
Sm
Log 6
Sd
Sm, Fl
Sh, Gm
Sd
Fl, Sh
Sg
Sr
Fl, Sm
Sg
Sm, Fl
Sd
Sg
Sm, Gm
Sm
Sm
cm
C Sl S G
LEGEND
Gravel, G
Gm: massive
Sands, S
Sm: massive (no structure)
Sd: sediment deformation
Sg: graded sands
Sr: rippled
Sh: horizontally bedded
Fine-grained, F
Fd: soft sediment deformation
Fl: laminated
Fining upward
Coarsening upward
Ripples
Slumping features
Deformation structures
Rip-up clasts
Pebbles
Fine intrusions

Figure 3.15: Sedimentary facies within an alluvial fan. A – Location of alluvial fan on the margin of Llaca Lake. Flow paths on the surface of the fan are indicated by the black arrows. Red box shows location of excavated pits for photos B, C and sedimentary logs shown in D. Figures in red box for scale. B – massive sands with clasts on the surface of the fan. C – fine-grained laminated silt and clay just below fan surface. D - sedimentary logs recorded in two small pits dug into the alluvial fan showing areas dominated by laminated fines and gravels (Log 7) and massive sands and gravels (log 8).

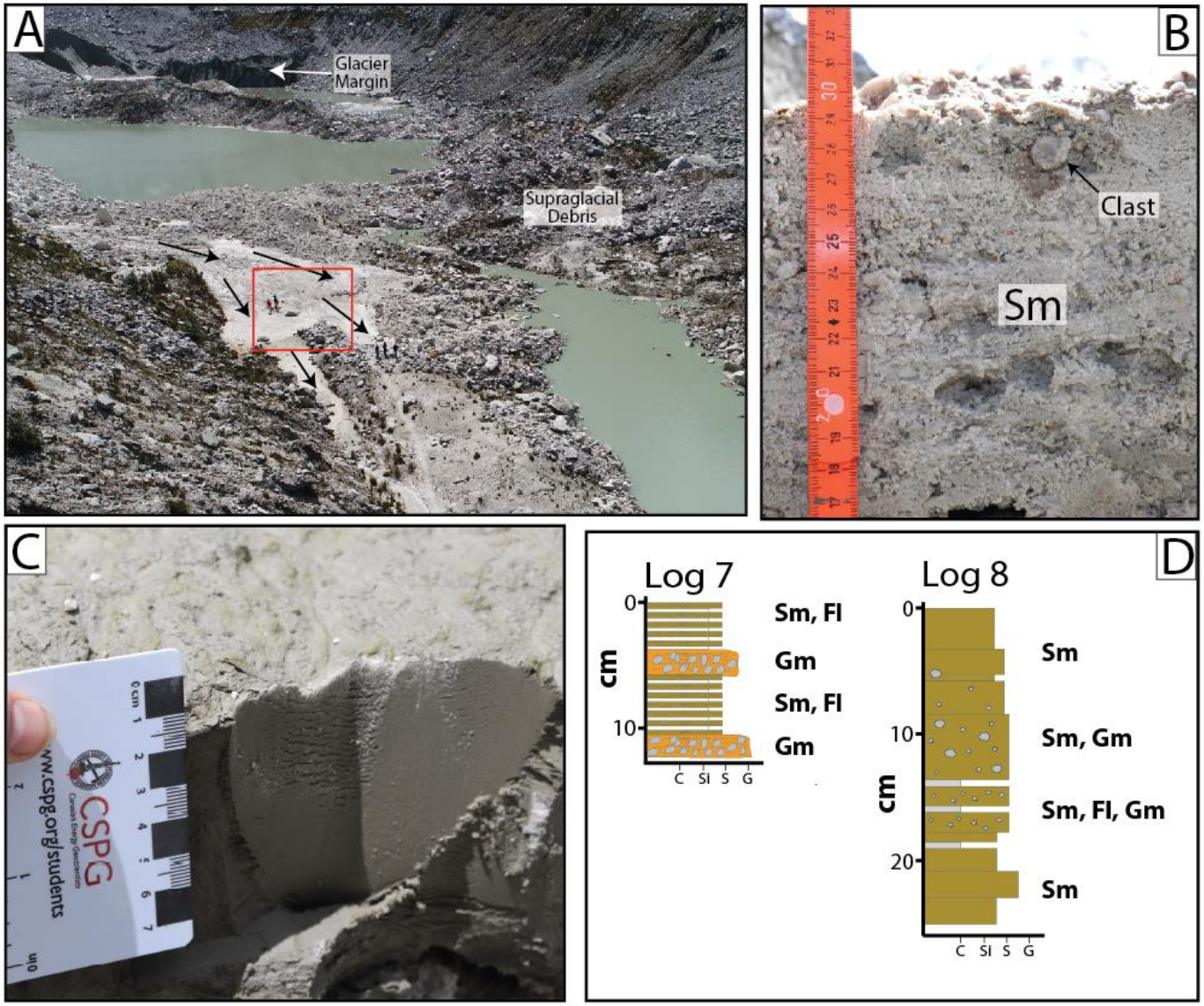
A
Glacier Margin
Supraglacial Debris
B
Clast
Sm
C
www.cspg.org/students
CSPG
D
Log 7
0
10
cm
C SI S G
Sm, Fl
Gm
Sm, Fl
Gm
Log 8
0
10
20
cm
C SI S G
Sm
Sm, Gm
Sm, Fl, Gm
Sm

(Figure 3.13) were identified in these exposures including laminated fines (Fl), deformed fines (Fd), horizontally bedded sand (Sh), massive sand (Sm), graded sand (Sg), rippled sand (Sr), deformed sand (Sd), and massive gravel (Gm).

3.6.1 Ice-cored hummokcs (Logs 1-6; Figure 14)

Fine-grained facies: Fine-grained facies dominate the sediments exposed on ice-cored hummocks (Figures 3.8B, 3.8C, 3.8D). Very fine-grained sand, silt and clay are grouped together as fine-grained facies and include laminated silts and clays (Fl; Figure 3.13I), deformed units of silt and clay (Fd; Figure 3.13J), and interbedded horizontally laminated sand (e.g. Sh, Fl; Fl, Sh; Figure 3.13J). Deformed fine-grained facies (Fd) contain soft sediment deformation structures (folds) and brittle deformation structures in the form of microfaults (Figure 3.13J). The thickness of deformed beds varies from 2 to 70 cm.

Fine-grained facies are interpreted as the product of deposition from overflows, interflows, and suspension settling of fine-grained sediment supplied by meltwater into the waters of Llaca Lake (e.g. Eyles, Clark and Clague, 1988; Eyles, 1993; Chikita, Jha and Yamada, 2001; Evans, Shulmeister and Hyatt, 2010; Eyles and Eyles, 2010). Laminated facies record changing supply mechanisms and energy levels in the lake; deformed facies (Fd; Figure 3.13J) record disruption of the sediment by water escape and/or slumping as underlying ice melts and sediment fails downslope (e.g. Eyles, 1979). Ductile deformation in these facies may also be the result of over-pressuring caused by rapid deposition of overlying sediment and readjustments of the sediment pile (Eyles, Clark and Clague, 1987).

Coarse-grained facies: Scattered angular clasts and a variety of sand facies are also exposed on the ice-cored hummocks. Angular clasts up to 1m diameter are commonly

found on the upper surface of hummocks and may be surrounded by finer-grained sand or silt (Figure 3.13K). Sand facies consist of horizontally bedded fine to medium grained sand (Sh; Figure 3.13B), massive (structureless) fine to medium grained sand (Sm; Figure 3.13B, 3.13C), graded fine to medium sand (Sg; Figure 3.13D), rippled sand (Sr; Figure 3.13E), and fine to medium grained deformed sand (Sd). Deformed sand facies show evidence of both brittle deformation (micro-faults; Figure 3.13F), and ductile deformation (folds, water escape structures; Figures 3.13G, 3.13H).

Angular clasts found on the surface of ice-cored hummocks were probably transported into the lake basin either by sediment gravity flows caused by slumping of lateral moraine walls or as ice-rafted material (Benn and Owen, 2002; Lukas et al., 2005). The presence of finer-grained sediment surrounding the clasts suggests they were emplaced subaqueously. Horizontally bedded sand (Sh; Figure 3.13B) and rippled sand (Sr; Figure 3.13E) are interpreted as the product of deposition from traction currents generated by underflows entering the lake (e.g. Eyles, Clark and Clague, 1987); structureless (Sm; Figure 3.13B, 3.13C) and normally graded (Sg; Figure 3.13G) sand facies record rapid deposition from sediment gravity flows and/or underflows. Deformed sand facies (Sd; Figure 3.13F, 3.13G) are interpreted as the product of disturbance caused by underlying ice melt, topographic inversion and slumping, as well as water escape caused by rapid sediment deposition (Eyles, 1979; Miall, 2010).

3.6.2 Alluvial fan (Logs 7-8; Figure 3.15):

Coarse-grained facies: Massive (structureless) sand and gravel facies (Sm, Gm; Figure 3.13A) dominate sediments exposed in pits dug into the alluvial fans rimming the

lake basin. Massive gravel facies contain subangular to subrounded clasts ranging in size from granules to boulders (5 mm to 30 cm; Figure 3.15) and have a matrix of coarse-grained to silty sand.

These facies are interpreted as the product of rapid deposition from sediment gravity flows generated along the steep interior slopes of the lateral moraines enclosing the basin. Limited sorting of sediment grain sizes during downslope transport has allowed the generation of distinct beds of gravel and sand; clasts are scattered throughout these deposits and their subangular to subrounded form suggests some abrasion has occurred during transport.

Fine-grained facies: Thin beds of massive fine sand and units of laminated silt are associated with coarser-grained sands and gravels in the alluvial fans (Figure 3.15C, 3.15D). These fine-grained facies have similar characteristics to those described in ice-cored hummocks and a similar subaqueous origin is proposed. It is likely that water level changes in the lake have permitted periodic flooding of the distal margins of the alluvial fans.

3.6.3 Depositional history of Llaca Lake

The sediment exposures recorded here provide a series of 'snap-shots' of depositional processes and environments that can exist in Llaca Lake at any one time. The majority of the exposures logged in ice-cored hummocks and fans extending into the lake show alternating beds of sand and fines (e.g. Sh, Fl; Fl, Sh; Figure 3.14 Logs 1, 2, 3, 5) that record deposition under changing energy regimes related to variations in meltwater production (ablation), and/or rainfall events. Periods of relatively low sediment input to the

lake are represented by units of laminated fine-grained sediment (Fl; Fl, Sh; Figure 3.14, Log 6,); sediment failure along the basin margins and/or rapid deposition caused by rapid melt and/or storm events are recorded by graded and deformed sand beds (Sg, Sd; Figure 3.14, Logs 1,2,4, 6). It is important to note that depositional conditions that prevailed during accumulation of these sediments may also have been significantly influenced by frequent lake level changes and topographic adjustments caused by underlying ice melt. The dynamic distribution of sediment exposures in Llaca Lake create complexity when attempting to create an idealized stratigraphic model to describe its sedimentological characteristics. However, the description of depositional processes and products captured in this research provide a framework for the creation of a generalized facies model when data from additional moraine-dammed supraglacial lakes are available.

3.7 LANDSYSTEM ZONES WITHIN LLACA LAKE

The geomorphological and sedimentological characteristics of Llaca Lake, a moraine-dammed supraglacial lake, are summarized in the schematic model shown in Figure 3.16 and can be synthesized into three landsystem zones: Zone 1: includes distal portions of Llaca Lake and the latero-frontal moraine; Zone 2: the central zone of ice-cored hummocks;

Figure 16: Summary diagram to show the landsystem zones (Zones 1-3), landsystem elements (circled numbers 1-10), and idealized sedimentary logs (A-F) characteristic of Llaca Lake, a moraine-dammed supraglacial lake. Active processes shown by inset circles at lower right.
Landsystem elements (circled numbers). 1 – outflow dam (Figure 4) built in 1970 to monitor lake levels and water discharge; 2 – latero-frontal moraine that dams Llaca Lake; 3 – main water body of Llaca Lake with a maximum depth of ~20 m; 4 – moraine slope failures (Figure 8B, 8C, 8D, 10) that originate from the inside of the latero-frontal moraine; 5 - ice-cored hummocks; 6 – undetermined lake substrate – subglacial, supraglacial and slope-derived sediment overlying bedrock; 7 – outer moraine trough; 8 – valley walls composed of granodiorite; 9 – debris covered glacier tongue covered by angular supraglacial debris ~1m thick (Figure 8B); 10 – rockfall and avalanche fans.
Idealized sedimentary logs of selected environments. A – the latero-frontal moraine (Figure 3) is likely to be composed of interbedded diamicts (Dmd, Dcm, Dmm) and fine-grained sediment (Fl, Sd). B – sediment found on the floor of Llaca Lake will include gravel (Gm) and sand (Sg, Sd, Sm) supplied by debris flows, turbidites, and/or slumping, and fine-grained sediment (Fl, Sh) from suspension; C – ice-cored hummocks contain sands carried into the lake by turbidites and/or underflows (Sg, Sm) and fines deposited from suspension (Fl). These facies will show vari¬¬ous amounts of soft sediment deformation (Sd, Fld); D – alluvial fans entering the lake from the valley walls (Figure 15) contain massive sands (Sm) and normally graded gravels that fine upwards (Gg); E – moraine slope failures consist of stratified diamict and units of coarse angular debris with little to no fine matrix (Cc); F – rockfall and avalanche fans are characterized by crudely bedded, coarse-grained angular debris (Figure 8A).
Active processes (inset circles). i – slumping of debris from hummocks; ii – melting of buried ice beneath lacustrine/supraglacial sediment; iii – backwasting of buried ice (Figure 8D); iv – active glacier terminus with supraglacial debris cover; v – meltwater inputs; vi – underflows generated by cold, dense incoming meltwater.

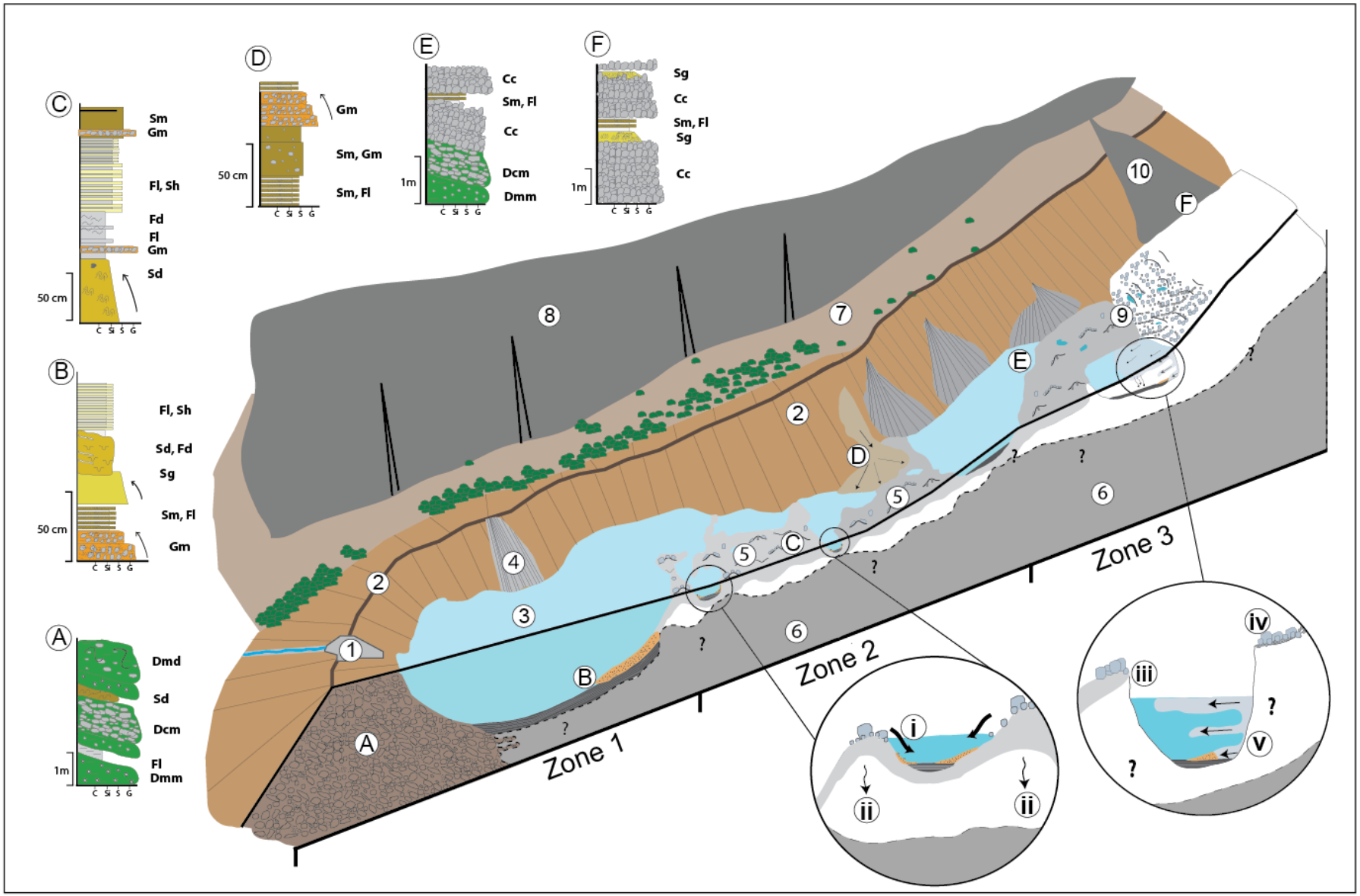
C
Sm
Gm
Fl, Sh
Fd
Fl
Gm
Sd
50 cm
C Si S G
B
Fl, Sh
Sd, Fd
Sg
Sm, Fl
Gm
50 cm
C Si S G
A
Dmd
Sd
Dcm
Fl
Dmm
1m
C Si S G
D
Gm
Sm, Gm
Sm, Fl
50 cm
C Si S G
E
Cc
Sm, Fl
Cc
Dcm
Dmm
1m
C Si S G
F
Sg
Cc
Sm, Fl
Sg
Cc
1m
C Si S G
Zone 1
Zone 2
Zone 3
1
2
3
4
5
6
7
8
9
10
?
i
ii
iii
iv
v

and Zone 3: the active glacier margin. These zones are differentiated based on the spatial distribution of landforms, sediments, and active depositional processes.

Zone 1: Distal Llaca Lake and Latero-frontal Moraine

Zone 1 is bounded at its southern margin by the latero-frontal moraine that dams Llaca Lake. Sediment exposures through the moraine are limited and the moraine surface is partially covered by scrubby vegetation. While the internal sedimentary architecture of the moraine is unknown, examination of sediments exposed in similar moraines enclosing nearby lakes (e.g. Palcacocha; Bowman et al., 2018) suggests that it contains a combination of clast- and matrix-supported massive diamicts with minor amounts of interbedded finer grained sediment. The inner side of the moraine is prone to failure resulting in the transport of coarse-grained material into the lake (Figure 3.10). The Zone 1 landsystem is also distinguished by the absence of ice-cored hummocks. Examination of historical images of the lake suggest that ice no longer underlies this distal region or is buried by deeper water; this is now the least dynamic zone within the moraine-dammed supraglacial lake landsystem (Figure 3.7).

Zone 2: Central Zone of Ice-cored Hummocks

Zone 2 is characterised by ice-cored hummocks exposed above the water surface in Llaca Lake (Figure 3.5, 3.6, 3.7, 3.88B). Sequential satellite imagery of this zone shows significant changes in the shape and size of these hummocks over time (Figure 3.11, 3.812) and suggests that the hummocks overlie progressively melting buried ice. Buried ice can be observed in debris covered hummocks close to the modern ice margin (Figure 3.8D) and it is possible that some of the buried ice is still connected to the main glacier. The uneven

thickness of debris on the surface of the ice results in uneven amounts of insulation and causes differential melting rates (Nicholson et al., 2018). Differential melting creates a hummocky topography on the debris-covered ice surface and ultimately results in topographic inversion as supraglacial debris mixes with meltwater to create debris flows that infill lows on the melting ice surface. Fine-grained sediment (dominantly silt and clay) introduced by inflowing meltwater from the glacier margin, accumulates as laminated deposits in areas covered by water. In addition to material that has been transported supraglacially and englacially, coarse grained sediment is also introduced into the lake and onto the surface of the buried ice by alluvial fans and debris flows from the steep inner slopes of the moraine (Figure 3.8B, 3.8C). Alluvial fans contain a mixture of sand and gravel (Sm, Gm; Figure 3.16 – Log D) and rockfall debris is dominated by large (between 50cm and 20m diameter), angular blocks (Figure 3.16 – Log E).

Zone 3: Glacier Margin

Zone 3 of the Llaca Lake landsystem includes the debris-covered terminus of Llaca Glacier (Figure 3.8A), including proximal areas where stagnant ice is melting below a thick supraglacial cover producing hummocky topography, and steep-sided lateral moraines that contribute coarse angular debris to the ice surface and adjacent water bodies. The thick debris cover on Llaca Glacier (Figure 3.8A) originates from rockfalls and avalanches from the steep bedrock valley walls. The terminus of the glacier is in contact with Llaca Lake and can be identified as an actively calving ice face (Figure 3.9). Subglacial meltwater issues from the ice margin and transports coarse- and fine-grained sediment into the basin; subaqueous mass flow processes including turbidity currents and sediment gravity flows

also transport sediment into the lake from areas proximal to the ice margin. Sediment failures from the debris-covered buried ice mass observed on the western margin of the lake body also contribute sediment to the lake (Figure 3.8C).

The extent and location of Zone 3 is dynamic and changes with the position of the active glacier terminus. As the glacier margin retreats, stagnant ice masses buried beneath the thick cover of supraglacial sediment and water of Llaca Lake slowly melt to produce an ice-cored hummocky topography similar to that present in Zone 2 (Figure 3.5, 3.9). The ice proximal topography changes dramatically as ice retreats, buried ice melts, and the lake extends, creating a highly dynamic depositional environment (Figure 3.5, 3.9). Since 2017, two consistently enlarging water bodies have been observed in front of the glacier terminus (Figure 3.5, 3.6, 3.7, 3.9C).

3.8 EVOLUTION OF THE MORAINE-DAMMED SUPRAGLACIAL LAKE LANDSYSTEM

This study is the first to describe landform-sediment assemblages in a tropical moraine-dammed supraglacial lake in the Cordillera Blanca. The moraine-dammed supraglacial lake landsystem presented here for Llaca Lake summarizes the active surface processes, sediments and resultant landforms that characterize this environment (Figure 3.16). Previous studies of glaciated valley landsystems have focused on those in temperate regions (i.e. Boulton and Eyles, 1979; Eyles, 1979; N. Eyles, 1983; Kirkbride and Spedding, 1996; Benn and Owen, 2002; Spedding and Evans, 2002; Benn et al., 2003). Many of the factors noted to control landform development in temperate glaciated valleys (such as topography, debris supply to the glacier surface, and efficiency of sediment transport from glacier to ice proximal environments; e.g. Benn et al., 2003), also operate at

Llaca Lake and Llaca Glacier. However, this study emphasizes the important role that ice-cored hummocks have in the distribution of fine- (Fl) and coarse-grained sediments (Sg, Sr, Sd) in the lake basin. Topographic inversion, caused by the uneven melting of buried ice, not only creates water filled topographic lows that form sediment depocentres, but also causes extensive mixing and deformation of accumulating sediment. The ice-cored hummocks in Llaca Lake are constantly changing in size and distribution (Figure 3.5, 3.11, 3.12) and those visible today will likely be submerged as buried ice continues to melt. It is difficult to predict the characteristics of the sediment stratigraphy that will eventually be preserved within the Llaca Lake basin other than to say there will be interbedding of both coarse-and fine-grained sediments which will be extensively deformed in places. It is also important to note that the progressive melting of buried ice in the Llaca Lake basin will increase the volume of water that can be contained within the basin and could ultimately increase the risk and impact of a GLOF. It will be important to continuously monitor ice melt and lake level fluctuations over the coming years as Llaca Glacier continues to melt.

Tropical glaciers are undergoing rapid glacier retreat (Veettil et al., 2017), with the total glaciated area in the Cordillera Blanca having decreased 46-52% between 1930 and 2016 (Georges, 2004; Silverio and Jaquet, 2017; INAIGEM, 2018). This retreat is causing the associated proglacial lakes to grow both in size and number (Tacsi Palacios et al., 2014; Emmer et al., 2016). Many of these enlarging lakes overlie buried and stagnant glacial ice and are therefore considered to be supraglacial (Iturrizaga, 2014; Tacsi Palacios et al., 2014). The description of landforms and sediments presented here for Llaca Lake provides

a framework for further landsystem analysis of these growing, and potentially dangerous supraglacial lakes.

3.9 CONCLUSIONS

This study presents a detailed geomorphological and sedimentological assessment of Llaca Lake, a moraine-dammed tropical supraglacial lake in the Cordillera Blanca, Perú. The use of UAV-derived photogrammetric orthomosaics and DEMs, in addition to field-based data and remotely sensed aerial imagery, allows high-resolution analysis of the landforms and surface sediments in the lake and the delineation of landform elements and three spatially distinct landsystem zones (Figure 3.16). These zones comprise the latero-frontal moraine and ice-distal open water areas (Zone 1), the central area of the lake dominated by ice-cored hummocks (Zone 2), and the ice-proximal area adjacent to the active glacier margin (Zone 3). The boundaries between each of these zones are constantly changing as depositional environments adjust to glacier margin retreat, buried ice melt, and water level changes. The geomorphological and sedimentological signature of such a dynamic environment is therefore complex and will vary according to changing conditions; the analysis of the Llaca Lake landsystem presented here should therefore be considered as a snapshot in time and a first step towards understanding the broad range of spatially and temporally variable processes operating in this type of environment.

Additional work is needed to document how surface processes change with further retreat of the ice margin and development of Llaca Lake; it is especially important to understand factors, including lake level changes, that affect stability of the moraine dams that impound these high-altitude lakes. As more is learned about processes operating in

such ice marginal lakes, the value of their longer-term sediment record to facilitate paleoclimatic and paleoenvironmental reconstructions increases in importance. There is a growing demand to understand the sedimentary records of glacial lakes in the Cordillera Blanca in order to better understand climatic change in the Holocene (Stansell et al., 2015; Mark, Stansell and Zeballos, 2017). Analysis of fine-grained lake sediments, including sedimentological, micropaleontological, and geochemical analyses, (i.e., Last and Vance, 2002; Haberzettl et al., 2007; Thomas and Briner, 2009; Larsen et al., 2011; Stansell et al., 2014) can provide valuable paleoclimatic information and it is important to understand depositional processes in these lakes to utilize these data most effectively. Tropical glaciers in the Cordillera Blanca are undergoing rapid retreat and melt, and the moraine-dammed supraglacial lake landsystem of Llaca Lake is dynamic and constantly changing. Understanding the nature of the landsystem elements, their changing spatial distribution, and the sedimentary record of these growing and highly dynamic glacial lakes, will greatly enhance understanding of the threat they pose to nearby communities, a threat that is very real in many areas of the Cordillera Blanca.

REFERENCES

Autoridad Nacional del Agua (ANA), 2020. Lagunas - Reservas de agua dulce en Áncash: Resultados de estudios de batimetría en 38 lagunas glaciares. Huaraz, Perú. Autoridad Nacional del Agua, Perú.

Baraer, M., Mark, B.G., McKenzie, J.M., Condom, T., Bury, J., Huh, K.-I., Portocarrero, C., Gómez, J., & Rathay, S., 2012. Glacier recession and water resources in Peru's Cordillera Blanca, Journal of Glaciology, 58 (207), pp. 134–150. doi: 10.3189/2012JoG11J186.

Barnett, T. P., Adam, J. C. and Lettenmaier, D. P., 2005. Potential impacts of a warming climate on water availability in snow-dominated regions', Nature, 438(7066), pp. 303–309. doi: 10.1038/nature04141.

Benn, D. I., Kirkibride, M.P., Owen, L.A., & Brazier, V., 2003. Glaciated valley landsystems. In Evans, D. J. A. (ed.) Glacial Landsystems. Arnold, pp. 372–406. doi: 10.4324/9780203784976.

Benn, D. I. and Owen, L. A., 2002. Himalayan glacial sedimentary environments: a framework for reconstructing and dating the former extent of glaciers in high mountains. Quaternary International, 97–98, pp. 3–25. doi: 10.1016/S1040-6182(02)00048-4.

Bennett, G. L., Evans, D.J.A., Carbonneau, P., & Twigg, D.R., 2010. Evolution of a debris-charged glacier landsystem, Kviárjökull, Iceland. Journal of Maps, 6(1), 40–67. doi: 10.4113/jom.2010.1114.

Boulton, G. S. and Eyles, N., 1979. Sedimentation by valley glaciers; a model and genetic

classification, in Schlüchter, C. (ed.) *Proceedings of an INQUA Symposium on Genesis and Lithology of Quaternary Deposits. Zurich.* Rotterdam: A.A. Balkema, Rotterdam, pp. 11–24.

Boulton, G. S. and Eyles, N., 1979. Sedimentation by valley glaciers; a model and genetic classification, in Schlüchter, C. (ed.) *Proceedings of an INQUA Symposium on Genesis and Lithology of Quaternary Deposits. Zurich.* Rotterdam: A.A. Balkema, Rotterdam, pp. 11–24.

Carey, M., 2005. Living and dying with glaciers: people's historical vulnerability to avalanches and outburst floods in Peru. Global and Planetary Change, 47(2–4), pp. 122–134. doi: 10.1016/j.gloplacha.2004.10.007.

Carey, M., 2010. *In the Shadow of Melting Glaciers: Climate Change and Andean Society*. New York: Oxford University Press. doi: 0.1093/acprof:oso/9780195396065.001.0001.

Carey, M., Huggel, C., Bury, J., Portocarrero, C., & Haeberli, W., 2012. An integrated socio-enviornmental framework for glacier hazard management and climate change adaptation: lesssons from Lake 513, Cordillera Blanca, Peru. Climatic Change, 112, 733-767. doi: 10.1007/s10584-011-0249-8.

Chandler, B. M. P., Evans, D.J.A., Chandler, S.J.P., Ewertowski, M.W., Lovell, H., Roberts, D.H., Schaefer, M., Tomczyk, A.M., 2020. The glacial landsystem of Fjallsjökull, Iceland: Spatial and temporal evolution of process-form regimes at an active temperate glacier. Geomorphology, 361, p. 107192. doi: 10.1016/j.geomorph.2020.107192.

Chevallier, P., Pouyand, B., Suarez, W., & Condom, T., 2011. Climate change threats to environment in the tropical Andes: glaciers and water resources. Regional Environmental Change, 11(S1), pp. 179–187. doi: 10.1007/s10113-010-0177-6.

Chikita, K., Jha, J., & Yamada, T., 2001. Sedimentary effects on the expansion of a Himalayan supraglacial lake. Global and Planetary Change, 28(1–4), pp. 23–34. doi: 10.1016/S0921-8181(00)00062-X.

Clague, J. and Evans, S. G., 2000. A review of catastrophic drainage of moraine-dammed lakes in British Columbia. Quaternary Science Reviews, 19(17–18), pp. 1763–1783. doi: 10.1016/S0277-3791(00)00090-1.

Clapperton, C.M., 1972. The Pleistocene Moraine Stages of West-Central Peru. Journal of Glaciology, 11, 62, 255-263. doi: 10.3189/S0022143000022243.

Cobbing, J., W. Pitcher, J. Baldock, W. Taylor, W. McCourt, & Snelling, N.J, 1981. Estudio geológico de la Cordillera Occidental del norte del Perú, Institute Geologico Minero y Metalurgico, Peru., 10(D), 1–252. Available at: https://hdl.handle.net/20.500.12544/330.

Concha, J. F., 1951. Origin de las lagunas. Huaraz, Perú.

Condom, T., Escobar, M., Purkey, D., Pouget, J.C., Suarez, W., Ramos, C., Apaestegui, J., Zapata, M., Gomez, J., & Vergara, W., 2011. Modelling the hydrologic role of glaciers within a Water Evaluation and Planning System (WEAP): a case study in the Rio Santa watershed (Peru). Hydrology and Earth System Sciences Discussions, 8(1), pp. 869–916. doi: 10.5194/hessd-8-869-2011.

Deverchère, J., Dorbath, C. and Dorbath, L., 1989. Extension related to a high topography: results from a microearthquake survey in the Andes of Peru and tectonic implications. Geophysical Journal International, 98(2), pp. 281–292. doi: 10.1111/j.1365-246X.1989.tb03352.x.

Ely, J. C., Graham, C., Barr, I.D., Rea, B.R., Spagnolo, M., & Evans, J., 2017. Using UAV acquired photography and structure from motion techniques for studying glacier landforms: application to the glacial flutes at Isfallsglaciären. Earth Surface Processes and Landforms, 42(6), pp. 877–888. doi: 10.1002/esp.4044.

Emmer, A. et al. (2016) '882 lakes of the Cordillera Blanca: An inventory, classification, evolution and assessment of susceptibility to outburst floods', CATENA, 147, pp. 269–279. doi: 10.1016/j.catena.2016.07.032.

Emmer, A. and Vilímek, V., 2013. Review Article: Lake and breach hazard assessment for moraine-dammed lakes: an example from the Cordillera Blanca (Peru). Natural Hazards and Earth System Sciences, 13(6), pp. 1551–1565. doi: 10.5194/nhess-13-1551-2013.

Emmer, A., Vilímek, V. and Zapata, M. L., 2018. Hazard mitigation of glacial lake outburst floods in the Cordillera Blanca (Peru): the effectiveness of remedial works. Journal of Flood Risk Management, 11, pp. S489–S501. doi: 10.1111/jfr3.12241.

Evans, D. J. A., 2003. Introduction to Glacial Landsystems. In Evans, D. J. A. (ed.) Glacial Landsystems. London: Arnold, pp. 1–11.

Evans, D. J. A., Ewertowski, M. and Orton, C., 2016. Fláajökull (north lobe), Iceland: active temperate piedmont lobe glacial landsystem. Journal of Maps, 12(5), pp. 777–789. doi: 10.1080/17445647.2015.1073185.

Evans, D. J. A., Ewertowski, M. and Orton, C., 2017. The glaciated valley landsystem of Morsárjökull, southeast Iceland', Journal of Maps, 13(2), pp. 909–920. doi: 10.1080/17445647.2017.1401491.

Evans, D. J. A., Lemmen, D. S. and Rea, B. R., 1999. Glacial landsystems of the southwest Laurentide ice sheet: Modern Icelandic analogues. Journal of Quaternary Science, 14(7), pp. 673–691. doi: https://doi.org/10.1002/(SICI)1099-1417(199912)14:7<673::AID-JQS467>3.0.CO;2-%23.

Evans, D. J. A., Shulmeister, J. and Hyatt, O., 2010. Sedimentology of latero-frontal moraines and fans on the west coast of South Island, New Zealand. Quaternary Science Reviews, 29(27–28), pp. 3790–3811. doi: 10.1016/j.quascirev.2010.08.019.

Evans, S. G. and Clague, J. J., 1994. Recent climatic change and catastrophic geomorphic processes in mountain environments', Geomorphology, 10(1–4), pp. 107–128. doi: 10.1016/0169-555X(94)90011-6.

Eyles, C. H. and Eyles, N., 2010. Glacial Deposits. In James, N. P. and Dalrymple, R. W. (eds) Facies Model 4. St. John's, Newfoundland & Labrador: Geological Association of Canada, pp. 73–104.

Eyles, N., 1979. Facies of supraglacial sedimentation on Icelandic and Alpine temperate glaciers. Canadian Journal of Earth Sciences, 16(7), pp. 1341–1361. doi: 10.1139/e79-121.

Eyles, N., 1983. Glacial Geology: A Landsystems Approach. In Eyles, N. (ed.) Glacial Geology: An Introduction for Engineers and Earth Scientists. Oxford: Pergamon Press.

Eyles, N., 1983. The Glaciated Valley Landsystem. In Glacial Geology. Oxford: Pergamon Press, pp. 91–110.

Eyles, N., 1993. Earth's glacial record and its tectonic setting. Earth-Science Reviews, 35(1–2), pp. 1–248. doi: 10.1016/0012-8252(93)90002-O.

Eyles, N. and Clark, B. M., 1988. Storm-influenced deltas and ice scouring in a late Pleistocene glacial lake. Geological Society of America Bulletin, 100(5), pp. 793–809. doi: 10.1130/0016-7606(1988)100<0793:SIDAIS>2.3.CO;2.

Eyles, N., Clark, B. M. and Clague, J. J., 1987. Coarse-grained sediment gravity flow facies in a large supraglacial lake. Sedimentology, 34(2), pp. 193–216. doi: 10.1111/j.1365-3091.1987.tb00771.x.

Fitzsimons, S. J., 2003. Ice-marginal Terrestrial Landsystems: Polar-Continental Glacier Margins', in Evans, D. J. A. (ed.) Glacial Landsystems. London: Arnold, pp. 89–110.

Gauthier, D., Wood, D. F. and Hutchinson, D. J., 2015. Natural geologic controls on rockfall hazard and mitigation on the Niagara escarpment, King' s Highway 403 at Hamilton , ON , Canada. In 66th Highway Geology Symposium. Sturbridge,

Massachusetts, pp. 520–534. Available at: http://www.highwaygeologysymposium.org/wp-content/uploads/66_HGS-OPT.pdf.

Georges, C., 2004. 20th-Century glacier fluctuations in the tropical Cordillera Blanca, Perú. Arctic, Antarctic, and Alpine Research, 36(1), pp. 100–107. doi: 10.1657/1523-0430(2004)036[0100:TGFITT]2.0.CO;2.

Giovanni, M.K., Horton, B.K., Garzione, C.N., McNulty, B., & Grove, M., 2010. Extensional basin evolution in the Cordillera Blanca, Peru: Stratigraphic and isotopic records of detachment faulting and orogenic collapse in the Andean hinterland. Tectonics, 29, TC6007, 1-21. pp. 1–21. doi: 10.1029/2010TC002666.

Glasser, N. F. and Hambrey, M. J., 2003. Ice-marginal terrestrial landsystems: Svalbard polythermal glaciers. In Evans, D. J. A. (ed.) Glacial Landsystems. London: Arnold, pp. 65–88.

Haberzettl, T., Coberlla, H., Fey, M., Janssen, S., Lucke, A., Mayr, C., Ohlendorf, C., Schäbitz, F., Schleser, G.H., Wille, M., Wulf, S., & Zolitschka, B., 2007. Lateglacial and Holocene wet-dry cycles in southern Patagonia: Chronology, sedimentology and geochemistry of a lacustrine record from Laguna Potrok Aike, Argentina. Holocene, 17(3), pp. 297–310. doi: 10.1177/0959683607076437.

Harrison, S., Kargel, J., S., Huggel, C., Reynolds, J., Shugar, D.H., Betts, R.A., Emmer, A., Glasser, N., Haritashya, U.K., Klimes, Reinhardt, L., Shaub, Y., Wiltshire, A., Regmi, D., & Vilímek, 2018. Climate change and the global pattern of moraine-dammed glacial lake outburst floods. The Cryosphere, 12(4), pp. 1195–1209. doi:

10.5194/tc-12-1195-2018.

Hock, R., Rasul, G., Adler, C., Cáceres, B., Gruber, S., Hirabayashi, Y., Jackson, M., Kääb, A., Kang, S., Kutuzov, S., Milner, A., Molau, U., Morin, S., Orlove, B., & Stelzer, 2019. High Mountain Areas. In Pörtner, H.-O. et al. (eds) IPCC Special Report Ocean and Cryosphere in a Changing Climate, pp. 131–202. Available at: https://www.ipcc.ch/site/assets/uploads/sites/3/2019/11/06_SROCC_Ch02_FINAL.pdf.

Hubbard, B., Heald, A., Reynold, J.M., Quincey, D., Richardson, S.D., Zapata Luyo, M., Santillan Portilla, N., & Hambrey, M.J., 2005. Impact of a rock avalanche on a moraine-dammed proglacial lake: Laguna Safuna Alta, Cordillera Blanca, Peru. Earth Surface Processes and Landforms, 30, 1251-1264. doi: 10.1002/esp.1198.

Huggel, C., Carey, M., Clague, J.J., Kääb, A., 2015. Introduction: human-environment dynamics in the high-mountain cryosphere. In Huggel, C. et al. (eds) *The High-Mountain Cryosphere - Environmental Changes and Human Risks*. New York: Cambridge University Press, pp. 1–6.

Instituto Nacional De Investigación en Glaciares y Ecosistemas de Montaña (INAIGEM), 2018. Inventario Nacional de Glaciares: Las Cordilleras Glaciares del Peru. Instituto Nacional de Investigación en Glaciares y Ecosistemas de Montaña Biblioteca y Publicaciones.

Iturrizaga, L., 2014. Glacial and glacially conditioned lake types in the Cordillera Blanca, Peru: A spatiotemporal conceptual approach. Progress in Physical Geography, 38, 5, 602-636. doi: 10.1177/0309133314546344.

Kaser, G., 2001. Glacier-climate interaction at low latitudes. Journal of Glaciology, 47(157), pp. 195–204. doi: 10.3189/172756501781832296.

Kershaw, J. A., Clague, J. J. and Evans, S. G., 2005. Geomorphic and sedimentological signature of a two-phase outburst flood from moraine-dammed Queen Bess Lake, British Columbia, Canada. Earth Surface Processes and Landforms, 30(1), pp. 1–25. doi: 10.1002/esp.1122.

Kirkbride, M. and Spedding, N., 1996. The influence of englacial drainage on sediment-transport pathways and till texture of temperate valley glaciers. Annals of Glaciology, 22, pp. 160–166. doi: 10.3189/1996AoG22-1-160-166.

Klimeš, J., Benešová, Vilímek, V., Bouška, P., & Cochachin Rapre, A., 2014. The reconstruction of a glacial lake outburst flood using HEC-RAS and its significance for future hazard assessments: an example from Lake 513 in the Cordillera Blanca, Peru. Natural Hazards, 71(3), pp. 1617–1638. doi: 10.1007/s11069-013-0968-4.

Klimeš, J., Vilímek, V. and Omelka, M., 2009. Implications of geomorphological research for recent and prehistoric avalanches and related hazards at Huascaran, Peru. Natural Hazards, 50(1), pp. 193–209. doi: 10.1007/s11069-008-9330-7.

Korup, O. and Tweed, F., 2007. Ice, moraine, and landslide dams in mountainous terrain. Quaternary Science Reviews, 26(25–28), pp. 3406–3422. doi: 10.1016/j.quascirev.2007.10.012.

Larsen, D. J., Miller, G.H., Geirsdóttir, Á., & Thordarson, T., 2011. A 3000-year varved record of glacier activity and climate change from the proglacial lake Hvítárvatn,

Iceland. Quaternary Science Reviews, 30(19–20), pp. 2715–2731. doi: 10.1016/j.quascirev.2011.05.026.

Last, W. M. and Vance, R. E., 2002. The Holocene history of Oro Lake, one of the western Canada's longest continuous lacustrine records. Sedimentary Geology, 148(1–2), pp. 161–184. doi: 10.1016/S0037-0738(01)00216-0.

Lukas, S., Nicholson, L.I., Ross, F.H., & Humlum, O., 2005. Formation, Meltout Processes and Landscape Alteration of High-Arctic Ice-Cored Moraines—Examples From Nordenskiold Land, Central Spitsbergen. Polar Geography, 29(3), pp. 157–187. doi: 10.1080/789610198.

Lukas, S., 2008. A test of the englacial thrusting hypothesis of "hummocky" moraine formation: case studies from the northwest Highlands, Scotland. Boreas, 34(3), pp. 287–307. doi: 10.1111/j.1502-3885.2005.tb01102.x.

Lynch, B.D., 2012. Vulnerabilities, competition and rights in a context of climate change toward equitable water governance in Peru's Rio Santa Valley. Global Environmental Change. Elsevier Ltd, 22(2), pp. 364–373. doi: 10.1016/j.gloenvcha.2012.02.002.

Margirier, A., Audin, L., Robert, X., Herman, F., Ganne, J., & Schwartz, S., 2016. Time and mode of exhumation of the Cordillera Blanca batholith (Peruvian Andes). Journal of Geographical Research: Solid Earth, 121, 6235-6249. doi: 10.1002/2016JB013055.

Margirier, A., Braun, J., Robert, X., & Audin, L., 2018. Role of erosion and isostasy in the Cordillera Blanca uplift: Insights from landscape evolution modeling (northern Peru, Andes). Tectonophysics, 728–72, 119–129. doi: 10.1016/j.tecto.2018.02.009.

Mark, B. G., Bury, J., McKenzie, J.M., French, A., & Baraer, M., 2010. Climate Change and Tropical Andean Glacier Recession: Evaluating Hydrologic Changes and Livelihood Vulnerability in the Cordillera Blanca, Peru. Annals of the Association of American Geographers, 100(4), pp. 794–805. doi: 10.1080/00045608.2010.497369.

Mark, B. G. and Seltzer, G. O., 2003. Tropical glacier meltwater contribution to stream discharge: a case study in the Cordillera Blanca, Peru. Journal of Glaciology, 49(165), pp. 271–281. doi: 10.3189/172756503781830746.

Mark, B. G. and Seltzer, G. O., 2005. Evaluation of recent glacier recession in the Cordillera Blanca, Peru (AD 1962–1999): spatial distribution of mass loss and climatic forcing.Quaternary Science Reviews, 24(20–21), pp. 2265–2280. doi: 10.1016/j.quascirev.2005.01.003.

Mark, B., Stansell, N. and Zeballos, G., 2017. The last deglaciation of Peru and Bolivia. Cuadernos de Investigación Geográfica, 43(2), p. 591. doi: 10.18172/cig.3265.

McNulty, B. and Farber, D., 2002. Active detachment faulting above the Peruvian flat slab. Geology, 30(6), p. 567. doi: 10.1130/0091-7613(2002)030<0567:ADFATP>2.0.CO;2.

Miall, A., 2010. Alluvial Deposits. In James, N. P. and Dalrymple, R. W. (eds) Facies Model 4. St. John's, Newfoundland & Labrador: Geological Association of Canada, pp. 105–138.

Miles, E. S., Watson, C.S., Brun, F., Berthier, E., Esteves, M., Quince, D.J., Miles, K.E., Hubbard, B., & Wagnon, P., 2018. Glacial and geomorphic effects of a supraglacial lake drainage and outburst event, Everest region, Nepal Himalaya. The Cryosphere, 12(12), pp. 3891–3905. doi: 10.5194/tc-12-3891-2018.

Nicholson, L. I., McCarthy, M., Pritchard, H.D., & Willis, I., 2018. Supraglacial debris thickness variability: impact on ablation and relation to terrain properties. The Cryosphere, 12(12), pp. 3719–3734. doi: 10.5194/tc-12-3719-2018.

Owen, L. A. and Derbyshire, E., 1989. The Karakoram glacial depositional system. Zeitschrift für Geomorphologie, Supplement(76), pp. 33–77.

Portocarrero, C. A., 2014. The Glacial Lake Handbook: reducing risk from dangerous glacial lakes in the Cordillera Blanca, Peru. Technical Report, United States Agency for International Development, Global Climate Change Office, Climate Change Resilient Development Project Washington, DC, (February), p. 80. Available at: https://pdf.usaid.gov/pdf_docs/PBAAA087.pdf.

Rabatel., A., Francou, B., Soruco, A., Gomez, J., Cáceres, B., Ceballos, J.L., Basantes, R., Vuille, M., Sicart, J.-E., Huggel, C., Scheel, M., Lejeune, Y., Arnoud, Y., Collet, M., Condom, T., Consoli, G., Favier, V., Jomelli, V., Galarrage, R., Ginot, P., Maisincho, L., Mendoza, J., Ménégoz, M., Ramirez, E., Ribstein, P., Suarez, W., Villacis, M., & Wagnon, P., 2013. Current state of glaciers in the tropical Andes: a

multi-century perspective on glacier evolution and climate change. The Cryosphere, 7, 81-102. doi: 10.5194/tc-7-81-2013.

Rangwala, I., Pepin, N., Vuille, M., & Miller, J., 2015. Influence of climate variability and large-scale circulation on the mountain cryosphere. In Huggel, C. et al. (eds) The High-Mountain Cryosphere - Environmental Changes and Human Risks. New York: Cambridge University Press, pp. 9–27.

Rodbell, D. T., 1992. Lichenometric and Radiocarbon Dating of Holocene Glaciation, Cordillera Blanca, Perú. The Holocene, 2(1), pp. 19–29. doi: 10.1177/095968369200200103.

Schauwecker, S., Roher, M., Acuña, D., Cochachin, A., Dávila, L., Frey, H., Giráldez, C., Gómez, J., Huggel, C., Jacques-Coper, M., Loarte, E., Salzmann, N., & Vuille, M., 2014. Climate trends and glacier retreat in the Cordillera Blanca, Peru, revisited. Global and Planetary Change, 119, 85-97. doi: 10.1016/j.gloplacha.2014.05.005.

Schneider, D., Huggel, C., Cochachin, A., Guillén, S., & García, J., 2014. Mapping hazards from glacier lake outburst floods based on modelling of process cascades at Lake 513, Carhuaz, Peru. Advances in Geosciences, 35, 145-155. doi: 10.5194/adgeo-35-145-2014.

Schomacker, A., Benediktsson, Í. Ö. & Ingólfsson, Ó., 2014. The Eyjabakkajökull glacial landsystem, Iceland: Geomorphic impact of multiple surges. Geomorphology, 218, pp. 98–107. doi: 10.1016/j.geomorph.2013.07.005.

Schwartz, D. P., 1988. Paleoseismicity and neotectonics of the Cordillera Blanca Fault Zone, northern Peruvian Andes. Journal of Geophysical Research: Solid Earth, 93(B5), pp. 4712–4730. doi: 10.1029/JB093iB05p04712.

Sigurðardóttir, M., 2013.The sedimentology and formation of the Gígjökull and Kvíárjökull latero-frontal moraines, Iceland. University of Iceland.

Silverio, W. and Jaquet, J. M., 2017. Evaluating glacier fluctuations in Cordillera Blanca (Peru) by remote sensing between 1987 & 2016 in the context of ENSO. Archives des Sciences, 69(2), pp. 145–161. Available at: https://archive-ouverte.unige.ch/unige:98197.

Smith, J. A., Seltzer, G.O., Farber, D.L., Rodbell, D.T., Finkel, R.C., 2005. Early Local Last Glacial Maximum in the Tropical Andes. Science, 308(5722), pp. 678–681. doi: 10.1126/science.1107075.

Somos-Valenzuela, M. A., Chisolm, R.E., Rivas, D.S., Portocarrero, C., & McKinney, D.C., 2016. Modeling a glacial lake outburst flood process chain: the case of Lake Palcacocha and Huaraz, Peru. *Hydrology and Earth System Sciences*, 20(6), pp. 2519–2543. doi: 10.5194/hess-20-2519-2016.

Spedding, N. and Evans, D. J., 2002. Sediments and landforms at Kvíárjökull, southeast Iceland: a reappraisal of the glaciated valley landsystem. Sedimentary Geology, 149(1–3), pp. 21–42. doi: 10.1016/S0037-0738(01)00242-1.

Stansell, N. D., Rodbell, D.T., Abbott, M.B., & Mark, B.G., 2013. Proglacial lake sediment records of Holocene climate change in the western Cordillera of Peru. Quaternary Science Reviews, 70, pp. 1–14. doi: 10.1016/j.quascirev.2013.03.003.

Stansell, N. D., Rodbell, D.T., Licciardi, J.M., Sedlak, C.M., Schweinsberg, A.D., Huss, E.G., Delgado, G.M., Zimmerman, S.H., & Finkel, R., 2015. Late Glacial and Holocene glacier fluctuations at Nevado Huaguruncho in the Eastern Cordillera of the Peruvian Andes. Geology, 43(8), pp. 747–750. doi: 10.1130/G36735.1.

Stokes, C. R., Tarasov, L., Blomdin, R., Cronin, T.M., Fisher, T.G., Gyllencreutz, R., Hätterstand, C., Heyman, J., Hindmarsh, R.C.A., Hughes, A.L.C., Jakobsson, M., Kirchner, N., Livingstonen, S.J., Margold, M., Murton, J.B., Noormets, R., Peltier, W.R., Peteet, D.M., Piper, D.J.W., Preusser, F., Renssen, H., Roberts, D.H., Rocher, D.M., Saint-Ange, F., Stroven, A.P., & Teller, J.T., 2015. On the reconstruction of palaeo-ice sheets: Recent advances and future challenges. Quaternary Science Reviews, 125(479), pp. 15–49. doi: 10.1016/j.quascirev.2015.07.016.

Tacsi Palacios, A., Colonia Ortiz, D., Torres Castillo, J., & Santiago Martel, A., 2014. Inventario de Lagunas Glaciares del Peru. Autoridad Nacional del Agua – Unidad de Glaciología y Recursos Hídricos. Huaraz, Perú.

Thomas, E. K. and Briner, J. P., 2009. Climate of the past millennium inferred from varved proglacial lake sediments on northeast Baffin Island, Arctic Canada. Journal of Paleolimnology, 41(1), pp. 209–224. doi: 10.1007/s10933-008-9258-7.

Torres Amado, L. N., Dávila Roller, L. R. and Vilca Gómez, O. (2016) Informe Técnico N°03 - Monitoreo Glaciológico en el Glaciar Llaca. Huaraz, Perú.

Veetil, B.K., Wang, S., Souza, S.F., Bremer, U.S., & Simões, J.C., 2017. Glacier monitoring and glacier-climate interactions in the tropical Andes: A review. Journal

of South American Earth Sciences, 77, 281-246. doi: 10.1016/j.jsames.2017.04.009.

Veettil, B. K., 2018. Glacier mapping in the Cordillera Blanca, Peru, tropical Andes, using Sentinel-2 and Landsat data. Singapore Journal of Tropical Geography, 39(3), pp. 351–363. doi: 10.1111/sjtg.12247.

Vilímek, V., Zapata, M.L., Klimes, J., Patzel, Z., & Santillán, N., 2005. Influence of glacial retreat on natural hazards of the Palcacocha Lake area, Peru. *Landslides*, 2(2), pp. 107–115. doi: 10.1007/s10346-005-0052-6.

Viviroli, D., Archer, D.R., Buytaer, W., Fowler, H.J., Greenwood, G.B., Hamlet, A.F., Huang, Y., Koboltsching, G., Litaror, M.I., López-Moreno, J.I., Lorentz, S., Schadler, B., Schreier, H., Schwaiger, K., Vuille, M, & Woods, R., 2011. Climate change and mountain water resources: overview and recommendations for research, management and policy. Hydrology and Earth System Sciences, 15(2), pp. 471–504. doi: 10.5194/hess-15-471-2011.

Vuille, M., Bradley, R.S., Werner, M., & Keimig, F., 2003. 20th century climate change in the tropical Andes: Observations and model results. Climatic Change, 59(1–2), pp. 75–99. doi: 10.1023/A:1024406427519.

Vuille, M., Francou, B., Wagnon, P., Juen, I., Kaser, G., Mark, B.G., & Bradley, 2008. Climate change and tropical Andean glaciers: Past, present and future. Earth-Science Reviews, 89(3–4), pp. 79–96. doi: 10.1016/j.earscirev.2008.04.002.

Vuille, M., Carey, M., Huggel, C., Buytaert, W., Rabatel, A., Jacobsen, D., Soruco, A., Villacis, M., Yarleque, C., Elison Timm, O., Condom, T., Salzmann, N., & Sicart,

J.-E., 2018. Rapid decline of snow and ice in the tropical Andes – Impacts, uncertainties and challenges ahead. Earth-Science Reviews, 176, 195-213. doi: 10.1016/j.earscirev.2017.09.019.

Watanabe, T., Lamsal, D. and Ives, J. D., 2009. Evaluating the growth characteristics of a glacial lake and its degree of danger of outburst flooding: Imja Glacier, Khumbu Himal, Nepal. Norsk Geografisk Tidsskrift - Norwegian Journal of Geography,

Wegner, S. A., 2014. Nota Técnica 7 - Lo que el Agua se Llevó: Consecuencias y Lecciones del Aluvión de Huaraz de 1941. *Notas Técnicas sobre Cambio Climáatico - MInisterio del Ambiente, Perú*. Lima, p. 85.

Wigmore, O. and Mark, B., 2017. Monitoring tropical debris-covered glacier dynamics from high-resolution unmanned aerial vehicle photogrammetry, Cordillera Blanca, Peru. The Cryosphere, 11(6), pp. 2463–2480. doi: 10.5194/tc-11-2463-2017.

CHAPTER 4: SEDIMENTARY ARCHITECTURE OF A LATERAL MORAINE, GÍGJÖKULL, ICELAND

ABSTRACT

Frontal and lateral moraines are large prominent landforms found in glaciated valley environments and commonly dam large proglacial lakes. Unfortunately, relatively little is known about the sedimentary architecture of such large moraines or their potential for failure due to the inaccessible nature of moraine faces. This study uses Uncrewed Aerial Vehicle (UAV) derived photographic analysis to identify and characterize the sedimentary architecture of the eastern lateral moraine of Gígjökull in southern Iceland. Seven lithofacies are identified within the moraine and can be grouped into three lithofacies associations (LFAs) based on their lateral and vertical facies relationships, bed contacts and facies architecture. LFA 1 consists of stacked units of massive and matrix-supported diamict and is interpreted as originating from matrix-rich subaerial debris flows generated from englacial and supraglacial positions. LFA 2 is coarser- grained, consisting predominantly of crudely stratified and clast-supported diamict with angular to subangular clasts generated predominantly by rockfalls. LFA 3 consists of diamict that displays both brittle and ductile deformation and is interpreted as fine-grained ice marginal sediment glaciotectonized during glacier expansion/overriding. Each of these lithofacies associations dip away from the current ice margin at between 10° and 25° and record changing sediment supply conditions during moraine formation.

4.1 INTRODUCTION

Large latero- frontal moraines are found in many modern glaciated environments in high relief temperate and tropical regions (e.g. European Alps – Small, 1983; Lukas et al., 2012; New Zealand –Evans, Shulmeister and Hyatt, 2010; Himalayas – Benn and Owen, 2002; Norway – Shakesby, 1989; Peruvian Andes –Smith and Rodbell, 2010). These large moraines record the position of glacier termini during periods of maximum advance or still-stand, and in regions experiencing present-day glacier retreat, large latero-frontal moraines can act as naturally occurring dams to impound proglacial lakes (e.g. Peruvian Andes – Emmer and Vilímek, 2013; Canadian Rockies – Kershaw, Clague and Evans, 2005; Miles et al., 2018). Displacement of proglacial lake water caused by various mechanisms such as landslides, rockfalls or icefalls, can lead to moraine dam breach and the sudden release of water as glacial lake outburst floods (GLOFs). These floods are catastrophic to communities living down-valley of the moraine-impounded lakes (Carey, 2005; Hubbard et al., 2005; Kershaw, Clague and Evans, 2005; Korup and Tweed, 2007; Emmer and Vilímek, 2013). It is therefore important to understand the sedimentary architecture and stability of these moraines in an attempt to mitigate and prevent future GLOFs.

Large latero-frontal moraines are also utilized in many regions to aid in the reconstruction of past ice margin fluctuations and glacier behavior in response to climatic forcing. The temporal development of such moraines can be estimated by dating boulders, found near or on the moraine crestline, using lichenometric, radiocarbon or radionuclide techniques (Matthews and Petch, 1982; Smith, Finkel, et al., 2005; Ivy-Ochs et al., 2006; Solomina et al., 2007; Jomelli et al., 2008; Owen et al., 2009; Smith and Rodbell, 2010).

Despite concerns regarding the accuracy of dating boulders found on moraines in order to reconstruct past glacier behaviour, particularly in high relief regions prone to sediment reworking (e.g. Humlum, 1978; Lukas, 2012; Barr and Lovell, 2014; Osborn et al., 2015), moraines continue to be used for this purpose (Smith, Seltzer, et al., 2005; Ivy-Ochs et al., 2006; Owen et al., 2009; Mark, Stansell and Zeballos, 2017).

Understanding the age, origin, structure, and stability of large latero-frontal moraines is extremely important, yet few sedimentological studies have sought to understand the mechanisms of moraine formation in high relief glaciated environments due to difficulties of collecting appropriate data (Humlum, 1978; Small, 1983; Benn and Owen, 2002; Benn et al., 2003; Owen et al., 2009; Evans, Shulmeister and Hyatt, 2010; Sigurðardóttir, 2013). This study aims to provide a detailed sedimentological and architectural analysis of the eastern lateral moraine of Gígjökull, an accessible outlet glacier of the Eyjafjallajökull Ice Cap in southern Iceland (Fig. 1) using data collected by UAV (Uncrewed Aerial Vehicle) and field observations. The large latero-frontal moraine of Gígjökull is thought to have formed during maximum ice advance during the Little Ice Age (LIA) around 1721 AD (Kirkbride and Dugmore, 2008) and was breached most recently by a GLOF triggered by the eruption of Eyjafjallajökull in 2010 (Dunning et al., 2013). The moraine itself is much larger than others formed at the margins of nearby glaciers, reaching over 80 m in height; study of the sedimentary architecture and depositional origin of this moraine will aid in understanding the formation and stability of these large proglacial features elsewhere.

4.2 BACKGROUND

4.2.1 Field site – Gígjökull Glacier

Gígjökull is a northern outlet glacier of the Eyjafjallajökull Ice Cap, located in south central Iceland (Figure 4.1). Eyjafjallajökull is a central volcano rising from sea level to an elevation of approximately 1640 m.a.s.l. and has been built over the last 800,000 years through numerous eruptions characterized by varying types of volcano-ice interactions (Kristjánsson et al., 1988). The volcano is currently capped by a small ice cap drained by a series of outlet glaciers, including Steinholtsjökull an outlet glacier in the north, and Seljavallajökull and Kaldajlifsjökull to the south (Figure 1). Gígjökull is a 4 km-long outlet glacier with an average slope of 22° (Kirkbride and Dugmore, 2008) that descends from ~1550 m.a.s.l. on the northwestern flank of the volcanic crater, to 250 m.a.s.l. at its terminus. It is estimated to have an area of 7.8 km2 and approximately 10-30% of its surface area is covered with debris, mostly on the front and lateral glacier margin (Scherler, Wulf and Gorelick, 2018). Large, steep-sided latero-frontal moraines identify the former extent of Gígjökull during the Little Ice Age (Figures 4.1 and 4.2). The preservation of such large latero-frontal moraines is not common in this part of Iceland; the only other south Icelandic glacier with prominent lateral moraines is Kvíárjökull which lies 150 km to the east (Spedding, 2000; Spedding and Evans, 2002; Sigurðardóttir, 2013).

The modern forefield of Gígjökull is fully enclosed by the latero-frontal moraine complex that is subdivided into western and eastern segments by the incision of a large proglacial river (Figure 4.1). The western moraine segment has a length of ~1.2 km, a maximum width of 230 m and a height of 70 m (Figure 1); the eastern moraine segment is ~1.7 km long, with a maximum width of between 440-570 m, and a height of 80 m

Figure 4.1: A – Location of Eyjafjallajökul in southern Iceland indicated by the small orange box. B – Location of Gígjökull on Eyjafjallajökull shown in the red box. C – Proglacial field of Gígjökull; the terminus of Gígjökull is shaded blue and lies in the south of the mapped area; the latero-frontal moraine of Gígjökull is shaded brown. The location of the studied section of the moraine is shown by the white rectangular box on the right; the smaller white box indicates the portion of the moraine shown in Figures 6 & 8. Location of sedimentological logs (see Figure 5) drawn from pits excavated in and adjacent to the moraine are indicated by the circled numbers.

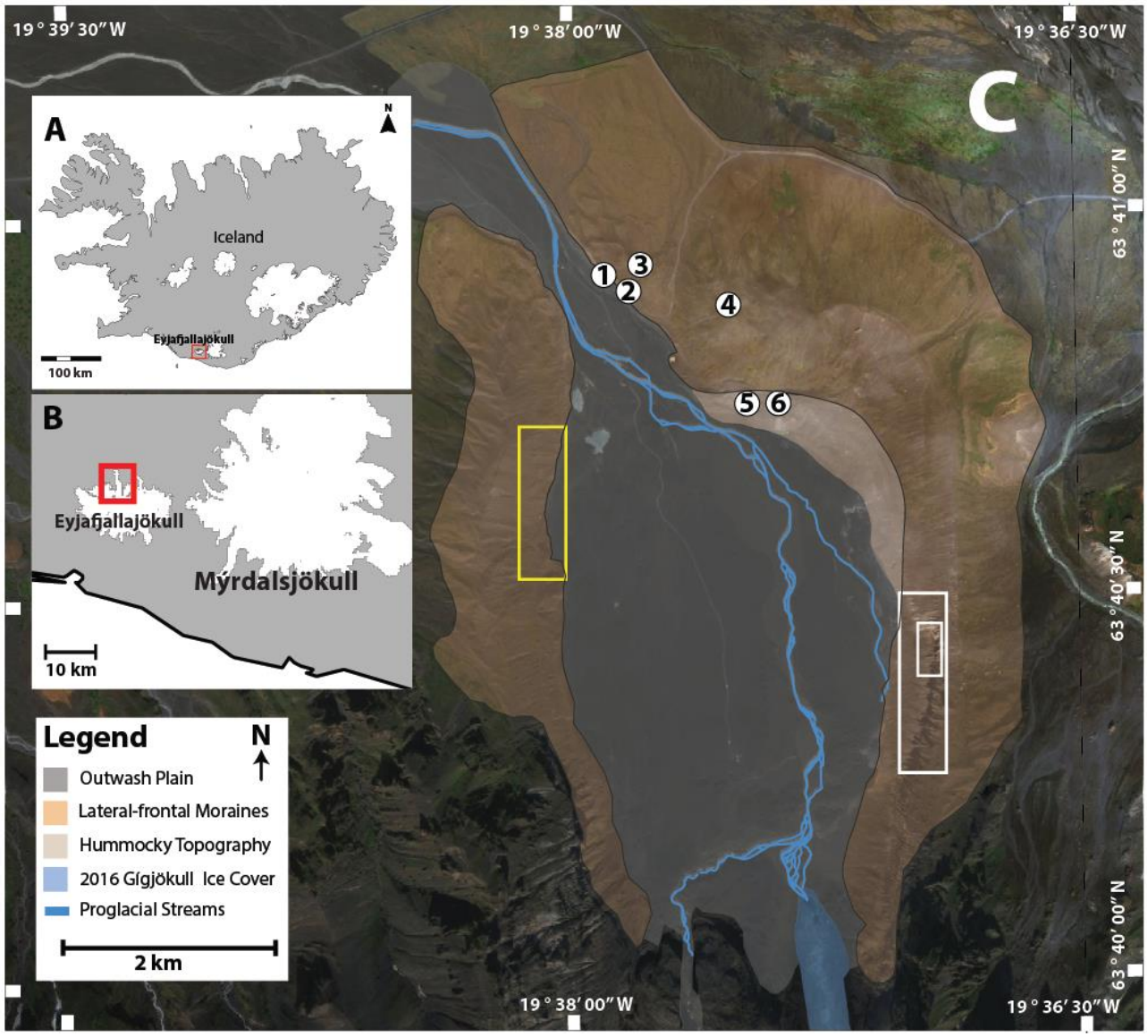
19 ° 39′ 30″ W
19 ° 38′ 00″ W
19 ° 36′ 30″ W
63 ° 41′ 00″ N
63 ° 40′ 30″ N
63 ° 40′ 00″ N
A
N
Iceland
Eyjafjallajökull
100 km
B
Eyjafjallajökull
Mýrdalsjökull
10 km
C
1
2
3
4
5
6
Legend
N
Outwash Plain
Lateral-frontal Moraines
Hummocky Topography
2016 Gígjökull Ice Cover
Proglacial Streams
2 km

Figure 4.2: Mapped terminus positions of Gígjökull from 1700 until 2016. Dashed lines indicate terminus positions based on dated landforms presented by Kirkbride & Dugmore (2008); terminus positions 1908 - 1988 are based on maps created by the Geodætisk Institut of Denmark and DMAHTC (Geodætisk Institut, 1908; Geodætisk Institut, 1957; Geodætisk Institut, 1982; DMAHTC, 1990; terminus positions for 2016 based on satellite imagery from ArcGIS Basemap (ESRI, 2020).

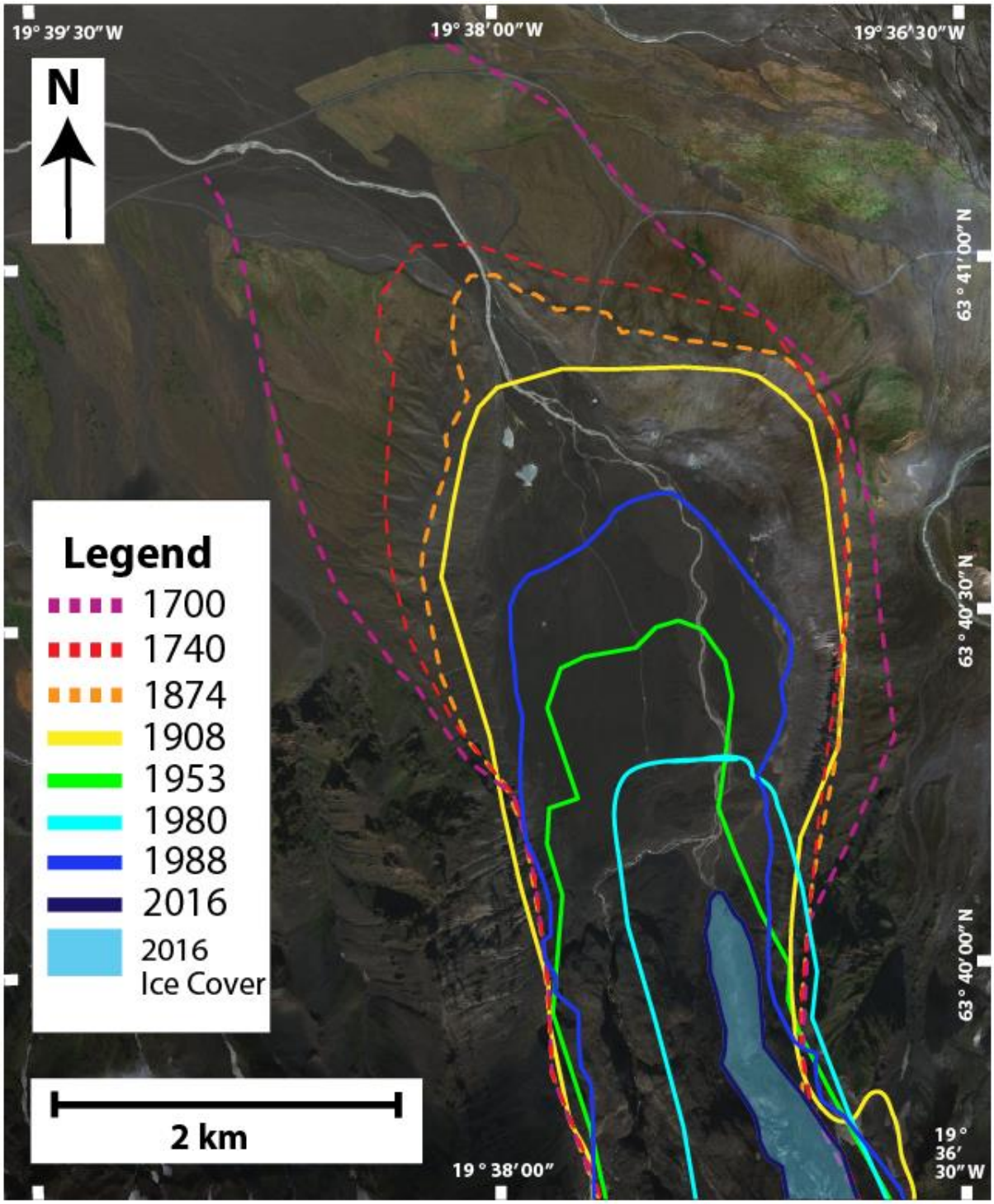
19° 39′ 30″ W
19° 38′ 00″ W
19° 36′ 30″ W
N
63 ° 41′ 00″ N
63 ° 40′ 30″ N
63 ° 40′ 00″ N
Legend
1700
1740
1874
1908
1953
1980
1988
2016
2016
Ice Cover
2 km
19 ° 38′ 00″
19 °
36′
30″ W

(Sigurðardóttir, 2013). Prior to the eruption of Eyjafjallajökull in April 2010, the forefield area enclosed by the moraine contained the ice-contact lake Gígkokulslón which had an area of ~0.6 km^2 and a depth of 20-30 m (Magnússon et al., 2012). Breaching of the moraine dam by floodwaters released by the 2010 Eyjafjallajökull eruption, drained the lake; proglacial streams now transport sediment and meltwater through the moraine breach, toward the ocean across the coastal sandur. The draining of Gígkokulslón increased accessibilitity to exposures through the eastern lateral moraine of Gígjökull allowing field observations and measurements of the internal moraine stratigraphy to be made. In addition, the low altitude of this proglacial field which lies close to sea level, provides ease in manuvouring a UAV to obtain high resolution images of the moraine interior

4.2.2. Glacial History of Gígjökull

The late Quaternary glacial history of Gígjökull is complex and not fully understood; however, the most recent glacier margin fluctuations are reasonably well documented (Figures 4.2, 4.3). Kirkbride and Dugmore (2008) dated the large latero-frontal moraine using tephra layers and concluded that Gígjökull had advanced both in the Neoglacial (~0 CE) period and between the 8th and 12th centuries CE. The glacier is thought to have reached its maximum Holocene extent during the Little Ice Age (LIA, Thorarinsson, 1943) at a time prior to 1721 CE (lichenometry date; Kirkbride and Dugmore, 2008). Dugmore (1987) postulates that although the maximum LIA and Holocene extent of Gígjökull is represented by the crestline of the large latero-frontal moraine, the glacier most likely reached this position several times previously during the Holocene. After the maximum LIA extent, during a period of overall recession, a series of

Figure 3.3: Cumulative retreat of Gígjökull from 1929 to 2012 (continuous orange line) based on data from the World Glacier Monitoring Service Fluctuation of Glaciers Database (WGMS FoG, 2020). Light blue bars represent yearly change - ice margin retreat is indicated below the 0 line and ice margin advance above the line. From 1929 to 2012, Gígjökull retreated ~1500 m with periodic episodes of advance in the early 1950's, 1961 and from 1970 to the mid 1990's.

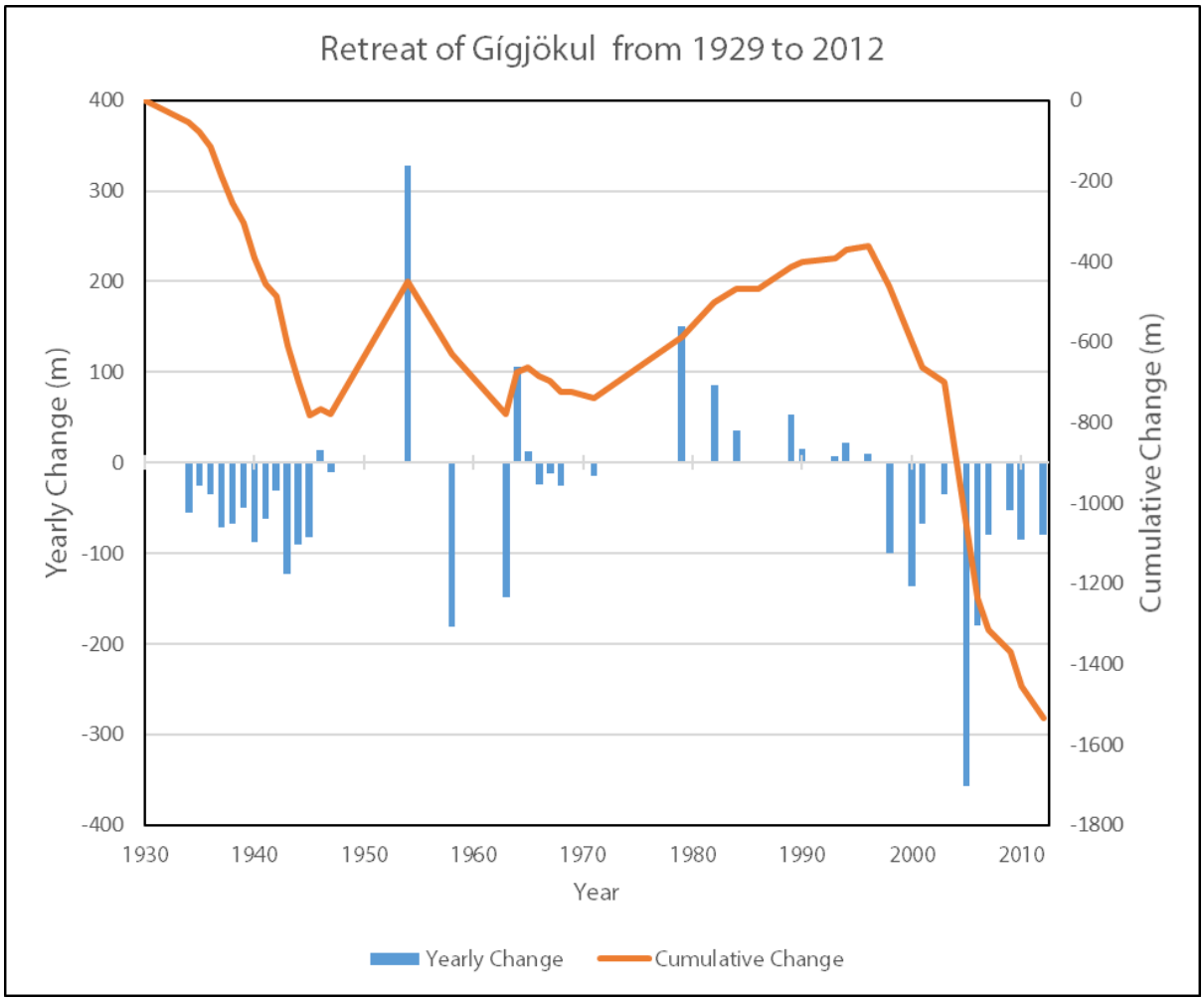
Retreat of Gígjökul from 1929 to 2012
Yearly Change (m)
Cumulative Change (m)
Year
400
300
200
100
0
-100
-200
-300
-400
0
-200
-400
-600
-800
-1000
-1200
-1400
-1600
-1800
1930
1940
1950
1960
1970
1980
1990
2000
2010
Yearly Change
Cumulative Change

at least five additional advances of the ice margin occurred prior to 1930 (Kirkbride and Dugmore, 2008).

Since the beginning of the 20th century, the margin of Gígjökull has experienced overall retreat with intervening periods of limited advance (Figures 4.2, 4.3). From 1907 to 1930 the margin of Gígjökull advanced as far as the proximal slopes of the frontal moraine (Dugmore, 1987). Between 1930 and 1958, the margin retreated approximately 675 m, and subsequently readvanced by 231m in the interval from 1958 to 1990 (Sigurðsson, 2000). Since 1990, the margin of Gígjökull has been steadily retreating (Figures 4.2, 4.3).

4.2.3 Eruption of Eyjafjallajökull

The eruption of Eyjafjallajökull in 2010, and the subsequent jökulhlaups (glacial outburst floods) triggered by the eruption, dramatically changed the geomorphology of the Gígjökull proglacial field (Magnússon et al., 2012; Dunning et al., 2013). The melting of approximately 0.08 km3 of ice during the first week of the eruption created a series of large flood events. The first large outburst of water began on April 14 when water drained from the ice cap both subglacially and supraglacially. As this water entered Gígjokulson, two rapidly prograding ice-contact fans began to extend into the lake (Dunning et al., 2013). On April 15, an additional jökulhlaup, with flows estimated to have peaked between 5000-15000 m3s-1, delivered more sediment to the lake and by the end of April 15, Gígjokulson was completely infilled with sediment and ice blocks. The volume of sediment delivered to the lake during this period is estimated to be 17.12 x 106 m3 (Dunning et al., 2013). Displaced water from the lake contributed ~12 x 106 m3 of water to the April 14 and 15

jökulhlaups that breached the moraine dam. The lake outflow was incised vertically by up to 6.2 m, with its cross-sectional area increasing from 40m2 to 500m2. Between April 20 and May 16, over 140 discrete outburst floods were recorded; after May 16, the discharge from Gígjökull returned to pre-eruption levels. Dunning et al. (2013) calculated an additional net sediment input of 2.47 x 106 m3 from May 15 to May 16, which was deposited as an aggraded debris fan that reached 35m above the sediment infill surface produced on April 15. In addition to the large volumes of sediment deposited during the jokulhlaup events, 0.6 x 106 m3 of the eastern moraine and lake floor infill were eroded by the flood waters (Dunning et al., 2013). Most of the erosion caused by the jökulhlaups was focused toward the lake outlet and the eastern part of the frontal moraine and caused further incision of several gullies on the eastern lateral moraine (Dunning et al., 2013). Despite this, the jökulhlaups did not cause significant erosion or loss of sediment from the large latero-frontal moraine limbs.

4.3 METHODOLOGY

In order to document the internal sedimentology and architecture of the Gígjökull latero-frontal moraine it was necessary to identify an area of the moraine that presented adequate exposure of the internal sediment stratigraphy. The focus of this study is therefore the southernmost section of the eastern lateral moraine of Gígjökull which provides a laterally extensive and unvegetated exposure through the upper part of the moraine (Figures 4.1 and 4.4). The western lateral moraine and frontal moraine were not investigated as they were mostly covered by talus and vegetation (Figure 4.4).

Figure 3.4: Panoramic view of the proglacial field of Gígjökull looking south. The exposed section of the eastern lateral moraine examined in this study is indicated in the white box on the left; the western lateral moraine, which is largely covered by talus and vegetation is indicated by the yellow box on the right.

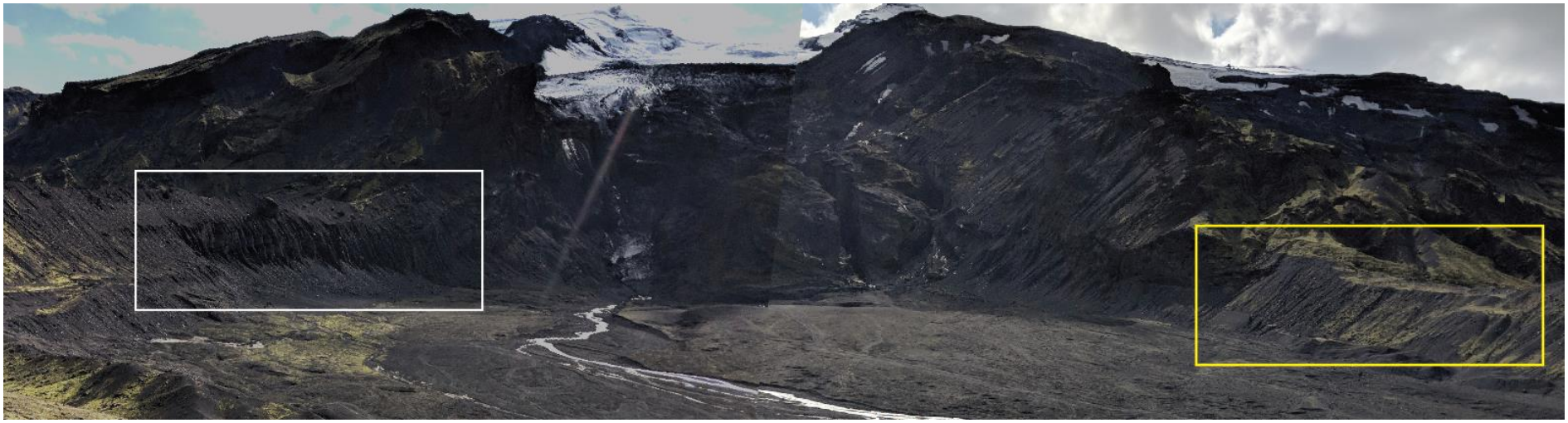

Geomorphological and sedimentological analysis and UAV photographic work was performed in the field during August 2018. Due to the height and steepness of the exposure it was not possible to directly examine and record sediment characteristics on one-dimensional, vertical sedimentological logs. Instead, a DJI Phantom -4 Advance UAV was employed to acquire high resolution photographs of the entire exposure, with images taken 8-10 m away from the moraine face. This allowed the collection and analysis of laterally continuous data to document facies architecture and reconstruct the processes and sequence of events that created this part of the moraine. The photographic survey covered the exposed area of the moraine lying approximately 500 m to 1 km north of the current glacier margin and approximately 60 m from the moraine crest to the base of the moraine (large white rectangle on Figures 4.1, 4.4). The northernmost section of the surveyed area was selected for detailed study as it had the highest resolution photogrammetry and appeared to be most representative of the moraine stratigraphy in that area. This detailed study area is approximately 50 m in height and 120 m in length (small white rectangle on Figure 4.1).

In order to identify and analyse the sedimentary architecture of the detailed study area a photogrammetric model was created using Agisoft Metashape Professional, a commonly used Structure from Motion Modelling Software (Ely et al., 2017). A processing workflow based on previous studies using Agisoft was completed (Gauthier, Wood and Hutchinson, 2015; Evans, Ewertowski and Orton, 2016). Data processing included alignment of photos, point-cloud generation, model refinement and the final output of the photomosaics (Figures 4.6). Unfortunately, ground control points (GCPs) were not established at the study site and this poses a limitation on the spatial accuracy of the

Figure 4.5: Sedimentary logs taken from the four pits excavated in the eastern lateral-frontal moraine of Gígjökull (Logs 1-4), and in hummocky topography on the southern side of the eastern frontal moraine (Logs 5,6). Location of logs is shown on Figure 1C.

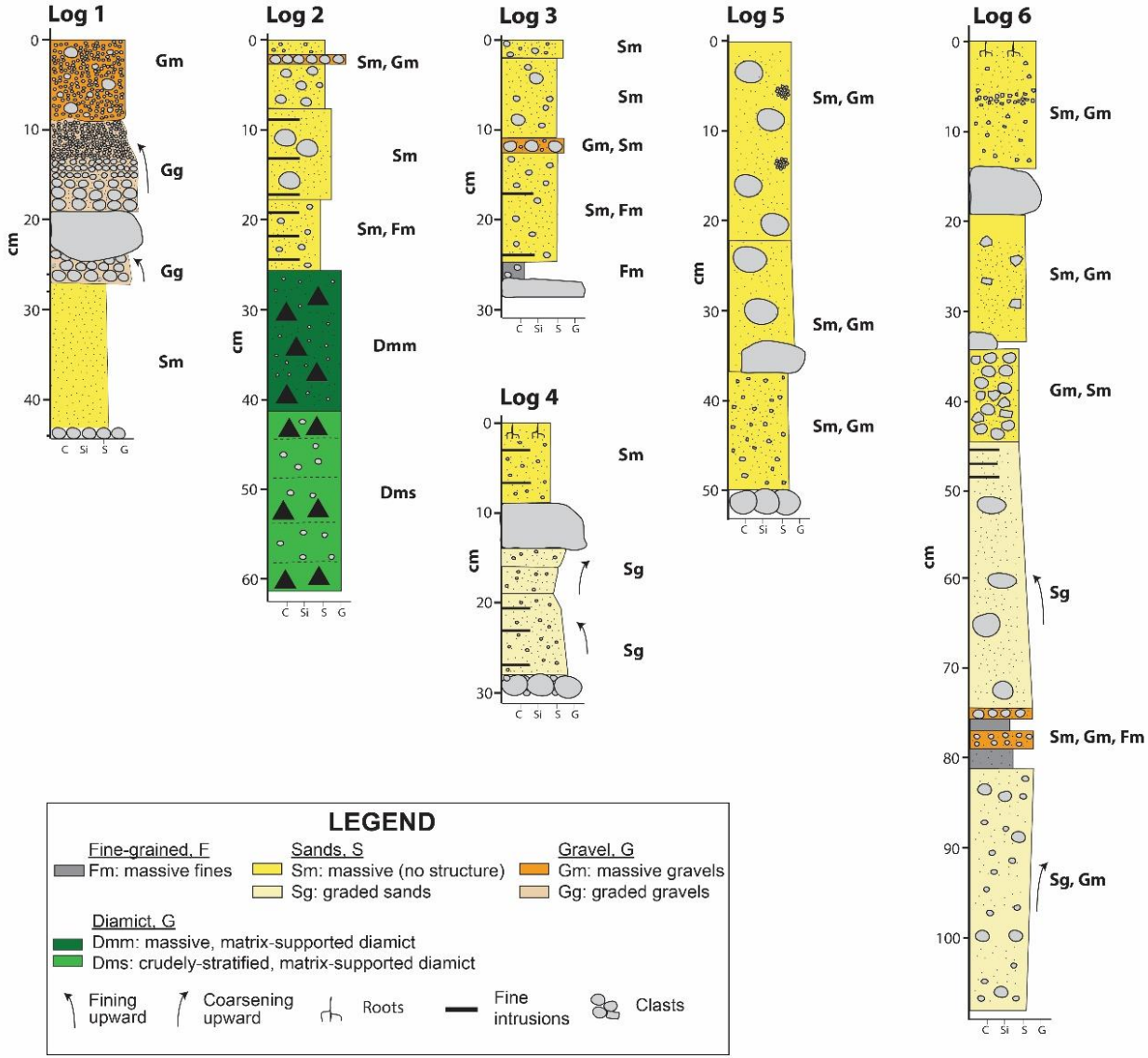
Log 1
Gm
Gg
Gg
Sm
Log 2
Sm, Gm
Sm
Sm, Fm
Dmm
Dms
Log 3
Sm
Sm
Gm, Sm
Sm, Fm
Fm
Log 4
Sm
Sg
Sg
Log 5
Sm, Gm
Sm, Gm
Sm, Gm
Log 6
Sm, Gm
Sm, Gm
Gm, Sm
Sg
Sm, Gm, Fm
Sg, Gm
cm
C Si S G
LEGEND
Fine-grained, F
Fm: massive fines
Sands, S
Sm: massive (no structure)
Sg: graded sands
Gravel, G
Gm: massive gravels
Gg: graded gravels
Diamict, G
Dmm: massive, matrix-supported diamict
Dms: crudely-stratified, matrix-supported diamict
Fining upward
Coarsening upward
Roots
Fine intrusions
Clasts

Figure 4.6: Photomosaic of the exposure through part of the eastern limb of the Gígjökull moraine (small white rectangle on Figures 4.1C, 4.4). The locations of detailed photographs shown in Figures 4.7A-I are indicated by the white boxes. The modern margin of the Gígjökull Glacier lies approximately 1km to the north (right) of this image. Red lines represent contacts between units. Clasts have been outlined in black to increase their visibility.

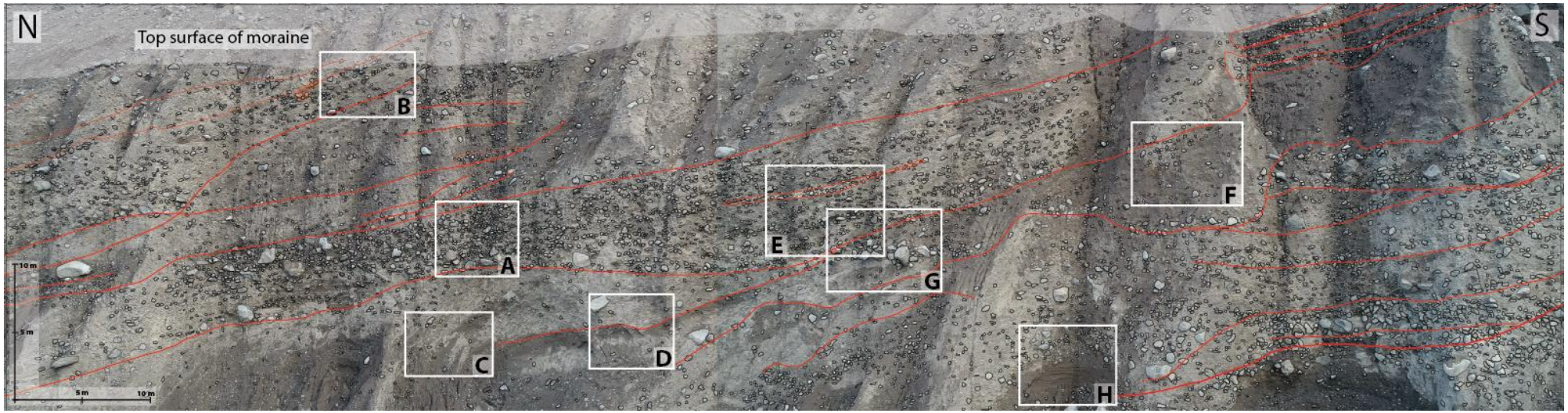
N
S
Top surface of moraine
A
B
C
D
E
F
G
H
10 m
5 m
5 m
10 m

photomosaics. However, for the purposes of the architectural analysis of the moraine, this was deemed an acceptable limitation.

To augment the UAV photography and modelling, several small pits were excavated into the accessible portion of the eastern frontal moraine (Figures 4.1, 4.5) to document sediment types and details of sediment texture, clast characteristics and sedimentary structures. In addition, landforms in the forefield area were examined and data recorded regarding their height, maximum lateral extent, sediment composition, and spatial relationship with other landforms.

4.4 LITHOFACIES CHARATERISTICS

4.4.1 Lithofacies of the eastern lateral moraine

Seven lithofacies types were identified from the photomosaic modelled from numerous UAV images of the detailed study area in the eastern limb of the Gígjökull moraine (Figure 4.6, 4.7A-I). These facies types include massive (Dcm) and crudely stratified (Dcs) clast-supported diamict; matrix-supported deformed (Dmd), crudely stratified (Dms), and massive (Dmm) diamict; massive and crudely stratified gravels (Gm, Gms), and laminated and deformed fine-grained facies (Fl, Fd). These facies types are each described below.

Massive, clast-supported diamict facies (Dcm; Figure 4.7A) contain clasts ranging in size from <10 cm to boulders with a long axis dimension greater than 1m. Clasts observed in these facies in the southern part of the moraine are mostly subrounded with few subangular clasts, while clasts observed in the northern part of the moraine are mostly subangular with few subrounded clasts. There is no clear imbrication of the clasts in this facies, although clasts between 50cm and 1m in diameter commonly form crude boulder horizons/trains.

Figure 4.7: Facies types identified in the eastern limb of the Gígjökull moraine (see Figures 1 & 6 for location). A: massive, clast-supported diamict (Dcm); B: crudely stratified, clast-supported diamict (Dcs); C: folded unit of matrix-rich diamict (arrowed) within deformed, matrix-supported diamict (Dmd); D: horizon of clast-poor, matrix-rich diamict within Dmd facies showing deformation by normal faulting or fracturing; E: crudely stratified, matrix-supported diamict (Dms) with gravel horizons (Gms); F: matrix-supported massive diamict (Dmm); G: boulder horizon (Gms) within diamict. Several clasts exceed 1m diameter; H: raft of horizontally laminated fine-grained sediment (Fl) within massive, clast-supported diamict (Dcm).

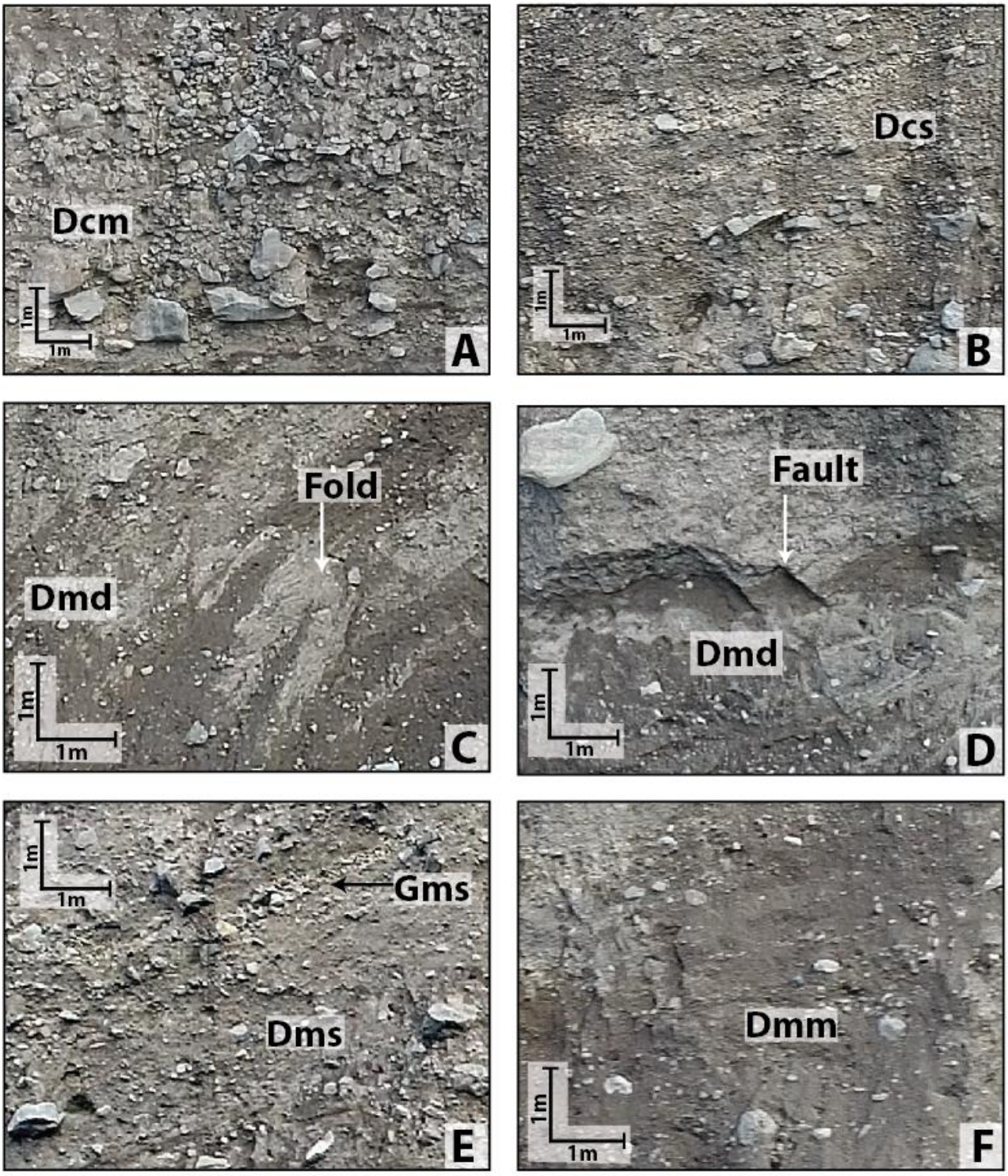
Dcm
1m
1m
A
Dcs
1m
1m
B
Fold
Dmd
1m
1m
C
Fault
Dmd
1m
1m
D
1m
1m
Gms
Dms
E
Dmm
1m
1m
F

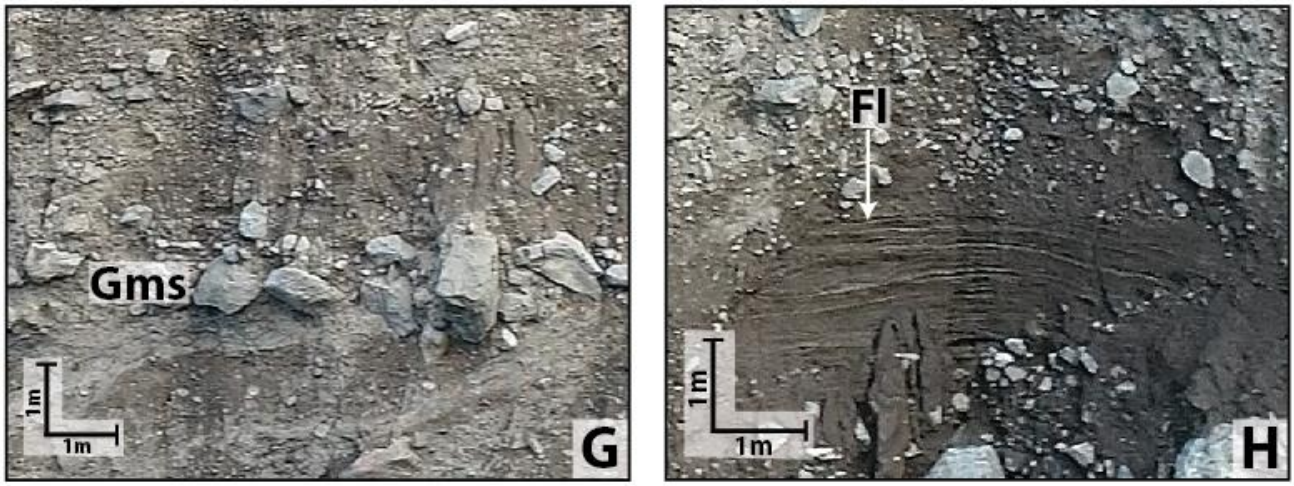
Gms
1m
1m
G
Fl
1m
1m
H

Crudely stratified, clast-supported diamict facies (Dcs; Figure 4.7B) are poorly sorted and contain clasts ranging in size from < 10 cm to <1 m, with occasional boulders greater than 1m diameter. Clasts in this facies range from subrounded to subangular and form laterally extensive 10-20 cm-thick horizons/trains of clasts that extend over 3 m along section; these horizons/trains create the crude stratification observed in this facies and dip towards the north at angles of between 14-18°. Dcs facies observed in the southern portion of the moraine, closer to the modern glacier margin, contain clasts that reach over 1m in diameter; clasts observed in Dcs facies in the midsection of the moraine are smaller with long axes generally <10cm. The size of clasts contained within Dcs facies are generally smaller than those in Dcm facies. Matrix appears to be similar to the silty-sand matrix of diamict exposed in pits dug in the frontal moraine. Massive clast-supported diamict facies with silt, sand, or sand and fine gravel matrix, have also been reported on the upper surface of the moraines at Gígjökull (Sigurðardóttir, 2013).

Matrix-supported deformed diamict facies (Dmd; Figure 4.7C) are found in the lower exposed parts of the northern sections of the moraine. These deformed facies show partially folded units of texturally distinct diamict, with fold structures becoming more apparent towards the southern part of the exposure (Figure 4.7C). There is also evidence of brittle deformation in the form of normal faults or fractures, approximately 0.7-0.8 m in length, that disrupt horizons of alternating diamict units with variably textured matrix (Figure 4.7D).

Crudely stratified, matrix-supported diamict facies (Dms; Figure 4.7E) have a relatively fine-grained matrix with subrounded to subangular ¬¬clasts ranging from < 10 cm to <1m.

Horizontally stratified gravel horizons between 0.5 m to 1.5 m thick, accentuate the crude stratification of the diamict. The clasts within these horizons vary in size from 10 cm to 1.2 m and are subrounded to subangular: clast horizons dip approximately 18-22° towards the north, away from the modern glacier margin. Relatively fine-grained sediment with few clasts separates the clast-rich horizons. Similar Dms facies excavated in pits in the frontal moraine have a matrix of silty-fine to coarse sand with subrounded clasts that range from 3-10 cm in diameter. Stratified, matrix-supported diamicts described from the upper surface of the Gígjökull moraine by (Sigurðardóttir, 2013) are characterized by a coarse-grained, sand-rich matrix.

Massive, matrix-supported diamict facies (Dmm; Figure 4.7F) have crude to no internal structure and are very poorly sorted. Clast size and abundance varies throughout these facies but most clasts are subangular to subrounded and range in size from less than 10 cm to over 1 m. This facies is most prevalent in the southern part of the moraine exposure close to the modern ice margin. Although matrix texture could not be determined in situ, similar Dmm facies examined in the frontal moraine have a matrix of fine sand with some silt; similar massive, matrix-supported diamict facies described by Sigurðardóttir (2013) contain clays and silts as well as sands and fine gravels.

Gravel facies (Gm, Gms) include a range of boulder and gravel horizons observed within the outcrop of the eastern moraine (Figure 4.6). These are commonly less than 0.75 m in thickness and vary in length from less than 4 m to over 10 m. These clast-rich units either have a horizontal orientation or dip toward the north (dips range from 12°-28°) away from the modern ice margin. Subangular to subrounded clasts contained within these facies are

mostly less than 1m diameter; clasts larger than 1m are only observed at one location (Figure 4.7G). The clasts observed within gravel facies in the excavated pits of the frontal moraine are much smaller than those observed in the lateral moraine and range from granules (>2mm) to pebbles/cobbles (2cm – 10cm).

Fine-grained facies (Fl, Fd) in the form of discrete lenses or clasts (Figure 4.7H) are observed in four different locations of the moraine section. Fine-grained lenses/clasts range in size from 0.5 cm to 2m in thickness and from 2 m to ~5.5 m in length and show both horizontal bedding and deformation structures. Fine-grained facies documented in the frontal moraine consist predominantly of silt or sandy silt and a similar texture is proposed for these facies.

4.4.2. Lithofacies of the eastern frontal moraine and associated hummocky topography

Sediment pits were dug at accessible locations on the eastern frontal moraine of Gígjökull (Logs 1-4; Figures 4.1 & 5) and in an area characterized by hummocky topography at the base of the eastern lateral moraine (Logs 5 and 6; Figures 4.1, 4.5 & 4.8). The sediment exposed in these pits provided additional information on sediment characteristics within the moraines at Gígjökull (e.g. sediment texture, clast characteristics and sedimentary structures) that could not be obtained from analysis of the UAV images alone.

The four shallow pits that were excavated into the eastern frontal moraine of Gígjökull exposed massive and stratified matrix-supported diamict (Dmm, Dms), massive and graded sands (Sm, Sg), and massive and graded gravels (Gm, Gg; Logs 1-4, Figure 4.5). Diamict facies were characterized by a silty-sand matrix and contained commonly striated, sub-rounded clasts between 5 cm and 50 cm in diameter. Massive sand facies were

Figure 4.8: Hummocky topography on inner margin of the frontal moraine of Gígjökull. Photo was taken from the top of the moraine looking southwards. B. Vegetation cover on parts of the inner moraine and adjacent hummocky topography. C. Sediment exposure through a hummock (sediment log 5; Figure 5) showing massive gravels and sands with subrounded to subangular clasts. Trowel for scale.

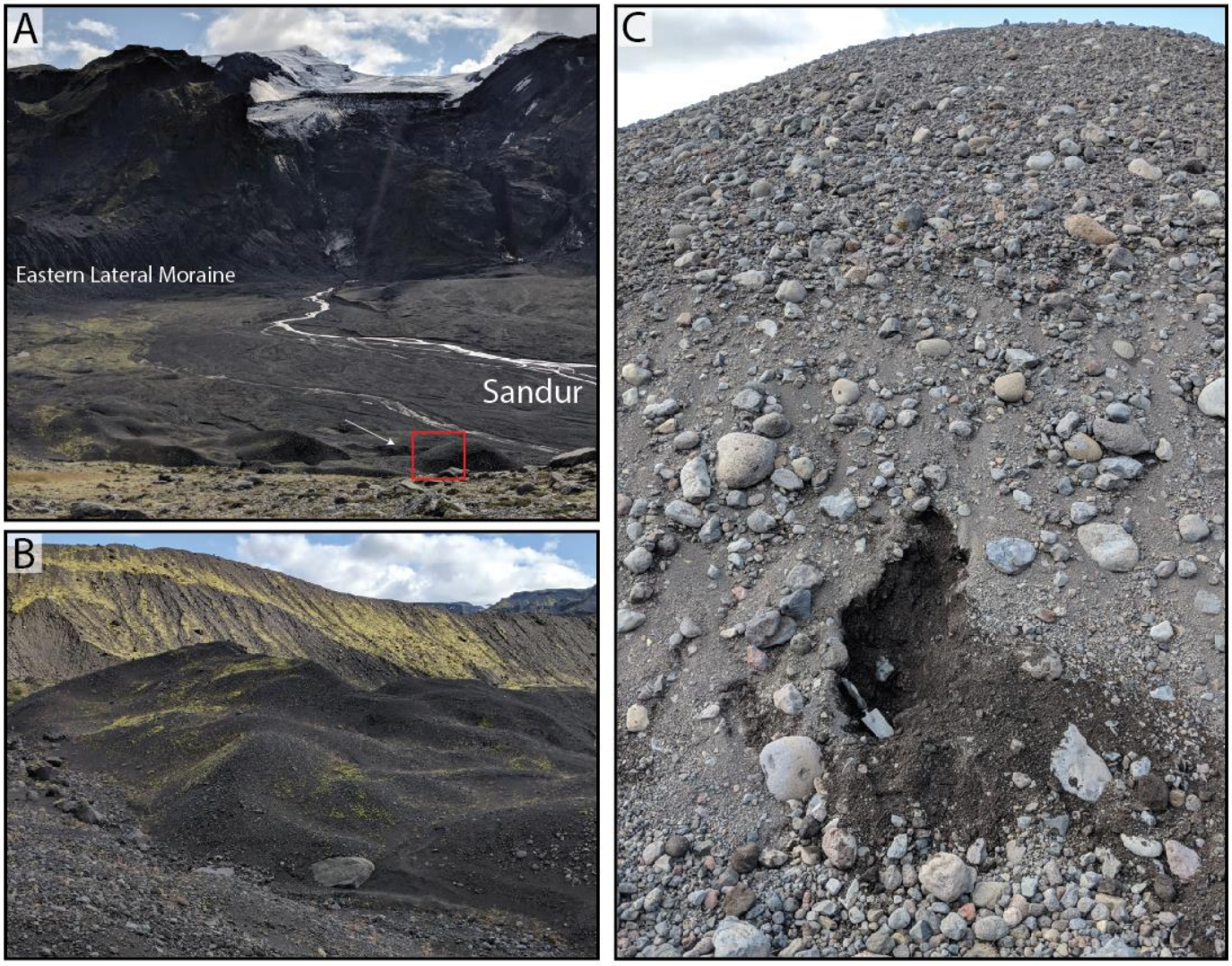
A
Eastern Lateral Moraine
Sandur
B
C

coarse grained and contained common clasts 0.5 to 5 cm diameter; gravel facies contained subrounded clasts up to 8 cm in diameter. These facies suggest that following subglacial or ice marginal deposition of the matrix- supported diamict facies and retreat of the ice margin, deposition on the exposed forefield was dominated by fluvioglacial processes resulting in the deposition of sands and gravels. The timing of deposition of these fluvioglacial sands and gravels is not certain as the forefield has been subjected to repeated jökulhlaup events (Dugmore et al., 2013). The silty-sand matrix of the diamict facies exposed in these pits can be used to infer a similar matrix texture for the diamicts (Dmm, Dms) found within the lateral moraine.

Sediment logs 5 & 6 (Figures 4.1, 4.5) were recorded from shallow pits dug into an area of hummocky topography on the southern side of the eastern frontal moraine (Figures 4.1, 4.9). These pits contained massive and graded sands (Sm, Sg), massive gravels (Gm) as well as some massive fines (Fm). Massive sand facies contained subrounded to subangular pebbles ranging from 1 cm to 7 cm in diameter, whereas graded sands contained smaller clasts less than 1 cm in diameter. The massive gravels (Gm) exposed in these pits contained larger subrounded clasts up to 12 cm in diameter. These thick units of interbedded gravels and massive and graded sands likely record deposition by flood waters following jökulhlaups or by fluvioglacial systems that migrated across the forefield during periods of ice recession. The presence of graded sands suggests rapid deposition of sediment from turbulent flows and supports the proposal that much of this sediment records jökulhlaup events. It is likely that the hummocky surface topography is being generated by the uneven melting of buried ice beneath the overlying cover of sands and gravels. This

ice may be part of the former ice margin that was buried by rapidly deposited glaciofluvial sediment or may be from ice blocks transported by jökulhlaups and trapped within the accumulating sediment.

4.5 LITHOFACIES ASSOCIATIONS

Individual lithofacies identified in the detailed study area of eastern moraine limb can be grouped into three lithofacies associations (LFA1 – 3) to facilitate interpretation of their depositional origin. Lithofacies associations are identified on the basis of lateral and vertical facies relationships, the nature of bed contacts, and the architecture of the sedimentary units they contain (Figure 4.9).

LFA 1 – Lithofacies association 1 is primarily composed of stacked units of massive to crudely stratified, matrix-supported diamict (Dmm, Dms). There are four distinct units of LFA 1 in the study section, all of which dip towards the north, away from the modern glacier margin, at angles of between 8 and 18°; crude stratification within Dms facies, produced by changes in matrix texture and clast content, dips in a similar manner. LFA 1 is characterized by clast-poor diamict containing few, small clasts (<10 cm) scattered throughout a fine-grained matrix; however, clast content does increase toward the north. The proportions of Dmm and Dms facies vary laterally within this facies association, with more frequent alternation of facies types in the southern portion of the unit, proximal to the modern glacier margin, and more consistent massive facies (Dmm) towards the northern, more distal section. Gravel horizons (Gm, Gms) are present in two of the LFA 1 units, attaining a maximum thickness of 1 m and length of up to 15 m, and accentuate the crude stratification of the unit (Figure 4.8). Close to the base of the lowermost unit of LFA 1 a

Figure 4.9: Architecture of lithofacies associations (LFA 1-3) identified within the eastern lateral moraine (for location see small white rectangle on Figures 4.1 and 4.4). Modern ice margin lies to the right of the photomosaic. Most lithofacies associations dip to the north (away from the glacier margin) at angles between 8 and 25°suggesting progressive construction of the moraine as the ice advanced northward.

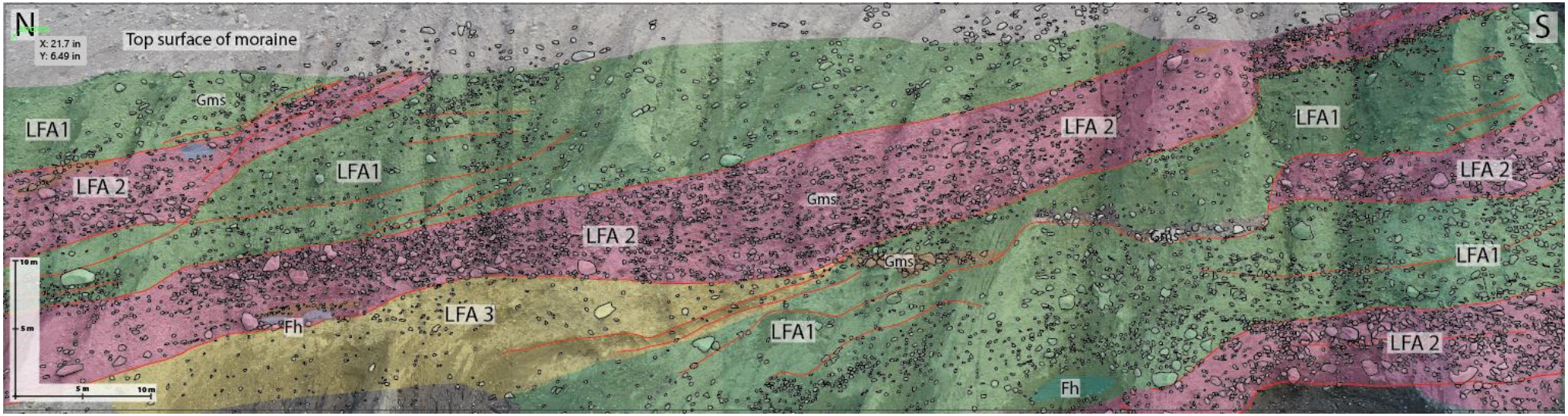
N
S
X: 21.7 in
Y: 6.49 in
Top surface of moraine
Gms
LFA1
LFA 2
LFA1
LFA 2
Gms
LFA 2
Gms
Gms
LFA 3
Fh
LFA1
LFA1
LFA 2
LFA 2
Fh
10 m
5 m
5 m
10 m

large intraclast (1 m in height by 8 m in length) of fine-grained material can also be seen (Fl, Fd; Figure 4.8).

Interpretation: LFA 1 comprises stacked units of massive and stratified matrix-supported diamict that often exhibit gradational contacts, suggesting deposition by closely related processes. Interbedded within these diamicts are laterally extensive gravel horizons (Gm, Gms) and occasional intraclasts of fine-grained sediment (Fl, Fd). This association of facies types and their gently northward-dipping orientation is strongly suggestive of deposition by subaerial debris-flows which originated from a supraglacial position and stacked up to form multiple units of diamict (Dmm, Dms) interbedded with fluvially-transported gravels (Gm, Gms; Evans et al., 2010; Humlum, 1978; Lukas & Sass, 2011; Lukas, 2005; Lukas et al., 2012; Owen & Derbyshire, 1989; Reinardy & Lukas, 2009; Small, 1983). Longer transport distances away from the ice margin may have resulted in greater amounts of homogenization of materials (increased proportion of massive facies) and loss of matrix material (increase in clast content) distal to the ice margin from which the flows were generated (Evans, Shulmeister and Hyatt, 2010). Discontinuous lenses and pockets of cobble-boulder gravels, and occasional fine-grained intraclasts, likely record the accumulation and remobilization of sediment from ephemeral stream channels or ponds, on or adjacent to the lateral margins of the glacier. The subrounded nature of some of the clasts in LFA1 is indicative of fluvial abrasion and suggests that the moraine includes sediments that were transported either by supraglacial or subglacial meltwater flows. Low gradient glaciers with extensive debris cover such as Gígjökull provide ideal conditions for the supraglacial transport of sediment by meltwaters (Kirkbride and Spedding, 1996;

Spedding, 2000; Benn et al., 2003). It has been suggested by previous workers that some of the fluvial sediment contained within the Gígjökull lateral-frontal moraine may have originated in a subglacial position and was subsequently elevated to englacial and supraglacial positions prior to final deposition (Kirkbride and Spedding, 1996; Spedding, 2000). Some of the gravel horizons observed within LFA1 may also have resulted from the concentration of clasts at the base of the debris flows or from the winnowing or interaction of clasts on the surface of flows (Lukas, and Sass, 2011; Lucas, 2005; Lawson, 1998; Benn, 1992).

The dipping units of massive and stratified diamict and associated gravels of LFA 1 are therefore interpreted to have resulted from the alternating accumulation of supraglacial debris flows and glaciofluvial sediments released from the ice margin (Benn et al., 2003; Evans, Shulmeister and Hyatt, 2010; Lukas and Sass, 2011; Lukas et al., 2012; Sigurðardóttir, 2013). Differential sorting and reworking by fluvial and slope processes may have contributed to the distinct lateral variability of diamict facies which transition from stratified facies proximal to the glacier to more massive facies distally (Benn et al., 2003; Evans et al., 2010).

LFA2 – This lithofacies association is characterized by massive to crudely stratified, clast-supported diamict (Dcm, Dcs; Figure 4.8). In comparison to LFA 1, this lithofacies association is clast-rich and contains an abundance of large subrounded to subangular clasts greater than 1m diameter (Figure 4.8). Four distinct units of LFA 2 can be discriminated in the studied section, all of which dip northward at angles ranging from 9° to 25° (Figure 4.8). All four units exhibit sharp upper and lower contacts accentuated by the absence of

clasts in the overlying and underlying units. A particularly prominent unit of LFA 2 crosses the entire studied section, traversing ~115m from south to north (right to left on Figure 4.8) and shows a clear transition from stratified Dcs facies in the south to massive Dcm facies in the north. Gravel horizons (Gm, Gms) are present in LFA 2 but are notably thinner than the gravel beds found in LFA1, with a thickness of less than 0.5 m and a lateral extent ranging from 15 – 20m (Figure 4.8). In the uppermost unit of LFA 2, large intraclasts of fine-grained sediment (Fl, Fd), up to 50cm in height and 1.8-2m long, can be seen. The lower contact of this laterally extensive unit of LFA 2 with LFA 3 below, is sharp and possibly erosive.

Interpretation: LFA 2 is composed of massive and crudely stratified clast-supported diamicts that often exhibit sharp contacts and is interpreted to record deposition from relatively coarse-grained debris flows originating from a supraglacial position (Humlum, 1978; Small, 1983; Owen and Derbyshire, 1989; Benn et al., 2003; Levansukas et al., 2012). The large size and predominantly subangular shape of the clasts indicates a supraglacial origin; this supraglacial debris accumulated as rockfall or avalanche debris on the margins of the glacier forming a lateral moraine (Benn et al., 2003; Evans et al., 2010, 2013; Humlum, 1978; Lukas et al., 2012; Owen & Derbyshire, 1989; Small, 1983). Rockfall debris may have originated from discrete large-scale rockfall events or accumulated gradually from more frequent failure of the valley walls or avalanches. The inclusion of smaller subrounded clasts indicates the inclusion of some water-worked debris, possibly from supraglacial streams or reworked subglacial material (Kirkbride & Spedding, 1996b; Spedding, 2000).

LFA 3¬¬ – Lithofacies association 3 occurs in only one location towards the base of the central-northern part of the outcrop (Figure 4.8). This association is dominated by a heavily deformed, matrix-supported diamict containing both Dmd and Dms facies. LFA 3 has a gradational contact with an underlying unit of LFA 1 and is sharply overlain by a unit of LFA 2. LFA 3 is ~54m in length and ranges in thickness from 1-8m; it pinches out to the south where it is truncated and erosively overlain by clast-rich facies of LFA 2 (Figure 4.8). Although the dominant structures visible within this association appear to be folds created by ductile deformational processes, several normal faults or fractures are also visible within the Dmd facies, particularly in the southern part of the unit (Figure 4.8).

Interpretation: LFA 3 contains matrix-supported stratified diamict that shows both brittle and ductile deformation structures. The deformed diamict appears to have a fine-grained matrix which suggests that it originated either subglacially or in a low energy, lacustrine setting in either a supra- or ice marginal location (Benn & Evans, 2010; Evans et al., 2010). The folding and faulting structures visible in this association are likely the result of localized ice overriding which caused glaciotectonic deformation of the sediments when a portion of the glacier margin advanced (or readvanced) over the fine-grained deposits (Evans et al., 2010; Lukas, 2005). Alternately, but less likely, deformation may have occurred as a result of loading and disruption of the relatively fine-grained diamict by the emplacement of the rapidly deposited sediments above (the diamict units of LFA 2). The presence of both brittle and ductile deformation structures suggests that the diamict was initially mobile and water-saturated when first disturbed, and dewatered and rigid during later stages of deformation. Given the stratigraphic position of LFA 3 close to the base of

the moraine limb, it is interpreted here as a unit of locally overridden fine-grained sediment, which may have formed originally in an ice marginal lake or pond during a period of ice retreat. Subsequent readvance of the ice is likely to have caused the glaciotectonic disturbance and deformation of the fine-grained sediments.

4.6 DISCUSSION

4.6.1. Interpretation of moraine-building processes

The overall architecture of the lithofacies units identified within the eastern lateral moraine of Gígjökull is characterized by alternating units of matrix-supported (LFA 1) and clast-supported diamict (LFA 2), overlying a unit of highly deformed diamict (LFA 3), all of which dip gently northwards away from the current position of the ice margin (Figure 4.8). Three distinct depositional mechanisms are suggested for the construction of the eastern lateral moraine of Gígjökull: 1) matrix-rich subaerial debris flows generated from supraglacial material, including sediment elevated from sub- and englacial positions, together with glaciofluvial sediments (LFA1); 2) clast-rich subaerial debris flows comprised of coarse-grained supraglacial debris (derived from rockfall events) that has undergone minimal modification (LFA 2); and 3) glaciotectonization of fine-grained sediment formed in supraglacial/ice marginal ponds (LFA 3).

Analysis of the sedimentary characteristics and architecture of the eastern lateral moraine of Gígjökull indicates that the depositional processes responsible for building the moraine were dominated by supraglacial debris flows containing some rounded glaciofluvial materials (LFA 1) and accumulations of angular rock-fall debris (LFA 2) released from valley walls and the ice margin. This arrangement of alternating units of

debris flows sourced by matrix-rich supraglacial sediment and clast-rich rock fall debris has been observed in other moraines where crudely to well-stratified bedding dips away from, or toward, the glacier margin, depending on whether the snout is advancing or receding respectively (Boulton & Eyles, 1979; Evans et al., 2010; Lawson, 1979; Small, 1983). Interbedded successions of diamicts, stratified sediments, and coarse, bouldery layers have also been interpreted to document deposition from intermittent debris flows, glaciofluvial processes, and the accumulation of glacially transported rock avalanche material (Humlum, 1978; Owen and Derbyshire, 1989).

The accumulation of matrix-rich LFA 1 facies along the lateral moraine occurred when the dominant sediment supply to the moraine was from supraglacial debris flows with minimal direct input from avalanches and/or rockfalls. During the ablation season, when melting occurs on the glacier surface releasing englacial, supraglacial and glaciofluvial sediment from the ice, water saturated debris flows can be readily generated (Small, 1983; Owen and Derbyshire, 1989; Benn et al., 2003). These gravity driven flows can move on the sloping glacier surface and accumulate along the lateral and frontal margins, contributing toward the growth of the moraines. Some of the material incorporated into the flows may have originated as relatively fine-grained subglacial material, thrust upwards onto the glacier surface by compression at the glacier margin (Kirkbride and Spedding, 1996; Spedding, 2000). During this stage of moraine formation, the ice margin is likely to have been stationary to slowly advancing, allowing substantial amounts of sediment to accumulate along its margins (Lukas et al., 2012).

In contrast, clast-rich LFA 2 facies represent periods dominated by accumulation of coarse-grained supraglacial material released from the valley walls. The amount of rockfall and/or avalanche debris released from valley walls is influenced by bedrock characteristics such as slope, aspect, bedrock erodibility, tectonic and volcanic activity, but also by climatic factors such as precipitation and temperature (Boulton and Eyles, 1979; Small, 1983; Benn and Owen, 2002; Benn et al., 2003). The repeated occurrence of LFA 2 units within the lateral moraine at Gígjökull indicates that large amounts of rockfall and/or avalanche debris were available for release from the ice at multiple times. Kirkbride and Spedding (1996) and Spedding (2000) described large amounts of poorly sorted, coarse-grained material on the eastern moraine in 1987, in areas where it was in contact with the glacier; the accumulation of coarse-grained supraglacial debris on the glacier margins must have been a frequent occurrence in the past and may have resulted in reduced ablation rates and ice marginal advance (Benn et al., 2003).

The architecture of alternating units of LFA 1 and LFA 2 within the analyzed section of the eastern lateral moraine of Gígjökull supports the construction of this moraine during episodes in which sediment was supplied alternately by predominantly fine-grained supraglacial/glaciofluvial sources and by coarse-grained rockfall/avalanche debris. The one unit of LFA 3 exposed in the studied section was probably formed during an episode of glacier readvance that overrode relatively fine-grained sediment previously deposited beneath and/or on the margins of the ice; the presence of only one unit of LFA 3 suggests that conditions conducive to the formation of such fine-grained deformed facies were not experienced very frequently.

4.6.2 Depositional Model of the Eastern Moraine of Gígjökull

A depositional summary model (Figure 4.10) is presented here to illustrate the formation of the Gígjökull eastern lateral moraine based on interpretation of its sedimentological and architectural characteristics.

Stage 1. During glacier advance, subaerial debris flow fans (containing supraglacial, englacial, and some glaciofluvial materials) are deposited from the front and lateral margins of the ice onto the surface of pre-existing sediment (Benn et al., 2003; Lukas, 2005). This body of pre-existing sediment probably included thickened wedges of material bulldozed or released from the ice in the form of an incipient moraine which was sufficient to obstruct the glacier from extending laterally and promoted ice thickening. Retardation of the forward movement of the ice resulted in thickening of the ice and allowed supraglacial debris to flow from the glacier surface onto the pre existing sediment (incipient moraine) as a series of steeply dipping beds of LFA1. A similar process of moraine growth has been suggested for large scale moraines elsewhere (Benn et al., 2003; Kirkbride and Winkler, 2012; Kirkbride and Deline, 2013). It is likely that the incipient moraine at Gígjökull was formed sometime between O and 900 AD when the glacier margin is thought to have reached the position of the current latero-frontal moraine (Kirkbride and Dugmore, 2008; Dugmore et al., 2013). Subsequent retreat of the ice margin was followed by readvance at the onset of the LIA; by the beginning of the 20th century, the large latero-frontal moraines of Gígjökull were recorded in historical documents as being almost fully formed. This suggests that formation of the units that are described here occurred sometime between the initial

Figure 4.10: Conceptual model of the processes that formed the eastern lateral moraine at Gígjökull. 1 – Stage 1: As the glacier advances and encounters a barrier to forward flow, debris bands are thrust from subglacial/englacial positions to the ice surface. The released sediment mixes with sediment from supraglacial streams and/or rockfall debris to create debris flows (LFA 1) that are deposited over existing material. 2 – Stage 2: Coarse-grained supraglacial debris from episodic rock falls and avalanches are deposited as clast-supported units of LFA 2. 3 – Stage 3: Supraglacial streams and ponds forming between the glacier ice and the developing moraine contribute fine-grained sediment to supraglacial debris flows. 4 – Stage 4: Accumulation of alternating units of matrix-rich debris flow (LFA 1) and coarse-grained rockfall debris (LFA 2) construct the moraine over time as the glacier retreats/readvances. During glacier readvance and/or thickening, the pressure of the glacier against units of fine-grained sediment can cause deformation (glaciotectonization; LFA 3). Large boulders (> 10m) on the uppermost surface of the moraine were probably emplaced during the final stages of maximum ice advance/thickness. The Gígjökull latero-frontal moraine was fully formed by the beginning of the 20th century and subsequently impounded the proglacial lake Gígjökulsón.

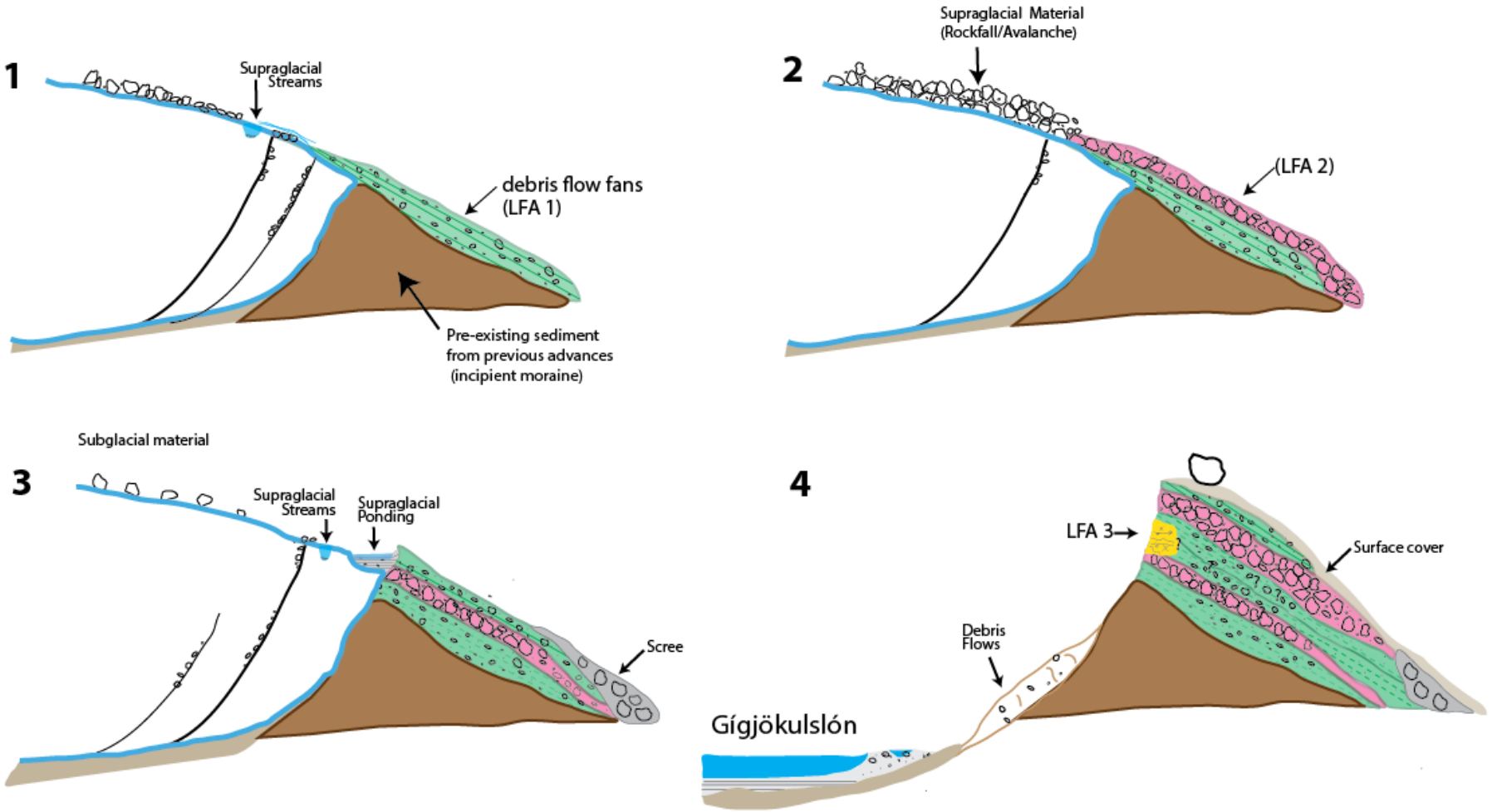
1
Supraglacial Streams
debris flow fans (LFA 1)
Pre-existing sediment from previous advances (incipient moraine)
2
Supraglacial Material (Rockfall/Avalanche)
(LFA 2)
3
Subglacial material
Supraglacial Streams
Supraglacial Ponding
Scree
4
LFA 3
Surface cover
Debris Flows
Gígjökulslón

expansion of glaciation at Gígjökull in the LIA (~1700AD) and the end of the last LIA advance that began around 1880 AD (Kirkbride and Dugmore, 2008).

Stage 2. Rockfall/avalanche debris is transported supraglacially and released onto the previously deposited debris flow material with similar dip angles. The size and quantity of rockfall debris will vary over time and during periods of low to no rockfall debris, deposition of debris flows generated from the surface of the glacier will dominate (e.g. Humlum, 1978; Small, 1983; Shakesby, 1989; Benn and Owen, 2002; Lukas et al., 2005). During such periods supraglacial streams will transport and rework clasts released by rock falls which may subsequently be incorporated into debris flows. The alternating accumulation of predominantly debris flow and predominantly rockfall materials creates much of the stratigraphy now exposed in the eastern moraine.

Stage 3. Supraglacial ponding between the moraine and the glacier ice during the ablation season allows the accumulation of fine-grained laminated sediment (e.g. Benn and Owen, 2002). This fine-grained sediment will undergo deformation and shearing if subsequently overridden/squeezed by the ice. Scree will also accumulate on the distal lower part of the moraine.

Stage 4. As the glacier retreats and thins, debris flow material and other collapsed sediment will accumulate as scree along the lower parts of the moraine. Isolated large boulders may remain on the surface of the moraine as the remnants of a more extensive cover of loose supraglacial debris, delivered from the glacier surface prior to its final retreat. Glacial lake Gígjökulslón formed in the topographically low area encircled by the latero-frontal moraine as the glacier withdrew; breaching of the moraine by

floodwaters released during the eruption of Eyjafjallajökull in 2010 drained this lake (Dunning et al., 2013).

As with many other lateral moraines (e.g. Benn et al., 1989, 2003; Benn & Evans, 2010; Matthews & Petch, 2008; Shakesby, 1989), the latero-frontal moraine at Gígjökull exhibits asymmetry, with the eastern lateral moraine being significantly larger than the western lateral moraine (Figures 4.1 & 4.4). Large lateral moraines are best developed on valley margins where there are extensive rockwalls to supply large amounts of debris to the glacier; cross valley differences in bedrock lithology or structure can therefore influence rates of debris supply either to the surface or bed of the glacier (Benn and Owen, 2002; Benn et al., 2003). Moraine asymmetry may also be attributed to differences in glacier dynamics where one margin of the glacier may be relatively slow moving or stable allowing the accumulation of a large lateral moraine, and the other margin may retreat at a faster rate, resulting in more dispersed sediment and a smaller moraine (Matthews and Petch, 1982; Benn et al., 2003; Benn and Evans, 2010).

4.6.3 Moraine Stability Implications for Glacial Lake Outburst Floods

Documentation of the sedimentary architecture of steep and inaccessible moraine faces at Gígjökull, primarily through use of UAV photographic analysis, has significant future applications to the understanding of the development of lateral moraines in other settings, and is particularly relevant to the study of large unstable moraines that dam proglacial lakes. In rapidly deglaciating areas such the Cordillera Blanca in Peru, the increasing size and number of glacial lakes induced by rapid glacier retreat, dramatically enhances the possibility of glacial lake outburst floods (GLOFs), which can have devastating impacts on

the communities located down valley from these lakes (Carey, 2005; Carey et al., 2012; Klimeš et al., 2016). To minimize the risk from GLOFs, remedial work to release water and strengthen the moraine dams, including the construction of spillways, tunnels and armoring of the dam, has been carried out in many of the lakes of Cordillera Blanca (Emmer and Vilímek, 2013; Emmer et al., 2016; Emmer, Vilímek and Zapata, 2016). In addition, quantitative modelling of moraine failure events and potential GLOFs has been conducted (Emmer and Vilímek, 2013; Klimeš et al., 2014; Schneider et al., 2014; Emmer, Vilímek and Zapata, 2016). However, inputs for these models are often limited to geometric characteristics such as moraine dimensions, lake dimensions, channel and valley floor dimensions (Worni et al., 2012; Schneider et al., 2014; Westoby et al., 2014; Emmer et al., 2016; Emmer, Vilímek and Zapata, 2016), and while acknowledged (MacDonald and Langridge-Monopolis, 1984; Blown and Church, 1985; McKillop and Clague, 2007), the sedimentary characteristics and architecture of these moraines are seldom used as model inputs.

The identification of individual facies types, sedimentary architectures, and the degree of sediment heterogeneity in such large moraine systems can allow inferences to be made regarding hydrogeological characteristics such as permeability (Freeze and Cherry, 1979; Slomka and Eyles, 2013). Understanding the location of areas of hydrogeological weakness can significantly augment the evaluation of moraine failure potential. Identification of areas of high permeability in a moraine (e.g. coarse-grained facies such as Dcm, or units such as LFA2), can enhance understanding of the structural integrity of the structure by identifying areas that are most prone to sediment loss through piping (Kenney

and Lau, 1985). The identification of units of fine-grained sediment (e.g. Fl) can also indicate areas of potential instability as such units may be undermined by water passing through adjacent coarse-grained facies and can trigger failure due to the build-up of high porewater pressures (Westoby et al., 2014). Enhanced understanding of the sedimentary architecture of lake-damming moraines in regions such as the Cordillera Blanca will not only aid in the development of more robust depositional models for these moraines but will also aid in the creation of effective monitoring and mitigation strategies for the glacial lakes they impound (A. Emmer et al., 2016; A. Emmer & Vilímek, 2014; Adam Emmer, 2017).

4.7 CONCLUSIONS

This study identifies the sedimentary architecture of part of the eastern lateral moraine of Gígjökull, a debris-covered valley glacier in southern Iceland. The study utilized a remotely operated UAV to obtain photographic data from steep and inaccessible exposures through the moraine and identified three distinctive lithofacies associations that record changing sediment sources and processes during moraine formation. These lithofacies associations record the alternating deposition of matrix-supported debris flows generated from englacial and supraglacial debris (LFA 1), coarse-grained supraglacial rock fall/avalanche debris (LFA 2), and the inclusion of occasional fine-grained deformed units (LFA 3).

Formation of the large eastern lateral moraine of Gígjökull began during the initial expansion of the glacier at the beginning of the LIA (~1700AD) (Kirkbride and Dugmore, 2008). As ice extended out onto the foreland, its forward movement was hindered by a sediment barrier formed by a remnant moraine that recorded glacier margin extent during earlier episodes of glaciation. Stalling of ice at this point, and retardation of forward flow,

allowed the continued supply of supraglacial debris provided by rockfalls and englacial sources, to be deposited as a growing latero-frontal moraine. The ample supply of debris allowed the development of a large latero-frontal moraine which reached its maximum size by the beginning of the 20th century. Subsequent ice marginal retreat of Gígjökull impounded a proglacial lake (Gígkokulslón) within the confines of the moraine until the eruption of Eyjafjallajökull and the breaching of the moraine dam by jokulhlaups. This study has application to other regions where high rates of glacial recession are creating large proglacial lakes dammed by unstable moraine dams such as the large latero-frontal moraine described here. Enhanced understanding of the sedimentary architecture and development of these moraines will allow the creation of more effective strategies for dam stabilization and flood mitigation.

REFERENCES

Barr, I. D. and Lovell, H., 2014. A review of topographic controls on moraine distribution. Geomorphology. Elsevier B.V., 226, pp. 44–64. doi: 10.1016/j.geomorph.2014.07.030.

Benn, D. I., Kirkbride, M.P., Owen, L.A., & Brazier, V., 2003. Glaciated valley landsystems, in Evans, D. J. A. (ed.) Glacial Landsystems. Arnold, pp. 372–406. doi: 10.4324/9780203784976.

Benn, D. I., 1989. Debris transport by Loch Lomond Readvance glaciers in Northern Scotland : basin form and the within-valley asymmetry of lateral moraines. Journal of Quaternary Science, 4 (3), 243–254.

Benn, D. I. and Evans, D. J. A. (2010) Glaciers & Glaciation. 2nd edn. London: Hodder Education.

Benn, D. I. and Owen, L. A., 2002. Himalayan glacial sedimentary environments: A framework for reconstructing and dating the former extent of glaciers in high mountains. Quaternary International 97–98, 3–25. doi: 10.1016/S1040-6182(02)00048-4.

Blown, I. and Church, M., 1985. Catastrophic lake drainage within the Homathko River basin, British Columbia. Canadian Geotechnical Journal 22(4), 551–563. doi: 10.1139/t85-075.

Boulton, G. S. and Eyles, N., 1979. Sedimentation by valley glaciers; a model and genetic classification', in Schlüchter, C. (ed.) Proceedings of an INQUA Symposium on

Genesis and Lithology of Quaternary Deposits. Zurich. Rotterdam: A.A. Balkema, Rotterdam, pp. 11–24.

Carey, M., 2005. Living and dying with glaciers: People's historical vulnerability to avalanches and outburst floods in Peru. Global and Planetary Change 47, 122–134. doi: 10.1016/j.gloplacha.2004.10.007.

Carey, M., Huggel, C., Bury, J., Portocarrero, C., & Haeberli, W., 2012. An integrated socio-environmental framework for glacier hazard management and climate change adaptation: Lessons from Lake 513, Cordillera Blanca, Peru. Climatic Change 112, 733–767. doi: 10.1007/s10584-011-0249-8.

Defense Mapping Agency Hydrographic/Topographic Cente (DMAHTC), 1990. Eyjafjallajökull, Ísland-Iceland [map]. 1:50,000. Edition: 1-DMA. Series: C761. Sheet 1812 III. Date of Measurement: 1988. Available at Landmælingar Íslands Map Collection: https://www.lmi.is/is/vefsjar/kortasjar/kortasafn-1

Dugmore, A. J., 1987. Holocene glacier fluctuations around Eyjafjallajökull, south Iceland : a tephrochronological study. PhD Thesis, University of Aberdeen.

Dugmore, A. J., Newton, A.J., Smith, K.T., & Mairs, K., 2013. Tephrochronology and the late Holocene volcanic and flood history of Eyjafjallajökull, Iceland. Journal of Quaternary Science 28(3), 237–247. doi: 10.1002/jqs.2608.

Dunning, S. A., Large, A.R.G., Russell, A.J., Roberts, M.J., Duller, R., Woodward, J, Mériaux, A., Tweed, F.S., & Lim, M., 2013. The role of multiple glacier outburst floods in proglacial landscape evolution: The 2010 Eyjafjallajökull eruption, Iceland. Geology 41(10), 1123–1126. doi: 10.1130/G34665.1.

Ely, J. C., Graham, C., Barr, I.D., Rea, B.R., Spagnolo, M., & Evans, J., 2017. Using UAV acquired photography and structure from motion techniques for studying glacier landforms : application to the glacial flutes at Isfallsglaciären. Earth Surface Processes and Landforms 42, 877–888. doi: 10.1002/esp.4044.

Emmer, A., Klimeŝ, Mergili, M., Vilímek, V., & Cochachin, A., 2016. 882 lakes of the Cordillera Blanca: An inventory, classification, evolution and assessment of susceptibility to outburst floods. Catena 147, 269–279. doi: 10.1016/j.catena.2016.07.032.

Emmer, A., 2017. Geomorphologically effective floods from moraine-dammed lakes in the Cordillera Blanca, Peru. Quaternary Science Reviews 177, 220–234. doi: 10.1016/j.quascirev.2017.10.028.

Emmer, A. and Vilímek, V., 2013. Review article: Lake and breach hazard assessment for moraine-dammed lakes: An example from the Cordillera Blanca (Peru). Natural Hazards and Earth System Sciences 13(6), 1551–1565. doi: 10.5194/nhess-13-1551-2013.

Emmer, A. and Vilímek, V., 2014. New method for assessing the susceptibility of glacial lakes to outburst floods in the Cordillera Blanca, Peru. Hydrology and Earth System Sciences 18(9), 3461–3479. doi: 10.5194/hess-18-3461-2014.

Emmer, A., Vilímek, V., & Zapata, M. L., 2016. Hazard mitigation of glacial lake outburst floods in the Cordillera Blanca (Peru): the effectiveness of remedial works. Journal of Flood Risk Management, 11, pp. S489–S501. doi: 10.1111/jfr3.12241.

ERSI, 2020. Basemap. Sources: DigitalGlobe (WV03_VNIR). Date of imagery: July 17, 2016. As shown in the 2019-12-12 version of the World Imagery Map. Available on ESRI World Imagery Wayback: https://livingatlas.arcgis.com/wayback/?active=4756&ext=-19.68909,63.64877,-19.55434,63.68604

Evans, D. J. A., Shulmeister, J. & Hyatt, O., 2010. Sedimentology of latero-frontal moraines and fans on the west coast of South Island, New Zealand. Quaternary Science Reviews 29, 3790–3811. doi: 10.1016/j.quascirev.2010.08.019.

Evans, D. J. A., Rother, H., Hyatt, O.M., & Shulmeister, J., 2013. The glacial sedimentology and geomorphological evolution of an outwash head/moraine-dammed lake, South Island, New Zealand. Sedimentary Geology 284–285, 45–75. doi: 10.1016/j.sedgeo.2012.11.005.

Evans, D. J. A., Ewertowski, M. & Orton, C., 2016. Fláajökull (north lobe), Iceland: active temperate piedmont lobe glacial landsystem. Journal of Maps 12(5), 777–789. doi: 10.1080/17445647.2015.1073185.

Freeze, R. A. and Cherry, J. A., 1979. Groundwater. Englewood Cliffs, New Jersey: Prentice-Hall, 604 pg.

Gauthier, D., Wood, D. F. & Hutchinson, D. J., 2015. Natural geologic controls on rockfall hazard and mitigation on the Niagara escarpment, King's Highway 403 at Hamilton, ON, Canada. In 66th Highway Geology Symposium. Sturbridge, Massachusetts, pp. 520–534.

Geodætisk Institut, 1908. Eyjafjallajökull 58 SV [map]. Scale: 1:50,000. Collection Number: 11.8.5.1. Date of Measurements: 1907. Available at Landmælingar Íslands Map Collection: https://www.lmi.is/is/vefsjar/kortasjar/kortasafn-1

Geodætisk Institut, 1957. Eyjafjallajökull 58 SV [map]. Scale: 1:50,000. Collection Number: 118.22.1. Date of Measurements: 1953-1954. Available at Landmælingar Íslands Map Collection: https://www.lmi.is/is/vefsjar/kortasjar/kortasafn-1

Geodætisk Institut, 1982. Eyjafjallajökull 58 [map]. Scale: 1:100,000. Collection Number: 99.12.1. Date of Measurements: 1980. Available at Landmælingar Íslands Map Collection: https://www.lmi.is/is/vefsjar/kortasjar/kortasafn-1

Hubbard, B., Heald, A., Reynolds, J.M., Quincey, D., Richardson, S.D., Zapata Luyo, M., Santillan Portilla, N., & Hambrey, M.J., 2005. Impact of a rock avalanche on a moraine-dammed proglacial lake: Laguna Safuna Alta, Cordillera Blanca, Peru. Earth Surface Processes and Landforms 30(10), 1251–1264. doi: 10.1002/esp.1198.

Humlum, O., 1978. Genesis of Layered Lateral Moraines: Implications for Paleoclimatology and lichenometry. Geografisk Tidsskrift, 77(1), 65–72. doi: 10.1080/00167223.1978.10649094.

Ivy-Ochs, S., Kerschner, H., Reuther, A., Maisch, M., Sailer, R., Schaefer, J., Kubik, P.W., Synal, H., & Schlüchter, 2006. The timing of glacier advances in the northern European Alps based on surface exposure dating with cosmogenic 10Be, 26Al, 36Cl, and 21Ne. Special Paper of the Geological Society of America 415, 43–60. doi: 10.1130/2006.2415(04).

Jomelli, V., Grancher, D., Brunstein, D., & Solomina, O., 2008. Recalibration of the yellow Rhizocarpon growth curve in the Cordillera Blanca (Peru) and implications for LIA chronology. Geomorphology 93(3–4), 201–212. doi: 10.1016/j.geomorph.2007.02.021.

Kenney, T. C. and Lau, D., 1985. Internal stability of granular filters. Canadian Geotechnical Journal 22(2), 215–225. doi: 10.1139/t85-029.

Kershaw, J. A., Clague, J. J. & Evans, S. G., 2005. Geomorphic and sedimentological signature of a two-phase outburst flood from moraine-dammed Queen Bess Lake, British Columbia, Canada. Earth Surface Processes and Landforms 30(1), 1–25. doi: 10.1002/esp.1122.

Kirkbride, M. P. and Deline, P., 2013. The formation of supraglacial debris covers by primary dispersal from transverse englacial debris bands. Earth Surface Processes and Landforms 38(15), 1779–1792. doi: 10.1002/esp.3416.

Kirkbride, M. P. and Dugmore, A. J., 2008. Two millennia of glacier advances from southern Iceland dated by tephrochronology. Quaternary Research 70(3), 398–411. doi: 10.1016/j.yqres.2008.07.001.

Kirkbride, M. P. and Winkler, S., 2012. Correlation of Late Quaternary moraines: impact of climate variability, glacier response, and chronological resolution. Quaternary Science Reviews 46(483), 1–29. doi: 10.1016/j.quascirev.2012.04.002.

Kirkbride, M. and Spedding, N., 1996. The influence of englacial drainage on sediment-transport pathways and till texture of temperate valley glaciers. Annals of Glaciology 22, 160–166. doi: 10.3189/1996aog22-1-160-166.

Klimeš, J., Benešová, M., Vilímek, V., Bouška, P., & Cochacin Rapre, A., 2014. The reconstruction of a glacial lake outburst flood using HEC-RAS and its significance for future hazard assessments: An example from Lake 513 in the Cordillera Blanca, Peru. Natural Hazards 71(3), 1617–1638. doi: 10.1007/s11069-013-0968-4.

Klimeš, J., Novotný, J., Novotná, I., Jordán de Urries, B., Vilímek, A., Emmer, A., Strozzi, T., Kusák, M., Cochachin Rapre, A., Harvich, F., & Frey, H., 2016. Landslides in moraines as triggers of glacial lake outburst floods: example from Palcacocha Lake (Cordillera Blanca, Peru). Landslides 13(6), 1461–1477. doi: 10.1007/s10346-016-0724-4.

Korup, O. and Tweed, F., 2007. Ice, moraine, and landslide dams in mountainous terrain. Quaternary Science Reviews 26(25–28), 3406–3422. doi: 10.1016/j.quascirev.2007.10.012.

Kristjánsson, L., Jóhannesson, H., Eiríksson, J., & Gudmundsson, A.I., 1987. Brunhes–Matuyama paleomagnetism in three lava sections in Iceland. Canadian Journal of Earth Sciences 25(2), 215–225. doi: 10.1139/e88-024.

Lawson, D. E., 1979. Sedimentological analysis of the western terminus region of the Matanuska glacier, Alaska. CCREL Report 79-9. US Cold Regions Research and Engineering Lab., Hanover, New Hampshire, U.S.A.

Lukas, S., 2005. A test of the englacial thrusting hypothesis of “hummocky” moraine formation: Case studies from the northwest Highlands, Scotland. Boreas 34(3), 287–307. doi: 10.1111/j.1502-3885.2005.tb01102.x.

Lukas, S., Nicholson, L.I., Ross, F.H., & Humlum, O., 2005. Formation, Meltout Processes and Landscape Alteration of High-Arctic Ice-Cored Moraines—Examples from Nordenskiold Land, Central Spitsbergen. Polar Geography 29(3), 157–187. doi: 10.1080/789610198.

Lukas, S., Graf, A., Coray, S., & Schlüchter, C., 2012. Genesis, stability and preservation potential of large lateral moraines of Alpine valley glaciers - towards a unifying theory based on Findelengletscher, Switzerland. Quaternary Science Reviews 38, 27–48. doi: 10.1016/j.quascirev.2012.01.022.

Lukas, S., 2012. Processes of annual moraine formation at a temperate alpine valley glacier: Insights into glacier dynamics and climatic controls. Boreas 41(3), 463–480. doi: 10.1111/j.1502-3885.2011.00241.x.

Lukas, S. and Sass, O., 2011. The formation of Alpine lateral moraines inferred from sedimentology and radar reflection patterns: a case study from Gornergletscher, Switzerland. In: Martini, I.P., French, H.M., and Perez Alberti, A. (Eds.), Ice-Marginal Periglacial Processes and Sediments. The Geological Society of London Special Publications, 354(1), 77–92. doi: 10.1144/SP354.5.

MacDonald, T. C. and Langridge-Monopolis, J., 1984. Breaching Characteristics of Dam Failures. Journal of Hydraulic Engineering 110(5), 567–586. doi: 10.1061/(ASCE)0733-9429(1984)110:5(567).

Magnússon, E., Gudmundsson, M.T., Roberts, M.J., Sigurðsson, G., Höskuldsson, F., and Oddsson, B., 2012. Ice-volcano interactions during the 2010 Eyjafjallajökull

eruption, as revealed by airborne imaging radar. Journal of Geophysical Research: Solid Earth 117(B7), 1-17. doi: 10.1029/2012JB009250.

Mark, B., Stansell, N. & Zeballos, G., 2017. The last deglaciation of Peru and Bolivia. Cuadernos de Investigación Geográfica 43(2), 591-628. doi: 10.18172/cig.3265.

Matthews, J. A. and Petch, J. R., 1982. Within-valley asymmetry and related problems of Neoglacial lateral moraine development at certain Jotunheimen glaciers, southern Norway. Boreas 11(3), 225–247. doi: 10.1111/j.1502-3885.1982.tb00716.x.

McKillop, R. J. and Clague, J. J., 2007. A procedure for making objective preliminary assessments of outburst flood hazard from moraine-dammed lakes in southwestern British Columbia. Natural Hazards, 41(1), 131–157. doi: 10.1007/s11069-006-9028-7.

Miles, E. S., Watson, C.S., Brun, F., Berthier, E., Esteves, M., Quincey, D.J., Miles, K.E., Hubbard, B., & Wagnon, P., 2018. Glacial and geomorphic effects of a supraglacial lake drainage and outburst event, Everest region, Nepal Himalaya. Cryosphere 12(12), 3891–3905. doi: 10.5194/tc-12-3891-2018.

Osborn, G., McCarthy, D., LaBrie, A., & Burke, R., 2015. Lichenometric dating: Science or pseudo-science? Quaternary Research 83(1), 1–12. doi: 10.1016/j.yqres.2014.09.006.

Owen, L. A., Robinson, R., Benn, D.I., Finkel, R.C., Davis, N.K., Yi, C., Putkonen, J., Li, D., & Murray, A.S., 2009. Quaternary glaciation of Mount Everest. Quaternary Science Reviews 28(15–16), 1412–1433. doi: 10.1016/j.quascirev.2009.02.010.

Owen, L. A. and Derbyshire, E., 1989. The Karakoram glacial depositional system. Zeitschrift für Geomorphologie Supplement (76), 33–77.

Reinardy, B. T. I. and Lukas, S., 2009. The sedimentary signature of ice-contact sedimentation and deformation at macro- and micro-scale: A case study from NW Scotland. Sedimentary Geology 221(1–4), 87–98. doi: 10.1016/j.sedgeo.2009.07.014.

Scherler, D., Wulf, H. &Gorelick, N., 2018. Supraglacial Debris Cover. V. 1.0. GFZ German Research Centre for Geosciences. doi: http://doi.org/10.5880/GFZ.3.3.2018.005.

Schneider, D., Huggel, C., Cochachin, A., Guillén, S., & García, J., 2014. Mapping hazards from glacier lake outburst floods based on modelling of process cascades at Lake 513, Carhuaz, Peru. Advances in Geosciences 35, 145–155. doi: 10.5194/adgeo-35-145-2014.

Shakesby, R. A., 1989. Variability in Neoglacial Moraine Morphology and Composition, Storbreen, Jotunheimen, Norway: Within-Moraine Patterns and their Implications. Geografiska Annaler: Series A, Physical Geography 71(1–2), 17–29. doi: 10.1080/04353676.1989.11880270.

Sigurðardóttir, M., 2013. The sedimentology and formation of the Gígjökull and Kvíárjökull latero-frontal moraines, Iceland. Masters Thesis, University of Iceland.

Sigurðsson, O., 2000. Jöklabreytingar 1930-1960, 1960-1990 og 1998-1999. Jökull 49, 83–90.

Slomka, J. M. and Eyles, C. H., 2013. Characterizing heterogeneity in a glaciofluvial deposit using architectural elements, Limehouse, Ontario, Canada. Canadian Journal of Earth Sciences 50(9), 911–929. doi: 10.1139/cjes-2013-0020.

Small, R. J., 1983.Lateral Moraines of Glacier De Tsidjiore Nouve: Form, Development, and Implications. Journal of Glaciology 29 (102), 250–259. doi: 10.3189/S0022143000008303.

Smith, J. A., Seltzer, G. O., Farber, D.L., Rodbell, D.T., & Finkel, R.C., 2005. Climate change: Early local last glacial maximum in the tropical Andes. Science, 308(5722), 678–681. doi: 10.1126/science.1107075.

Smith, J. A., Finkel, R. C., Farber, D.L., Rodbell, D.T., and Seltzer, G.O., 2005. Moraine preservation and boulder erosion in the tropical Andes: Interpreting old surface exposure ages in glaciated valleys. Journal of Quaternary Science 20(7–8), 735–758. doi: 10.1002/jqs.981.

Smith, J. A. and Rodbell, D. T., 2010. Cross-cutting moraines reveal evidence for north atlantic influence on glaciers in the tropical Andes. Journal of Quaternary Science 25(3), 243–248. doi: 10.1002/jqs.1393.

Solomina, O., Jomelli, V., Kaser, G., Ames, A., Berger, B., & Pouyaud, B., 2007. Lichenometry in the Cordillera Blanca, Peru: “Little Ice Age” moraine chronology. Global and Planetary Change 59(1–4), 225–235. doi: 10.1016/j.gloplacha.2006.11.016.

Spedding, N., 2000. Hydrological controls on sediment transport pathways : implications for debris-covered glaciers. Debris-Covered Glaciers (Proceedings of a workshop held at Seattle, Washington, USA, September 2000). IASH Publ. no. 264, 133-142.

Spedding, N. and Evans, D. J., 2002. Sediments and landforms at Kvíárjökull, southeast Iceland: a reappraisal of the glaciated valley landsystem. Sedimentary Geology 149(1–3), 21–42. doi: 10.1016/S0037-0738(01)00242-1.

Thorarinsson, S., 1943. Vatnajökull. Scientific Results of the Swedish Icelandic Investigations 1936-37-38. Chapter XI: Oscillations of the Iceland glaciers during the last 250 years. Geografiska Annaler 25(2), 1-54. doi: 10.2307/519895.

Westoby, M. J., Glasser, N.F., Brasington, J., Hambrey, M.J., Quincey, D.J., and Reynolds, J.M., 2014. Modelling outburst floods from moraine-dammed glacial lakes. Earth-Science Reviews 134, 137–159. doi: 10.1016/j.earscirev.2014.03.009.

World Glacier Monitoring Service Fluctuation of Glaciers dallatabase (WGMS FoG), 2020. Gigjokull (IS) – WWGMS ID: 3079. Database version: 2020-08-24. DOI: 10.5904/wgms-fog-2020-08

Worni, R., Stoffel, M., Huggel, C., Volz, C., Casteller, A., & Luckman, B., 2012. Analysis and dynamic modeling of a moraine failure and glacier lake outburst flood at Ventisquero Negro, Patagonian Andes (Argentina). Journal of Hydrology 444–445, 134–145. doi: 10.1016/j.jhydrol.2012.04.013.

CHAPTER 5: CONCLUSIONS

5.1 INTRODUCION

The main objective of this thesis is to investigate the origin, sedimentological characteristics, and paleoglacial significance of large latero-frontal moraines in deglaciating regions of the Cordillera Blanca, Perú and southern Iceland. This was achieved by utilizing a glacial sedimentological and geomorphological approach to investigate the relationship between current and past glacial processes in the study areas. As glaciers around the world continue to retreat, glacial lakes continue to increase in volume and in many high-altitude regions the risk for glacial lake outburst floods (GLOFs), from moraine-dammed lakes in particular, is increasing (Aggarwal et al., 2017; Harrison et al., 2018; Wilson et al., 2018; Shugar et al., 2020). Moraines that dam these glacial lakes are also used to determine past glacier behaviour and extent through geochronological analysis of boulders found near or on the crestline of the moraine, using a variety of methodologies such as lichenometry, radiocarbon dating, and surface exposure dating (i.e. Matthews and Petch, 1982; Ivy-Ochs et al., 2006; Jomelli et al., 2009; Owen et al., 2009; Smith and Rodbell, 2010). The research findings presented in this thesis utilize a glacial sedimentological and geomorphological approach to investigating the relationship between current and past glacial processes in the study areas, and the role that these processes play in determining the characteristics and stability of large ice marginal moraines that impound glacial lakes. Identifying and determining these relationships may be applied to better understand the role of large moraines damming glacial lakes in other high-altitude regions such as the Himalayas, British Columbia, Patagonia, and New Zealand (Figure 1) as well

as to aid in the reconstruction of the glacial and deglacial history of an area by understanding the chronology of moraine formation.

5.2 SUMMARY OF FINDINGS

To achieve the objectives above, this thesis established a qualitative chronological framework of the glacial history of the Cordillera Blanca, Perú through the compilation and mapping of dated moraines reported in the literature (Chapter 2). In many modern glaciated environments latero-frontal moraines are used to indicate the former positions of glacier termini and are dated using various geochronological technologies (i.e., Smith and Rodbell, 2010; Solomina et al., 2015; Mark, Stansell and Zeballos, 2017). To evaluate the recent glacial history of the Cordillera Blanca, available data on the location of moraines and their dates were compiled and mapped (Chapter 2). Six stages of glacial activity could be identified from this compilation ranging in age from older than 35 thousand years (Stage 1) to modern (Stage 6); the formation of numerous moraines by different glaciers in the same region at approximately the same time can be interpreted to indicate that regional climate conditions were favourable for glacier expansion and/or equilibrium. Regional differences in the spatial distribution of dated moraines occur between the northern and southern regions of the Cordillera Blanca which may result from differences in bedrock type, valley morphology, surface processes, and/or the inaccuracy of dating methodologies. It is important to note that topographic relief in the northern and central parts of the Cordillera Blanca (~3km) is also greater than in the southern part (~1km; Margirier et al., 2016) and may encourage higher rates of valley incision by glacial and fluvial processes as

well as enhancing the effectiveness of mass wasting processes in the redistribution of material from steep valley walls.

The current rapid recession of glaciers in the Cordillera Blanca has allowed the development and growth of numerous moraine dammed lakes. The geomorphology and sedimentology of an enlarging moraine-dammed, supraglacial lake (Llaca Lake) in the Cordillera Blanca is presented in Chapter 3 of this thesis and is the first study to describe the landform-sediment assemblages in a tropical moraine-dammed supraglacial lake. The integration of remotely sensed data collected by an uncrewed aerial vehicle (UAV) with field based sedimentological observations and geomorphological mapping, allowed for a landsystem model to be created that summarized the current geomorphic and sedimentologic environments of Llaca Lake into three landsystem zones (Chapter 3). These zones comprise the latero-frontal moraine and ice-distal open water areas (Zone 1), the central area of the lake dominated by ice-cored hummocks (Zone 2) and the ice-proximal area adjacent to the active glacier margin (Zone 3). The Cordillera Blanca, in addition to other glaciated regions of the world, contain enlarging lakes that overlie buried and stagnant glacial ice (Iturrizaga, 2014; Tacsi Palacios et al., 2014; Irvine-Fynn et al., 2017); the results of this study provide a framework for further landsystem analysis of these growing supraglacial lakes. This is especially important as the buried ice in the lake is slowly melting and thereby contributing to the available water for a GLOF event (Watson et al., 2016).

To aid in the understanding of the limitations of the use of moraines as indicators of past glacier behaviour (Humlum, 1978; Evans, Shulmeister and Hyatt, 2010; Osborn et al., 2015), and of the stability and structure of moraine dams in areas at risk to GLOF events

(Clague and Evans, 2000; McKillop and Clague, 2007; Westoby et al., 2014), this thesis characterized the sedimentary architecture of the eastern lateral moraine of Gígjökull, southern Iceland (Chapter 4). A DJI Phantom -4 Advance UAV was employed to acquire high resolution photographs of an exposure through the eastern lateral moraine of Gígjökull that allowed the identification of seven lithofacies types and three lithofacies associations (LFA 1-3). LFA 1 consists of stacked units of massive and matrix-supported diamict, interpreted to originate from matrix-rich subaerial debris flows, LFA 2 is coarser- grained, with angular to subangular clasts generated predominantly by rockfalls, and LFA 3 consists of deformed diamict interpreted as fine-grained ice marginal sediment glaciotectonized during glacier expansion/overriding. A depositional summary model is presented to illustrate the formation of the Gígjökull eastern lateral moraine based on interpretation of its sedimentological and architectural characteristics (Chapter 4). Documentation of the sedimentary architecture of the eastern lateral moraine of Gígjökull has significant applications to the understanding of moraine development in other glaciated settings and to the identification of areas of hydrogeological weakness that can reduce the structural integrity of the moraine.

This thesis has investigated select examples of moraines and moraine-dammed lakes in the Cordillera Blanca, Perú (Chapter 2 and 3) and in southern Iceland (Chapter 4) to aid in the understanding of moraine stability and lake characteristics, important factors in GLOF risk assessment. The landsystem model of Llaca Lake presented in this thesis provides a useful foundation for enhanced understanding of sedimentary processes in supraglacial lakes in high-altitude settings but may not be representative of all supraglacial

lakes. The sedimentological investigation of additional examples is required before a comprehensive depositional model for such environments can be developed. Similarly, the sedimentary architecture identified within the Gígjökull moraine may not be representative of all lateral moraines but adds to the suite of examples needed to build a comprehensive model.

5.3 FUTURE WORK

Despite the new insights that this research provides into the paleoglacial significance and potential stability of large latero-frontal moraines in deglaciating regions (Chapter 2, 4), and the nature of active surface processes in modern glacial lakes that are at risk of a GLOF (Chapter 3), additional work is required to adequately characterize the sedimentary characteristics of moraines, and the glacial lakes impounded by such moraines.

The methodology used in this thesis to characterize the sedimentary architecture of a lateral moraine (Chapter 4) can be applied in other glaciated areas where moraines dam glacial lakes. The growing number of large glacial lakes in the Cordillera Blanca, Perú continues to pose a serious risk of GLOF events that would severely impact communities in the region (Emmer et al., 2016, 2020). Investigation of the sedimentary architecture of moraines, via UAV-derived photogrammetry, in glacial lakes that are at risk of a GLOF event in the Cordillera Blanca such as Lake Palcacocha (Somos-Valenzuela and Mckinney, 2011; Emmer and Vilímek, 2013; Mergili et al., 2020), would create additional insight into the stability and origin of these landforms.

The research reported in this thesis for Lake Llaca (Chapter 3) is the first attempt at characterizing landform-sediment assemblages at an enlarging supraglacial lake.

Previous work on this lake (Wigmore and Mark, 2017), used UAV-derived photogrammetry to analyze glacier dynamics of the tongue of Llaca Glacier and ice-proximal ice-cored hummocks (Zone 3 in this thesis) over a one-year period. To better understand the dynamics and rate of change of the ice-cored hummocks over time, comprehensive aerial surveys of the entire lake should be conducted over several years to allow quantification of the surface processes operating in this lake.

Finally, there is a growing need to study the detailed paleoclimatic record of lacustrine sediments preserved in high-altitude lakes in the Cordillera Blanca to better understand the chronology of glacier recession and its response to past climate changes (Stansell et al., 2013; López-Moreno et al., 2017). Actively enlarging glacial lakes, such as Llaca Lake, can preserve an important record of changing sediment input during periods of relatively high ablation as has been experienced in recent years. Changing sedimentation characteristics and rates related to changes in ENSO precipitation and ablation rates can also be analysed and will provide valuable information regarding the behaviour of tropical glacial environments under conditions of global climate warming. Hence, the enlarging glacial lakes of the Cordillera Balance should be viewed as a great repository of data recording recent paleoclimatic changes in South America.

The data and analyses presented in this thesis augment current understanding of latero-frontal moraines, their origin, sedimentological characteristics, paleoglacial significance, and implications for generating GLOF events. The Cordillera Blanca, Perú contains the highest number of tropical glaciers in the world; these glaciers are rapidly retreating and enlarging the volume and number of glacial lakes that lie on their margins,

increasing risk of GLOF events that can devastate surrounding communities. Using a sedimentologic and geomorphic approach to characterize the sediment-landform assemblages of these lacustrine environments, as well as the sedimentary architecture of their impounding moraines, furthers our understanding of the dynamic surface processes occurring in the Cordillera Blanca and the risk of GLOF events.

REFERENCES

Aggarwal, S., Rai, S.C., Thakur, P.K., & Emmer, A., 2017. Inventory and recently increasing GLOF susceptibility of glacial lakes in Sikkim, Eastern Himalaya. Geomorphology 295, pp. 39–54.

Clague, J. and Evans, S. G., 2000. A review of catastrophic drainage of moraine-dammed lakes in British Columbia. Quaternary Science Reviews, 19(17–18), pp. 1763–1783. doi: 10.1016/S0277-3791(00)00090-1.

Emmer, A., Klimes, Mergili, M., Vilímek, V., & Cochachin, A., 2016. 882 lakes of the Cordillera Blanca: An inventory, classification, evolution and assessment of susceptibility to outburst floods. CATENA, 147, pp. 269–279. doi: 10.1016/j.catena.2016.07.032.

Emmer, A., Harrison, S., Mergili, M., Allen, S., Frey, H., & Huggel, C., 2020. 70 years of lake evolution and glacial lake outburst floods in the Cordillera Blanca (Peru) and implications for the future. Geomorphology, 365, p. 107178. doi: 10.1016/j.geomorph.2020.107178.

Emmer, A. and Vilímek, V., 2013. Review Article: Lake and breach hazard assessment for moraine-dammed lakes: an example from the Cordillera Blanca (Peru). Natural Hazards and Earth System Sciences, 13(6), pp. 1551–1565. doi: 10.5194/nhess-13-1551-2013.

Evans, D. J. A., Shulmeister, J. and Hyatt, O., 2010. Sedimentology of latero-frontal moraines and fans on the west coast of South Island, New Zealand. Quaternary Science Reviews, 29(27–28), pp. 3790–3811. doi:

10.1016/j.quascirev.2010.08.019.

Harrison, S., Kargel, J., S., Huggel, C., Reynolds, J., Shugar, D.H., Betts, R.A., Emmer, A., Glasser, N., Haritashya, U.K., Klimes, Reinhardt, L., Shaub, Y., Wiltshire, A., Regmi, D., & Vilímek, 2018. Climate change and the global pattern of moraine-dammed glacial lake outburst floods. The Cryosphere, 12(4), pp. 1195–1209. doi: 10.5194/tc-12-1195-2018.

Humlum, O., 1978. Genesis Of Layered Lateral Moraines. Geografisk Tidsskrift-Danish Journal of Geography, 77(1), pp. 65–72. doi: 10.1080/00167223.1978.10649094.

Irvine-Fynn, T. D. L., Porter, P.R., Rowan, A.V., Quincey, D.J., Gibson, M.J., Bridge, J.W., Watson, C.S., Hubbard, A., 7 Glasser, N.F., 2017. Supraglacial Ponds Regulate Runoff From Himalayan Debris-Covered Glaciers. Geophysical Research Letters, 44(23), pp. 11,894-11,904. doi: 10.1002/2017GL075398.

Iturrizaga, L., 2014. Glacial and glacially conditioned lake types in the Cordillera Blanca, Peru: A spatiotemporal conceptual approach. Progress in Physical Geography, 38, 5, 602-636. doi: 10.1177/0309133314546344.

Ivy-Ochs, S., Kerschner, H., Reuther, A., Maisch, M, Sailer, R., Schaefer, J., Kubik, R.W., Synal, H.A., & Schlucter, C., 2006. The timing of glacier advances in the northern European Alps based on surface exposure dating with cosmogenic 10Be, 26Al, 36Cl, and 21Ne. In Situ-Produced Cosmogenic Nuclides and Quantification of Geological Processes. Geological Society of America, pp. 43–60. doi: 10.1130/2006.2415(04).

Jomelli, V., Favier, V., Rabate, A., Brunstein, D., Hoffman, G., & Francou, B., 2009. Fluctuations of glaciers in the tropical Andes over the last millennium and paleoclimatic implications: A review. Palaeography, Palaeoclimatology, Palaeoecology, 281, 269-282. doi: 10.1016/j.palaeo.2008.10.033.

López-Moreno, J. I., Valero-Garcés, B., Mark, B., Condom, T., Revuelto, J., Azorín-Molina, C., Bazo, J., Frugone, M., Vincente-Serrano, S.M., Alejo-Cochachin, J., 2017. Hydrological and depositional processes associated with recent glacier recession in Yanamarey catchment, Cordillera Blanca (Peru). Science of The Total Environment, 579, pp. 272–282. doi: 10.1016/j.scitotenv.2016.11.107.

Margirier, A., Audin, L., Robert, X., Herman, F., Ganne, J., & Schwartz, S., 2016. Time and mode of exhumation of the Cordillera Blanca batholith (Peruvian Andes). Journal of Geographical Research: Solid Earth, 121, 6235-6249. doi: 10.1002/2016JB013055.

Mark, B., Stansell, N. and Zeballos, G., 2017. The last deglaciation of Peru and Bolivia. Cuadernos de Investigación Geográfica, 43(2), p. 591. doi: 10.18172/cig.3265.

Matthews, J. A. and Petch, J. R., 1982. Within-valley asymmetry and related problems of Neoglacial lateral moraine development at certain Jotunheimen glaciers, southern Norway. Boreas, 11(3), pp. 225–247. doi: 10.1111/j.1502-3885.1982.tb00716.x.

McKillop, R. J. and Clague, J. J., 2007. A procedure for making objective preliminary assessments of outburst flood hazard from moraine-dammed lakes in southwestern British Columbia. Natural Hazards, 41(1), pp. 131–157. doi: 10.1007/s11069-006-9028-7.

Mergili, M., Pudasaini, S., P., Emmer, A., Fisher, J.T., Cochachin, A., Frey, H., 2020. Reconstruction of the 1941 GLOF process chain at Lake Palcacocha (Cordillera Blanca, Peru). Hydrology and Earth System Sciences, 24(1), pp. 93–114. doi: 10.5194/hess-24-93-2020.

Osborn, G., McCarthy, D., LaBrie, A., & Burke, R., 2015. Lichenometric dating: Science or pseudo-science? Quaternary Research, 83, 1-12. doi: 10.1016/j.yqres.2014.09.006.

Owen, L. A., Robinson, R., Benn, D.I., Finkel, R.C., Davis, N.K., Yi, C., Putkonen, J., Li, D., & Murray, A.S., 2009. Quaternary glaciation of Mount Everest. Quaternary Science Reviews, 28(15–16), pp. 1412–1433. doi: 10.1016/j.quascirev.2009.02.010.

Shugar, D. H., Burr, A., Haritashya, U.K., Kargel, J.S., Watson, C.S., Kennedy, M.C., Bevington, A.R., Betts, R.A., Harrison, S., & Strattaman, K., 2020. Rapid worldwide growth of glacial lakes since 1990. Nature Climate Change, 10(10), pp. 939–945. doi: 10.1038/s41558-020-0855-4.

Smith, J. A. and Rodbell, D. T., 2010. Cross-cutting moraines reveal evidence for north atlantic influence on glaciers in the tropical Andes. Journal of Quaternary Science, 25(3), pp. 243–248. doi: 10.1002/jqs.1393.

Solomina, O. N., Bradley, R.S., Hodgson, D.A., Ivy-Ochs, S., Jomelli, V., Mackinstosh, A.N., Nesje, A., Owen, L.A., Wanner, H., Wiles, G., & Young, N.E., 2015. Holocene glacier fluctuations. Quaternary Science Reviews, 111, pp. 9–34. doi: 10.1016/j.quascirev.2014.11.018.

Somos-Valenzuela, M. A., Chisolm, R.E., Rivas, D.S., Portocarrero, C., & McKinney, D.C., 2016. Modeling a glacial lake outburst flood process chain: the case of Lake Palcacocha and Huaraz, Peru. Hydrology and Earth System Sciences, 20(6), pp. 2519–2543. doi: 10.5194/hess-20-2519-2016.

Stansell, N. D., Rodbell, D.T., Abbott, M.B., & Mark, B.G., 2013. Proglacial lake sediment records of Holocene climate change in the western Cordillera of Peru. Quaternary Science Reviews, 70, pp. 1–14. doi: 10.1016/j.quascirev.2013.03.003.

Tacsi Palacios, A., Colonia Ortiz, D., Torres Castillo, J., & Santiago Martel, A., 2014. Inventario de Lagunas Glaciares del Peru. Autoridad Nacional del Agua – Unidad de Glaciología y Recursos Hídricos. Huaraz, Perú.

Watson, C. S., Quincey, D.J., Carrivick, J.L., & Smith, M.W., 2016. The dynamics of supraglacial water storage in the Everest region, central Himalaya. Global and Planetary Change. Elsevier B.V., 142, pp. 14–27. doi: 10.1016/j.gloplacha.2016.04.008.

Westoby, M. J., Glasser, N.F., Brasington, J., Hambrey, M.J., Quincey, D.J., Reynolds, J.M., 2014. .Modelling outburst floods from moraine-dammed glacial lakes. Earth-Science Reviews, 134, pp. 137–159. doi: 10.1016/j.earscirev.2014.03.009.

Wigmore, O. and Mark, B., 2017. Monitoring tropical debris-covered glacier dynamics from high-resolution unmanned aerial vehicle photogrammetry, Cordillera Blanca, Peru. The Cryosphere, 11(6), pp. 2463–2480. doi: 10.5194/tc-11-2463-2017.

Wilson, R., Glasser, N.F., Reynolds, J.M., Harrison, S., Iribarren Anacona, P., Schaefer, M., Shannon, S., 2018. Glacial lakes of the Central and Patagonian Andes. Global and Planetary Change, 162, pp. 275–291. doi: 10.1016/j.gloplacha.2018.01.004.